A THEORETICAL AND EXPERIMENTAL STUDY OF TUNNEL BORING BY MACHINE WITH AN EMPHASIS ON BOREABILITY PREDICTION AND MACHINE DESIGN

William A. Hustrulid

Colorado School of Mines

Prepared for:

Advanced Research Projects Agency
Bureau of Mines

18 February 1972

DISCLAIMER NOTICE

THIS DOCUMENT IS THE BEST QUALITY AVAILABLE.

COPY FURNISHED CONTAINED A SIGNIFICANT NUMBER OF PAGES WHICH DO NOT REPRODUCE LEGIBLY.

MISSING PAGE
NUMBERS ARE BLANK
AND WERE NOT
FILMED

"A Theoretical and Experimental Study of Tunnel Boring by Machine With an Emphasis on Boreability Prediction and Machine Design"

Bureau of Mines Contract H0210043
Principal Investigator: Dr. W. A. Hustrulid
Contractor: Colorado School of Mines

Sponsored by
Advanced Research Projects Agency

14 KEY WORDS	LINK A		LINK B		LINK C	
	ROLE	WT	ROLE	WT	ROLE	WT
Boreability						
Cutter						
Tunnel						
Linear Cutting Machine						
Disc Cutter						
Specific Energy						
Cutting Coefficient						
Tunnel Boring Prediction						

UNCLASSIFIED
Security Classification

DOCUMENT CONTROL DATA - R & D

(Security classification of title, body of abstract and indexing annotation must be entered when the overall report is classified)

1. ORIGINATING ACTIVITY (Corporate author)
Colorado School of Mines
Department of Mining Engineering

2a. REPORT SECURITY CLASSIFICATION
UNCLASSIFIED

2b. GROUP
----

3. REPORT TITLE
A Theoretical and Experimental Study of Tunnel Boring by Machine With an Emphasis on Boreability Prediction and Machine Design

4. DESCRIPTIVE NOTES (Type of report and inclusive dates)
Interim Report

5. AUTHOR(S) (First name, middle initial, last name)
William A. Hustrulid

6. REPORT DATE	7a. TOTAL NO OF PAGES	7b. NO. OF REFS
February 18, 1972	268 281	11

8a. CONTRACT OR GRANT NO	9a. ORIGINATOR'S REPORT NUMBER(S)
H0210043	
b. PROJECT NO ARPA Order No. 1579, Amendment No. 2	
c.	9b. OTHER REPORT NO(S) (Any other numbers that may be assigned this report)
d.	

10. DISTRIBUTION STATEMENT
Distribution of this document is unlimited.

11. SUPPLEMENTARY NOTES	12. SPONSORING MILITARY ACTIVITY
	Advanced Research Projects Agency 1400 Wilson Boulevard Arlington, Virginia 22209

13. ABSTRACT

This report discusses the results of the first 12 months of a proposed 3-year research effort. The ultimate goal of this project was to develop scaling relationships required to predict field-boring performance from tests performed on small cores from along the proposed tunnel line. Fundamentals of failure of hard rock under cutters of various shapes and sizes were studied by performing both small-scale and full-size linear cutter tests.

Average horizontal and vertical forces, actual penetration, specific energy, cutting coefficient and cutting size distribution were calculated, through the use of an analog-digital computer, from the results of laboratory experiments using a small linear cutter on rock samples from the Nast, Lawrence, and Climax Tunnels. The results of that testing are presented here.

A large linear cutting machine, capable of being operated either at a constant force or a constant penetration mode has been designed and constructed. The contractor has proposed that the effect of the depth of cut and indexing distance on specific energy, vertical force, horizontal force, fragment size and cutting coefficient could be studied with this machine.

DD FORM 1473

ARPA Order Number: 1579

Contract Number: HO210043

Program Code Number:
1-F-10

Principal Investigator and Telephone Number: William A. Hustrulid, 303-279-3381, ext. 444

Name of Contractor:
Colorado School of Mines

Project Scientist or Engineer and Telephone Number: Same

Effective Date of Contract:
February 19, 1971

Short Title of Work: A Theoretical and Experimental Study of Tunnel Boring by Machine With an Emphasis on Boreability Prediction and Machine Design

Contract Expiration Date:
February 18, 1972
(No-cost extension to
August 18, 1972)

Amount of Contract: $71,812

INTERIM FINAL REPORT

February 19, 1971 - February 18, 1972

This research was supported by the Advanced Research Projects Agency of the Department of Defense and was monitored by the U.S. Bureau of Mines under Contract No. HO210043.

Preface

In this report is discussed the results obtained by the Mining Department of the Colorado School of Mines during the first year of a proposed three year effort on research contract HO 2100#3 entitled, "A Theoretical and Experimental Study of Tunnel Boring by Machine With Emphasis on Boreability Prediction and Machine Design." It is perhaps instructive to review the background leading to proposing this research before describing the present work.

During the period 1968-1970, the Mining Department worked with the United States Bureau of Reclamation (U.S.B.R.) on the development of tests that could be performed on test samples (diamond drill cores and larger samples from the portal regions) available from along the proposed tunnel line that might give useful information to potential contractors for the Bureau's tunnels. It was hoped that this would lead to better estimates of machine applicability and thereby avoid delays in construction and cost overruns that must be absorbed by the contractors or the U.S. Government. It was found that:

1. No particular method of estimating boreability was common to all manufacturers of boring machines and cutting tools. Details of the methods used were sketchy if available at all.

2. Complete operating data from previous tunnel boring operations had either not been recorded or was considered company confidential. Rock samples from these operations were generally not available.

Faced with these obstacles it was decided to gather operating data from the River Mountains Tunnel being bored at that time for the

U.S.B.R., collect rock samples from along the tunnel line, perform laboratory tests on these samples, and then try and correlate field and laboratory results. Linear cutter, button indentation, and physical property tests were performed in the laboratory. Although trends were found to exist; for example, the boring rate decreased as the uniaxial compressive strength of the rock increased, the scaling factors required to predict quantitatively the boring rate from these tests on small samples were not found. Specific energy values (energy required to remove a unit volume of rock) obtained from the laboratory linear cutter tests were always higher than those found in the actual boring. The specific energies ratios were not at all constant. This was not unexpected since in the field boring the rock weaknesses which can be expected in the removal process are normally different from those encountered in the laboratory studies. If the weaknesses were the same in both cases, then the scaling would be expected to be one to one.

Examining average depth of penetration and cutter spacings used on most boring machines, it was seen that major possible rock weakening structures such as bedding planes and joints are ignored by designers of machines and cutters. In fact, the presence of these structures can very seriously hamper the progress of present machines. Thus the rock is presently removed primarily by crushing and the average particle size is small. The tensile strength of intact rock is of the order of 1/10 to 1/20 of the uniaxial compressive strength. For the rock mass itself with joints, etc., the tensile strength can approach zero and under the cutting edge the rock is in a state of triaxial compression so the comparison of

strengths being attacked in the two cases will be even more different than by a factor of 10 or 20. It was with this background that the present program outlined below was designed.

1. The scale factors involved in predicting present boring machine performance would be examined by performing small and large linear cutting experiments on blocks of rock taken from sections of tunnel for which the actual boring data was known. The large linear cutter capable of cutting blocks about a cubic meter in size would be constructed in the first year of the contract and preliminary tests run. A comparison of laboratory and field results would be made.

2. In particular, the possibilities of employing other cutter designs would be investigated. The large linear cutter would be capable of using fixed pick type of tungsten carbide cutters. It is felt that this type of tool could presently be used on medium hard rock tunneling machines to advantage. Deeper depths of cut could be achieved at lower thrusts. Since the depth of cut is deeper the volume of rock being attacked is larger and the possibility of a major weakening feature in that volume greater. Thus the specific energy required would be less. For a particular power input the boring rate would be expected to be larger than a machine equipped with more conventional cutters. This portion of work will not be discussed in much detail in this report as it is scheduled for the second contract year. However, a few comments as to the reasons for its attractiveness are perhaps in order. The rotary power is the largest by far of the components making up the total power. This application of the rotary power depends on the torque developed which is roughly proportional to the depth

of cut. With present cutter designs the force required to achieve the cut increases non-linearly with the depth. The total force that can be applied is limited by the bearing capacity (approximately 30,000 lbs/cutter) and thus the depth of cut is limited quite severely. Since the pick cutters are fixed, this limitation is not applicable. Concern must, of course, then be focused on the main drive bearing. However, the possible contact surfaces are much larger and in theory at least, the bearing problem should be much less.

Originally it was hoped that the large linear cutter could be built in the first 6 months of the contract. However, because of construction delays primarily in the delivery of the MTS system, we are approximately 6 months behind schedule on this part of the first year's program. This will certainly be completed at the end of the 6 month no-cost extension phase in which we are presently working. This interim final report will consist of the following sections:

1. Linear cutter, button indentation, physical property, and field boring results from the Nast, Climax, and Lawrence Tunnels.
2. Design and construction of the large linear cutter.
3. Translations of certain Japanese articles on tunnel boring.

Acknowledgments

The authors are pleased to acknowledge the help, cooperation and advice of many people during the contract period to date. Some of these people are listed below.

1. The Climax Molybdenum Company, in particular Mr. Ken Harrelson and Mr. Bob Elder, for allowing cores to be drilled and large samples taken from along the Climax tunnel line.

2. The United States Bureau of Reclamation, in particular Mr. McGannis, Mr. Dewey Geary, and Mr. Jerry Bartell, for supplying boring data and allowing access to the Nast tunnel site.

3. The Lawrence Manufacturing Company, in particular Mr. William Hamilton, Mr. Howard Handewith, and Mr. Pete Gadzuk, for providing cutters for the large linear cutter, information and samples from the Lawrence Avenue tunnel.

4. The Smith Tool Company, in particular Mr. Tom Brassfield, Jr. and Alan Newcomb, for discussion regarding boreability prediction and boring data from the Climax tunnel.

5. The CSM instrument shop, in particular Mr. Earl Dickens and Mr. Al Wade, for their help in constructing the large linear cutter.

6. The White Pine Copper Company, in particular Mr. Joe Patrick, Dr. Cliff Hanninen, and Mr. Jerry Bennett, for providing samples for the small linear cutting experiments.

7. The MTS Corporation, in particular Mr. Bob Churchill, Mr. Keith Zell, Mr. Bob Beall, and Mr. Bob Sorenson, for advice regarding the design of the large cutter.

8. Dr. Donald Dick, Department of Electrical Engineering, University of Colorado, Boulder, Colorado, for his help in analyzing the linear cutter data.

9. Mr. Raymond Frahm, Research Technician, Department of Mining, CSM, for his help and suggestions in the construction of the large cutter.

10. The CSM Department of Buildings and Grounds, in particular, Col. Lemke and Mr. John Picktal, for providing men and equipment when needed in the construction phases of the large cutter.

PART I

SMALL LINEAR CUTTING RESULTS, SOME ACTUAL TUNNEL BORING RESULTS, AND THEIR ANALYSIS

by

K. O. Hakalehto*

---

*Post-doctorate Fellow, Department of Mining, Colorado School of Mines, Golden, Colorado.

1. INTRODUCTION

Tunnel boring machines using mechanical cutters have improved greatly during the past few years and it is now possible to cut very hard rocks. The question that remains, however, is whether the rocks can be bored economically. Presently, at least for medium to hard rocks, this question is sometimes only answered after a very expensive lesson of using and then removing an inappropriately chosen (or used) machine. The fact that such costly mistakes do happen reflect our present inability to make reasonable performance predictions on the basis of the small samples available before the tunnel is begun. Since the sample size is generally small, the number and variety of tests that can be used is rather small. In the past, generally only physical property data such as the uniaxial compressive strength, Young's modulus, etc. and perhaps small hand samples have been available on which bids were to be made. Over the past several years the CSM Mining Department has developed a small linear cutter that can be used to cut these samples and provide some information regarding the forces and energies required. At present, unfortunately, the scaling relationships required to translate these forces and energies into full scale are not available. The relationships, however, can only be developed by comparing the laboratory and field boring results in a manner similar to that discussed in this report.

In this part of the report the results of tests in which the small linear cutter was used to cut samples taken from the Nast,

Lawrence, and Climax tunnels are described. Field boring data is also given for the Nast and Lawrence tunnels. A comparison of laboratory and field results is made and the difference discussed.

Physical property data and button indentation results for these same rocks will be presented in a subsequent report.

2. EXPERIMENTS

2.1 Laboratory Testing

2.1.1 Linear Cutter

The small linear cutter used in this project is shown in Fig. 2.1. As can be seen, the cutter head is mounted to an old milling machine. The design force limitations are 7000 lbs vertical and 3000 lbs horizontal. The operational loads, which can be seen from the recorded forces (Appendix A), were generally below these design limits. In testing a few samples the peak values approached the maximum limit of vertical force, and therefore the cutter support system should be as rigid as possible. The testing method employed requires constant displacement. The maximum horizontal force is limited by the power output of the milling machine motor. With higher force levels it may not be powerful enough to maintain constant table speed.

For the highest loads the stiffness of the horizontal support arms of the unit was barely adequate. This can be observed in some of the records by the presence of elastic rebound force. This occurs when the cutter, after high horizontal loading, reached a hole in the sample where the horizontal component of the rock reaction is zero. The stored elastic energy in the support system is then released causing the arms to go momentarily into tension. This effect can be seen in some of the curves of the horizontal force in Appendix A. This rebound effect does not significantly affect the average results. It does affect the value of the cutting coefficient (the ratio of the horizontal to the vertical

Fig. 2.1. Linear cutter unit in the laboratory.

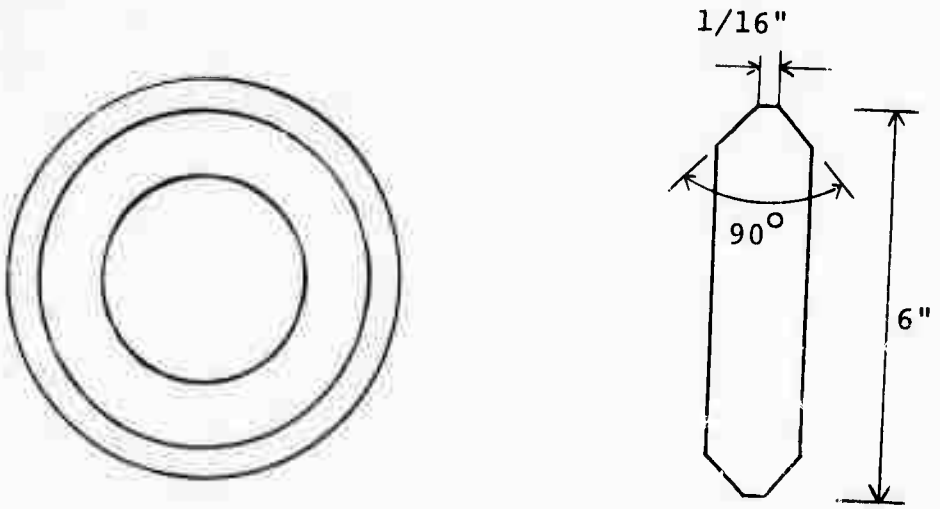

Fig. 2.2. Disk type kerf cutter used in the laboratory.

force) although the effect is felt only over a short distance. It has practically no effect on the calculated total energy along a cut.

The design of the cutting unit is such that cutters of different diameters and types may be employed. The cutter unit is constructed of mild steel except for the cutter which is made of Ketos steel (Crucible Steel Co., type AISI 01). The cutter was hardened to 58-62 Rockwell hardness after machining and then ground to a final cutting edge with a 90 degree included angle. The cutter is 6 inches in diameter and 1/2 inch thick, and has a 1/16 inch flat wear flat on the cutting edge. A diagrammatic representation of the cutter is shown in Fig. 2.2. This cutter was used throughout the tests. The controls of the milling machine allowed for accurate (±.002 in.) settings of penetration and indexing.

2.1.2 Instrumentation

The instrumentation was modified from that used earlier with the linear cutter system to include recording on magnetic tape. The tape was used as the input to the hybrid computer. The signals from the vertical and horizontal arms had to be amplified for input to the tape. The circuit is shown in Fig. 2.3.

Strain gages (120 ohm, G.F. 2.04, type SR-4) mounted on two sides of the restricted sections of each of the support arms were connected in series to compensate for any bending. A constant voltage of 10 volts was maintained across the Wheatstone bridge circuit. The sensitivities were 4410 lbs/mv for the vertical and 3310 lbs/mv for the horizontal arms. Temperature compensating gages

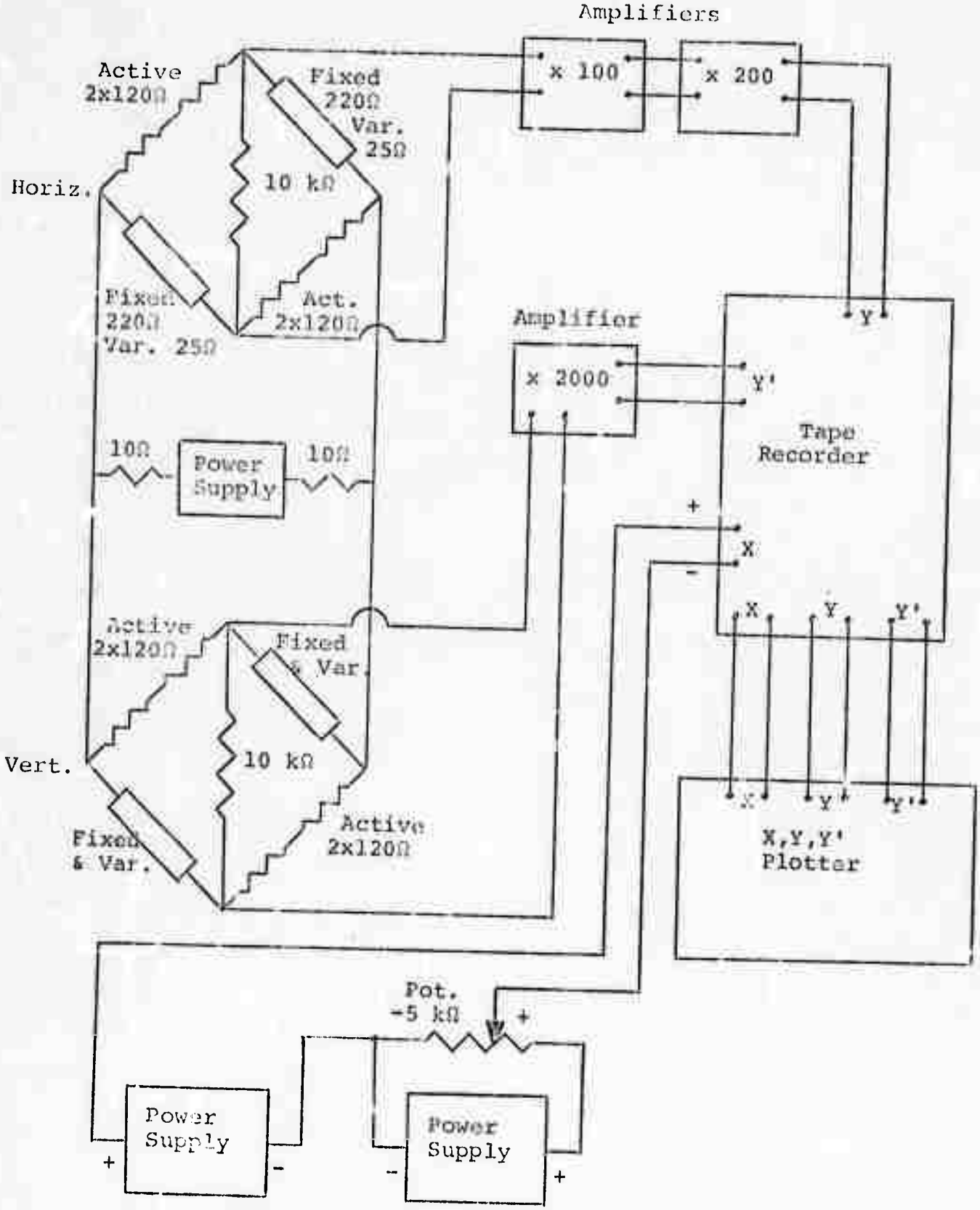

Fig. 2.3. Circuit for the Linear Cutter.

were not employed in these circuits. It was originally thought that since testing was done under laboratory conditions, and the time required per cut was less than one minute, temperature effects would be minimal. It was found on some occasions, however, that temperature compensation would have been an improvement. Because of the low output from the gages, they actually were sensitive to temperature changes and careful observation of the zero point had to be maintained before and after each cut. The sudden temperature changes were due to opening of a door from the laboratory straight to the winter weather outside. This effect was eliminated by careful checking of zeros and by choosing the moment for cutting.

The main problem in the electrical circuit was in the amplification of the vertical signal. This caused a delay of more than a month in the start of the tests. The Dana amplifiers, which were used in the horizontal circuit performed well and had excellent noise reflection levels. A new Honeywell amplifier (ACCUDATA 122) in the vertical circuit caused us trouble due to the noise pick up with high amplification. This problem was finally overcome when the design engineer of the amplifier made some changes in the amplifier to fit the noise problem in the laboratory. The amplifications were, in the final tests, 2000 in the vertical and 20,000 in the horizontal arm.

The movement of the linear cutter table was monitored with a 5 k ohm 10 turn potentiometer connected to balancing circuit. The output from the circuit was connected to one channel of the tape recorder.

Three channels were used in the tape recorder (Honeywell 8100): one for displacement, one for vertical force, and one for horizontal force. The tape recorder was calibrated to -2 volts to +2 volts peak to peak value. Hard copy records were made by playing the tape into an XYY' recorder. For the calibration of the output from the tape, calibration voltages were put at the beginning of each tape. The tape was then used to provide the input to the hybrid computer.

2.1.3 Sample Preparation

All the samples used from the Climax tunnel were in the form of 6 inch diameter cores. The samples from Nast and Lawrence tunnels were taken from blocks. The cores were sawed in half lengthwise and one half was used for cutting and the other half to prepare samples for the physical testing.

The core halves and the samples which were sawed from the blocks were mounted in a channel iron mold and surrounded with hydro-stone. After the hydro-stone had set at least twelve hours the surface of the samples were ground to the smoothness of ±.003 inch using a surface grinder. The smooth surface was necessary to assure reproducibility of results and to provide an accurate reference for volume measurements. After drying 48 hours at room temperature, the samples were clamped into a support frame on the table of the linear cutter and checked to insure a level of the surface. Testing could then be commenced.

2.1.4 Testing Method

After a sample was prepared and mounted on the machine, a testing procedure was established depending on the sample properties.

To eliminate "end" effects the first 1 1/2 inches and the last 1 to 2 inches of the cut were marked out and not included in the area and volume measurements. The samples were cut through from one end to the other.

Rather than a constant vertical force, a fixed penetration depth was set on the adjustable mobile table. The penetration depth was set when the cutter was free of the rock sample so that each force-displacement recording began with a zero vertical and horizontal force. The starting point of the table movement was set a sufficient distance ahead of the point of contact with the sample so that a zero load recording could be obtained on the tape for the setting of the zero in the hybrid computer.

The indexing was fixed to 0.30 in. in all tests, except in the last pass in the sample Climax #7. In hard rocks this indexing was too wide to cause breaking between the cuts on the first pass; it was, however, adequate for successive passes. The indexing was not taken as a variable in these experiments because it was understood that indexing was constant in the tunnel boring machine, and because the comparison is made between laboratory results and field data.

In this report a cut means one linear indentation along the surface of the sample. A pass is defined as the removal of one layer of rock resulting from several indexed cuts. The first pass consisted of eleven cuts on the 6" core samples which left 1.5 in. wide area on both sides which was not cut. At least as wide an area was left on the sides of the narrower samples when only seven or nine cuts were cut on the first pass. To minimize the effect of confinement on the results the outer two lines were dropped

after each volume measurement from the next pass. Because the last pass consisted in each case of at least three cuts, two consecutive passes had the same amount of cuts on some samples.

The set penetration for different passes could be maintained constant only for hard samples. It was necessary to vary the penetration for softer rock to compensate for the overbreak from the previous passes and to obtain a relatively equivalent force curve for all passes. The set penetration in hard rocks was usually 0.030 in. but was increased up to 0.120 in. in soft rock.

To determine the specific energy (the energy required to break a unit volume of rock), it was necessary to measure the volume of the removed material. It had been found earlier by Ross (1) that it was impossible to determine the volume of an individual cut and therefore a system was established to measure the volume of an entire pass. Ross compared different ways of measuring the volume (volume displacement of cuttings, sand filling, molding silicone rubber and cross section profile measurement), and concluded that sand filling was fast, as accurate as the others, and readily adaptable to the variations in the cuts.

Dry sand was used in this work for volume measurement. Sand of screen sizes -65/+150 mesh was used. The missing ends of the craters were replaced along the marked lines using ordinary putty. The top of the crater was planed with a rigid straight edge using the ground surface of the rock sample as a guide. The volume of sand was determined using a graduated cylinder. Because the volume of sand depends on the packing and because the sand-filled crater was almost unpacked, the volume of sand was taken to be the

value which was obtained when sand was poured into the cylinder without any more packing. Because errors may easily result in hasty volume measurement, much care was put into performing the determination consistently each time. To eliminate the occasional errors the measurements were repeated.

2.2 Calculation of the Laboratory Results

From the laboratory experimental results the following quantities were calculated:

1. Average horizontal and vertical forces
2. Actual penetration
3. Specific energy
4. Cutting coefficient
5. Cutting size distribution

By the analog-digital computer the following quantities were determined continuously along the length of a cut:

1. Cutting coefficient
2. Work done

2.2.1 Average Forces

To get the average horizontal and vertical forces, the areas under the marked portions of the recorded force versus displacement curves were determined using a planimeter. Dividing this area by the marked length we obtained the average forces for each cut. The average of the forces for each cut of the pass was taken as the average force of the pass.

2.2.2 Actual Penetration

The penetration, which was set on the machine, was not always

the same as the actual penetration realized in the cutting. The reason for the differences is that rock did not break exactly to the depth of the set penetration; in some cases there occurred much "overbreaking" and in some cases in hard rocks the actual penetration did not reach the set penetration.

To obtain the average actual penetration for a pass, the measured pass volume was divided by the plan area of the pass between the marks on the sample. This average penetration for a pass is denoted in the results as a calculated penetration.

A calculated penetration for a given sample is the average value of the calculated penetrations for each pass made on the sample.

2.2.3 Specific Energy

The energy for each cut was determined using the average horizontal force and the distance between the marks on the sample.* As will be discussed later, the energy was also determined by a hybrid (analog-digital) computer continuously along the length of the cut.

The energies for each cut used in the marked area were summed to give the energy used for each pass. Dividing the energy used in a pass by the measured volume of the same pass we obtained a value for energy per volume. This is called the specific energy.

---

*This is justified, because the displacement in the vertical direction is very small compared to the displacement in the horizontal direction. The energy from the vertical load is thus a very small part of the total energy.

The specific energy of a sample is the average value of the specific energies for each of the passes.

2.2.4 Cutting Coefficient

The cutting coefficient is defined as the ratio between the horizontal force (F_H) and the vertical force (F_V).

$$\mu = \frac{F_H}{F_V}$$

From the average values of the forces, the average cutting coefficient was determined for each cut. The cutting coefficient of a pass is the average value of the cutting coefficients of the cuts. The cutting coefficient of the sample is the average value of the cutting coefficients of the passes.

A continuous record of the variation of the cutting coefficient along the length of the sample was found using the hybrid computer.

2.2.5 Cutting Size Distribution

The cuttings from each pass were collected as carefully as possible for the determination of the size distribution. The sieving was performed using sieves from 4 mesh to 325 mesh. The results are, however, presented in a collected form.

The reliability of the sieving analysis cannot be too good as the amount of the material is small and there may be some losses of material, too. On the other hand, the results of various passes on one sample show so much consistency that some notes based on size distribution are justified.

A power frequency analysis program was also prepared for the hybrid computer and tried. The program works, but due to needed minor improvements in the program and the time limitations, we

could not perform the extensive calculations for this report. It is hoped that these calculations can be done later.

2.2.6 Calculations in the Hybrid Computer

The hybrid computer at the University of Colorado (C.U.), Boulder, Colorado, was used to determine the cutting coefficient and energy along a cut on the sample. Dr. Donald Dick from C.U. prepared the needed programs (Appendix B) and advised in the use of the computer.

The magnetic tape on which the cutting results were recorded was taken to Boulder where it was played back by the tape recorder and this output was fed into the analog part of the computer. The analog computer did the sampling of the data, usually taking 500 samples along the seven inch length of the sample. After sampling, the calculations were performed by the digital part of the computer. The output from the computer was then taken on an X-Y plotter.

After some difficulties at the beginning, especially with the tape recorders, the system began to work smoothly. DC calibration signals (zero, positive, and negative voltages) were recorded on each tape in the laboratory for calibration of the tape output.

The most time consuming part of the computer calculations was the plotting of the output. To complete one cut from the input of data to the end of the recording of the output took 5 to 10 minutes.

The output from the computer gave us continuous records of the cutting coefficient and total energy along the cut. The cutting coefficient was calculated for each sampling point and the output was given so that the displacement axis was scaled at a 1:1 ratio

with the actual displacement on the sample. The plots (Appendix A) show very large variations along the length of the cut.

The output of energy is given as a total energy at each point. The energy calculated for each sampling distance was added to the total energy of the preceding sampling point.

2.3 Tunnel Boring Data

Up to date tunnel boring data was received from the Nast tunnel in Colorado and to a certain extent from the Lawrence tunnel in Chicago. The promised data from the drift bored in the Climax mine arrived in February 1972 and was incomplete, so that it could not be used properly to calculate specific energies or cutting ccefficients. More data is being asked from the Smith Tool Co. Data from the White Pine mine was not available at the time of this report. The first blocks for laboratory testing arrived in the middle of February, but could not be immediately tested.

2.3.1 Nast Tunnel

The Nast tunnel is being bored using a Wirth machine, by Peter Kiewit and Sons, as part of the Fryingpan-Arkansas project for the United States Bureau of Reclamation. The bored tunnel has a diameter of 9'10" and will have a length of about 15,700 ft. The alignment and profile of the tunnel are given in Fig. 2.4 (2).

The machine is shown in Fig. 2.5, and the cutting head in Fig. 2.6. In the picture of the cutting head, four bits are absent. The cutters were tungsten carbide button bits. For a short distance disk type cutters were tried in porphyritic type granite, but they were removed as the boring rate was not improved. This was not

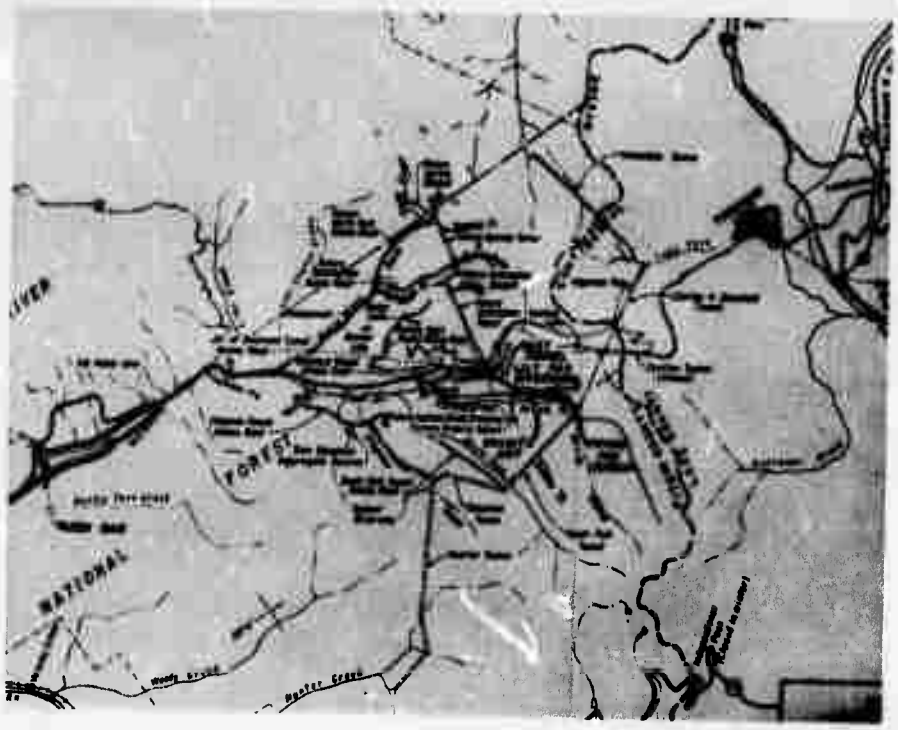

Fig. 2.4. Alignment and profile of the Nast tunnel.

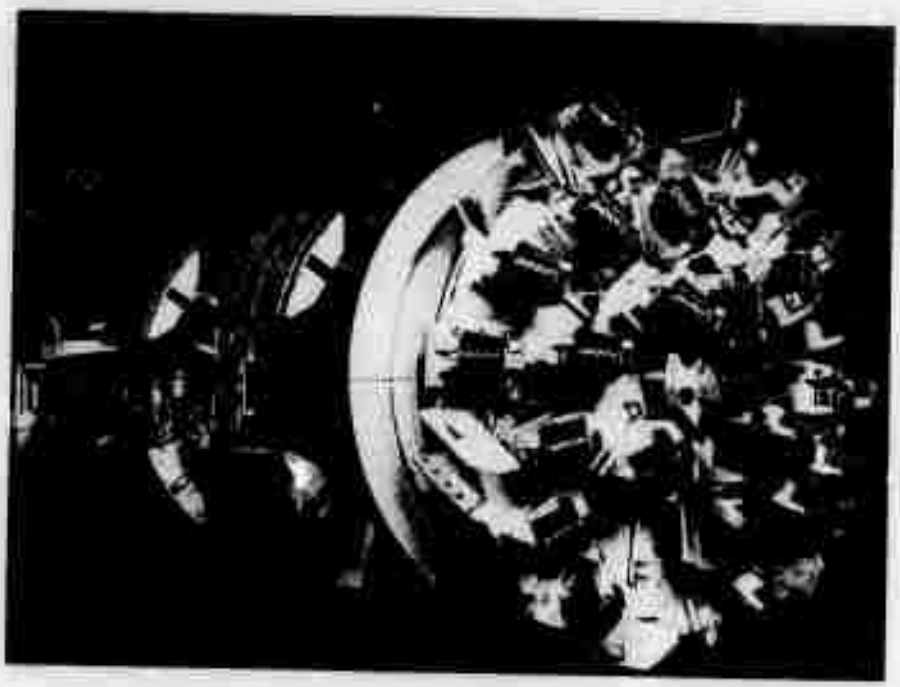

Fig. 2.5. The Wirth boring machine used in the Nast tunnel.

Fig. 2.6. The cutting head used in the Nast t. rel to the end of 1971.

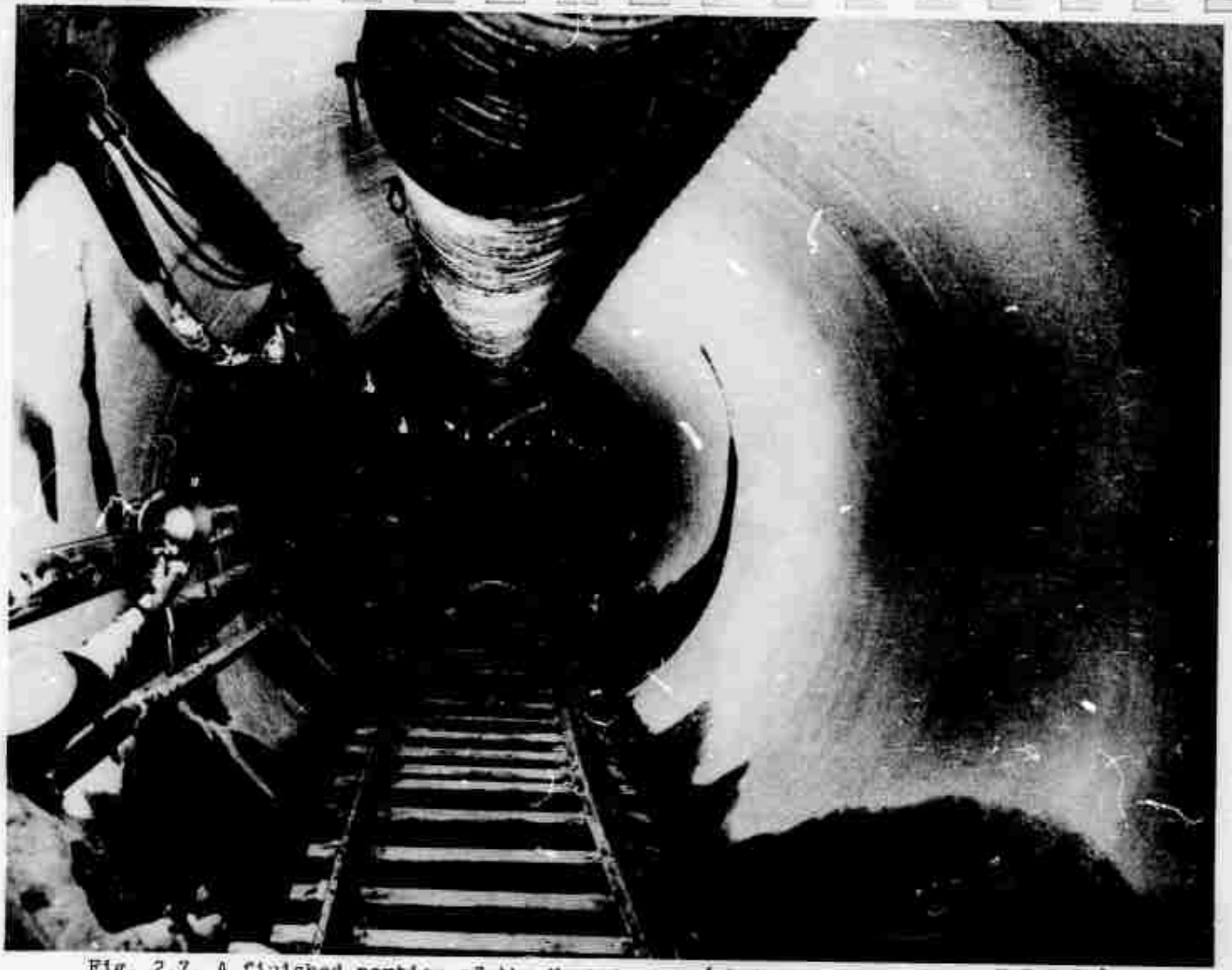

Fig. 2.7. A finished portion of the Nast tunnel (photo courtesy of the U.S.B.R.).

necessarily the fault of the cutters, since some other difficulties were present at the same time.

The head was changed at the end of 1971 to a flat face head. This is thought to cause less bending in the head and the cutter saddles and it is hoped in this way to eliminate some of the repairs.

A portion of the finished tunnel is shown in Fig. 2.7. The data collected from the Nast tunnel by the U.S.B.R. for each shift was provided to us for our use. It covers the tunnel bored from November 1970 to January 1972. The length of the tunnel was about 5,500 ft at the end of the period under consideration in this work.

2.3.2 Lawrence Tunnel

Data was received from the Chicago sewer tunnel bored using the Lawrence machine. The tunnel has the diameter of 13'8" and the final length of 12,451 ft. Our data is from one month, July 1971, and corresponds to the advancement of 1,150 ft.

The machine employs disk type cutters. The total number of cutters on the head is 27.

The received logs included time and advancement, thrust (psi), and the hydraulic pressure used to rotate the head. From this information, boring rate and specific energy could be calculated by knowing the relationship between rotary hydraulic pressure and the rotary power.

2.3.3 Calculation of Field Specific Energy

Hustrulid and Ross (3,1) have earlier derived the theory for the calculation of specific energy and cutting coefficient from the

field data. A summary of the theory is presented below.

The total input power to the rock can be given with the expression

$$P = 2\pi nt + T \times B_r' \qquad (2.1)$$

where

P = power (ft-lbs/min)

n = RPM, rotation speed of the head

t = torque (ft-lbs)

T = thrust (lbs)

B_r' = boring rate (ft/min)

The rate of rock volume removal is

$$V_T = \frac{\pi}{4} D^2 B_r' \qquad (2.2)$$

where

V_T = volume/time (ft^3/min)

D = tunnel bore diameter (ft)

The energy/volume or specific energy is the total input to the rock divided by the volume of the removed rock.

$$E_V' = \frac{P}{V_T} = \frac{2\pi nt + T\ B_r'}{\frac{\pi}{4} D^2 \times B_r'} \qquad (2.3)$$

In this expression E_V' has the units ft-lbs/ft^3.

The boring rate and the specific energy are normally given in ft/hr and the specific energy in in.-lbs/$in.^3$, respectively. The expression 2.3 can be modified to the following form

$$E_V = \frac{2\pi nt + T \frac{B_r}{60}}{0.6\pi D^2 B_r} \qquad (2.4)$$

where

E_V = specific energy (in.-lbs/in.^{3})

B_r = boring rate (ft/hr)

Because the rotary power term ($2\pi nt$) is usually much larger than that due to the thrust ($TB_r/60$), E_V can be approximated by

$$E_V = \frac{2\pi nt}{0.6\pi D^2 B_r} \tag{2.5}$$

In many cases the rotary power is given in terms of horsepower and E_V can be expressed by

$$E_V = \frac{55{,}000\ hp}{\pi D^2 B_r} \tag{2.6}$$

2.3.4 Calculation of Field Cutting Coefficient

There is evidence (4) that in the cutting of rock, the relationship between the cutting (t_i) and normal (N_i) forces can be given

$$t_i = \mu N_i \tag{2.7}$$

where

t_i = tangential (cutting) force of each cutter

N_i = thrust force per cutter

μ = coefficient of cutting friction.

Assuming that the cutter head is rigid, then the thrust force is the same for all cutters

$N_i = N$ (Constant).

We then have

$T = nN$

where

T = total thrust

n = number of cutters.

The tangential force (t_n) can be expressed from equation (2.7)

$$t_i = \mu \frac{T}{n} . \tag{2.8}$$

The total applied cutting head torque then becomes

$$t = \mu \frac{T}{n} \sum_{i=1}^{n} r_i \tag{2.9}$$

where

t = total torque

r_i = radius arm of each cutter.

Assuming that the n cutters are evenly distributed,

$$\frac{1}{n} \sum_{i=1}^{n} r_i = \frac{R}{2}$$

where

R = radius of tunnel bore.

The expression for the total torque becomes

$$t = \mu T \frac{R}{2} \tag{2.10}$$

and cutting coefficient (μ) becomes

$$\mu = \frac{2}{R} \frac{t}{T} \tag{2.11}$$

3. DISCUSSION OF RESULTS

3.1 Laboratory Cutting

The summary of the results of the laboratory samples, which represented different types of rock, are given in Table 3.1. Sometimes the first pass did not break material enough so that volume measurements could be made. In these cases the figures given for the second pass represent the first and second passes together. The energy used in the first pass varied between 12% and 17% of the combined energy of the first and second passes.

The results in figures 3.1-3.6 are given as a function of the calculated penetration. Calculated penetration is considered to be the most relevant measure in the laboratory to the boring rate in the field.

Each point in the figures represents one sample. In Fig. 3.6 where four samples are chosen for a more detailed representation, each point represents one pass on the sample.

3.1.1 Specific Energy

Fig. 3.1 shows that there exists an inverse relationship between calculated penetration and specific energy when cutting in different rock types. The inverse relationship does not necessarily represent the relationship in an individual sample. On the contrary, there is some slight evidence of an opposite relationship. This is not, however, well established in these experiments and can be partly the result of the bottom conditions of the cuts.

The cutting method used (cutter, constant indexing) in most cases limits the sizes of the particles produced. Some evidence of this may be found in the size distribution of the cuttings (Table 3.2), where only the Lawrence #1 sample clearly exhibits coarser cuttings than the others. The first pass usually gives coarser cuttings than the later passes, which is due to the unfractured material under the cutter. On each sample, the material right under the edge of the cutter was pulverized and packed. The cutting method may thus effectively limit the value of specific energy obtained.

The average results of the different samples are the most representative for comparing with field boring in different types of rock. It is worth noting that the indexing was kept constant and no attempt was made to find the optimum indexing-penetration ratio for different samples.

3.1.2 Cutting Coefficient

The cutting coefficient shows a direct relationship with calculated penetration (Fig. 3.2). This means that the deeper the cut, the greater is the cutting coefficient. The individual samples do not, in this case, differ remarkably from the trend of the average values of different samples.

In our tests we could increase the forces only by setting a deeper penetration in the cutting machine. The results show that increasing the penetration affects the horizontal force relatively more than the vertical force.

Table 3.1. Linear Cutter Testing Data.

Pass	Average Horiz. Force (lbs)	Average Vertical Force (lbs)	Cutting Coefficient	Penetration Set (in x 10^{-3})	Penetration Calculated (in x 10^{-3})	Specific Energy ($\frac{\text{in-lbs}}{\text{in}^3}$)
			Nast #2			
1	35	2430	.014	30		
2	236	3420	.070	30	42	21700
3	119	2510	.048	30	21	18700
4	202	3220	.063	40	38	17900
5	176	2710	.065	40	42	13800
			Lawrence #1			
1	111	3050	.037	40	46	8100
2	127	2110	.060	60	52	8100
3	233	3070	.076	70	75	10400
4	245	3840	.064	70	83	9900
			Climax #1			
1	26	2290	.011	30		
2	197	3310	.060	30	53	14100
3	78	1370	.057	30	35	7500
4	162	2300	.069	50	53	10200
5	118	1710	.068	40	37	10500
6	137	2000	.068	40	41	10900
			Climax #2			
1	40	2970	.014	35		
2	256	3870	.068	30	59	16800
3	131	2310	.057	40	42	10200
4	196	2800	.070	50	41	16000
5	204	3050	.067	50	52	13000
			Climax #7			
1	80	1160	.070	40	70	3800
2	42	566	.074	60	37	3800
3	120	1370	.088	90	108	3700
4*	168	1870	.092	120	65	5200
			Climax #13			
1	76	1100	.072	50	65	3900
2	57	794	.073	60	35	5400
3	120	1340	.090	70	77	5200
4	141	1470	.097	90	108	4400

*indexing .60 in.

Table 3.1. (Continued)

Pass	Average Horiz. Force (lbs)	Average Vertical Force (lbs)	Cutting Coefficient	Penetration Set (in x 10^{-3})	Penetration Calculated (in x 10^{-3})	Specific Energy ($\frac{\text{in-lbs}}{\text{in}^3}$)
			Climax #15			
1	116	2260	.052	50	41	9400
2	185	2110	.088	60	72	8600
3	148	1750	.084	70	82	6000
4	201	2140	.094	90	103	6500
5	249	2630	.095	110	81	10200
			Climax #18			
1	33	2470	.014	35		
2	162	4140	.042	30	53	12400
3	137	2130	.065	30	29	15800
4	120	2250	.053	30	28	14000
5	133	2220	.060	30	29	15000

Table 3.2. Particle Size Distribution of the Cuttings (%).

Nast #2

	P 1+2	P 3	P 4	P 5
+14	44.9	45.7	45.1	45.0
-14→+150	37.6	37.2	38.9	40.1
-150	17.5	17.1	15.9	14.9

Lawrence #1

	P 1	P 2	P 3	P 4
+14	85.1	69.4	69.0	64.7
-14→+150	10.7	21.2	20.8	24.9
-150	4.1	9.4	10.2	10.5

CX #2

	P 1+2	P 3	P 4	P 5
+14	53.3	48.1	46.6	39.2
-14→+150	33.6	37.7	38.7	43.5
-150	13.1	14.1	14.8	17.3

CX #7

	P 1	P 2	P 3	P 4
+14	64.7	51.1	49.3	53.6
-14→+150	27.5	36.6	37.4	34.8
-150	7.8	12.3	13.3	11.5

CX #15

	P 1	P 2	P 3	P 4	P 5
+14	73.0	45.3	48.4	48.5	40.6
-14→+150	22.6	34.4	41.6	41.7	47.7
-150	4.3	9.4	10.1	9.9	11.8

CX #18

	P 1+2	P 3	P 4	P 5
+14	70.4	59.3	56.6	53.6
-14→+150	19.5	26.5	28.7	29.1
-150	10.0	14.1	14.8	17.4

CX #1

	P 1+2	P 3	P 4	P 5	P 6
+14	67.3	57.8	59.1	57.3	57.1
-14→+150	26.9	35.2	34.2	35.2	36.7
-150	5.9	7.0	6.8	7.6	6.2

CX #13

	P 1	P 2	P 3	P 4
+14	66.3	49.0	54.7	53.2
-14→+150	26.9	38.3	34.1	35.8
-150	6.9	12.8	11.2	11.0

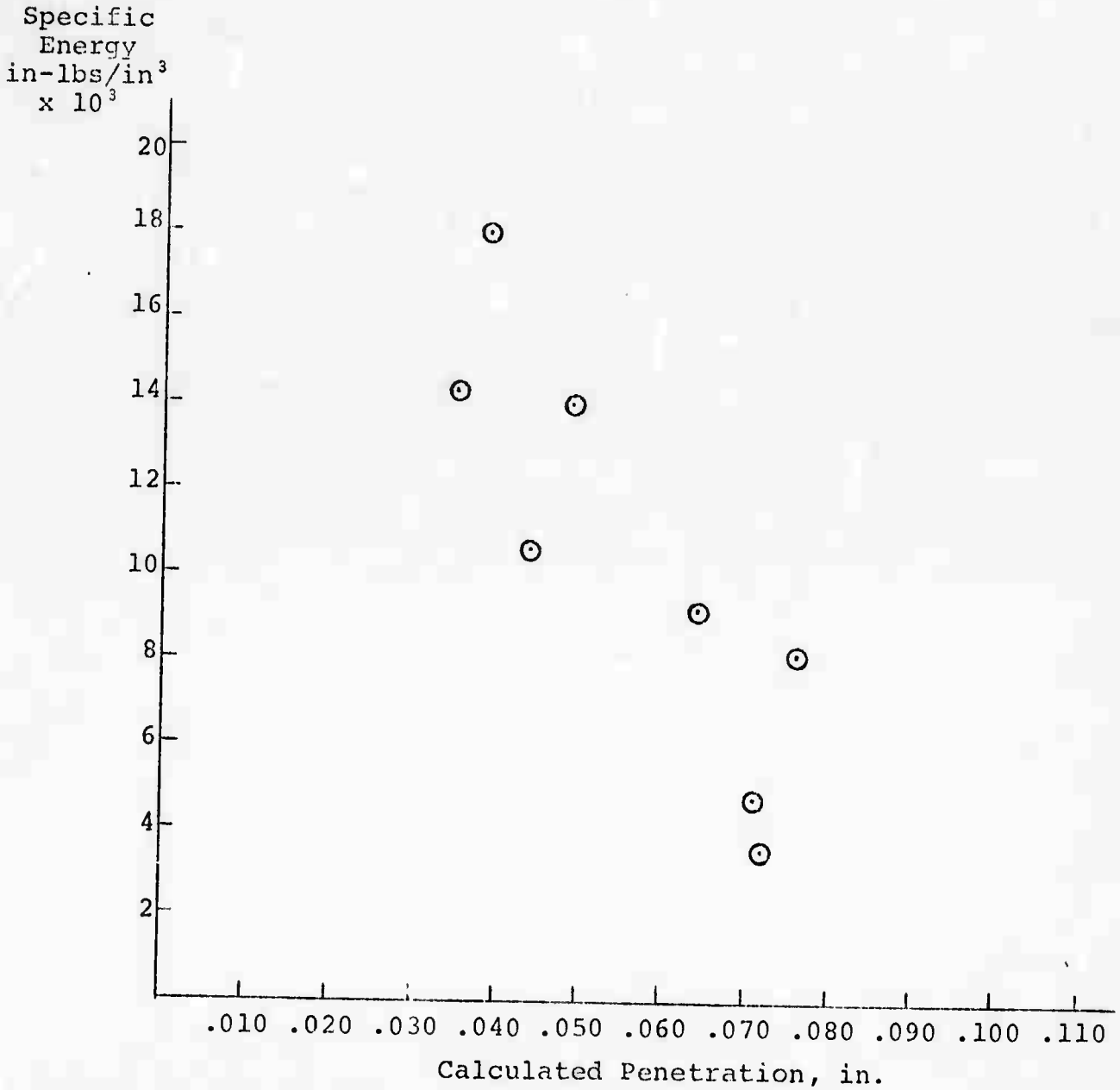

Fig. 3.1. Relationship between specific energy and penetration for laboratory samples.

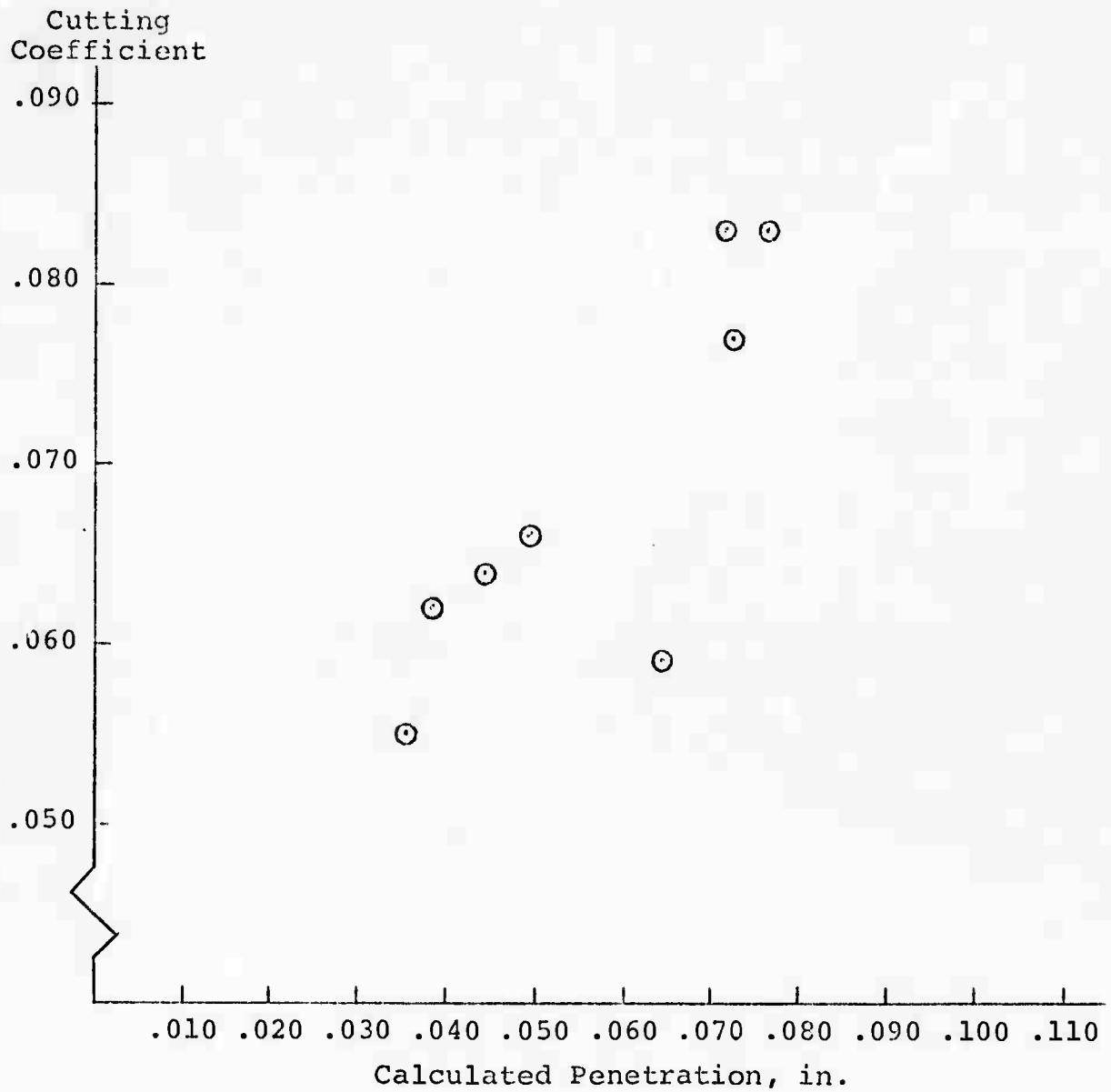

Fig. 3.2. Relationship between cutting coefficient and penetration for laboratory samples.

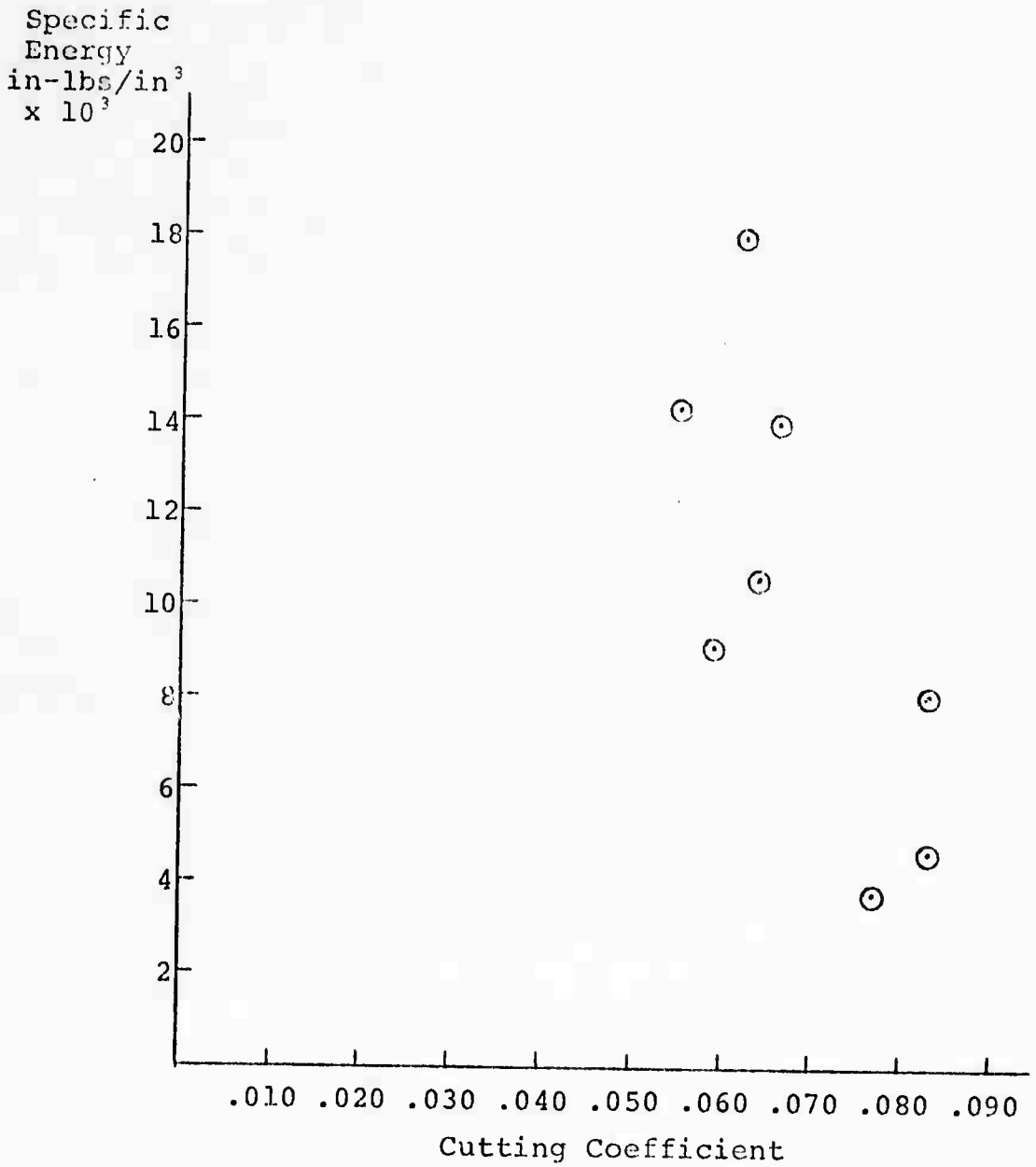

Fig. 3.3. Relationship between specific energy and cutting coefficient for laboratory samples.

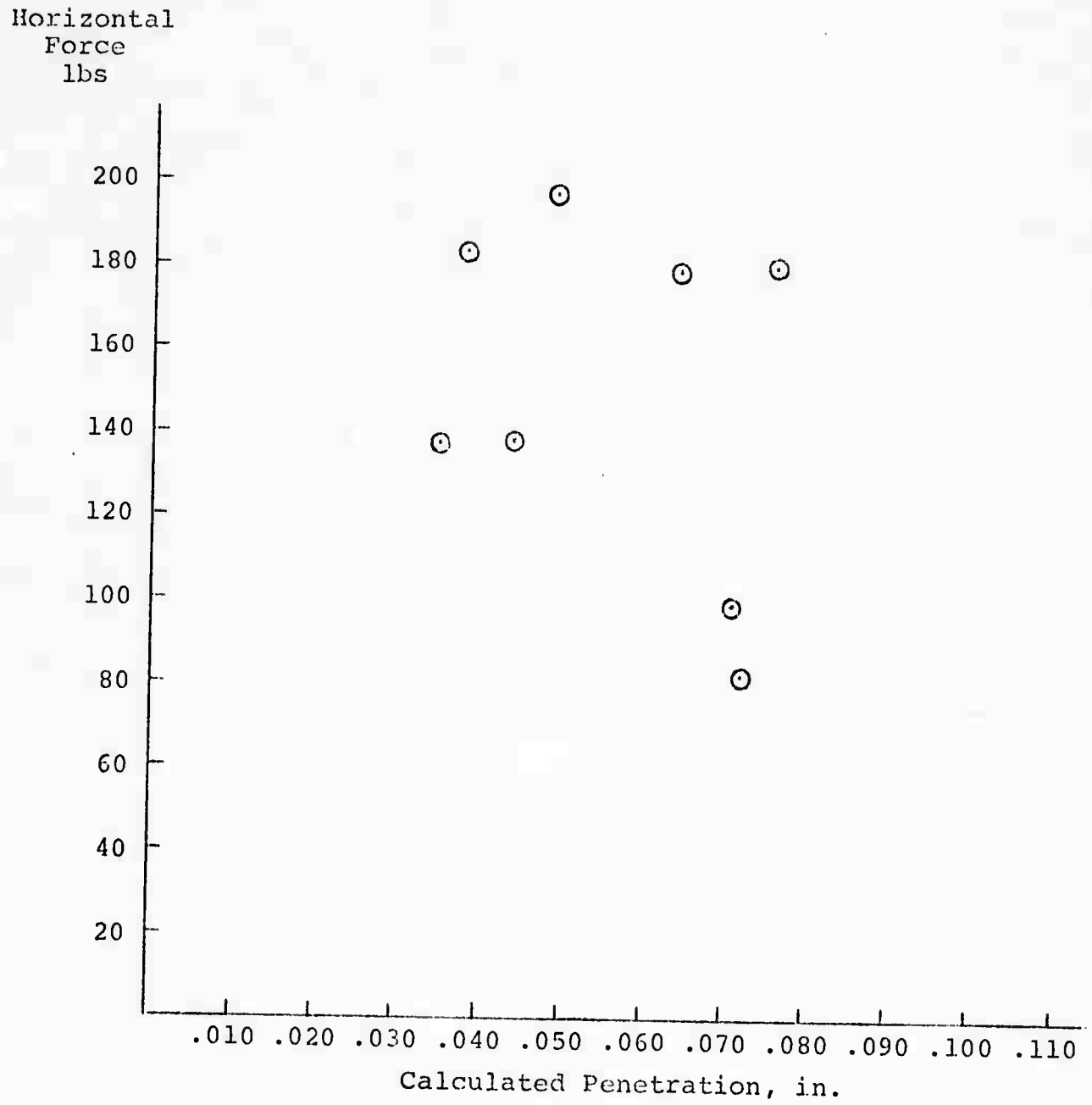

Fig. 3.4. Relationship between horizontal force and penetration for laboratory samples.

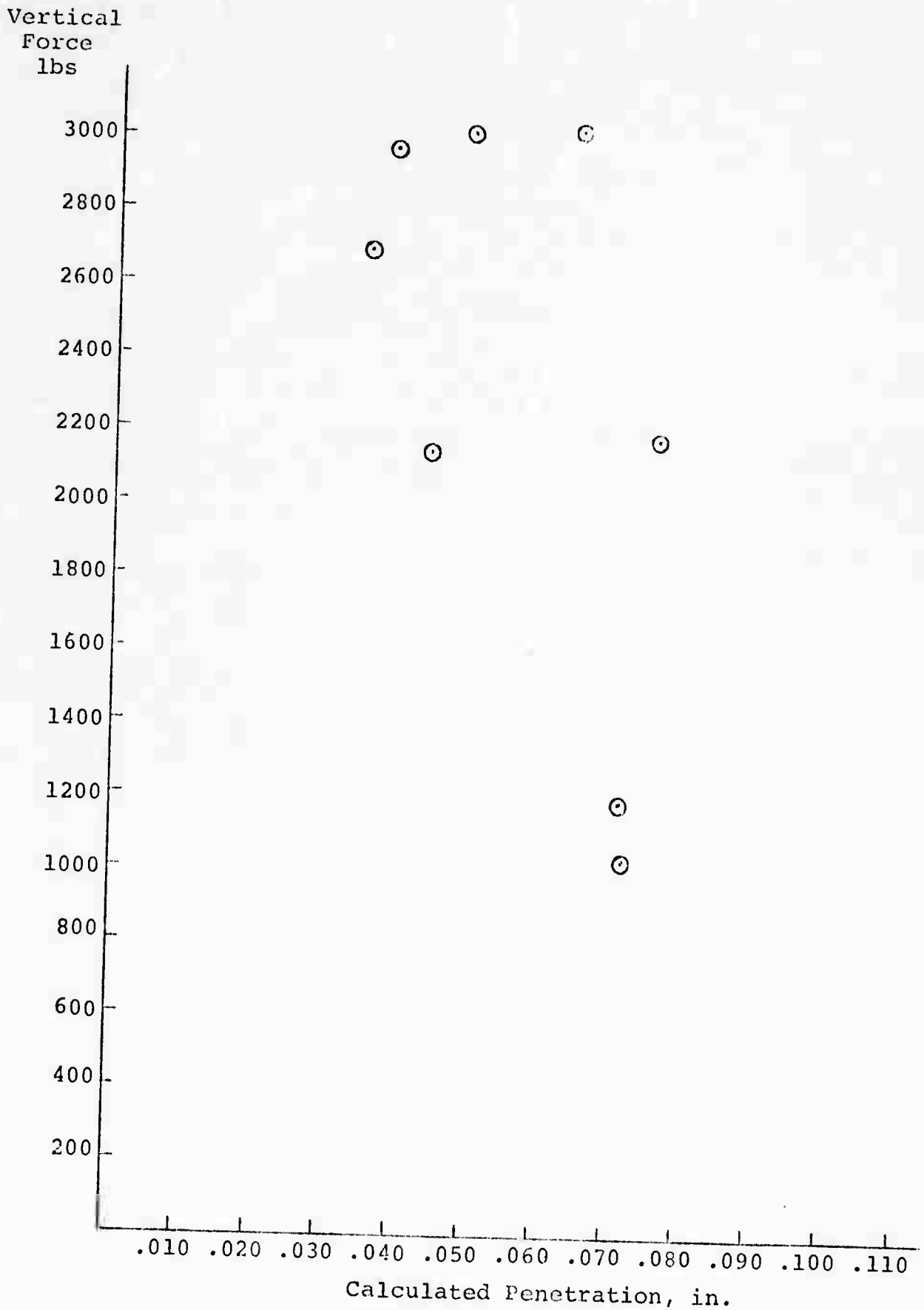

Fig. 3.5. Relationship between vertical force and penetration for laboratory samples.

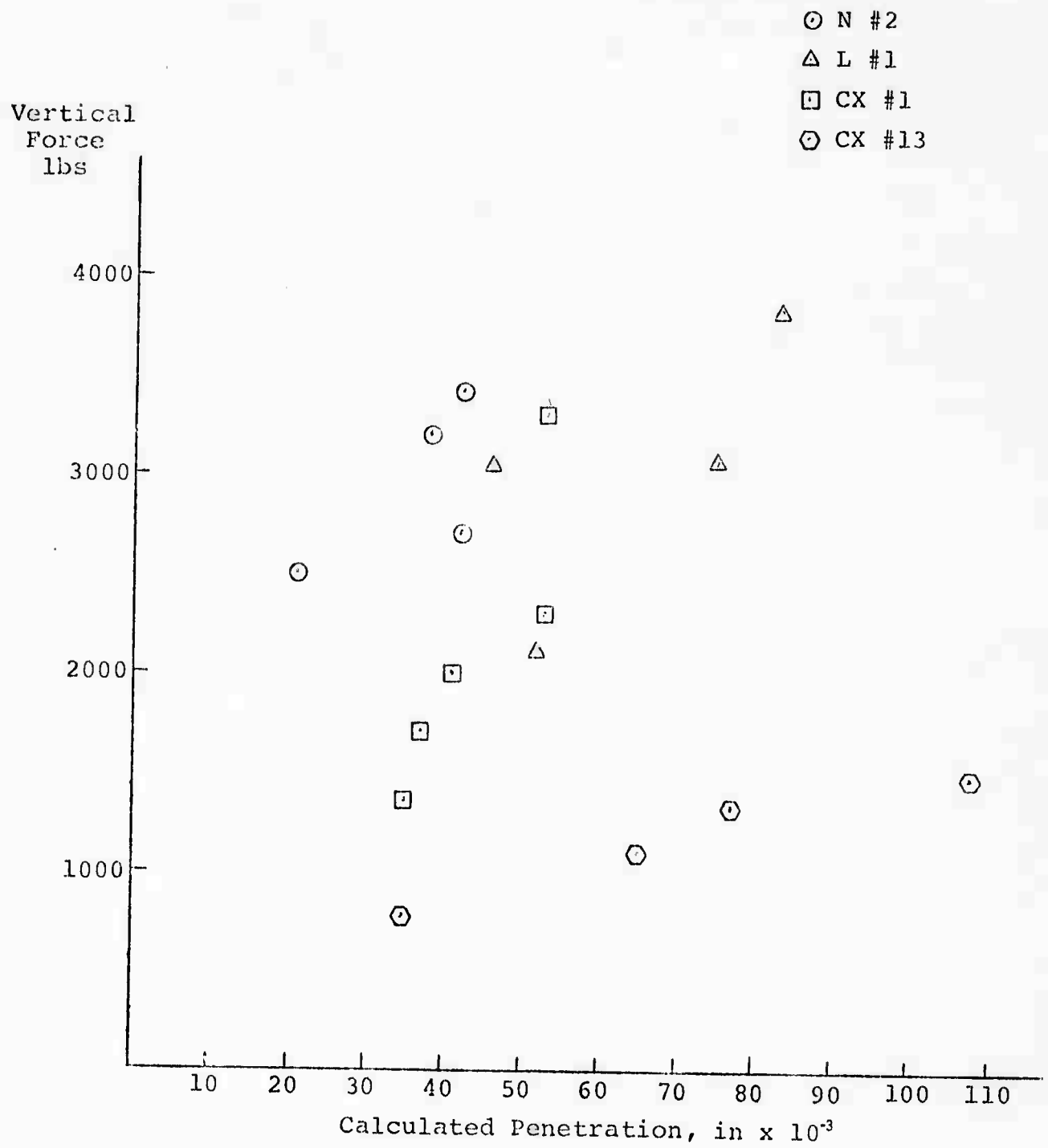

Fig. 3.6. Relationship between vertical force and penetration for the different passes on some laboratory samples.

3.1.3 Specific Energy - Cutting Coefficient

The representation of specific energy as a function of cutting coefficient (Fig. 3.3) shows, as expected, an inverse relationship. This inverse relationship may not represent the situation in one sample. This exception from the average behavior of different samples is due to the same possible reasons mentioned in the discussion of the specific energy earlier.

3.1.4 Horizontal Force

The horizontal force (Fig. 3.4) does not show any clear general relationship with the penetration. In no case the horizontal force alone is any good measure for penetration of the cutter in a rock. On the other hand, horizontal force has quite a dominating role in the cutting coefficient (this is also seen in Appendix A), and the cutting coefficient was shown to have clear inverse relationship with penetration.

The horizontal force increases relatively more with the depth of cut than the vertical force. The Japanese (5,6,7) have reported the same type of relationship for cuts in which no interaction occurred between the cuts.

3.1.5 Vertical Forces

The vertical force shows some inverse relationship with calculated penetration (Fig. 3.5). This inverse relationship occurs with the average values of different samples. What this actually tells us is that in the rocks which are easier to cut we get a certain penetration with a lower vertical force than in a rock which is hard to cut.

Earlier work (8,9,10) has shown that the vertical force and penetration should have a direct linear relationship. If we plot the values obtained for different passes on one sample, we get a relationship between vertical force and penetration, which is more or less direct for one sample (Fig. 3.6). The rise for harder rocks is steeper than for softer rocks. Let us note again that no bottoming occurred with our kerf type cutter.

3.2 Laboratory Cutting Results Calculated by the Hybrid Computer

The results from some representative cuts for each sample are shown in Appendix A. The cutting coefficient (μ) and total energy (W) along the cut are given as a function of the displacement along the sample. The curves are copies of the actual recorded computer output. Together with the cutting coefficient and energy curves are shown the corresponding vertical (F_V) and horizontal (F_H) force curves. In the figures are included the values of set penetration, indexing, average vertical force, average horizontal force, and average cutting coefficient for the cut.

The sample from the Nast tunnel (N #2) was rather homogeneous and hard. The results show a variation in cutting coefficient which is typical for hard rock where chipping occurs. In pass 3, cut 4 we can see that the horizontal force goes negative (tension). This is an inherent behavior of the cutting system. When the force on the measuring arms is removed suddenly, there is some rebound effect in the measuring arms due to the slight softness in the system. This rebound effect is measured by the strain gages and recorded as tension. Although this tension does not

reflect true behavior of the sample, it is of such a small magnitude that it does not produce critical errors in the final results.

The work done increases almost linearly across sample N #2. The changes in cutting coefficient can be seen on the energy curve, but they are of a minor nature. This seems to be the general behavior in homogeneous samples.

The sample from the Lawrence tunnel in Chicago (L #1) was homogeneous and very fine-grained. The very typical behavior when cutting this sample was that large chips were formed. This can be seen also from the sieving analysis (Table 3.2). On some recordings the formation of large chips can be seen clearly. In pass 4, cut 4 the major cutting coefficient lows and highs follow each other almost in sequence.

The energy increases monotoniously and also here the major changes in the cutting coefficient can only slightly be seen in the energy curve.

In pass 4, cut 6 the decrease in the horizontal force is seen at the end of the energy curve. The cutting coefficient does not show this as the vertical force decreases at the same time. The shape of the cutting coefficient curve, however, closely follows the horizontal force curve.

Only the cutting coefficient curves are given for sample Climax #1. In pass 1, cut 1 we can see a typical curve for the first pass on the ground surface of hard rocks when no chipping occurs. The curves are rather smooth and the horizontal force is low. The cutting coefficient curve is low and smooth. The kick

in the middle of the cutting coefficient curve is due to a crack which went across the sample. The effect of this crack cannot be seen so clearly on the later passes as the cutting coefficient varies also due to chipping along the cut.

In passes 3 and 5 the rebound of the horizontal arms can be seen because the penetration was not enough to reach the bottom of the chips of the earlier pass.

The first and often also the second pass are not very representative of the sample. The consistency of the results from pass to pass depends on many factors and is demonstrated in the results of the sample Climax #1. The basic shape of the cutting coefficient curve is rather consistent from the second to the sixth pass. The changes in the magnitude of the cutting coefficient, however, are not consistent.

On the curves of sample Climax #2 the effect of the bottom of the cut can be seen. Pass 4, cut 3 shows the effect of deep chipping in the earlier pass. The two negative rebounds are due to the holes created by the cut on the earlier pass. Also the vertical force drops and there is practically no penetration at the bottom of the hole.

The sharp peaks of the earlier cutting coefficient curves are reduced since the scale has been changed. The linearity of the energy curve is a measure of the homogeneity of the sample. On a homogeneous sample the cutting coefficient curve may show large and fast variations due to the chipping. This has, however, minor effect on the total energy curve, which increases rather linearly.

Climax #7 was a very soft sample to cut. It had veins of harder material in the soft matrix. This is the main cause of the changes in the cutting coefficient. Deep cuts could be taken in this sample and as we can see from the energy curve, a relatively large amount of work could be done on the rock. The volume of the removed rock was also large and the specific energy value was thus low. The linear cutter penetrated this sample easily and increasing the set penetration had the result of producing more cutting than chipping.

In sample Climax #13 a small layer of mica encountered during the second pass resulted in the removal of material much below the set penetration over a limited area on the sample. The effect of this hole can be seen on the curves which represent pass 4.

The specific energy value of this sample is rather low. The changes in cutting coefficient are, however, noticeable even if the effect of the major hole is left out. This sample was easy to cut, but the force curves show that variable forces experienced by the cutter.

Climax #15 was very inhomogeneous with soft and hard portions. This can be seen in both the forces and cutting coefficient curves. The low force and energy values at the beginning are obtained in soft material. When the cutter hits hard veins the forces increase and an even more remarkable change is seen in the cutting coefficient. The reason why the changes in the cutting coefficient are so large and sudden is that when the cutter hits hard rock after cutting in softer rock the horizontal force increases slightly before the vertical force. This happens also when the

cutter hits the edge of a hole.

The cutting coefficient curve does not necessarily reveal what kind of rock we are cutting. The energy curve indicates the quality of the rock, i.e., if it is soft or hard to cut. If we examine pass 2, cut 6 of CX #15, we see that there has first been soft material and then harder and more variable material is cut. The first pass has removed material in front of a hard vein so that there is a hole and during the second pass this is experienced in the horizontal force as a rebound effect. Just after this the cutter hits the hard vein and the cutting coefficient jumps up. This vein is, however, narrow and followed by an area of rather soft rock with harder inclusions. The energy curve is still rather flat. Then the cutter enters a harder portion of the sample; energy rises, but the cutting coefficient becomes lower. From the cutting coefficient alone it is hard to tell what kind of rock is cut, because the curve could represent the same kind of material which was cut at the beginning. Near the end of the energy curve we can see the effect of cutting a softer portion followed at the end by harder rock. This explanation was substantiated by examining the surface of the sample.

The sample Climax #18 was hard to cut. This is shown by the high specific energy values, low cutting coefficients, and low penetration. The low average cutting coefficient does not, however, correspond to the changes along a cut. The cutting coefficient varies from actually zero to the maximum of about 1.4. The forces are high and the changes in the cutting coefficient correspond to large force differences.

The cutting coefficient curves in Appendix A show that for each rock type the cutting coefficient changes remarkably along the cut. The only exception to this is for the first cut on a hard ground rock surface when no chipping occurs. This has, however, no resemblance to a real cutting situation. The changes in vertical and horizontal forces and cutting coefficients along the cut are due to the changes in the rock and to the chipping action.

The shape of the cutting coefficient curve is dominated by the shape of the horizontal force curve. Horizontal force reacts more sensitively to the changes under the cutter than vertical force.

The average cutting coefficient gives only partial information of the rock. The cutting coefficient alone does not give full information of the sample, but together with the total energy curve rather much can be told about the type of rock which is cut.

3.3 Tunnel Boring Results

3.3.1 Nast Tunnel

Boring rate, thrust, torque, cutting coefficient, and specific energy were calculated for each shift from the data provided from the data provided from the Nast tunnel (11). These results are given in the plots in Appendix C along the length of the tunnel. The dots are the values for each shift and the crosses are weighted average values for each 100 ft advance. Thrust and torque are expressed only as weighted averages. There existed an error in the station marks in the tunnel around the station +467 -00. This error is taken into account in the presentation of the results.

The rock along the tunnel was classified in the geologic logs as excellent, good, fair, or poor and as qualities between these. The classification is based mainly on the structure of rock, and has consistency, although it is mainly qualitative in nature.

The calculated data was grouped according to the rock qualities in seven different groups. The results are given in Table 3.3 and Figs. 3.7 - 3.11. Rock quality grouping gives perhaps the best idea about the factors affecting rock boreability in the tunnel.

The general trend is that the boring rate increases when going from excellent to poor rock with exception that between fair and poor rocks. The specific energy decreases with increasing boring rate. The cutting coefficient tends to increase when going from excellent to poor rock; more exceptions than in the boring rate and specific energy occur though. Thrust and torque do not show any clear tendency in the results in Table 3.3, though thrust has been higher in excellent and excellent-good rocks than in the others.

The other quantities are given as a function of boring rate in Figs. 3.7 - 3.10. Figure 3.11 gives the relationship between specific energy and cutting coefficient. We had only one laboratory sample from the Nast tunnel, therefore we have to compare these field boring results to the average behavior of all laboratory samples.

Specific Energy

As expected, the specific energy is observed to vary inversely with the boring rate. Laboratory results with different samples

Table 3.3. Boring Data from Nast Tunnel

Rock Quality	Boring Rate ft/hr	Specific Energy in-lbs/in^3	Cutting Coefficient	Thrust lbs x 10^3	Torque ft-lbs x 10^3
Excellent	2.31	16600	.088	522	112
Excellent Good	2.67	15200	.086	518	109
Good	2.88	12800	.095	461	104
Good Fair	3.06	12300	.092	500	109
Fair	3.66	8600	.105	401	102
Fair Poor	3.22	10200	.100	463	111
Poor	4.21	8800	.112	423	114

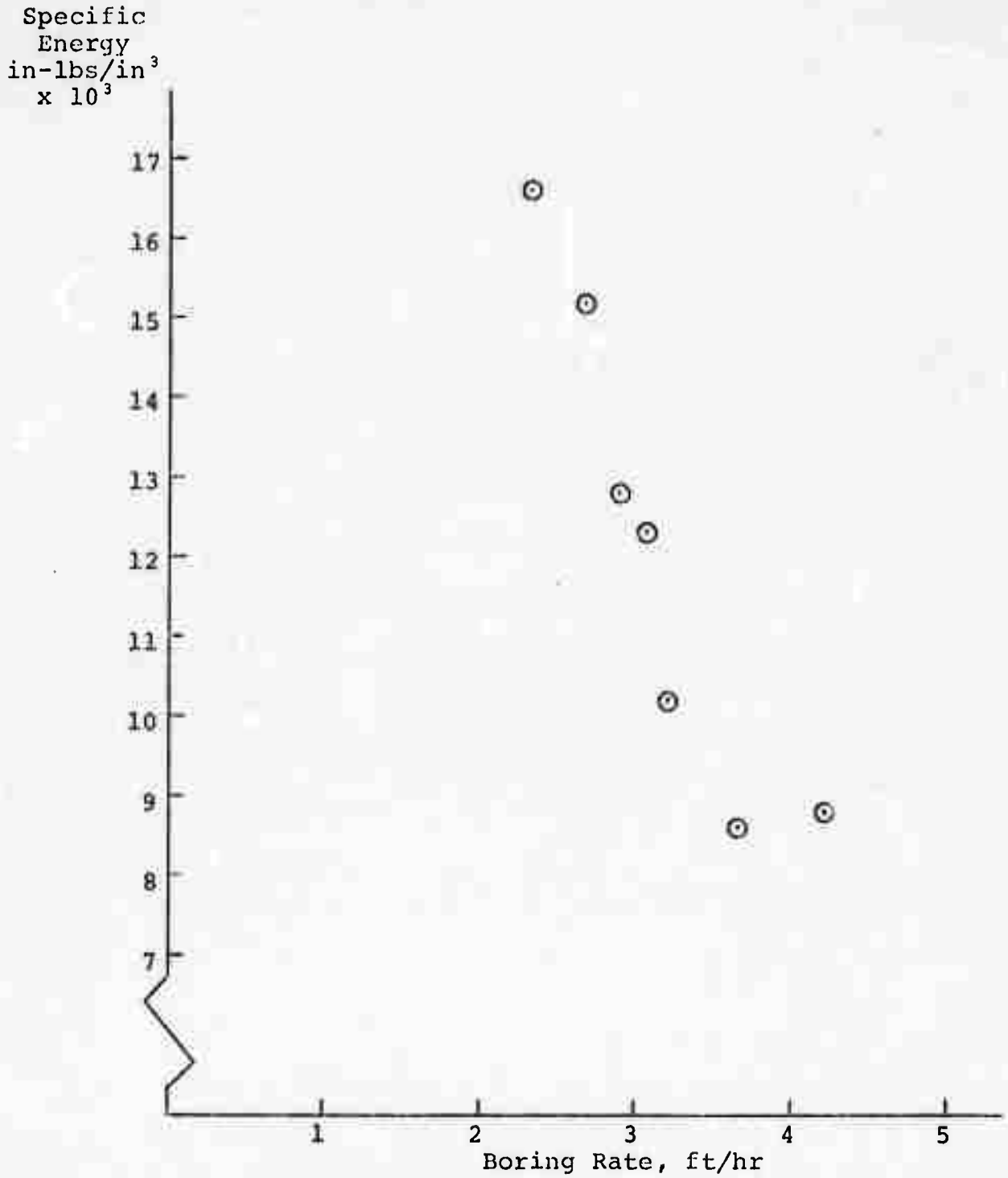

Fig. 3.7. Relationship between specific energy and boring rate for the Nast tunnel data. Points represent the average values of the seven groups of geological classification.

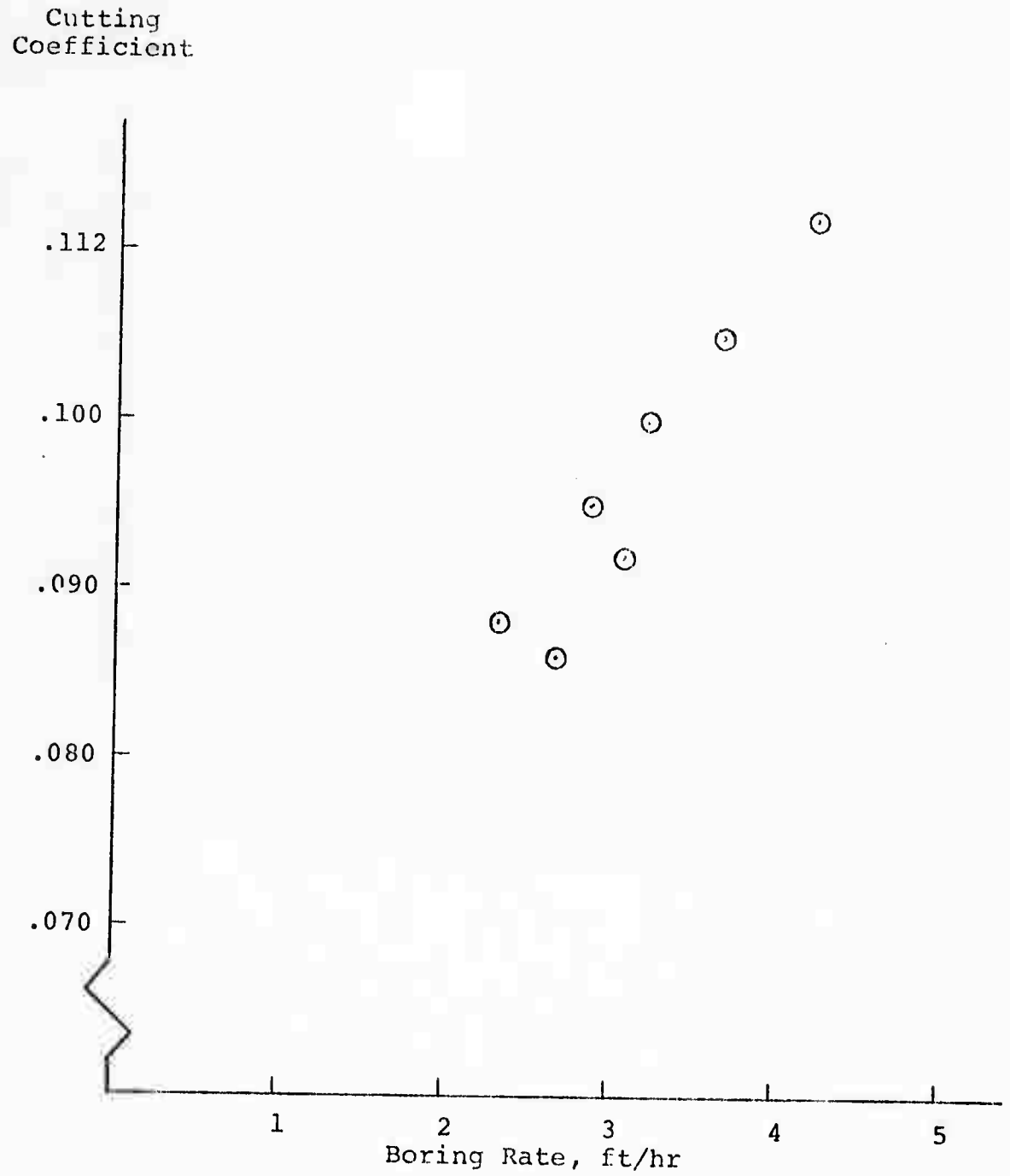

Fig. 3.8. Relationship between cutting coefficient and boring rate for the Nast tunnel data. Points represent the average values of the seven groups of geological classification.

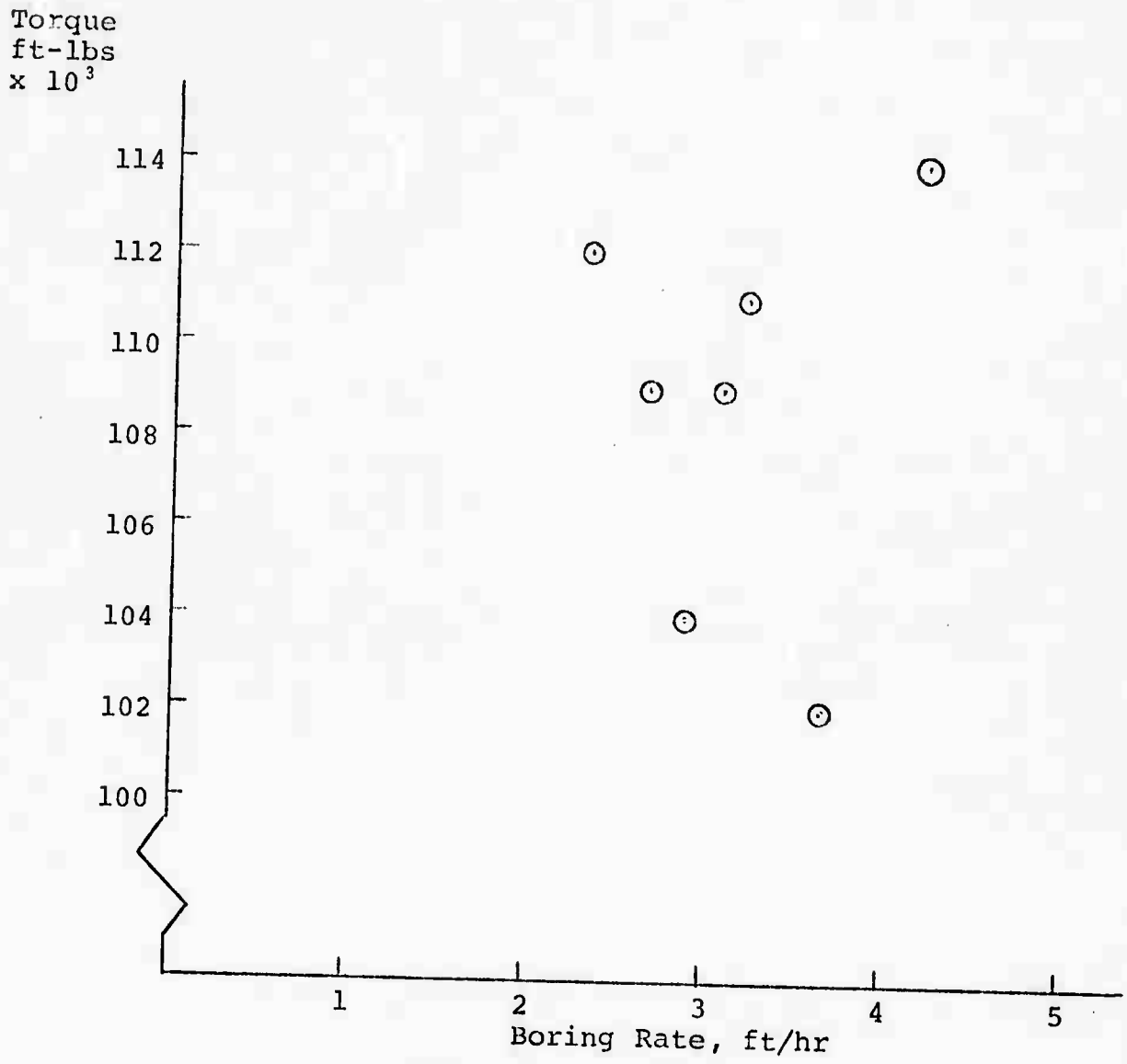

Fig. 3.9. Relationship between torque and boring rate for the Nast tunnel data. Points represent the average values of the seven groups of geological classification.

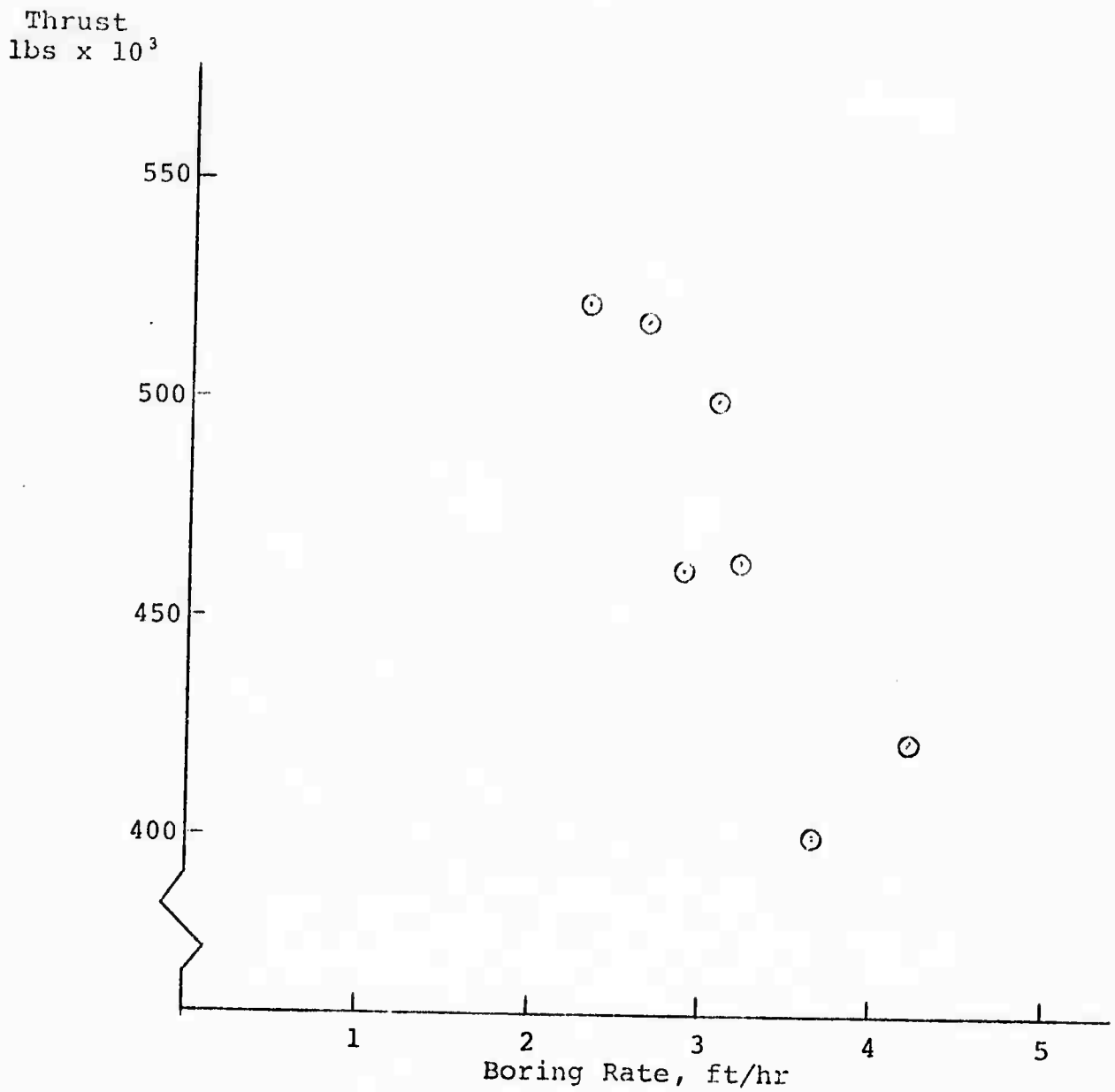

Fig. 3.10. Relationship between thrust and boring rate for the Nast tunnel data. Points represent the average values of the seven groups of geological classification.

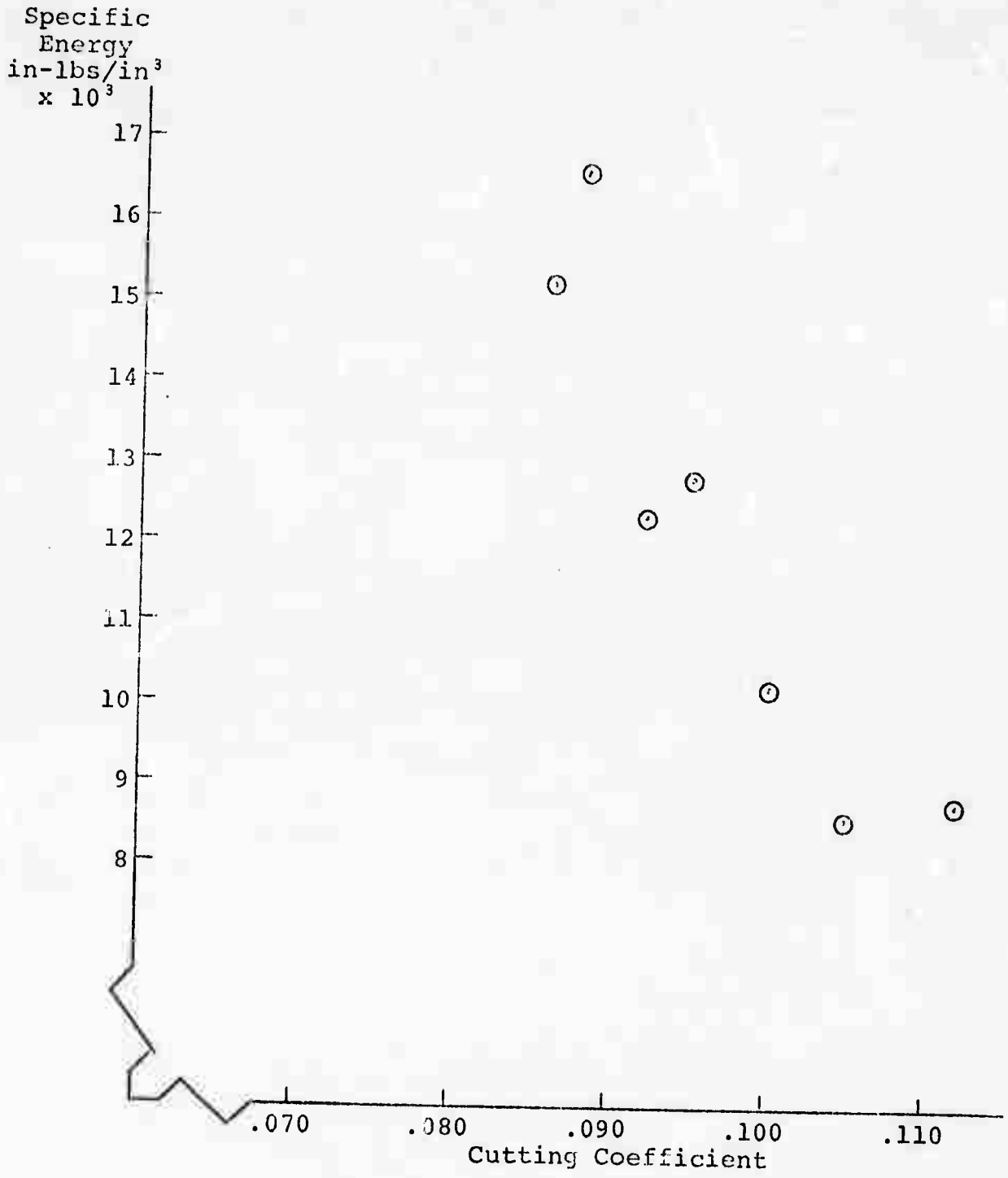

Fig. 3.11. Relationship between specific energy and cutting coefficient for the Nast tunnel data. Points represent the average values of the seven groups of geological classification.

(Fig. 3.1) showed the same type of relationship between specific energy and calculated penetration. In both cases the higher boring rates or deeper penetrations and lower specific energies are obtained in poorer rock. Because the rotation speed of the cutting head varied in the field, boring rate and penetration per revolution are not exactly the same measure. The variations in rotation speed were, however, such that they should not prevent us from comparing field and laboratory results.

The Nast laboratory sample gave the specific energy value of 18,300 in.-lbs/in.^{3}. The sample was taken from the area which is classified as good-fair. The sample was intact and did not include any major structural weaknesses and thus can better be compared with excellent rock quality. When boring in excellent rock, the field specific energy was 16,600 in.-lbs/in.^{3}. As can be expected, the laboratory value is higher probably due to finer cuttings.

Cutting Coefficient

The boring rate has an almost direct linear relationship with the cutting coefficient (Fig. 3.8).

The laboratory results of different samples (Fig. 3.2) also gave direct relationships between the cutting coefficient and penetration. In this respect, the field and laboratory results are consistent. The higher cutting coefficient value means deeper penetration and faster boring.

The Nast laboratory sample gave the average cutting coefficient as 0.062 (the first pass excluded). This is below the lowest field cutting coefficient value which is 0.086 for excellent-good rock.

Specific Energy - Cutting Coefficient

There is an inverse relationship between specific energy and cutting coefficient (Fig. 3.11). This inverse relationship was also observed in laboratory experiments (Fig. 3.3). We cannot compare the results in one sample to the field results with different rocks, since we also had differences in the laboratory results of one sample and of all samples.

3.3.2 Lawrence Tunnel

From data of Lawrence tunnel in Chicago, boring rate and specific energy were calculated and are given in the plots of Appendix D along the tunnel. The dots are values for each shift and the crosses are the weighted averages of each 100 ft.

The boring in the Lawrence tunnel has been very consistent and "homogeneous" compared to the boring in the Nast tunnel. The achieved boring rates are twice as much as in the Nast tunnel and specific energies remarkably lower.

We had one laboratory sample from the Lawrence tunnel.

Specific Energy

Specific energy was calculated from the rotation horsepowers. The points in Figs. 3.10 and 3.13 represent the weighted averages of each one hundred feet.

Specific energy and boring rate (Fig. 3.12) have an inverse relationship which is almost linear. The inverse relationship was also found in the results of the Nast tunnel.

The average specific energy value of the Lawrence tunnel laboratory sample was 9100 in.-lbs/in.^{3}. This is much higher than the specific energy values obtained in the field boring. An

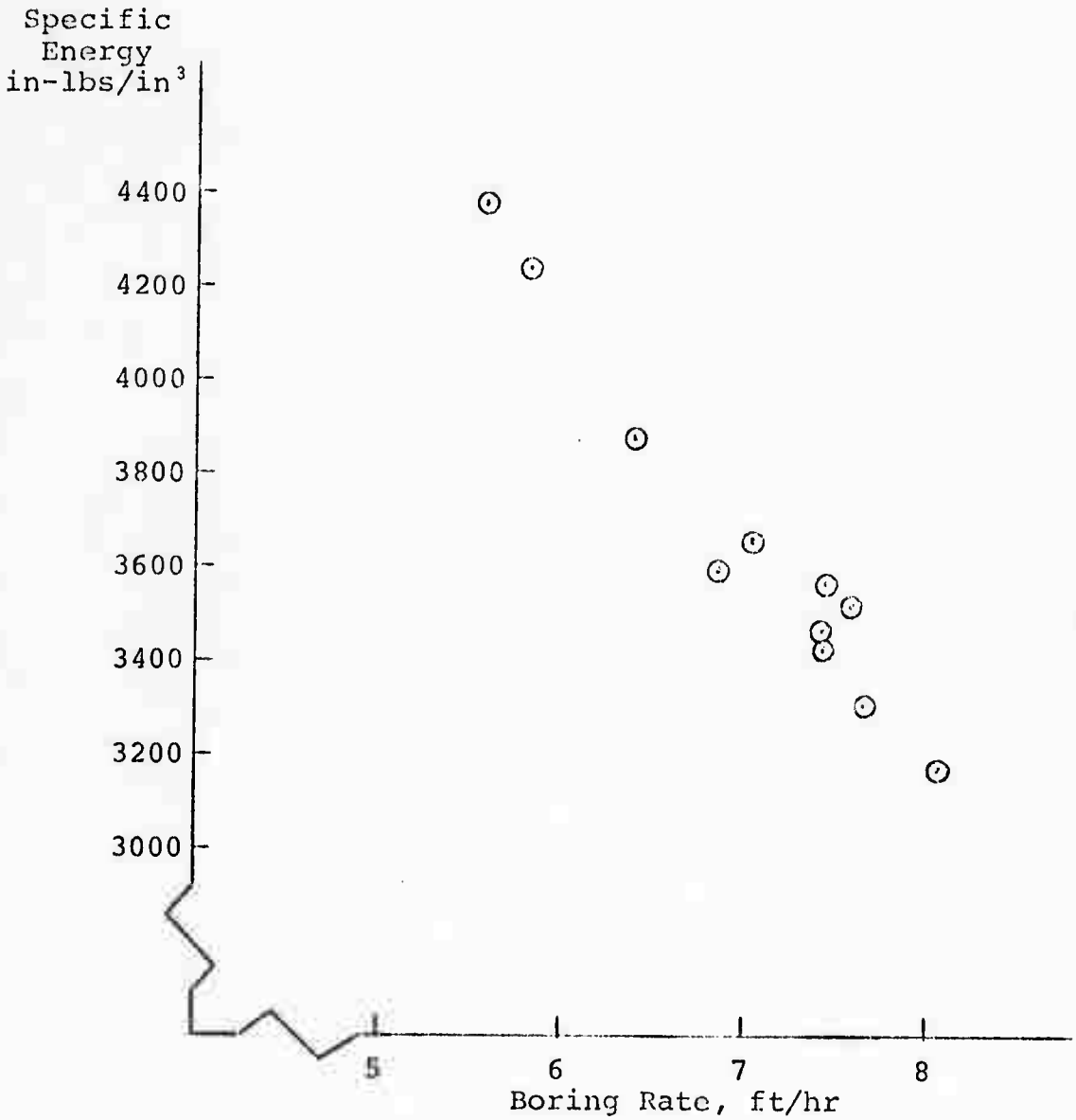

Fig. 3.12. Relationship between specific energy and boring rate for the Lawrence tunnel data. Points represent the average values of each one hundred feet.

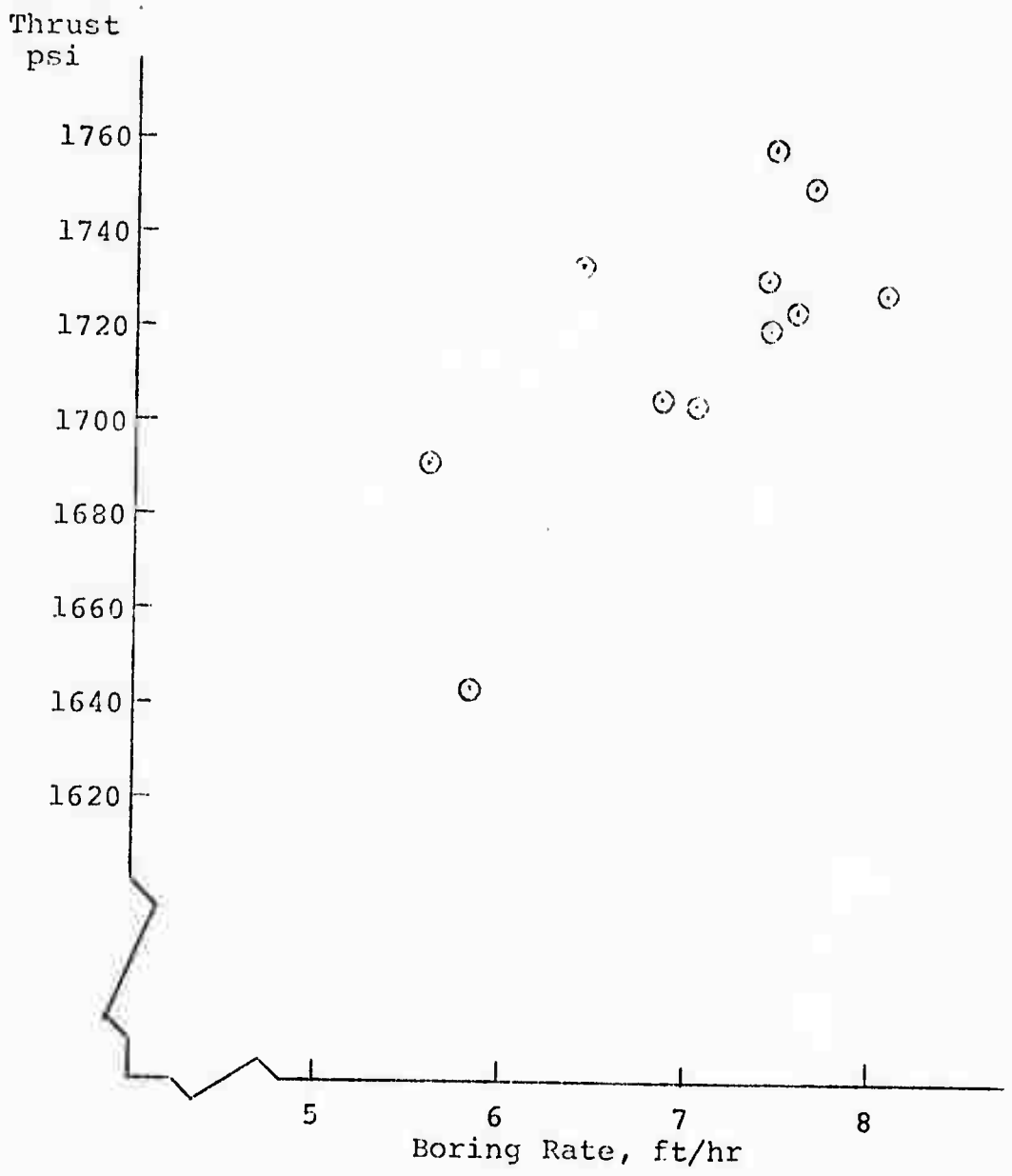

Fig. 3.13. Relationship between thrust and boring rate for the Lawrence tunnel data. Points represent the average values of each one hundred feet.

explanation of this large difference may be that very effective chipping occurred in this rock. This causes large differences in the particle sizes of field and laboratory cuttings.

Thrust

The most remarkable difference when Lawrence tunnel data is compared with the results of the Nast tunnel is that thrust has a direct relationship with boring rate in the Lawrence tunnel (Fig. 3.13).

Two factors: (1) disk type cutters have been used in the Lawrence machine and with these cutters bottoming does not occur, and (2) the rock in the tunnel has been rather homogeneous, may be the main reasons for this direct relationship.

The direct relationship was also found in the results of different passes in the laboratory sample (Fig. 3.6). This seems to be the real behavior when rock type is not changed and if the cutter does not cause limitations. If the strength of rock is low, it limits the thrust which can be used.

3.4 Prediction of Boring Rate

Both the field boring data and the laboratory cutting results give an inverse relationship between specific energy and cutting coefficient. This suggests that using the equations (2.5) and (2.10) we could derive boring rate for field boring.

$$E_V = \frac{2\pi nt}{0.6\pi D^2 \times B_r} \qquad (2.5)$$

$$t = \mu T \frac{R}{2} = \mu T \frac{D}{4} \qquad (2.10)$$

where

E_V = specific energy (in.-lbs/in.^{3})

t = torque (ft-lbs)

n = RPM

D = diameter of bore (ft)

B_r = boring rate (ft/hr)

T = thrust (lbs)

μ = cutting coefficient.

We get from (2.5)

$$t = \frac{0.6\pi D^2 \times B_r \times E_V}{2\pi n} \qquad (3.1)$$

Equating (3.1) and (2.10) and arranging the terms we obtain

$$B_r = \frac{nT}{1.2D} \frac{\mu}{E_V} \qquad (3.2)$$

Thus by knowing cutting coefficient and specific energy we should be able to determine boring rate in various conditions.

The results of this work and also earlier research (1) show that cutting coefficient is very much dependent on the cutter design. In any case we should be able to obtain the limits for cutting coefficient from the design. The Nast tunnel data (Table 3.3) shows that cutting coefficient increases by 27% from excellent to poor rock, but boring rate increases by 82% at the same time.

The specific energy value which is obtained in the laboratory is generally higher than that obtained from field data. Two basic reasons can be pointed out as a reason for this. First, the laboratory sample does not include structural weaknesses of the rock in situ (or only in minor extent). Second, the size of cuttings is smaller than in the field.

In our results for the Nast tunnel the difference between laboratory specific energy and field specific energy for excellent rock type is small. The reason may be that cuttings in the Nast tunnel were fine, especially in excellent rock type. The difference between laboratory and field specific energy values for the Lawrence tunnel is remarkable. This may be due to the great ability of this rock to chip, which causes differences in particle size between laboratory and the field results.

We can obtain the upper limit to specific energy from laboratory cutting, but our value may be much too high depending on the rock. Without particle size analysis or a method with which we can take into account the effect of particle size to specific energy, we can only poorly relate laboratory and field specific energies. Because the structural features are very dominant in the field we should have a means to estimate their influence to the specific energy in boring.

For the time being the main difficulty in using equation (3.2) for boring rate prediction is the uncertainty in specific energy.

The equation (3.2) shows also the direct relationship between boring rate and thrust. This can be seen in the results only if specific energy and cutting coefficient remain constant. This explains the difference between the data of the Nast and Lawrence tunnels (Figs. 3.10 and 3.13).

4. CONCLUSIONS

This work shows that structural features, rock weaknesses, have a dominating role in rock cutting. The machine design should make much better use of these weaknesses than is presently done.

The determination of the real field specific energy value is the main difficulty in the boring rate prediction at the present time.

Laboratory cutting using intact rock samples gives higher specific energy values than field boring. This work did not reveal a means to scale the laboratory results to field. Certain definite relationships are shown which call for better knowledge of the particle size of cuttings and the structure of rock to be bored.

The inverse relationship between specific energy and cutting coefficient, both in the field and in the laboratory, supports the idea that machine design should try to increase cutting coefficient to obtain better boring results. For the time being, the machine design puts a limit on the cutting coefficient.

Cutting coefficients can be increased by taking deeper cuts. This results also in coarser cuttings. Cutting coefficient varies very much along a cut. This causes very variable loads on the cutters.

REFERENCES

1. Ross, N. A., "Theoretical and Experimental Analysis of Tunnel Boreability," M.S. Thesis, Colorado School of Mines, 1970.

2. "Nast Tunnel, Fryingpan Conduit, and Lily Pad Diversion North Side Collection System," United States Bureau of Reclamation, Specifications No. DC-6829.

3. Ross, N. A. and Hustrulid, W. A., "Some Comments on the Design of Medium to Hard Rock Tunnel Boring Machines," Dynamic Rock Mechanics.

4. Teale, R., "The Mechanical Excavation of Rock - Experiments with Roller Cutters," Int. Jour. of Rock Mech. Min. Sci., v. 1, no. 1, pp. 63-78, 1964.

5. Sasaki, K., Yamakado, N., Siohara, Z., and Tobe, M., "Studies on the Cutting Resistance of Rock," Jour. of Mining and Metallurgy Institute of Japan, v. 77, no. 881, Nov. 1961, pp. 975-980. (Translation by CSM)

6. Takaoka, S., Hayamizu, H., and Misawa, S., "Studies on the Fracture of Rock by Rotary Cutters - Rock Fracturing by Disk Cutters," Jour. of the Min. Met. Inst. of Japan, v. 84, no. 960, April 1968, pp. 427-432. (Translation by CSM)

7. Takaoka, S., Hayamizu, H., Misawa, S., and Uuriyagawa, M., "Studies on the Fracture of Rock by Rotary Cutters - by a Spherical Chip Cutter and a Milled Tooth Cutter," Jour. of Min. Met. Inst. of Japan, v. 85, no. 975, July 1969, pp. 491-496. (Translation by CSM)

8. Teale, R., "The Concept of Specific Energy in Rock Drilling," Int. Jour. Rock Mech. Min. Sci., v. 2, no. 1, pp. 57-72, 1965.

9. Cook, N. G. W., "Analysis of Hard-Rock Cuttability for Machines," Conf. on Tunnel and Shaft Excavation, Univ. Minnesota, Minneapolis, Minn. (1968).

10. Bruce, and Morrell, R., "Principles of Rock Cutting Applied to Mechanical Boring Machines," Symp. II on Rapid Excavation Proc., Sacramento, Calif., Oct. 1969.

11. Private Communication, Mr. H. E. McInnis, Construction Engineer, United States Bureau of Reclamation, 1972.

APPENDIX A

HORIZONTAL (F_H) AND VERTICAL (F_V) FORCES, CUTTING COEFFICIENT (μ), AND ENERGY (W) ALONG SOME CUTS ON LABORATORY SAMPLES.

SET PENETRATION, INDEXING, AVERAGE HORIZONTAL (F_H) AND VERTICAL (F_V) FORCES, AND AVERAGE CUTTING COEFFICIENT (μ) FOR THE CUT ARE INCLUDED IN THE TABLES SHOWN IN THE FIGURES OF CUTTING COEFFICIENT AND ENERGY.

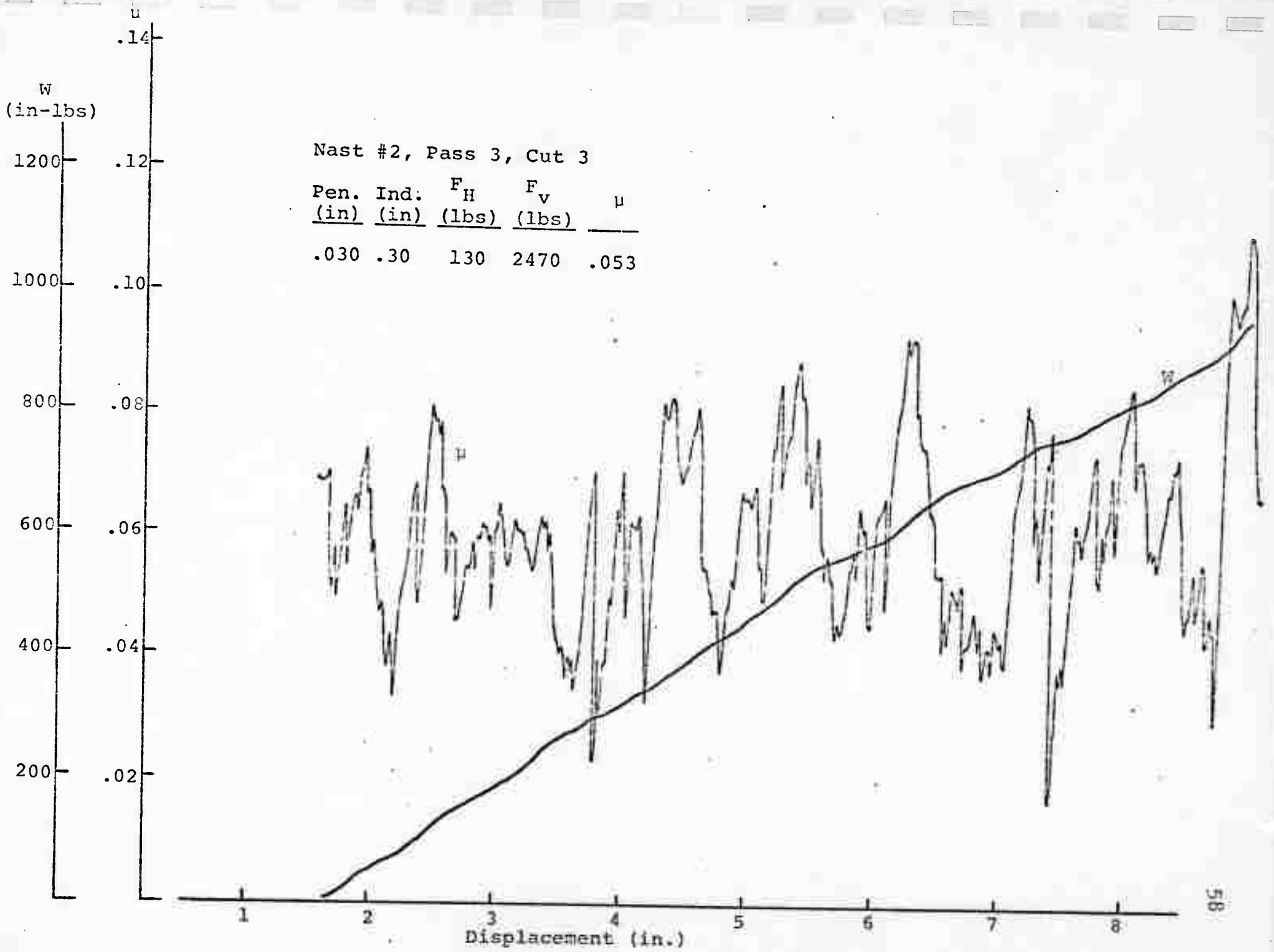
μ
.14
W
(in-lbs)
1200
.12
1000
.10
800
.08
600
.06
400
.04
200
.02
Nast #2, Pass 3, Cut 3
Pen. (in) Ind. (in) F_H (lbs) F_V (lbs) μ
.030 .30 130 2470 .053
μ
W
1
2
3
4
5
6
7
8
Displacement (in.)

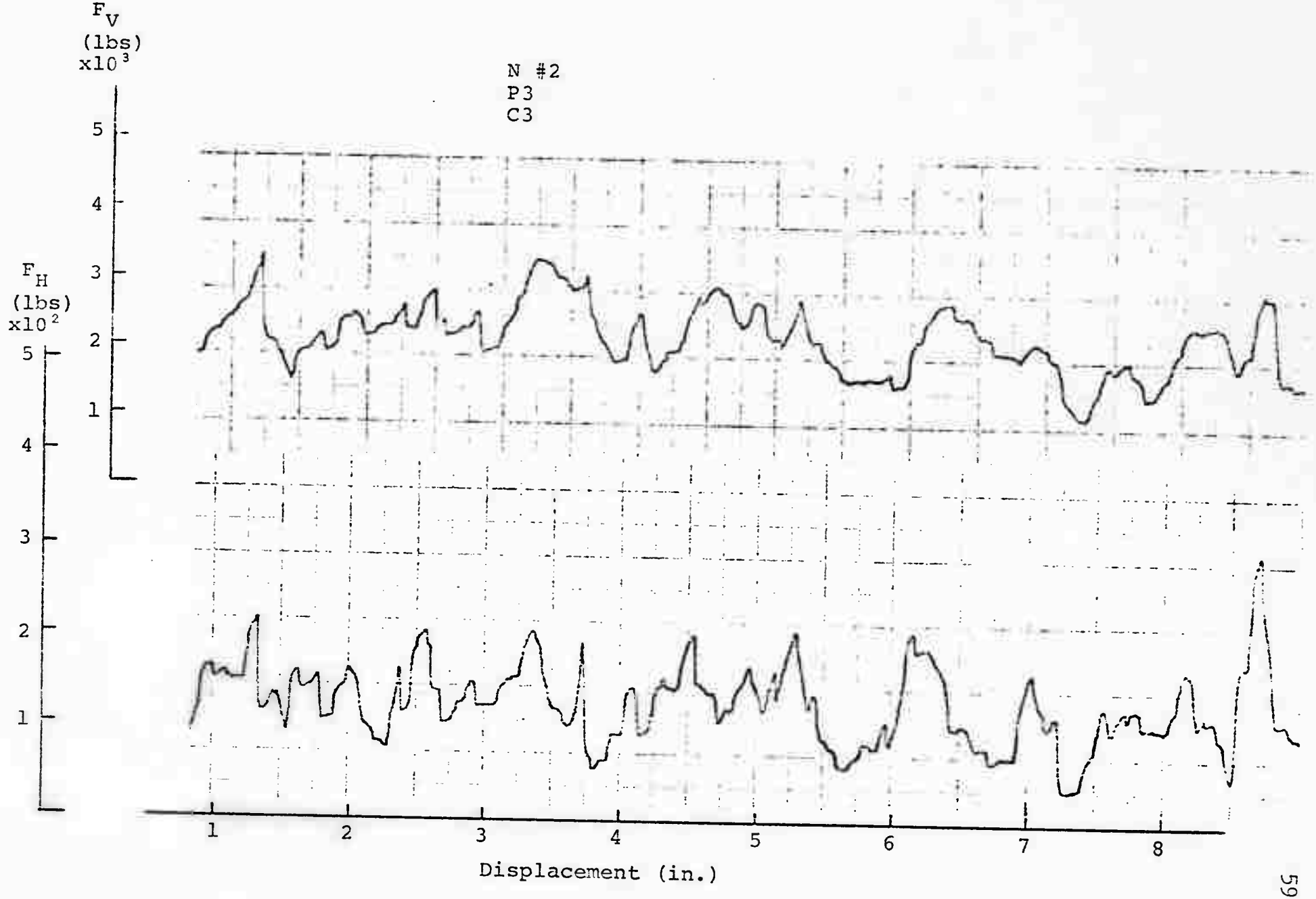
N #2
P3
C3
F_V (lbs) x10^3
5
4
3
2
1
F_H (lbs) x10^2
5
4
3
2
1
1
2
3
4
5
6
7
8
Displacement (in.)

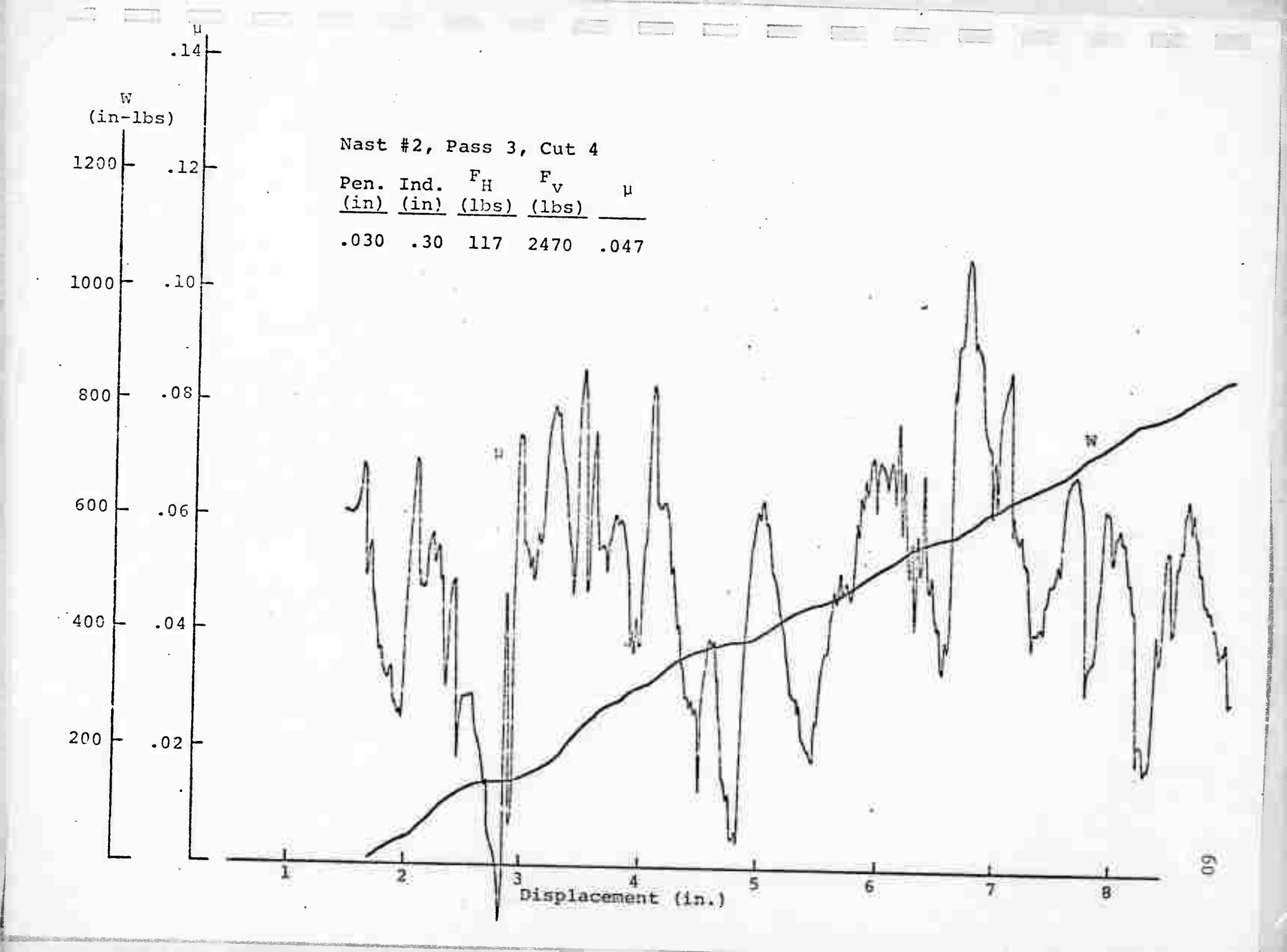
Nast #2, Pass 3, Cut 4
Pen. (in) Ind. (in) F_H (lbs) F_V (lbs) μ
.030 .30 117 2470 .047
μ
.14
.12
.10
.08
.06
.04
.02
W (in-lbs)
1200
1000
800
600
400
200
W
1
2
3
4
5
6
7
8
Displacement (in.)
60

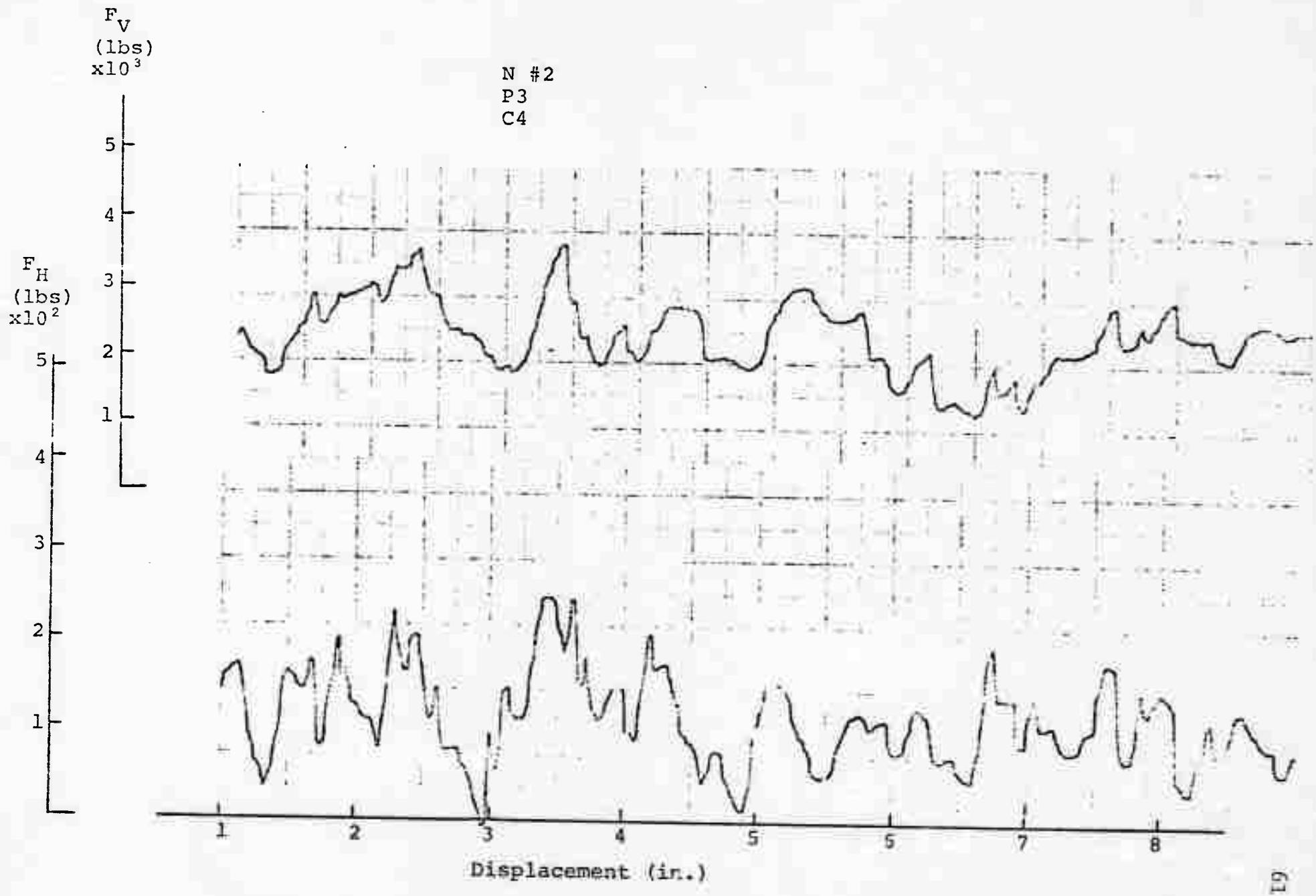
F_V (lbs) x10^3
N #2
P3
C4
5
4
3
2
1
F_H (lbs) x10^2
5
4
3
2
1
1
2
3
4
5
6
7
8
Displacement (in.)

Nast #2, Pass 3, Cut 5

Pen. (in)	Ind. (in)	F_H (lbs)	F_V (lbs)	μ
.030	.30	120	2390	.050

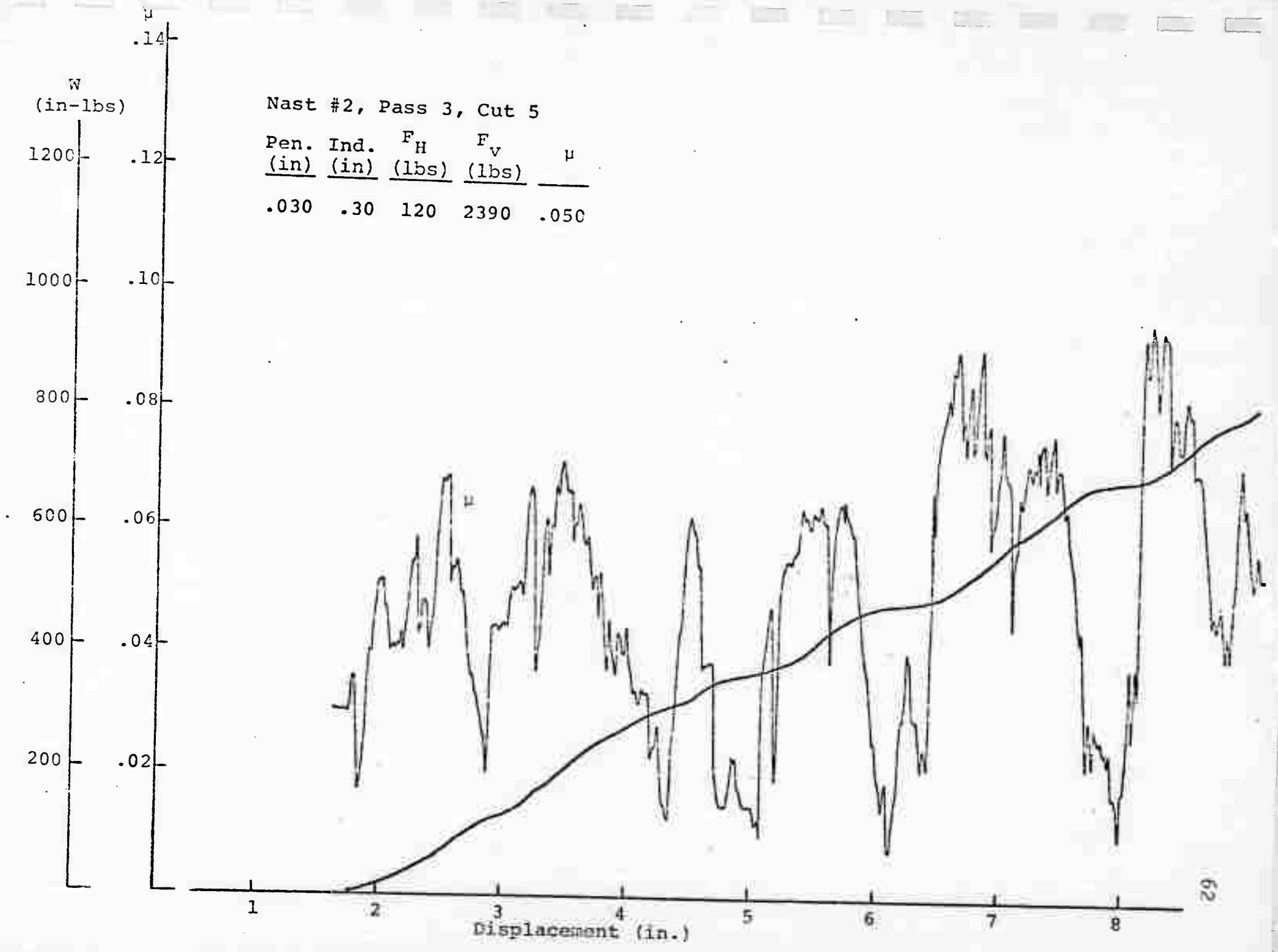

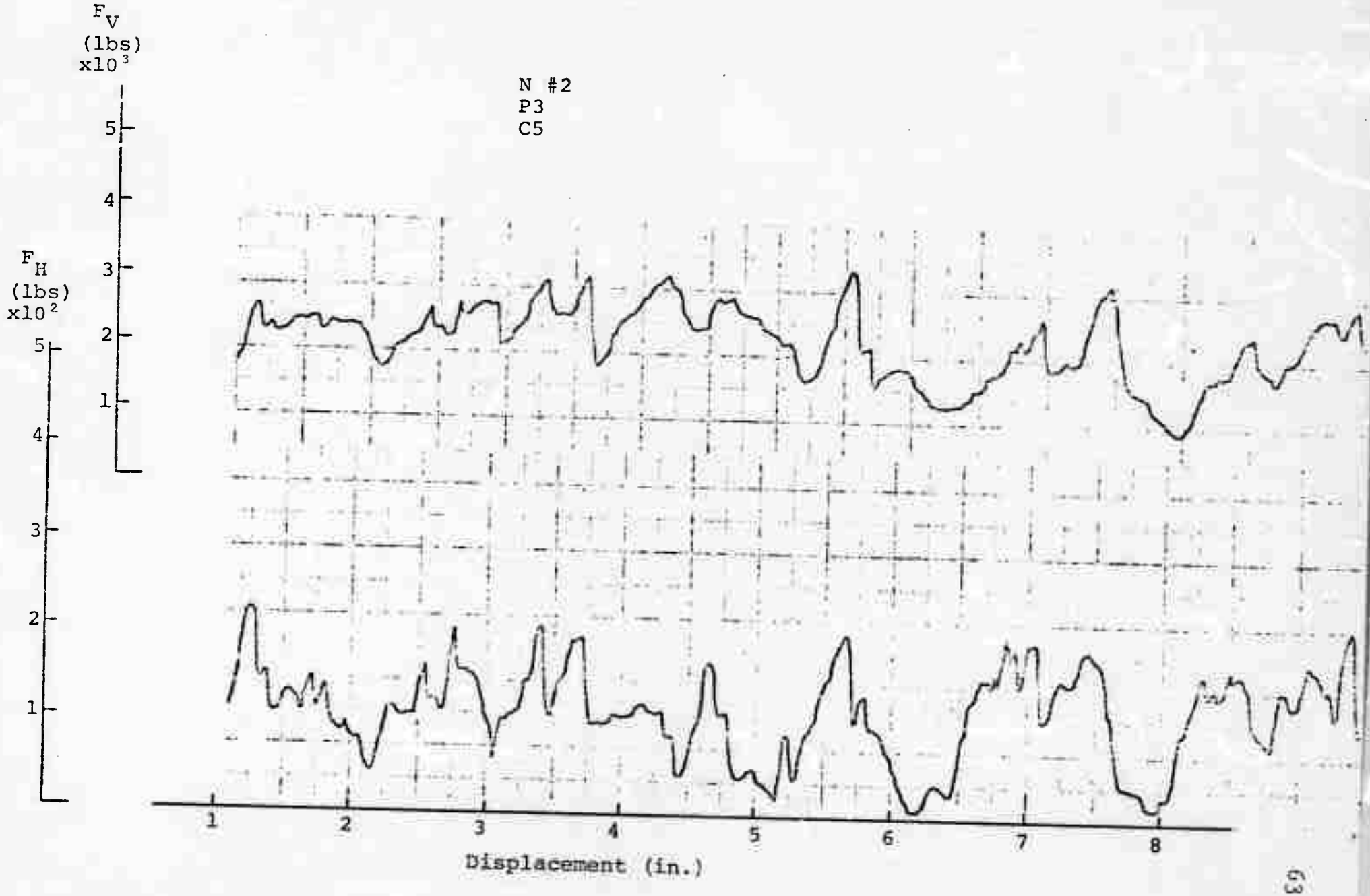
F_V (lbs) x10^3
5
4
3
2
1
F_H (lbs) x10^2
5
4
3
2
1
N #2
P3
C5
1
2
3
4
5
6
7
8
Displacement (in.)

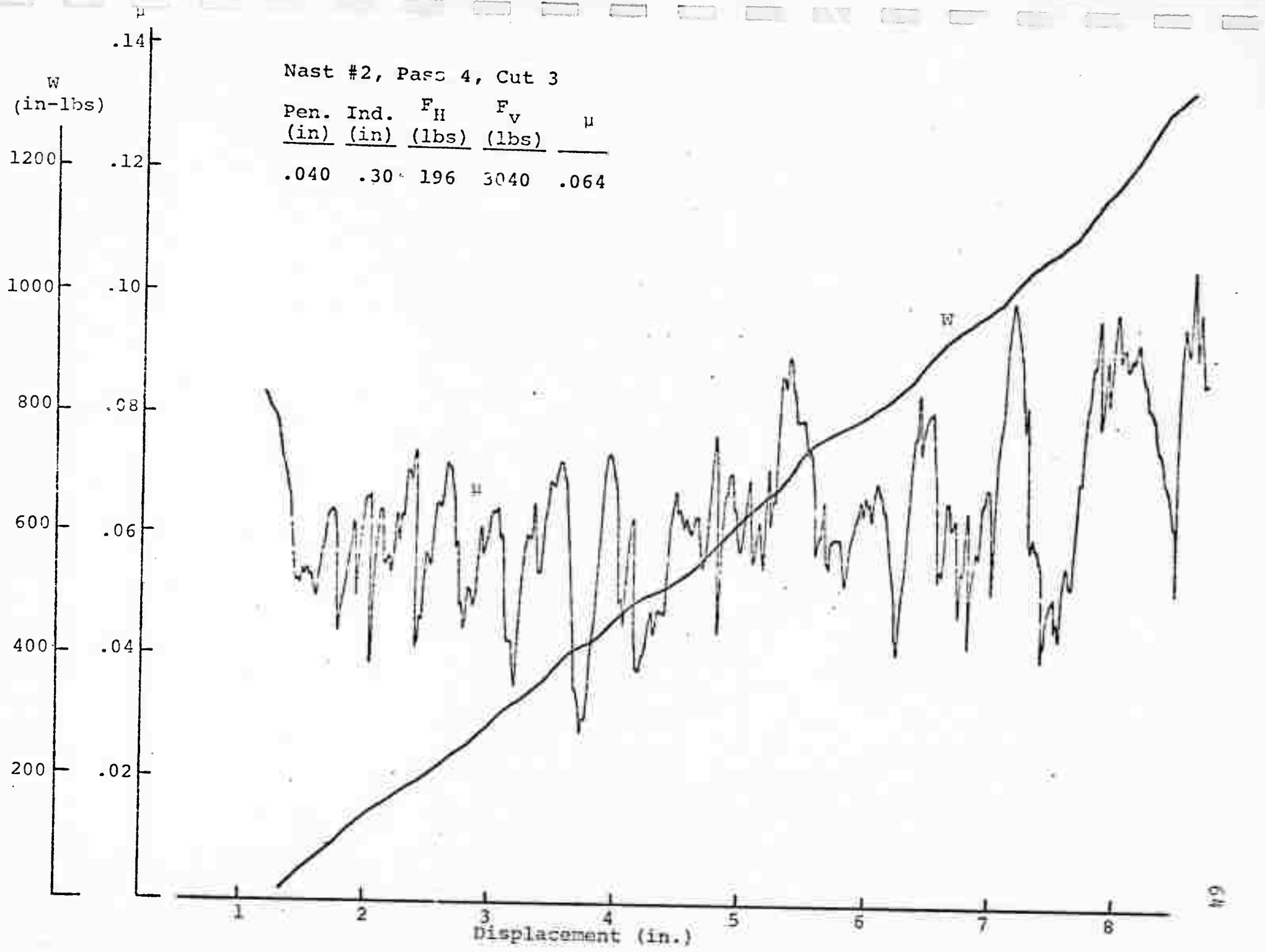
Nast #2, Pass 4, Cut 3
Pen. (in) | Ind. (in) | F_H (lbs) | F_V (lbs) | μ
.040 | .30 | 196 | 3040 | .064
W (in-lbs)
μ
1200
1000
800
600
400
200
.14
.12
.10
.08
.06
.04
.02
W
μ
1
2
3
4
5
6
7
8
Displacement (in.)

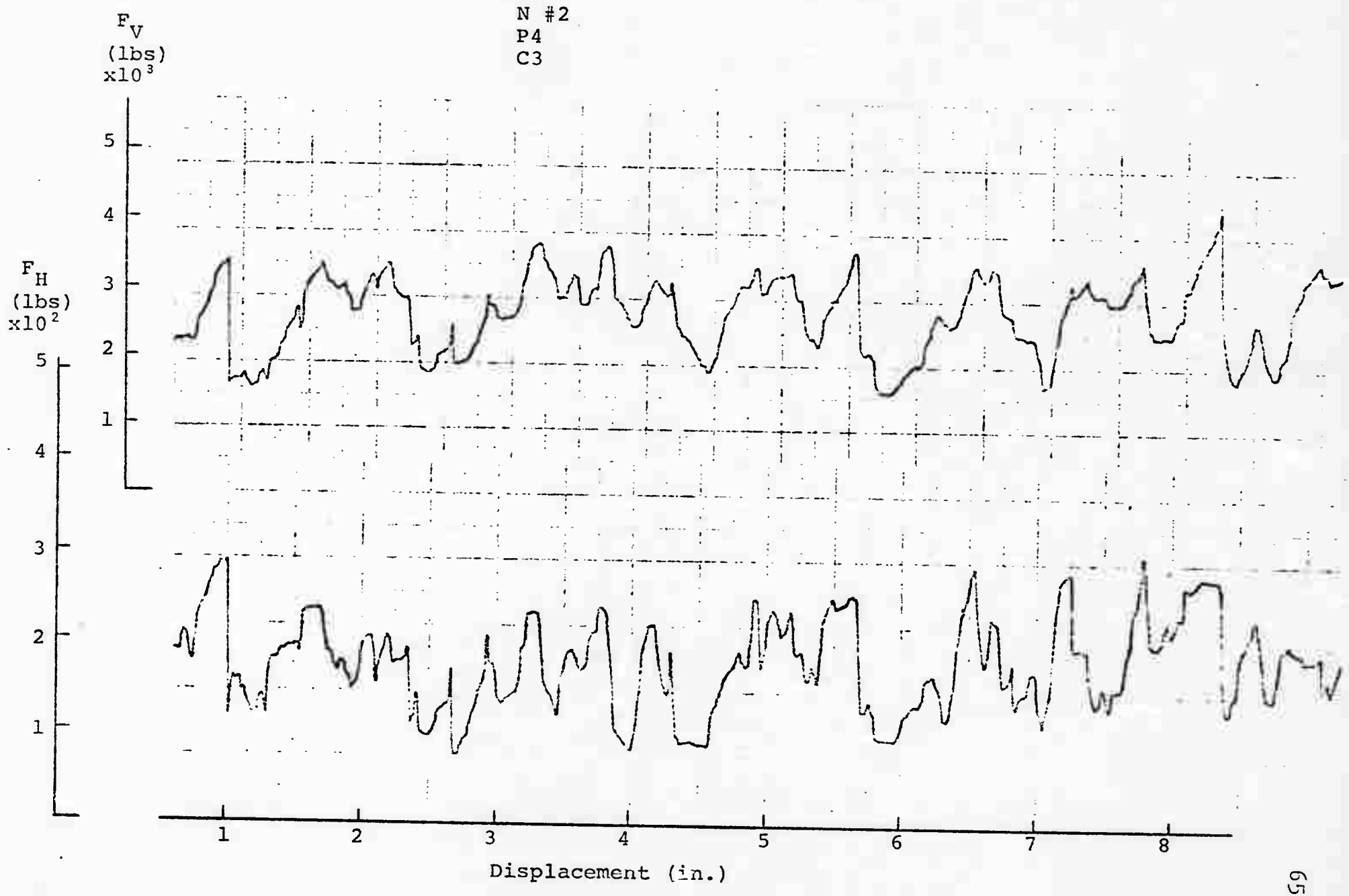
N #2
P4
C3
F_V (lbs) x10^3
5
4
3
2
1
F_H (lbs) x10^2
5
4
3
2
1
1
2
3
4
5
6
7
8
Displacement (in.)

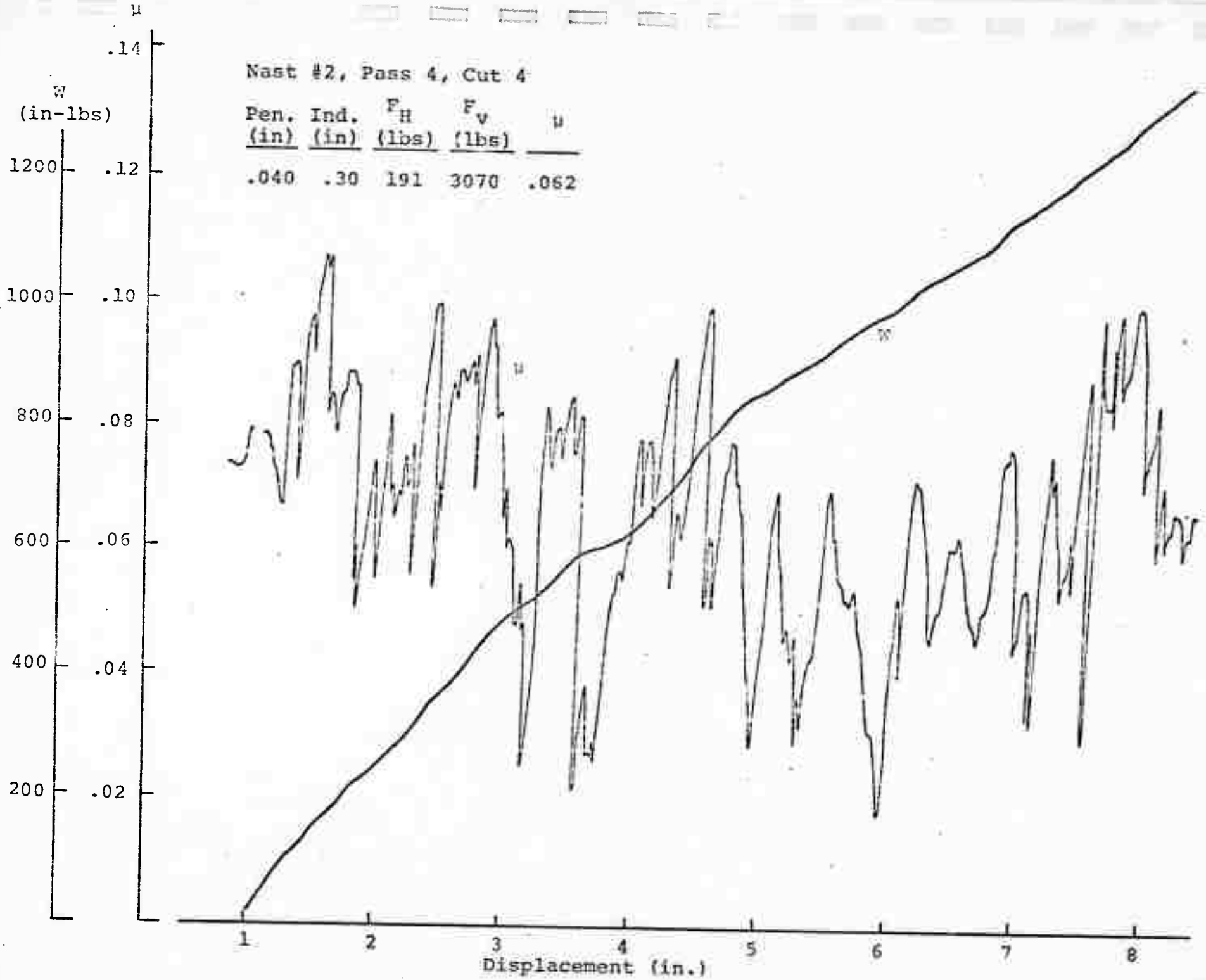
μ
.14
W
(in-lbs)
1200
.12
1000
.10
800
.08
600
.06
400
.04
200
.02
Nast #2, Pass 4, Cut 4
Pen. (in) Ind. (in) F_H (lbs) F_V (lbs) μ
.040 .30 191 3070 .062
W
μ
1
2
3
4
5
6
7
8
Displacement (in.)

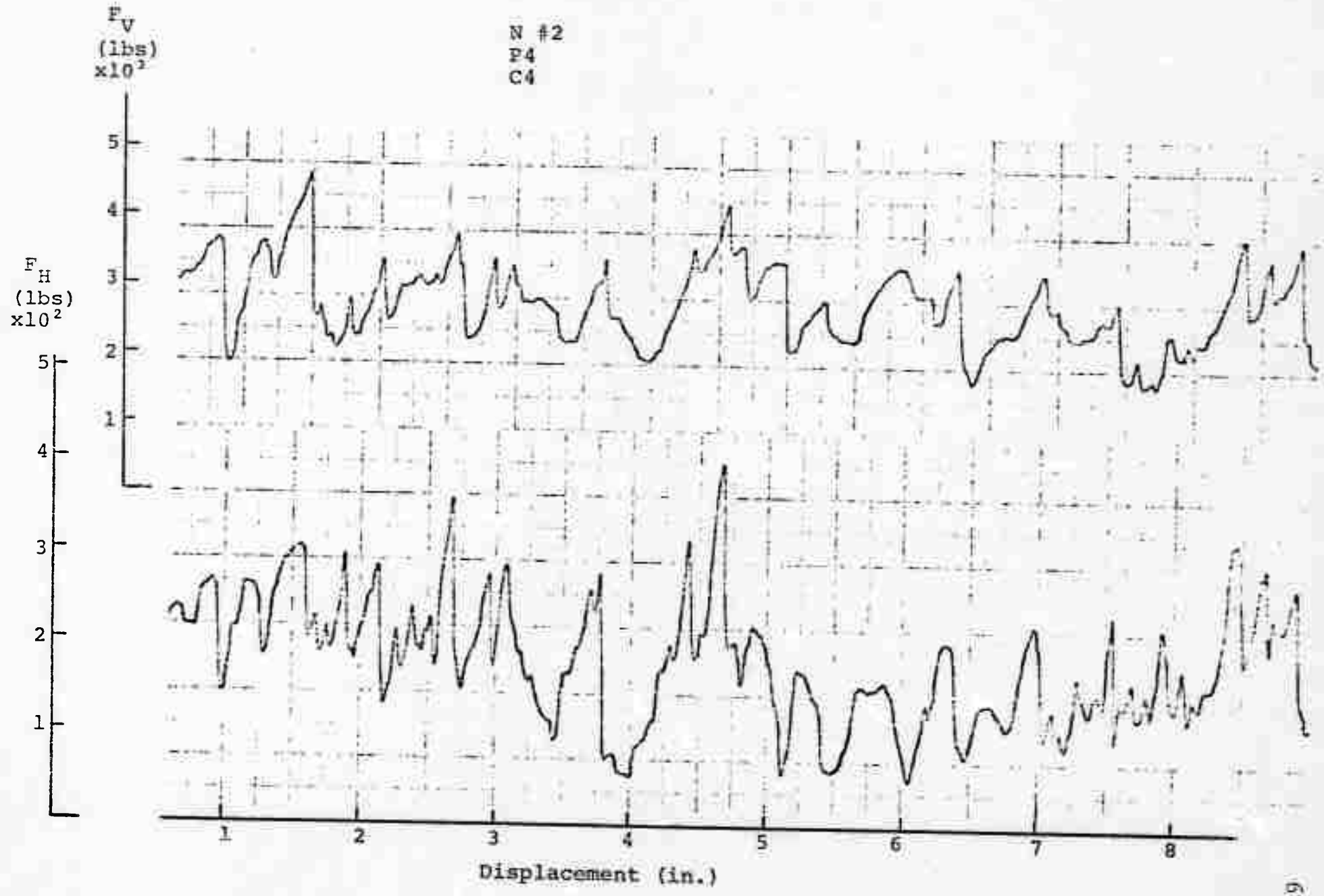
N #2
P4
C4
F_V (lbs) x10²
5
4
3
2
1
F_H (lbs) x10²
5
4
3
2
1
1
2
3
4
5
6
7
8
Displacement (in.)

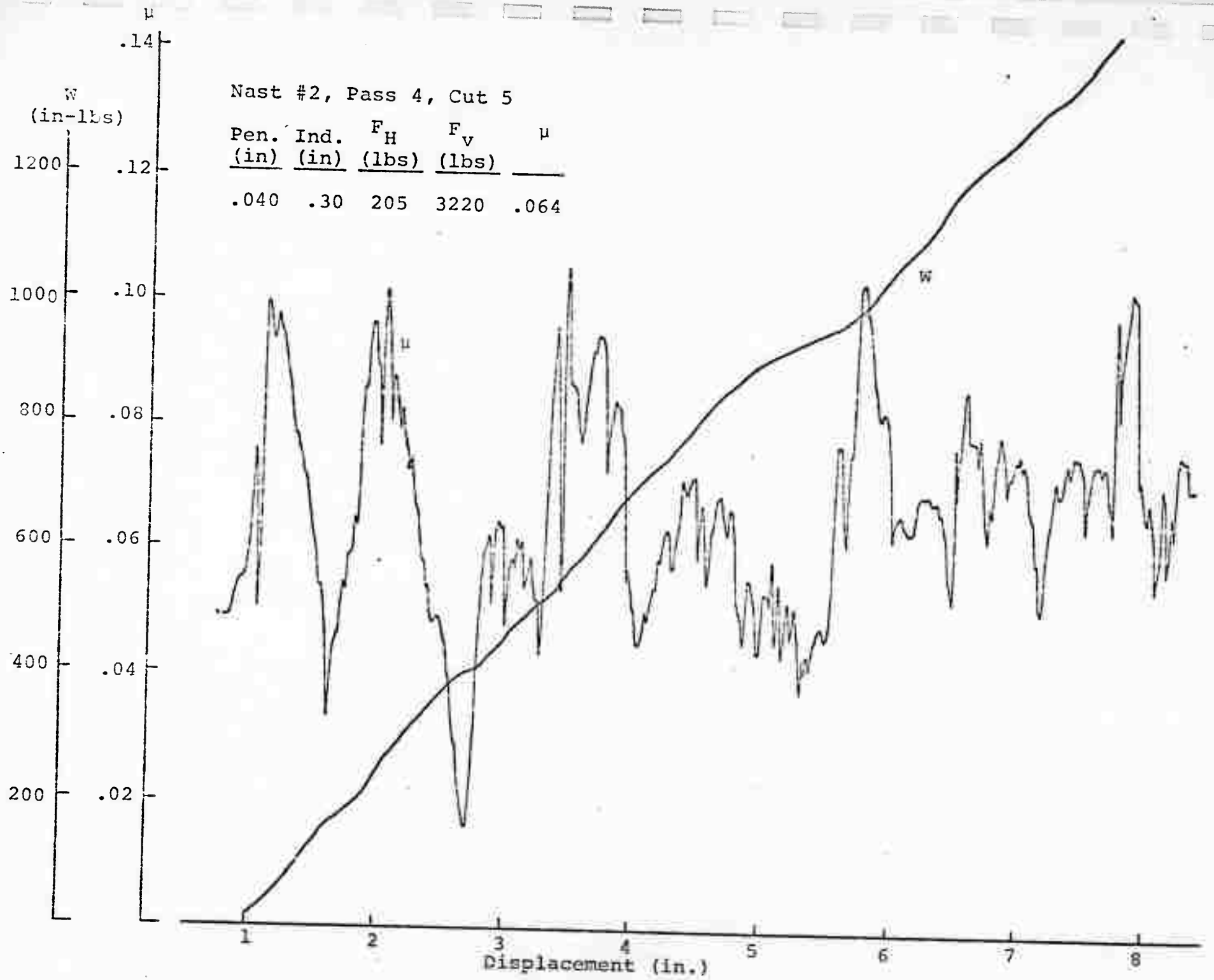
μ
.14
W
(in-lbs)
Nast #2, Pass 4, Cut 5
Pen. (in) Ind. (in) F_H (lbs) F_V (lbs) μ
.040 .30 205 3220 .064
1200
.12
1000
.10
800
.08
600
.06
400
.04
200
.02
μ
W
1
2
3
4
5
6
7
8
Displacement (in.)

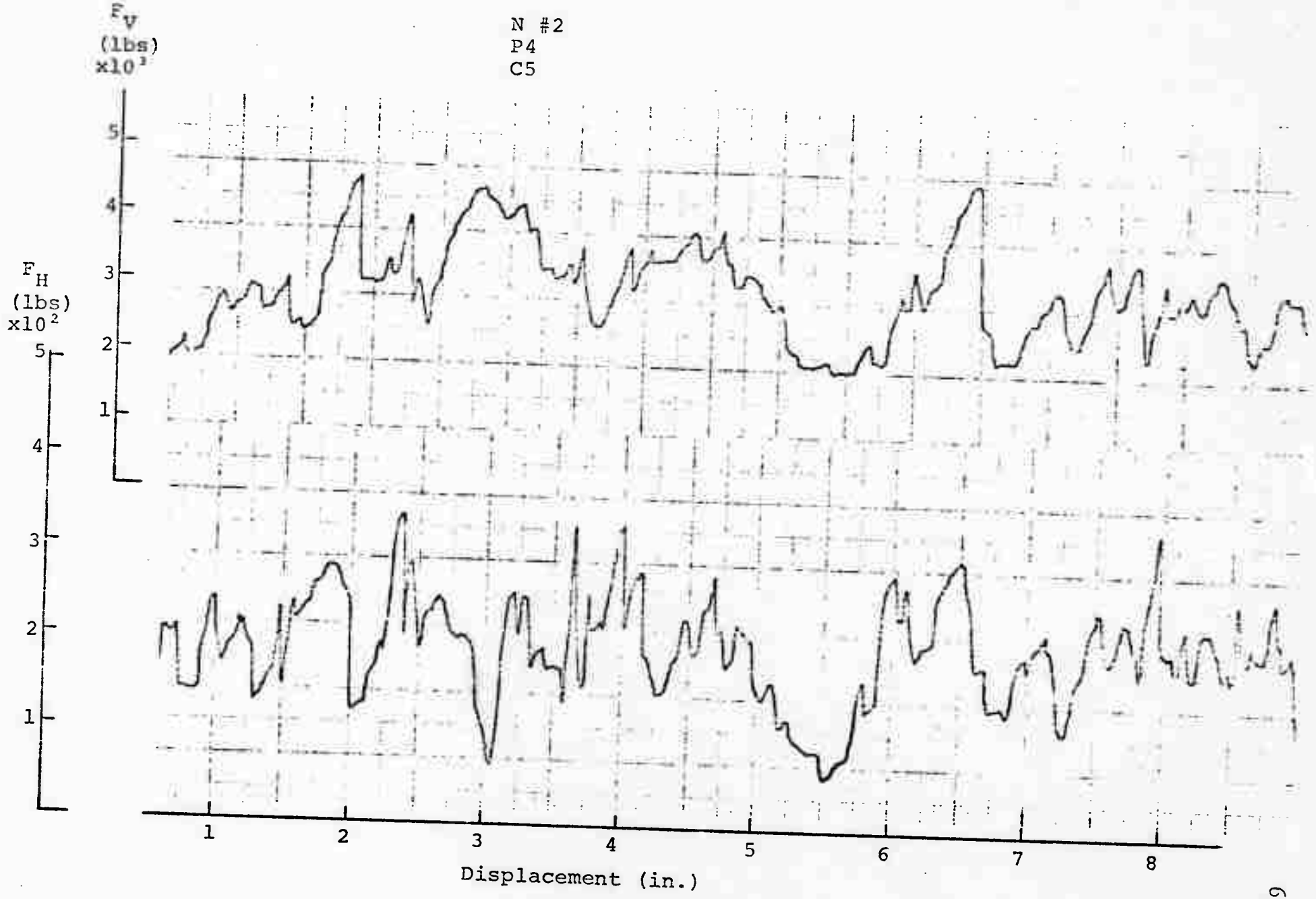
N #2
P4
C5
F_V (lbs) x10³
5
4
3
2
1
F_H (lbs) x10²
5
4
3
2
1
1
2
3
4
5
6
7
8
Displacement (in.)

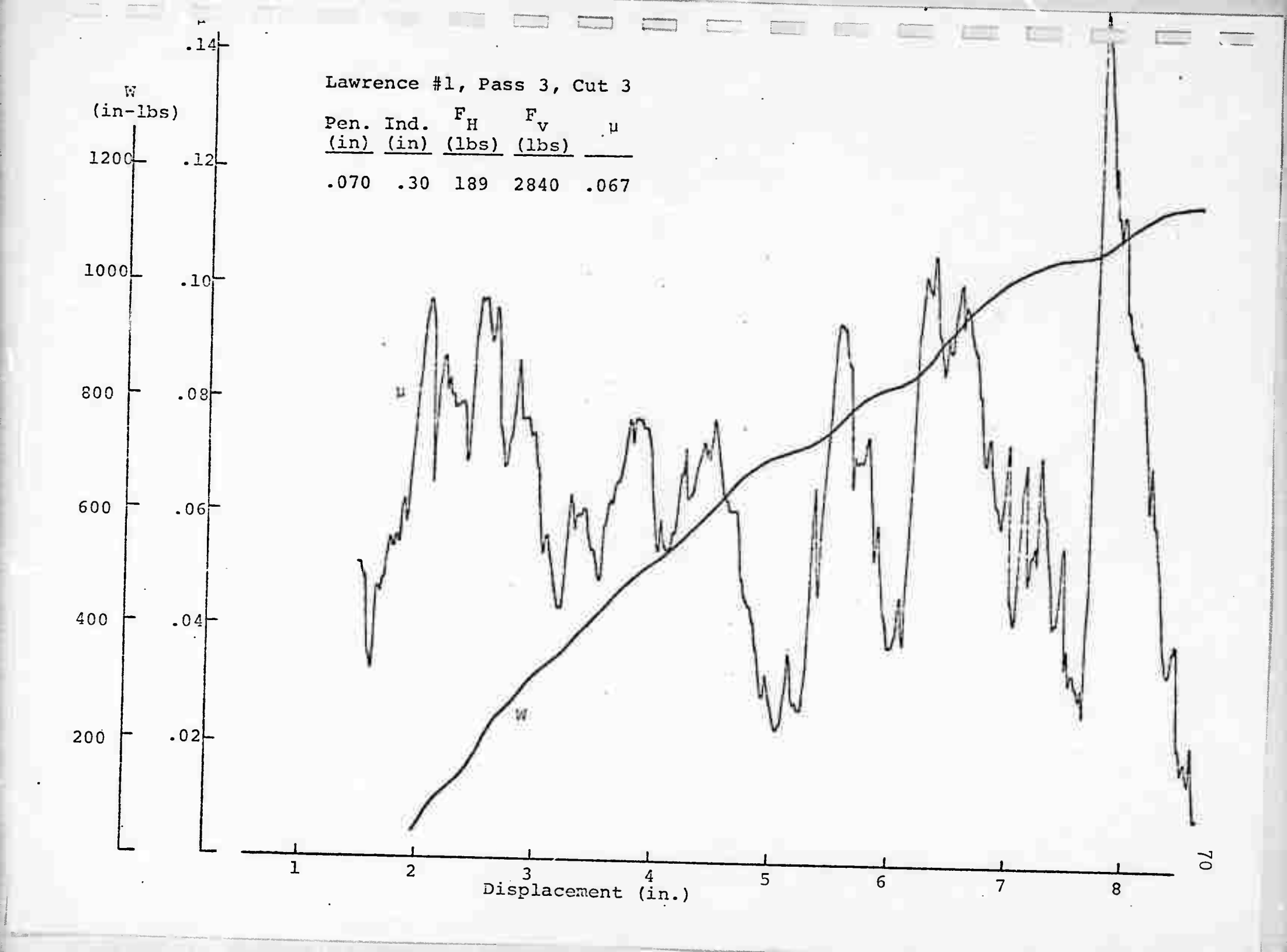
Lawrence #1, Pass 3, Cut 3
Pen. (in) Ind. (in) F_H (lbs) F_v (lbs) μ
.070 .30 189 2840 .067
W (in-lbs)
1200
1000
800
600
400
200
.14
.12
.10
.08
.06
.04
.02
μ
W
1
2
3
4
5
6
7
8
Displacement (in.)
70

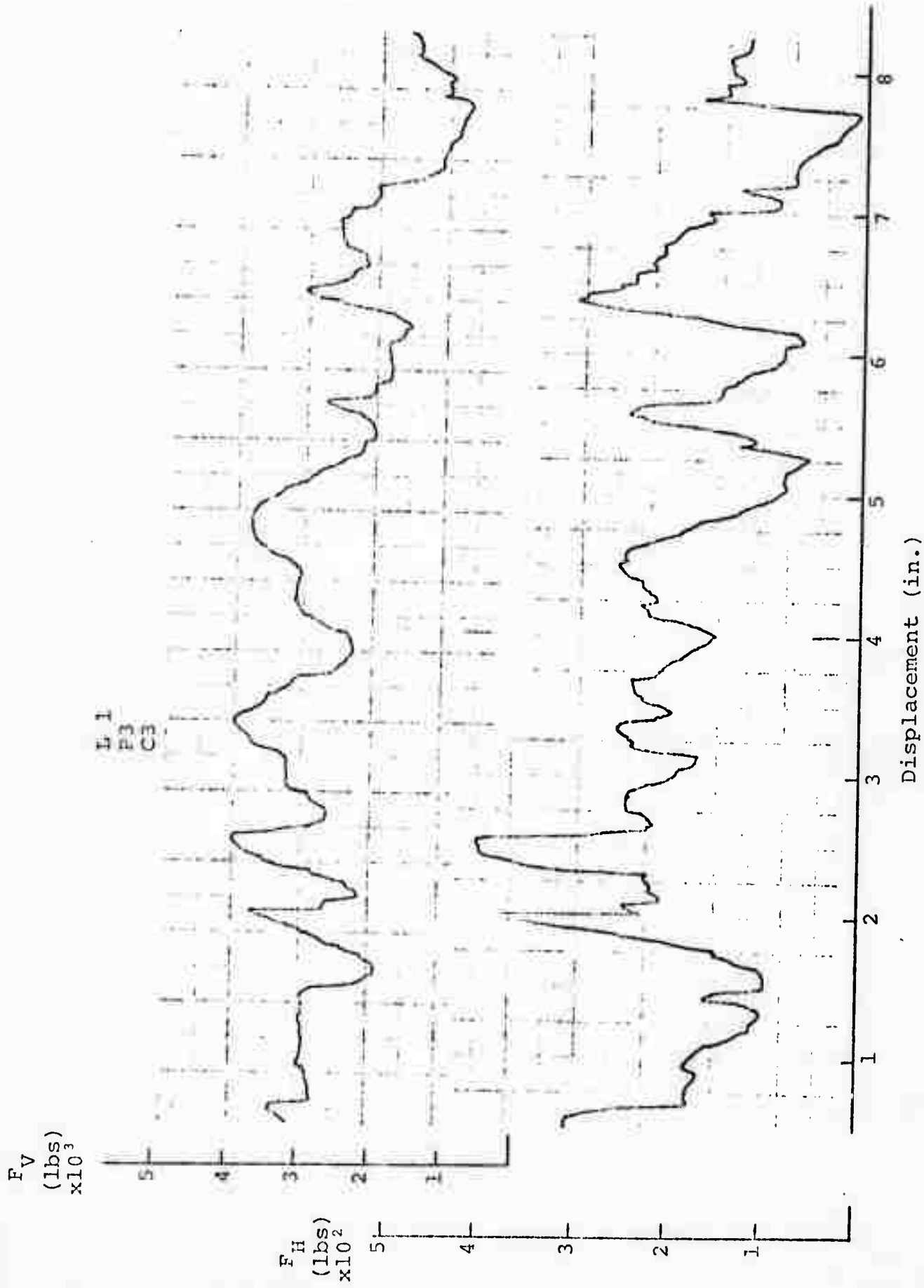
L 1
P3
C3
F_V (lbs) x10^3
F_H (lbs) x10^2
Displacement (in.)

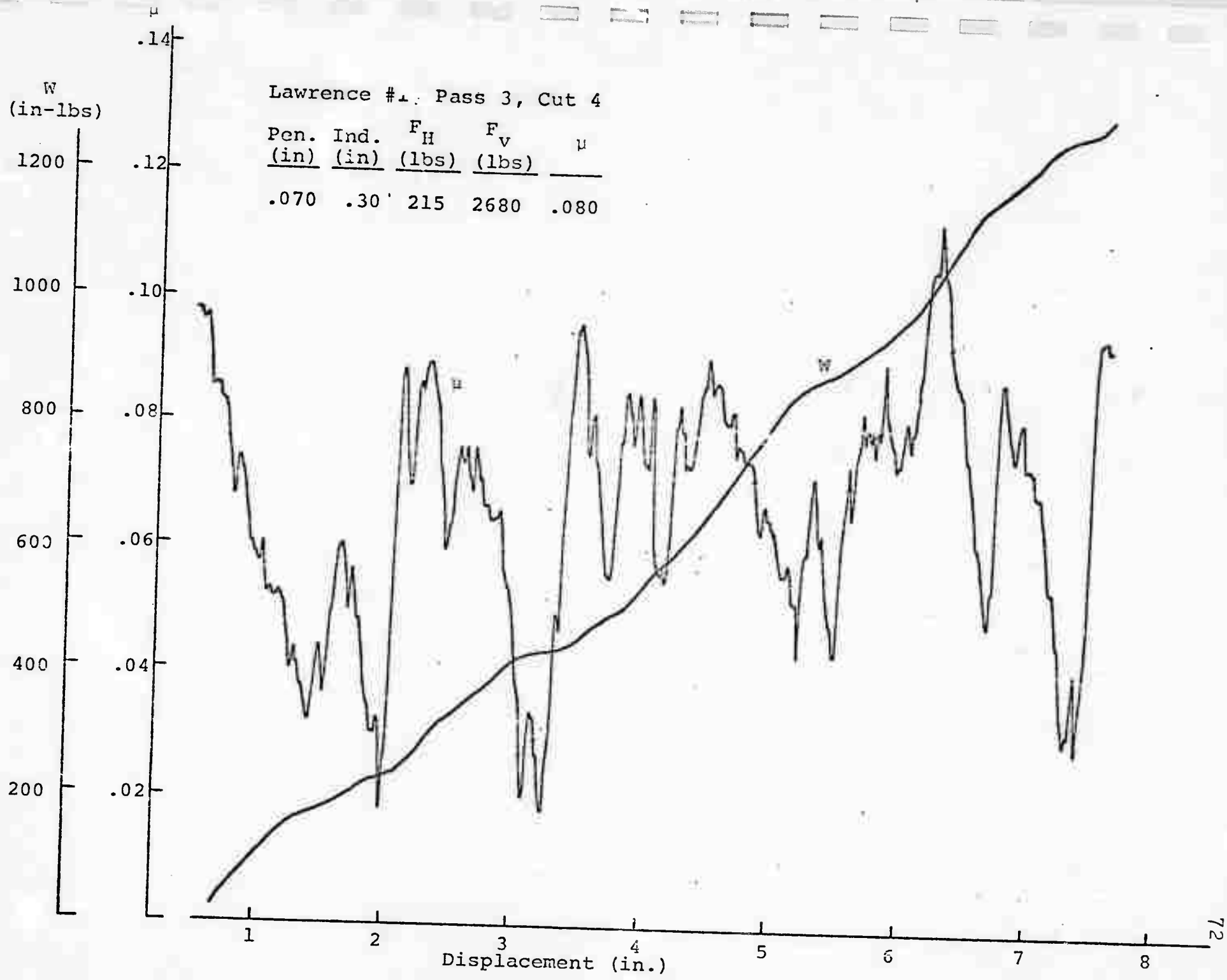
Lawrence #1. Pass 3, Cut 4
Pen. (in) | Ind. (in) | F_H (lbs) | F_V (lbs) | μ
.070 | .30 | 215 | 2680 | .080
W (in-lbs)
μ
1200
1000
800
600
400
200
.14
.12
.10
.08
.06
.04
.02
W
μ
1
2
3
4
5
6
7
8
Displacement (in.)

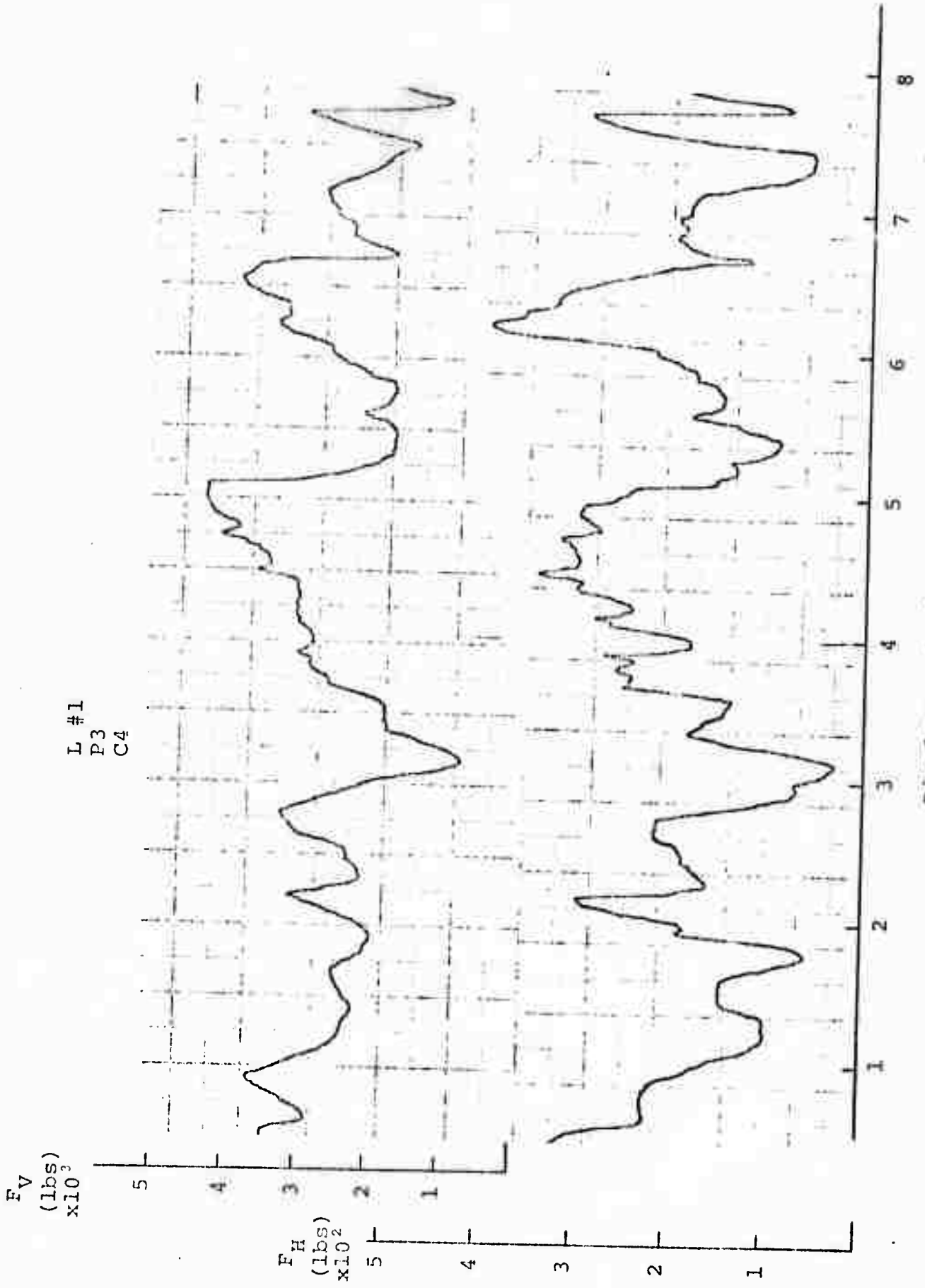
L #1
P3
C4
F_V (lbs) x10^3
F_H (lbs) x10^2
Displacement (in.)

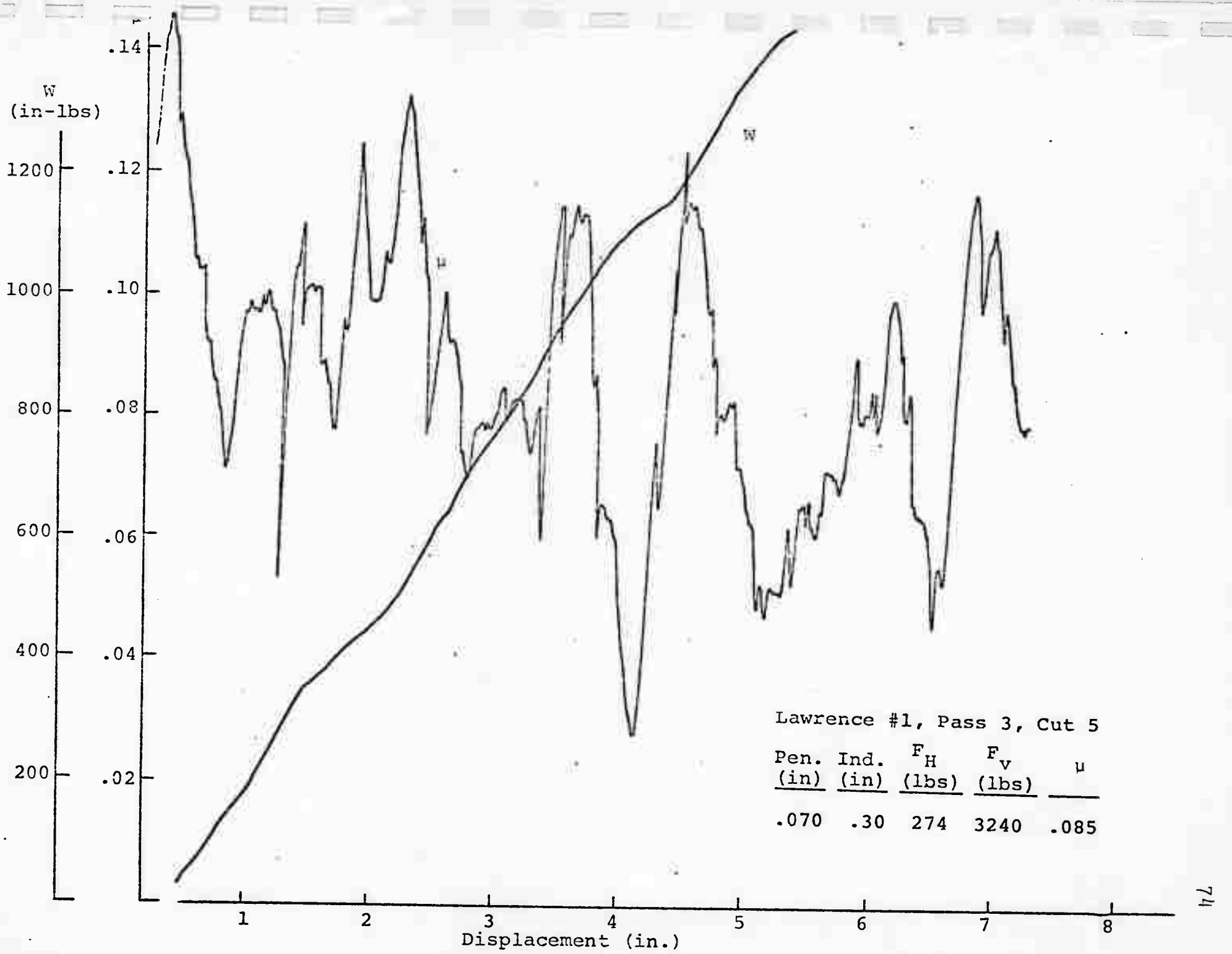

Lawrence #1, Pass 3, Cut 5

Pen. (in)	Ind. (in)	F_H (lbs)	F_V (lbs)	μ
.070	.30	274	3240	.085

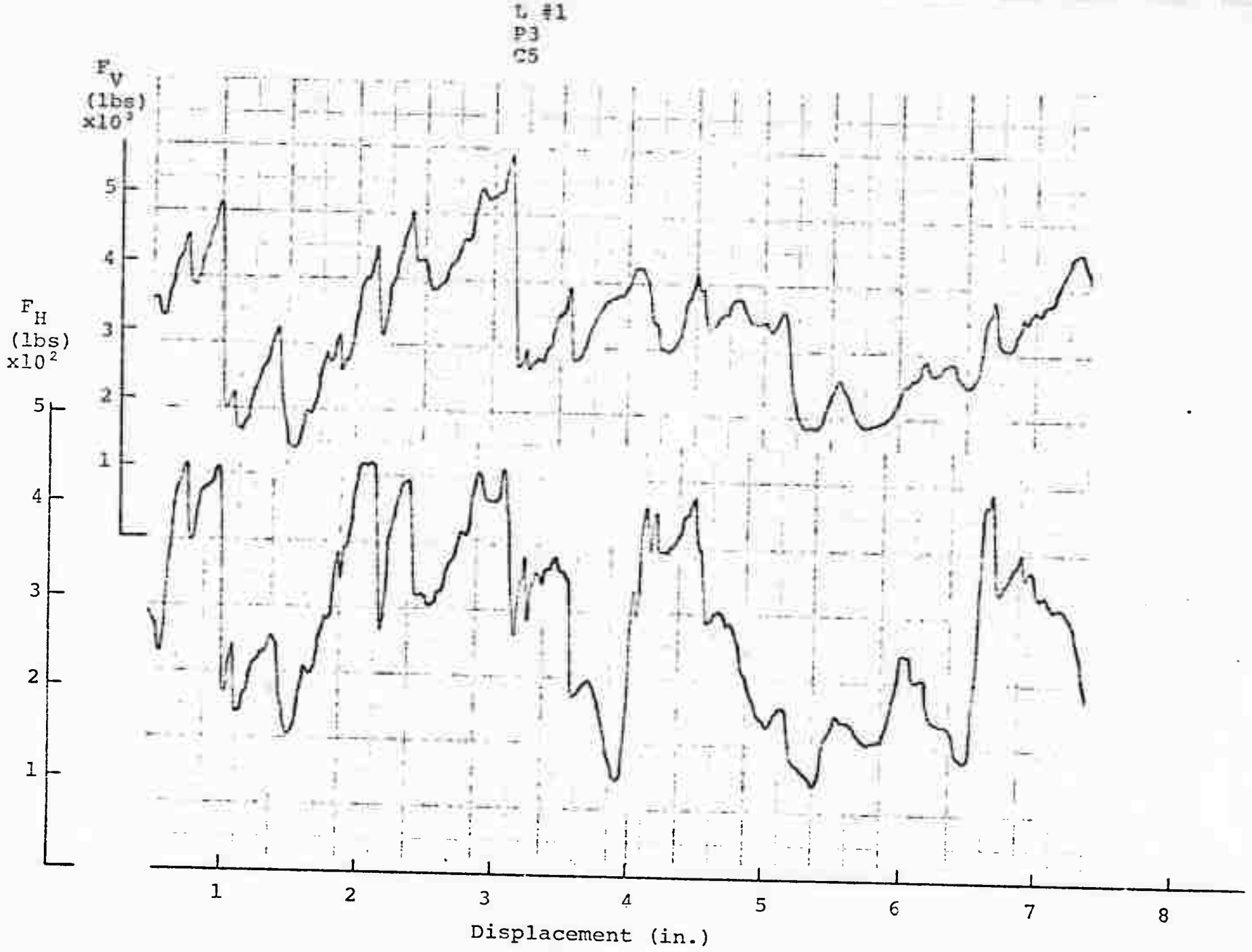
L #1
P3
C5
F_V (lbs) x10³
5
4
3
2
1
F_H (lbs) x10²
5
4
3
2
1
1
2
3
4
5
6
7
8
Displacement (in.)

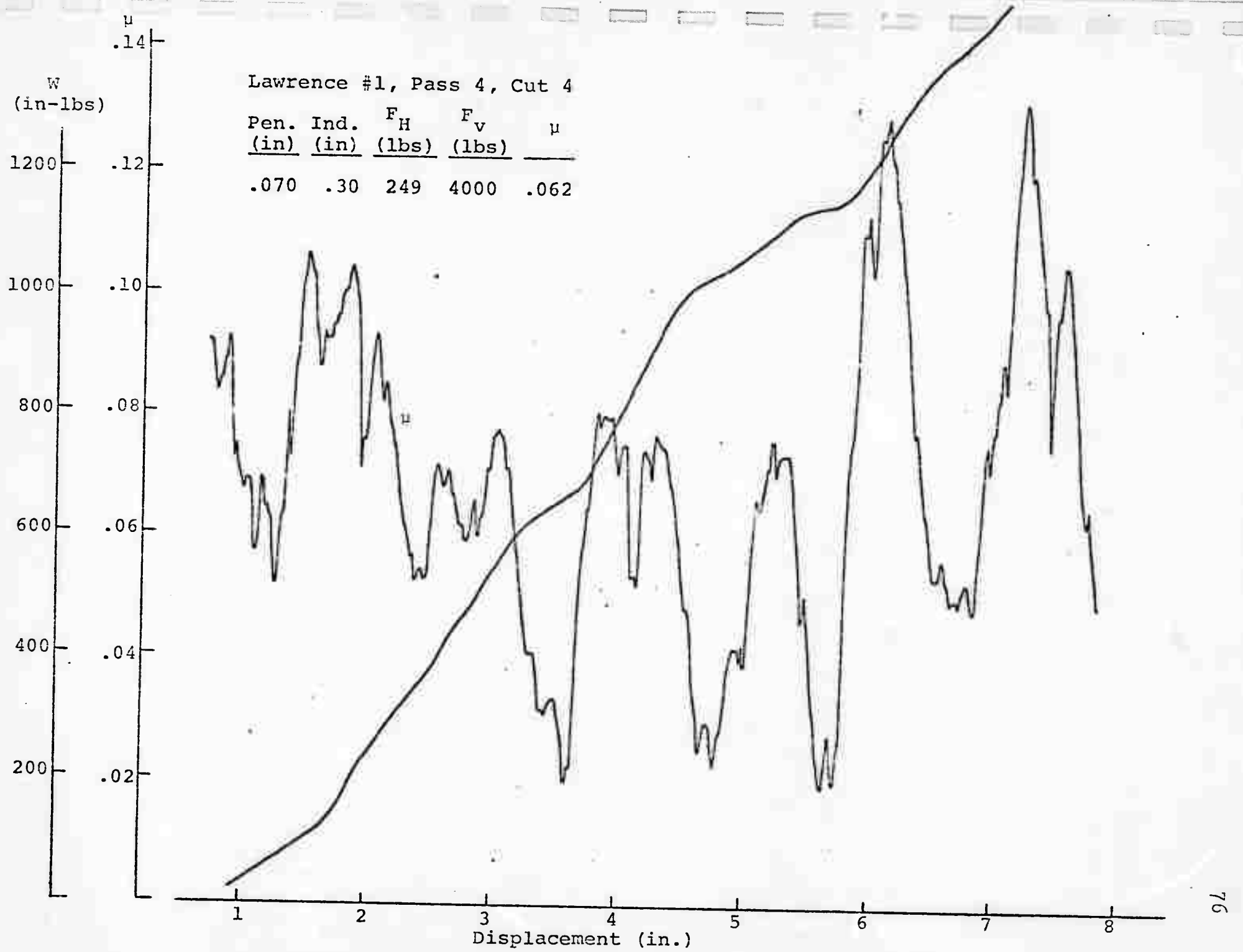
Lawrence #1, Pass 4, Cut 4
Pen. (in) | Ind. (in) | F_H (lbs) | F_v (lbs) | μ
.070 | .30 | 249 | 4000 | .062
W (in-lbs)
μ
1200
1000
800
600
400
200
.14
.12
.10
.08
.06
.04
.02
1
2
3
4
5
6
7
8
Displacement (in.)

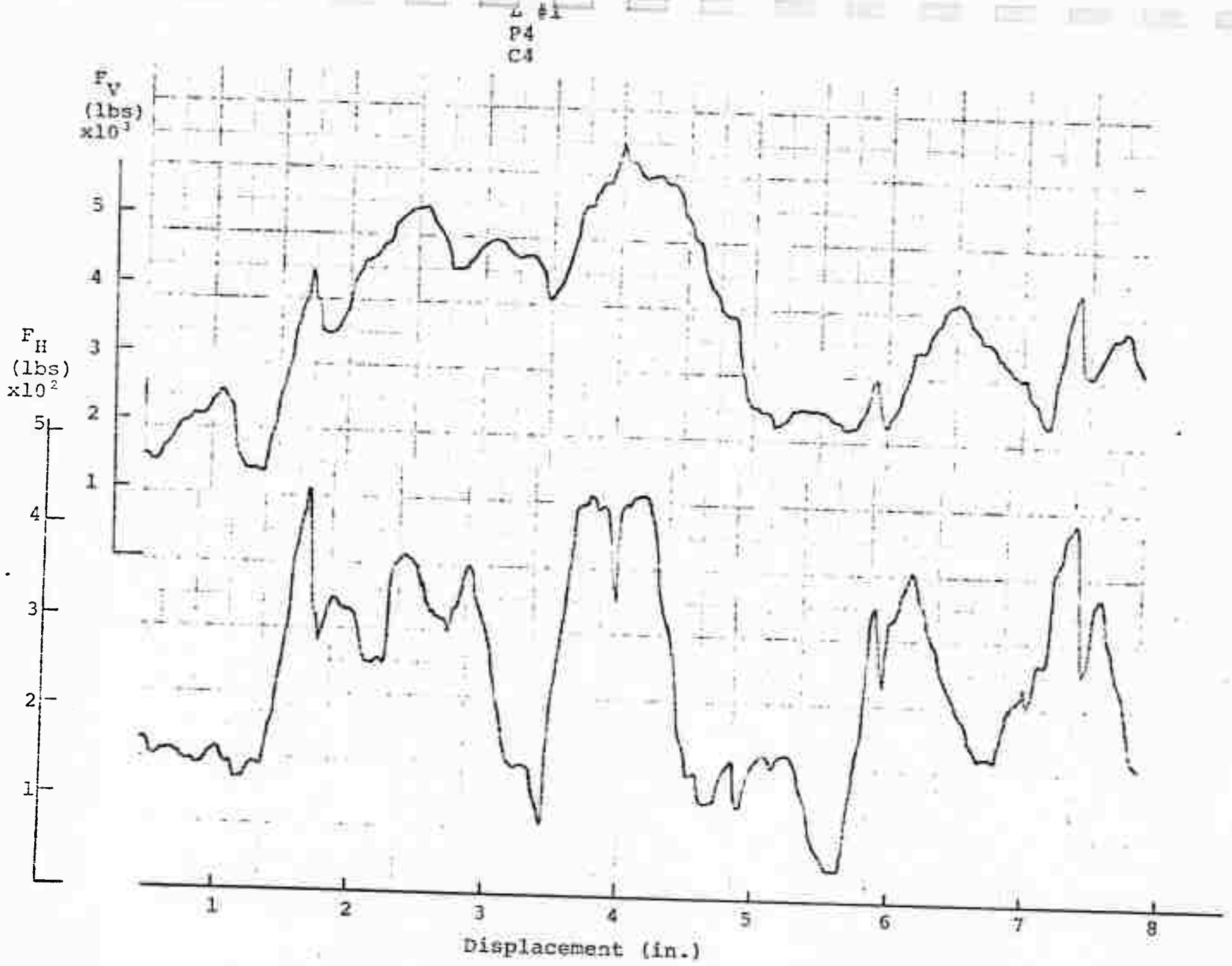
P4
C4
F_V (lbs) x10^3
5
4
3
2
1
F_H (lbs) x10^2
5
4
3
2
1
1
2
3
4
5
6
7
8
Displacement (in.)

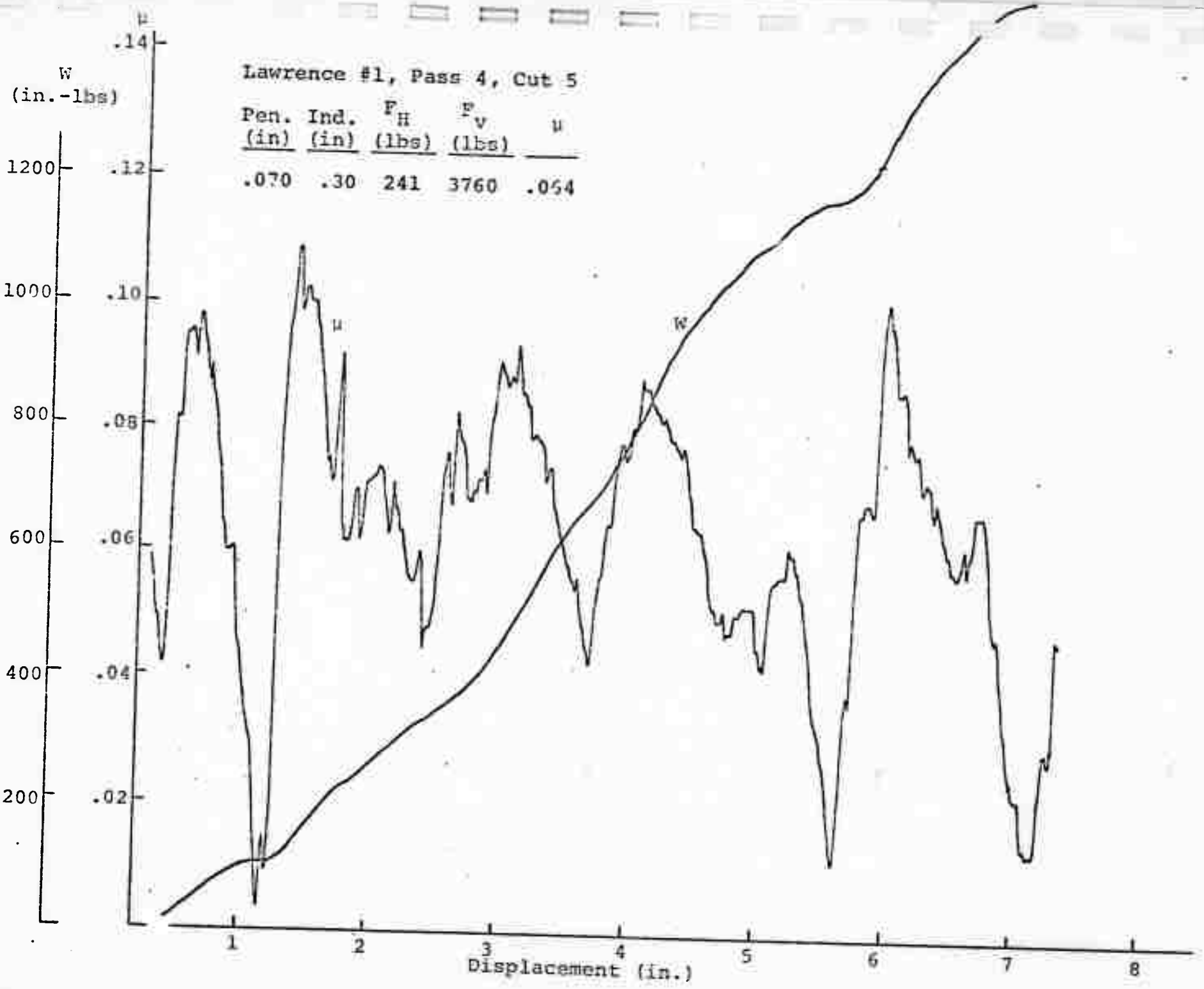
Lawrence #1, Pass 4, Cut 5
Pen. Ind. (in) .070
F_H (lbs) 241
F_V (lbs) 3760
μ .054
W (in.-lbs)
μ
1200
1000
800
600
400
200
.14
.12
.10
.08
.06
.04
.02
μ
W
1
2
3
4
5
6
7
8
Displacement (in.)

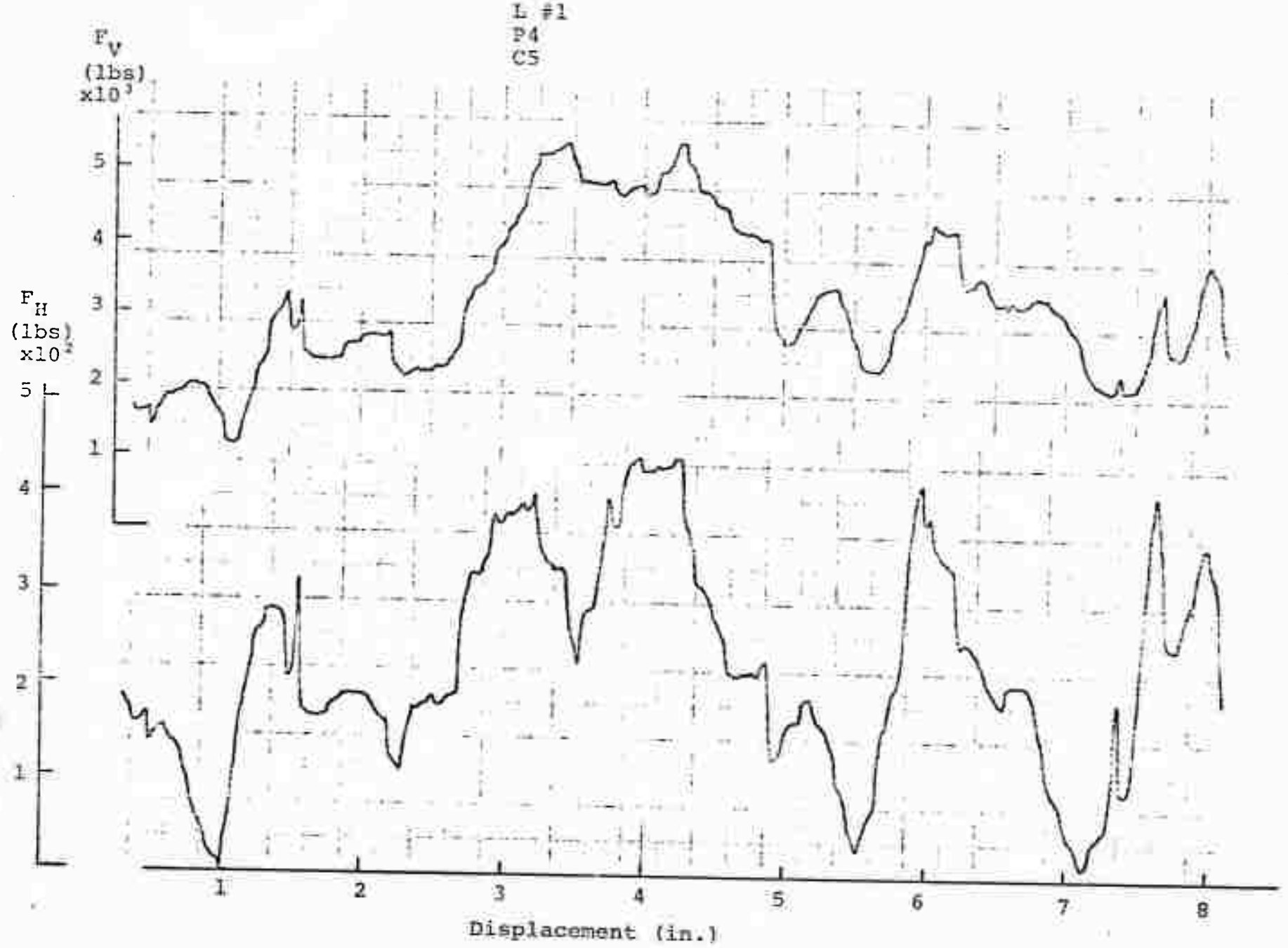
L #1
P4
C5
F_V (lbs) x10³
5
4
3
2
1
F_H (lbs) x10²
5
4
3
2
1
1
2
3
4
5
6
7
8
Displacement (in.)

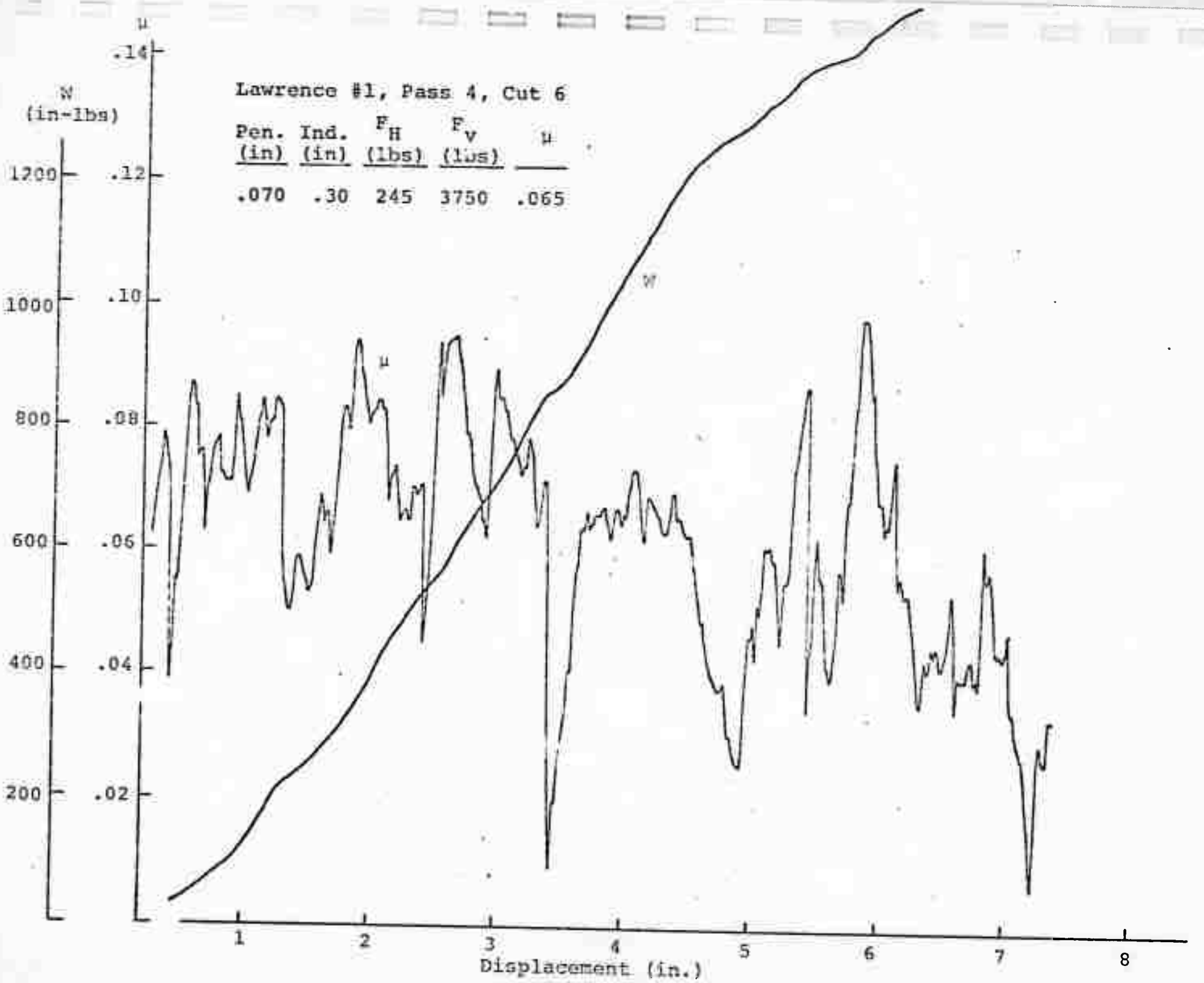
Lawrence #1, Pass 4, Cut 6
Pen. (in) Ind. (in) F_H (lbs) F_V (lbs) μ
.070 .30 245 3750 .065
W (in-lbs)
μ
1200
1000
800
600
400
200
.14
.12
.10
.08
.06
.04
.02
W
μ
1 2 3 4 5 6 7 8
Displacement (in.)

L #1
P4
C6

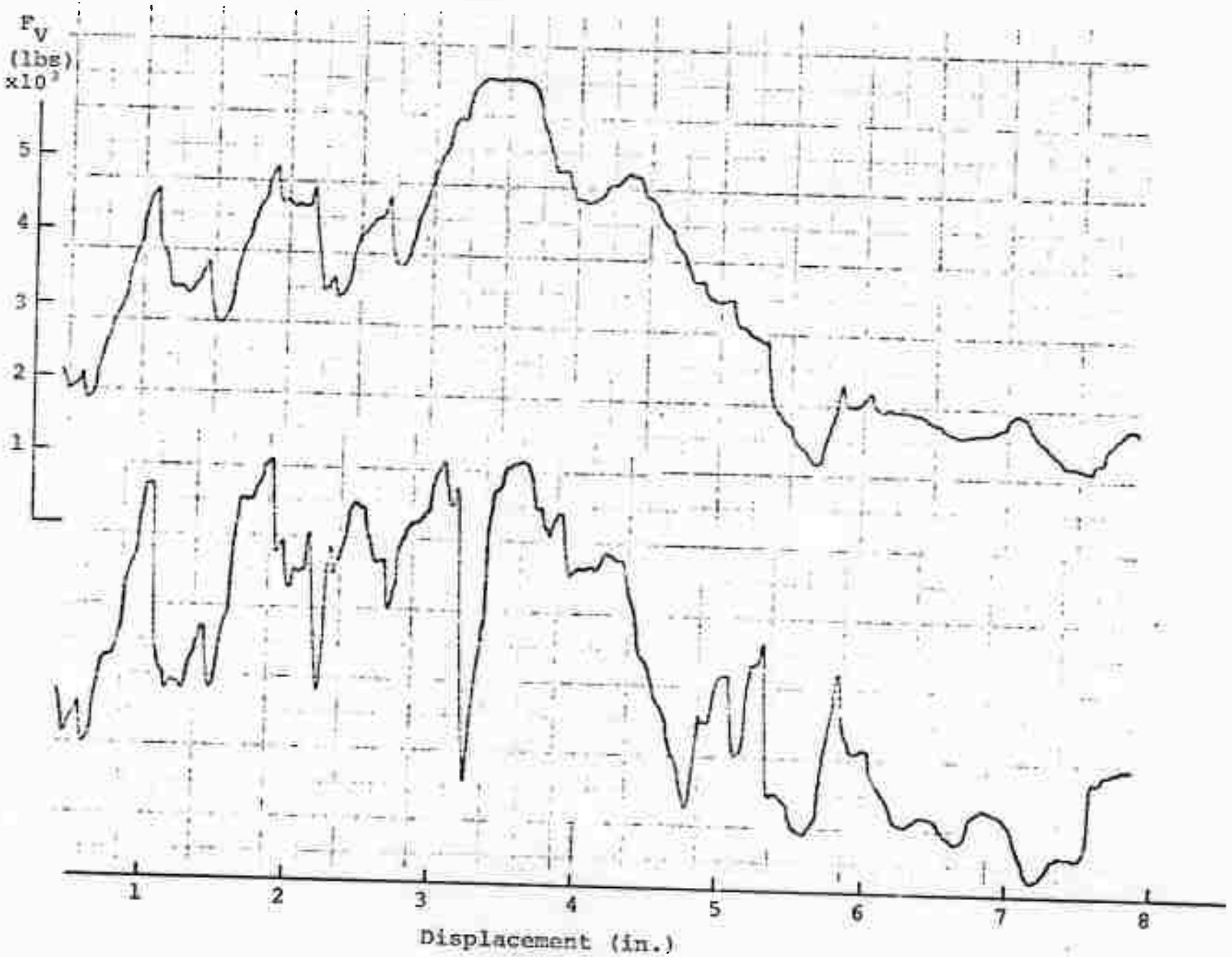

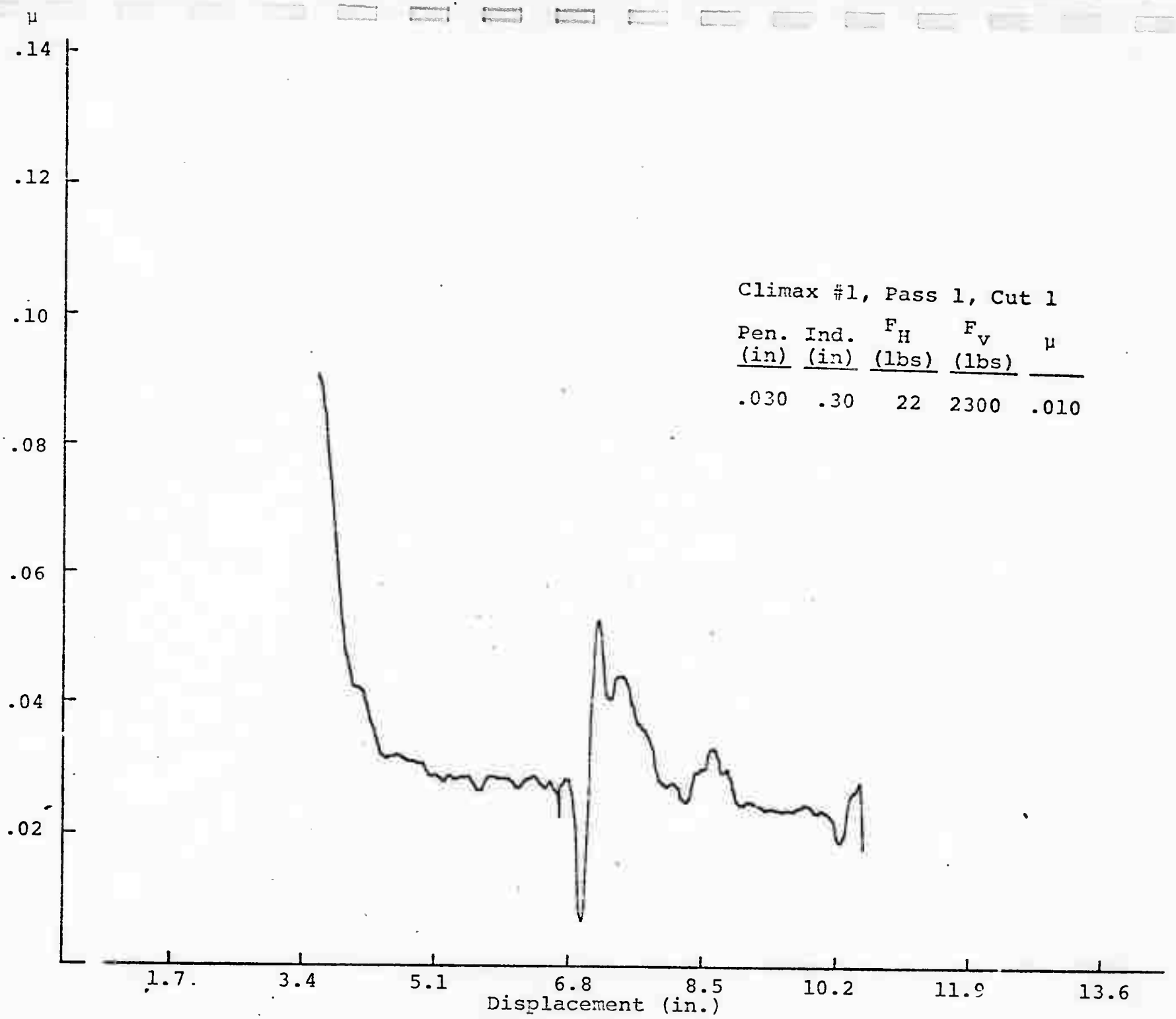
μ
.14
.12
.10
.08
.06
.04
.02
Climax #1, Pass 1, Cut 1
Pen. (in) Ind. (in) F_H (lbs) F_v (lbs) μ
.030 .30 22 2300 .010
1.7
3.4
5.1
6.8
8.5
10.2
11.9
13.6
Displacement (in.)

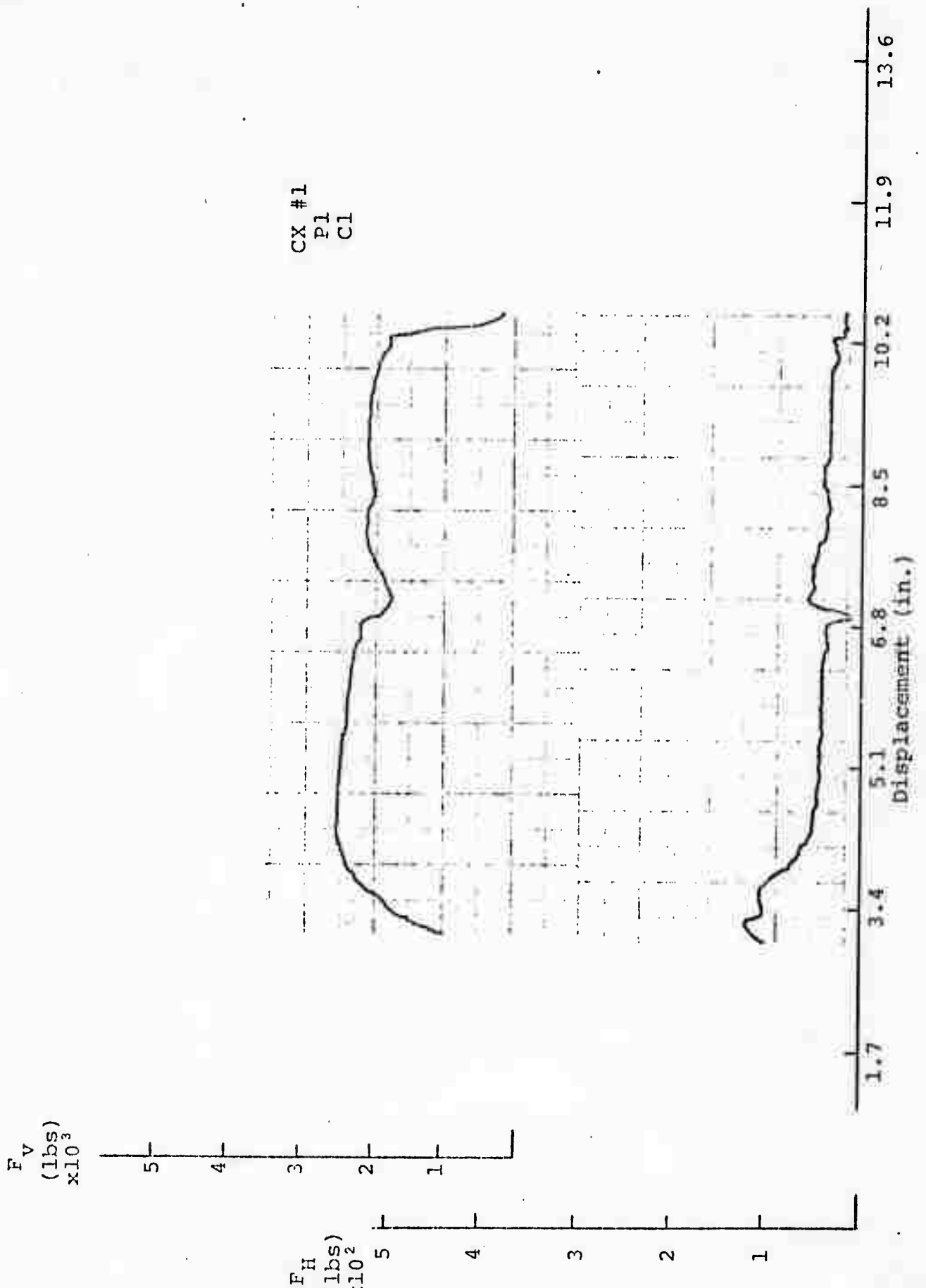
CX #1
P1
C1
F_V (lbs) x10^3
F_H (lbs) x10^2
Displacement (in.)
1.7
3.4
5.1
6.8
8.5
10.2
11.9
13.6

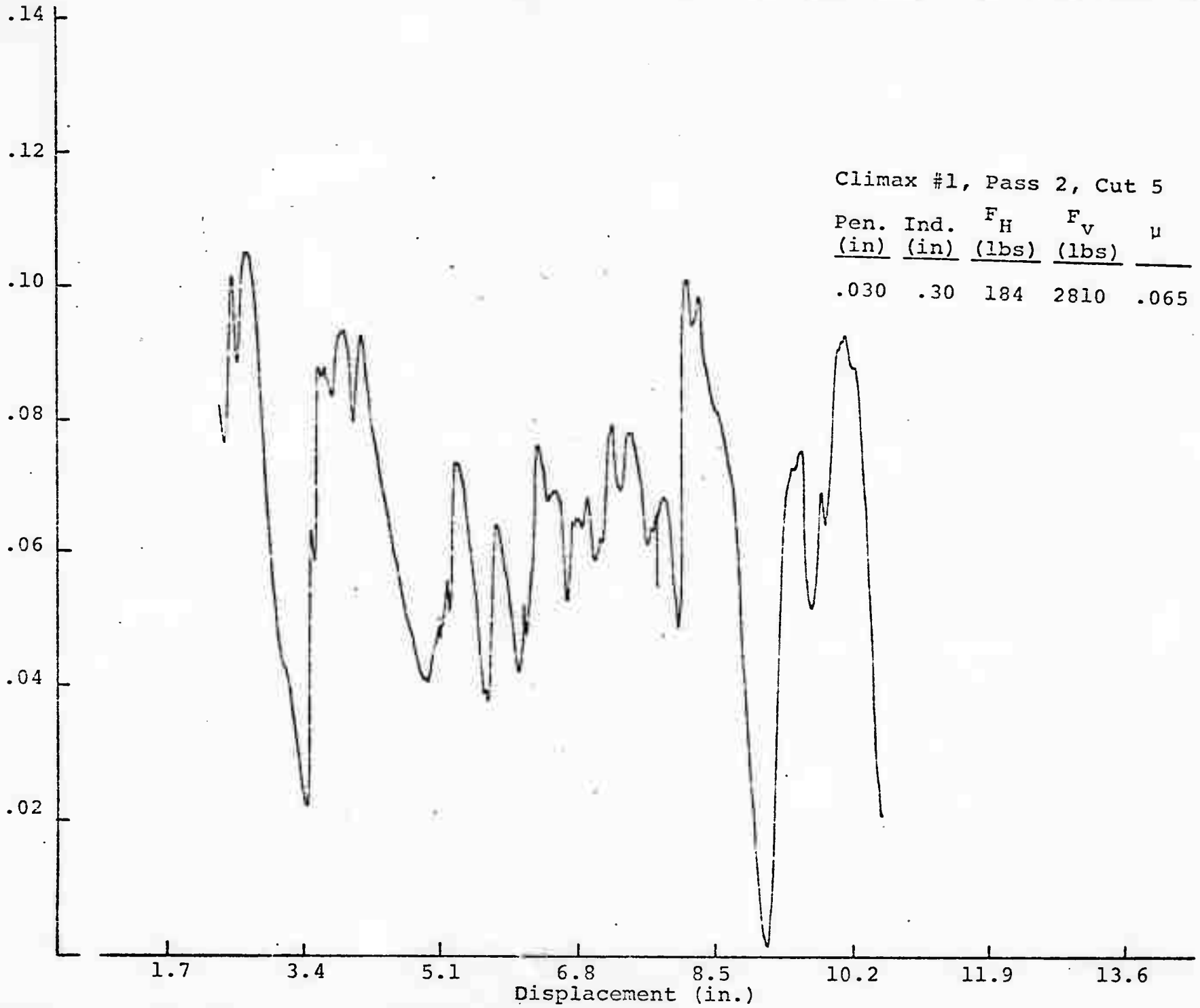
.14
.12
.10
.08
.06
.04
.02
1.7
3.4
5.1
6.8
8.5
10.2
11.9
13.6
Displacement (in.)
Climax #1, Pass 2, Cut 5
Pen. (in) Ind. (in) F_H (lbs) F_V (lbs) μ
.030 .30 184 2810 .065

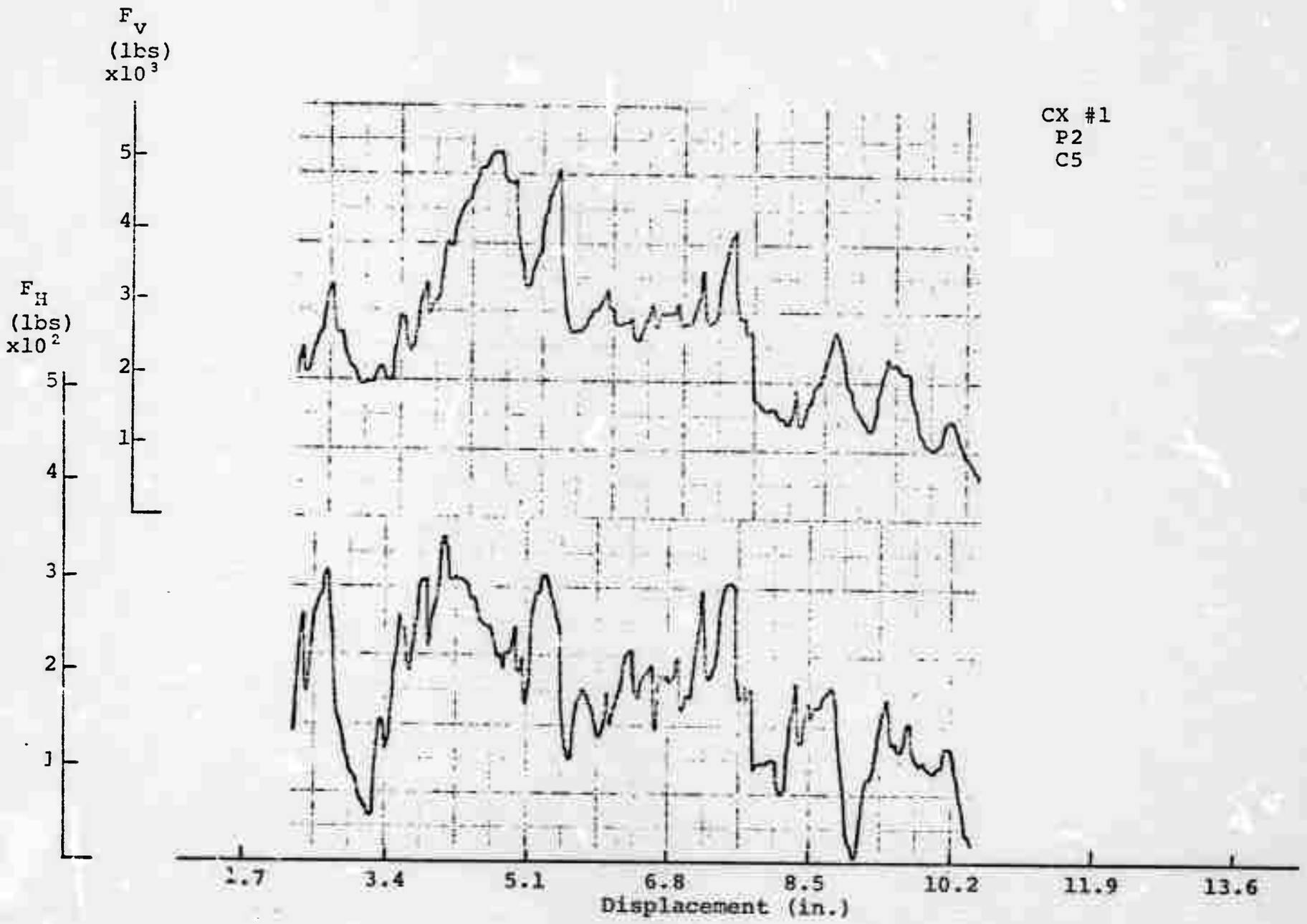
F_V (lbs) x10^3
5
4
3
2
1
F_H (lbs) x10^2
5
4
3
2
1
CX #1
P2
C5
2.7
3.4
5.1
6.8
8.5
10.2
11.9
13.6
Displacement (in.)

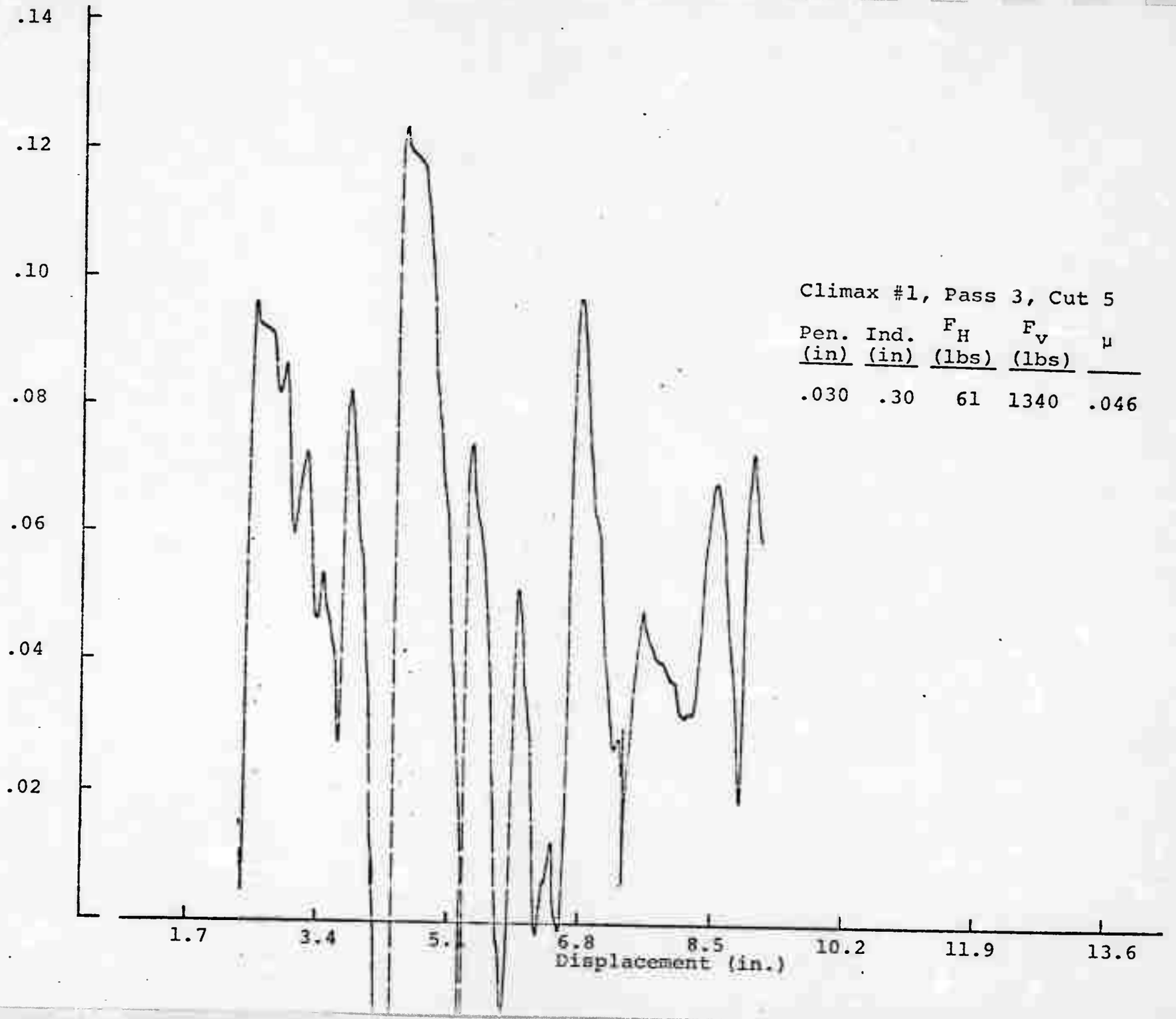

Climax #1, Pass 3, Cut 5

Pen. (in)	Ind. (in)	F_H (lbs)	F_V (lbs)	μ
.030	.30	61	1340	.046

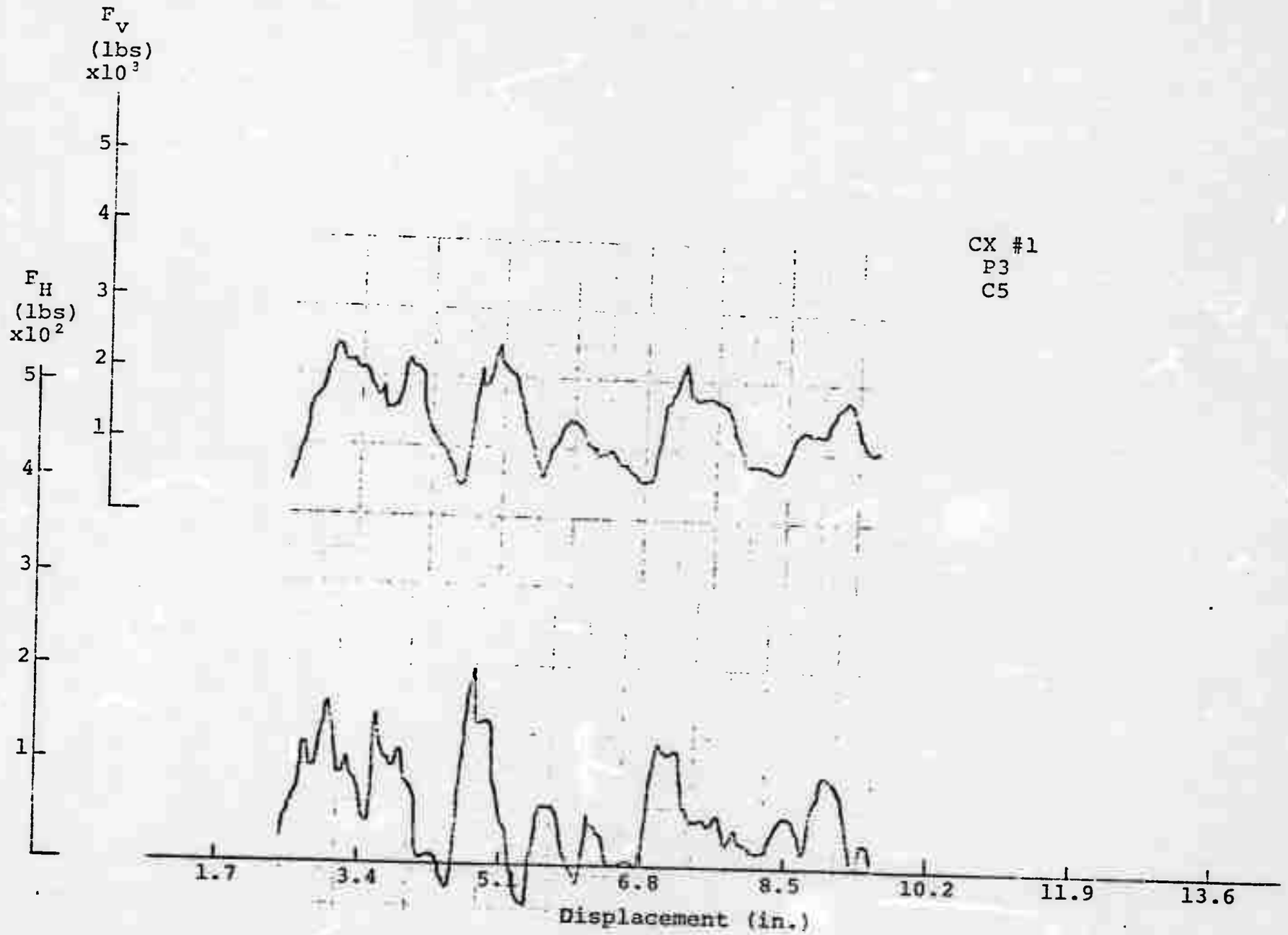
F_V (lbs) x10^3
5
4
3
2
1
F_H (lbs) x10^2
5
4
3
2
1
CX #1
P3
C5
1.7
3.4
5.1
6.8
8.5
10.2
11.9
13.6
Displacement (in.)

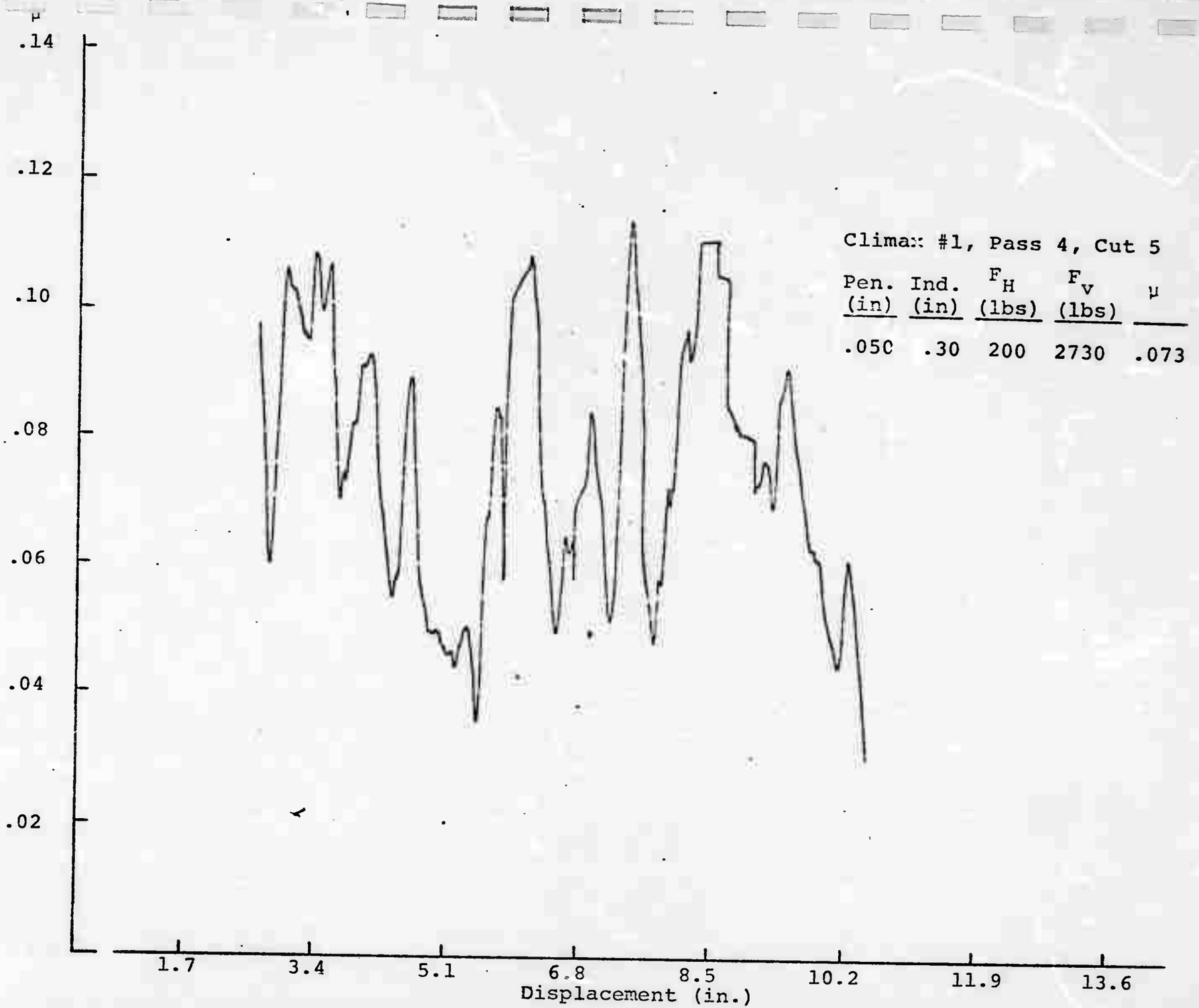

Climax #1, Pass 4, Cut 5

Pen. (in)	Ind. (in)	F_H (lbs)	F_V (lbs)	μ
.050	.30	200	2730	.073

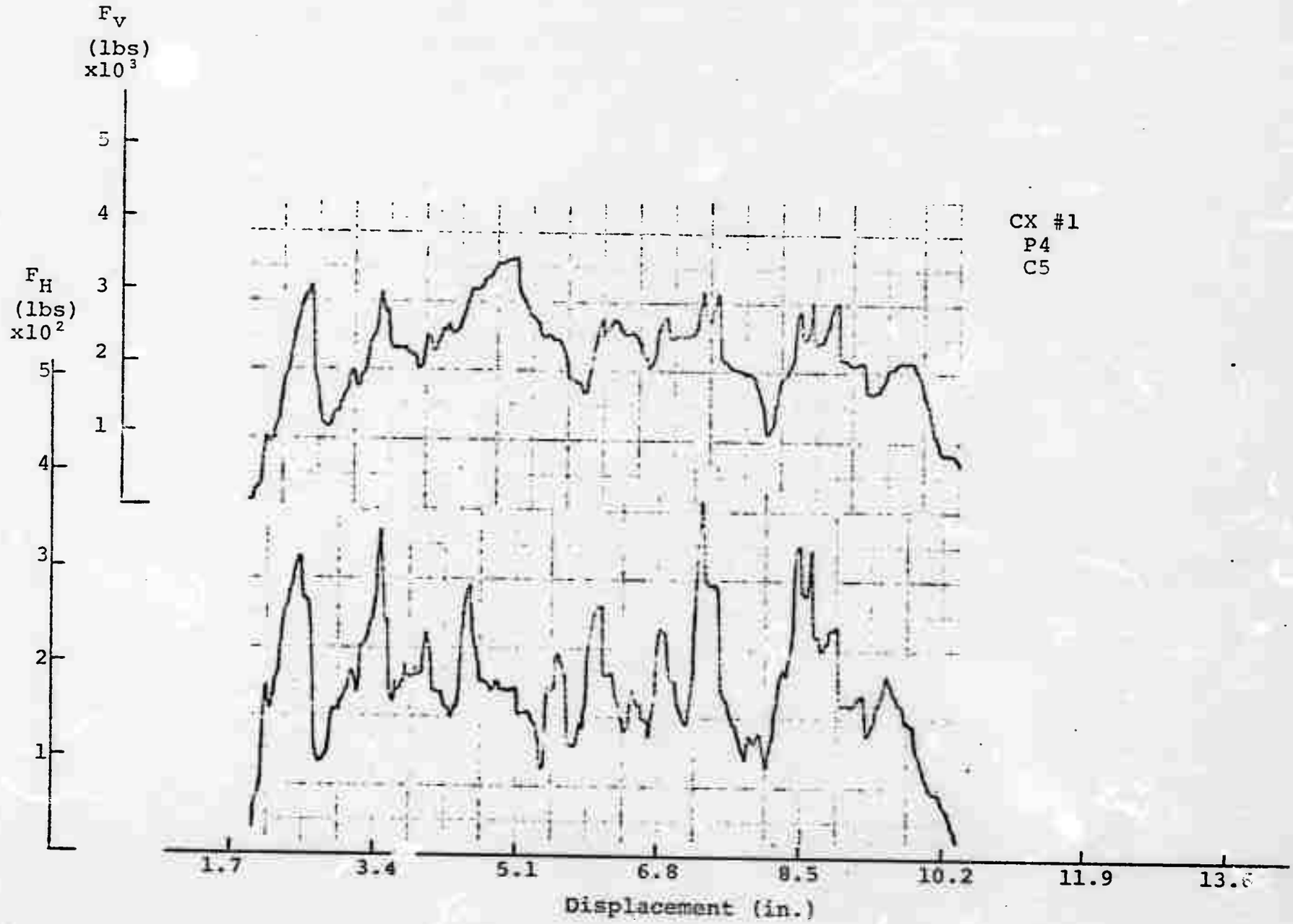
F_V (lbs) x10^3
5
4
3
2
1
F_H (lbs) x10^2
5
4
3
2
1
CX #1
P4
C5
1.7
3.4
5.1
6.8
8.5
10.2
11.9
13.6
Displacement (in.)

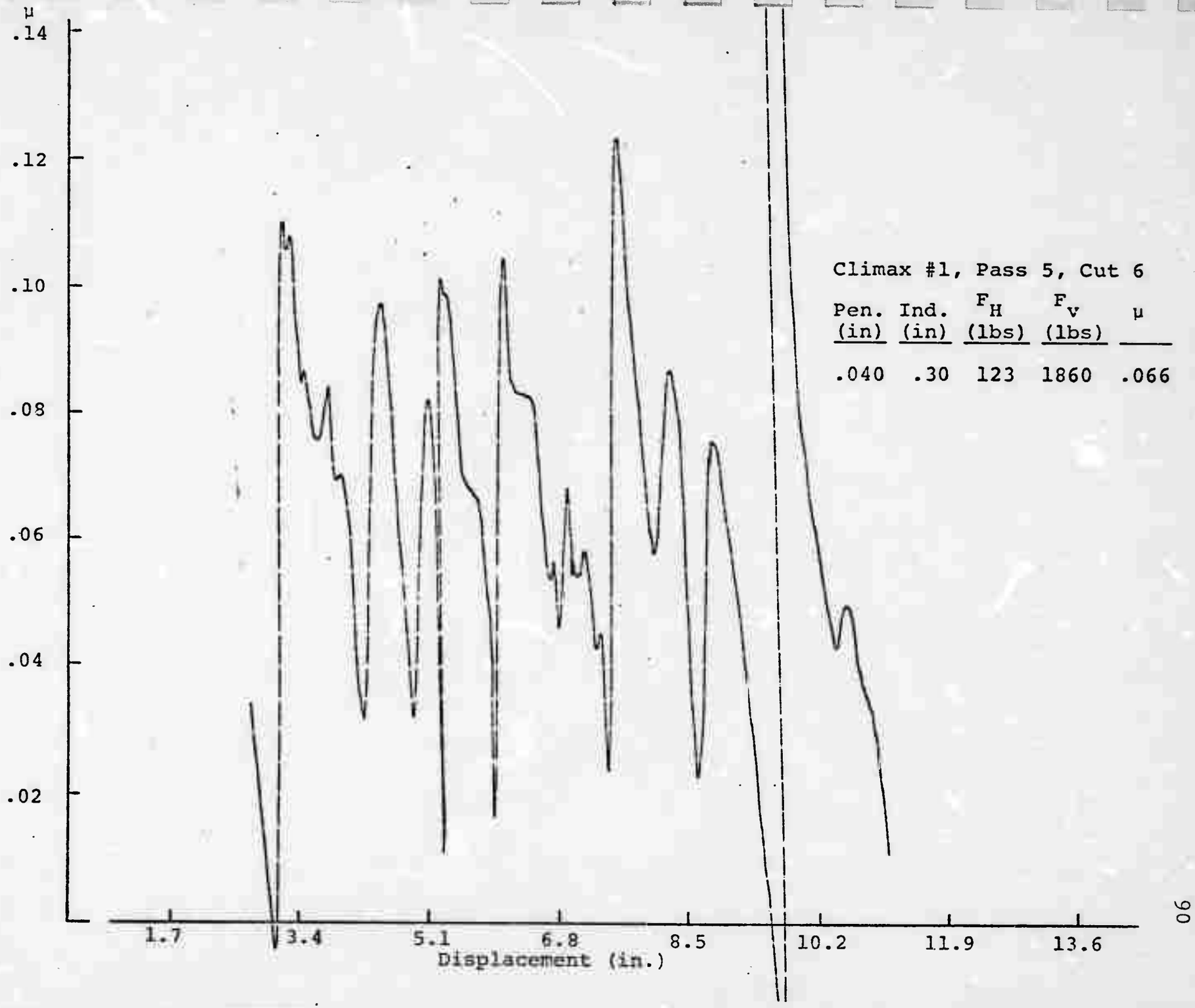

Climax #1, Pass 5, Cut 6

Pen. (in)	Ind. (in)	F_H (lbs)	F_v (lbs)	μ
.040	.30	123	1860	.066

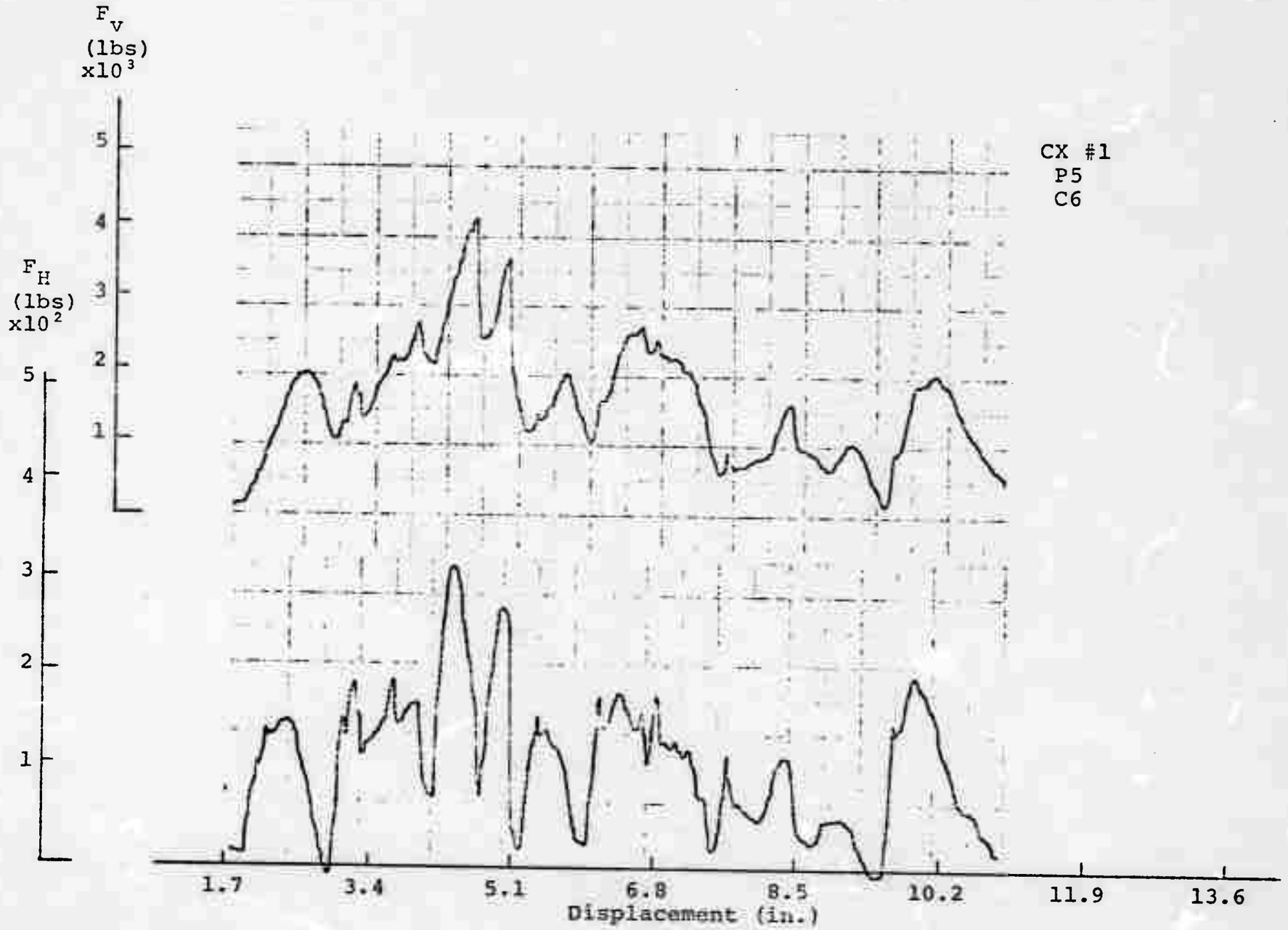
F_V (lbs) x10³
5
4
3
2
1
F_H (lbs) x10²
5
4
3
2
1
CX #1
P5
C6
1.7
3.4
5.1
6.8
8.5
10.2
11.9
13.6
Displacement (in.)

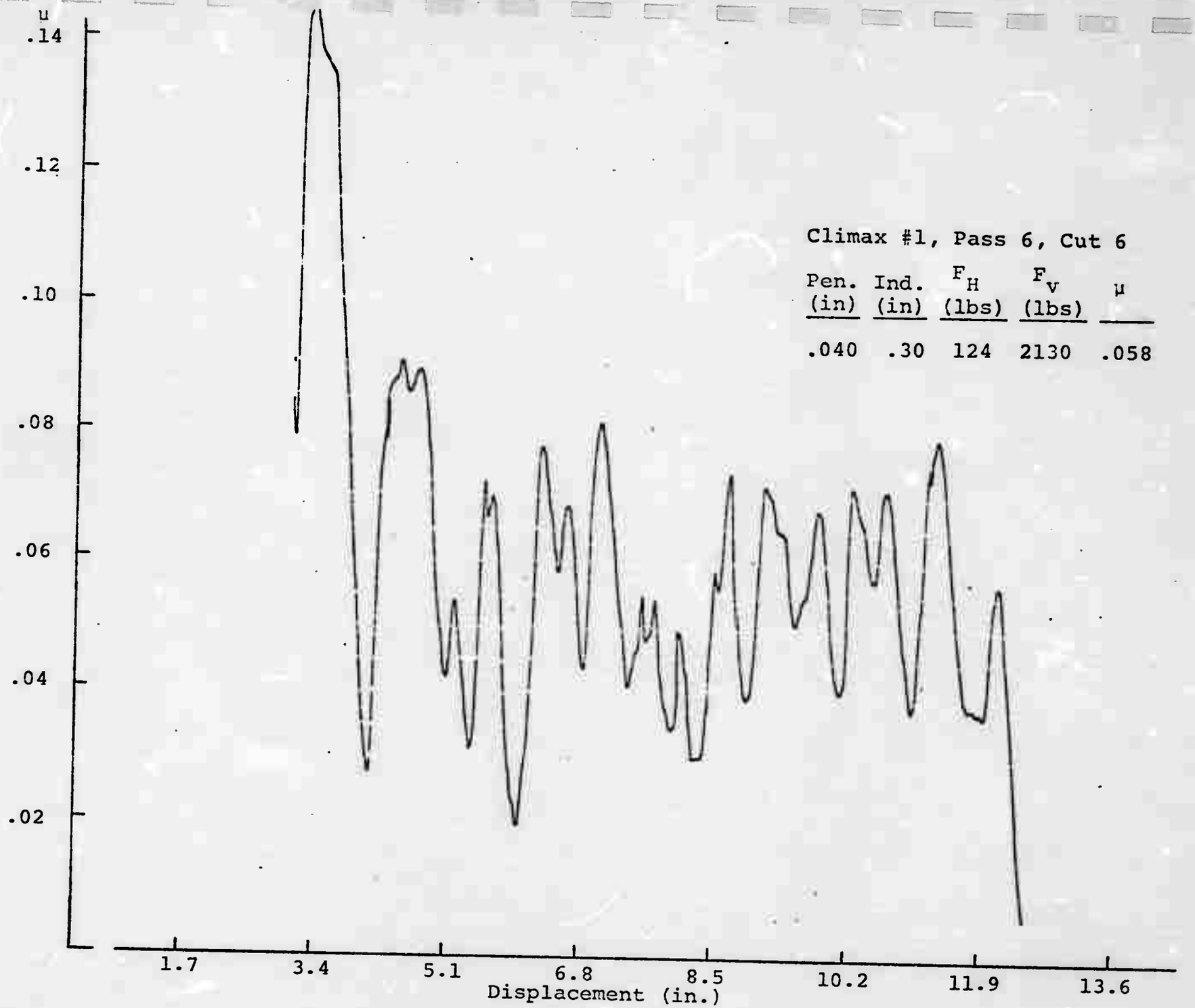

Climax #1, Pass 6, Cut 6

Pen. (in)	Ind. (in)	F_H (lbs)	F_V (lbs)	μ
.040	.30	124	2130	.058

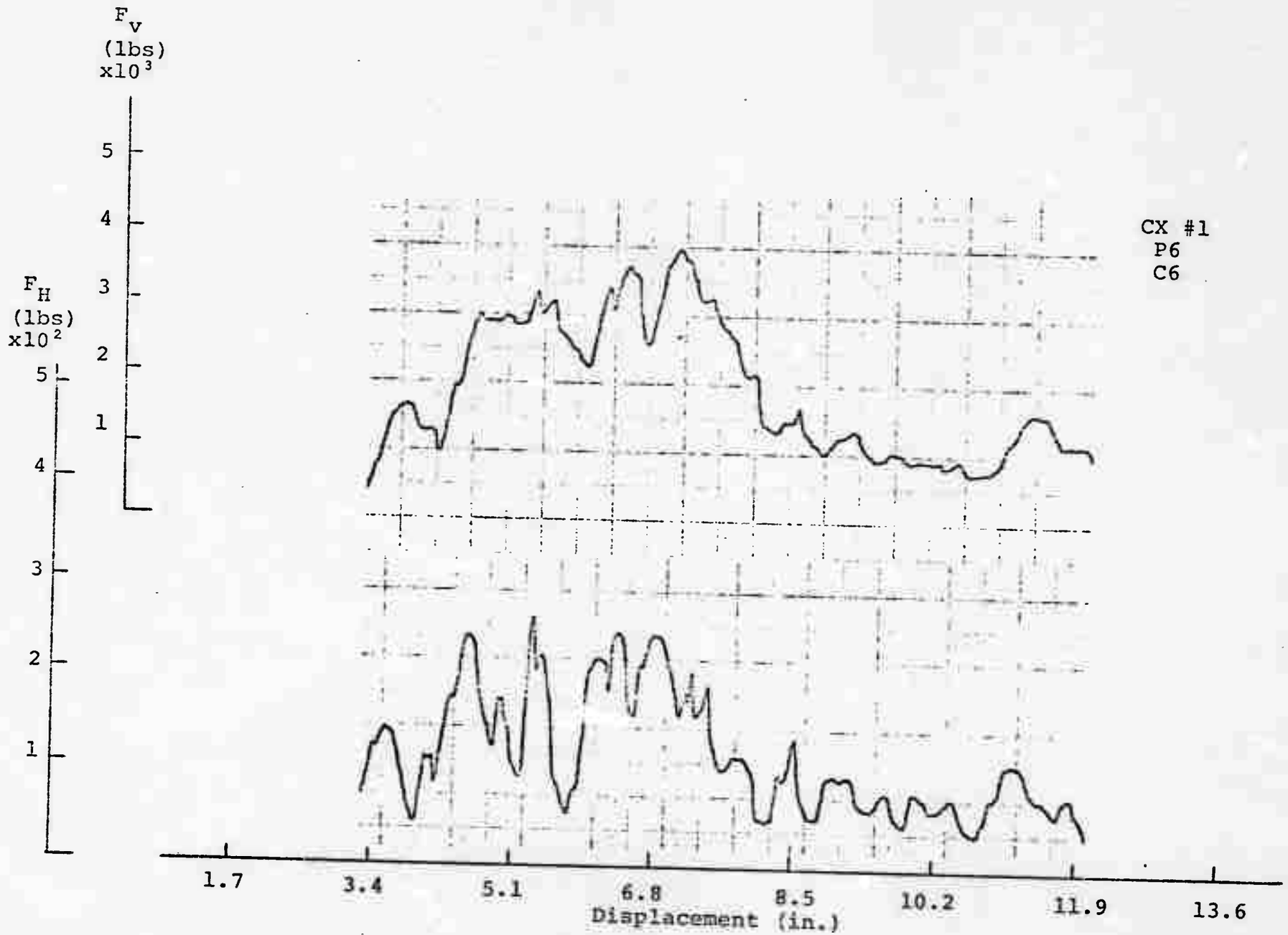
F_V (lbs) x10^3
5
4
3
2
1
F_H (lbs) x10^2
5
4
3
2
1
CX #1
P6
C6
1.7
3.4
5.1
6.8
8.5
10.2
11.9
13.6
Displacement (in.)

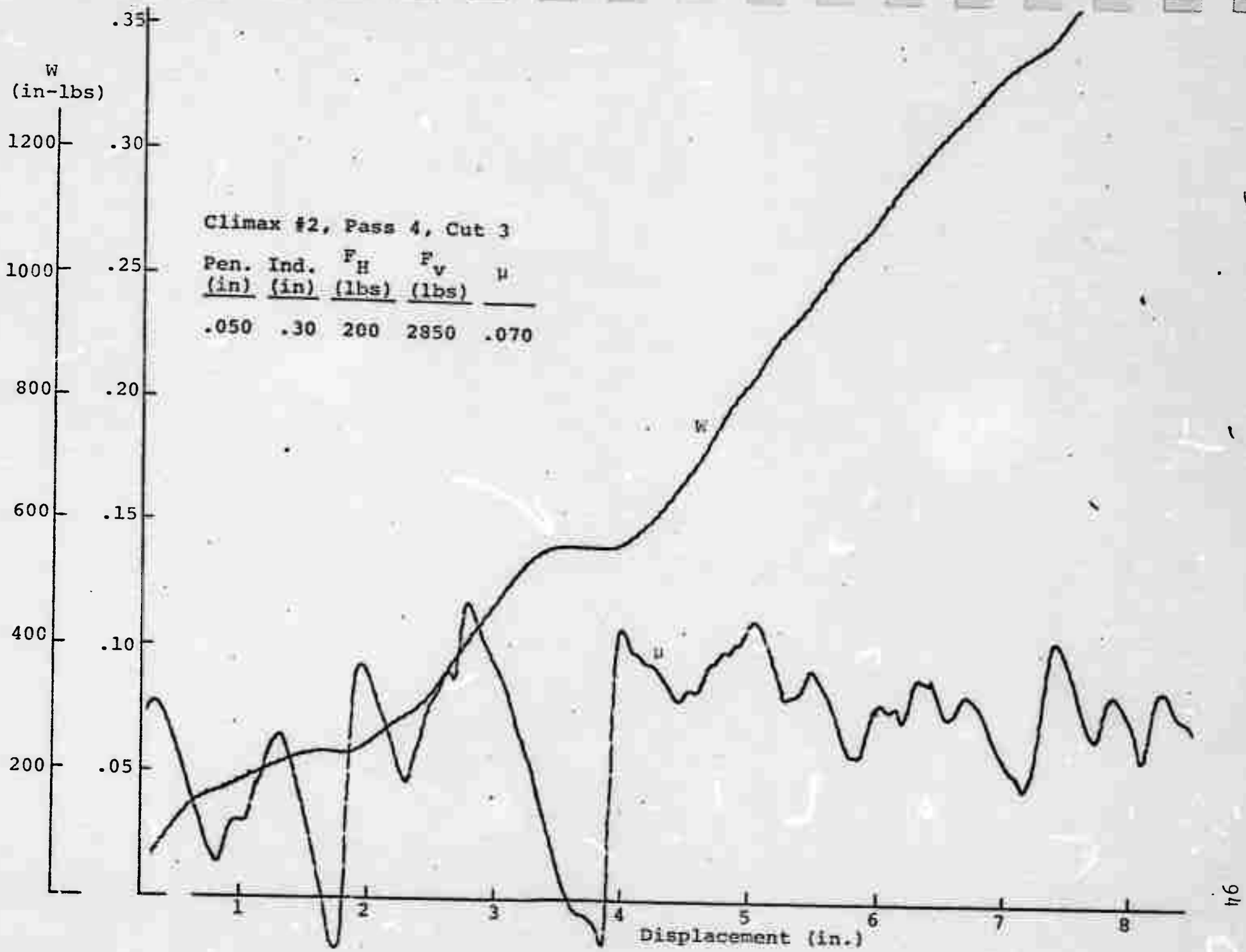
W
(in-lbs)
1200
1000
800
600
400
200
.35
.30
.25
.20
.15
.10
.05
Climax #2, Pass 4, Cut 3
Pen. (in) Ind. (in) F_H (lbs) F_V (lbs) μ
.050 .30 200 2850 .070
W
μ
1
2
3
4
5
6
7
8
Displacement (in.)

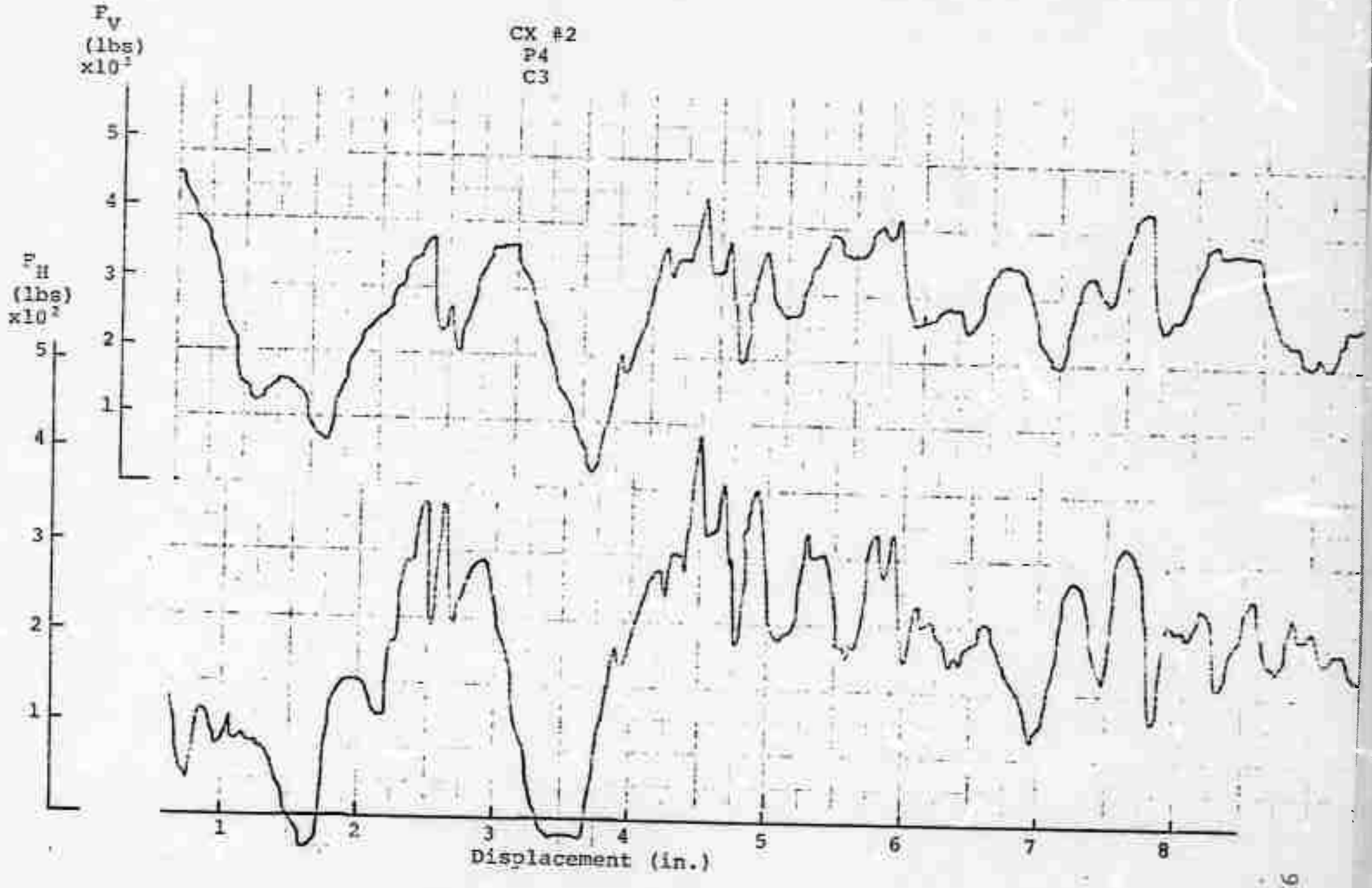
CX #2
P4
C3
P_V (lbs) x10²
P_H (lbs) x10²
1
2
3
4
5
Displacement (in.)
6
7
8

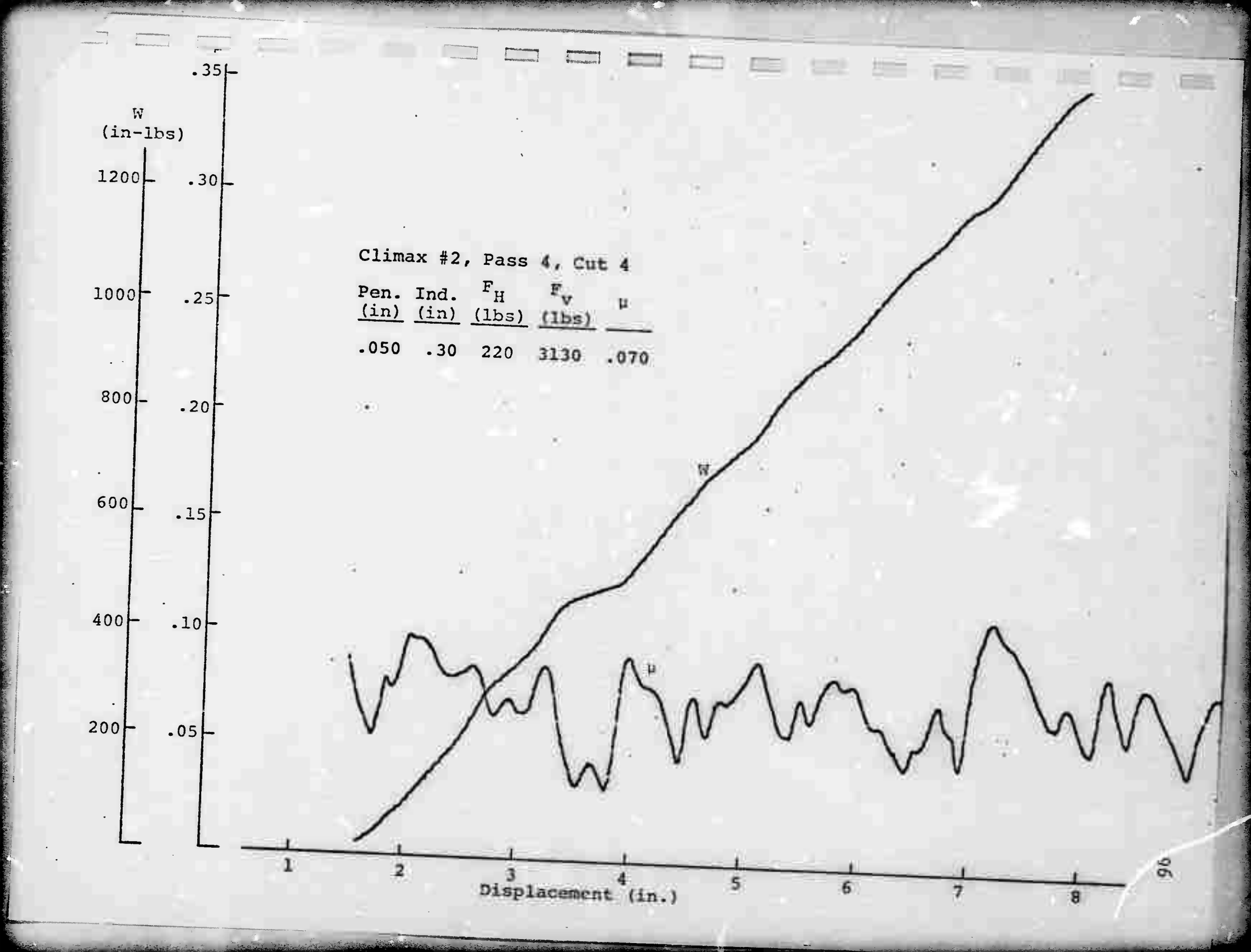
W
(in-lbs)
1200
1000
800
600
400
200
.35
.30
.25
.20
.15
.10
.05
Climax #2, Pass 4, Cut 4
Pen. Ind. F_H F_V μ
(in) (in) (lbs) (lbs)
.050 .30 220 3130 .070
W
μ
1
2
3
4
5
6
7
8
Displacement (in.)

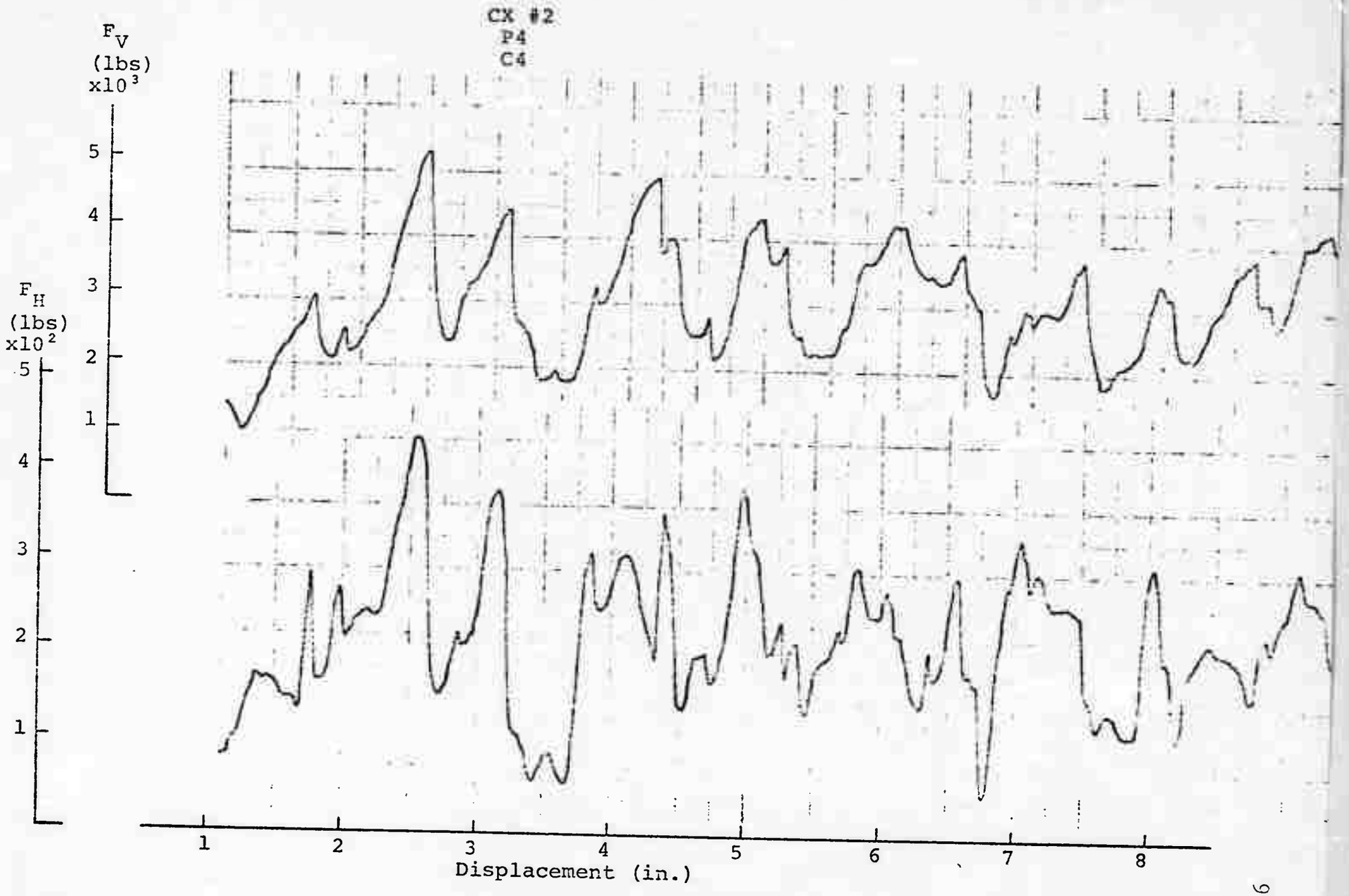
CX #2
P4
C4
F_V (lbs) x10^3
5
4
3
2
1
F_H (lbs) x10^2
5
4
3
2
1
1
2
3
4
5
6
7
8
Displacement (in.)

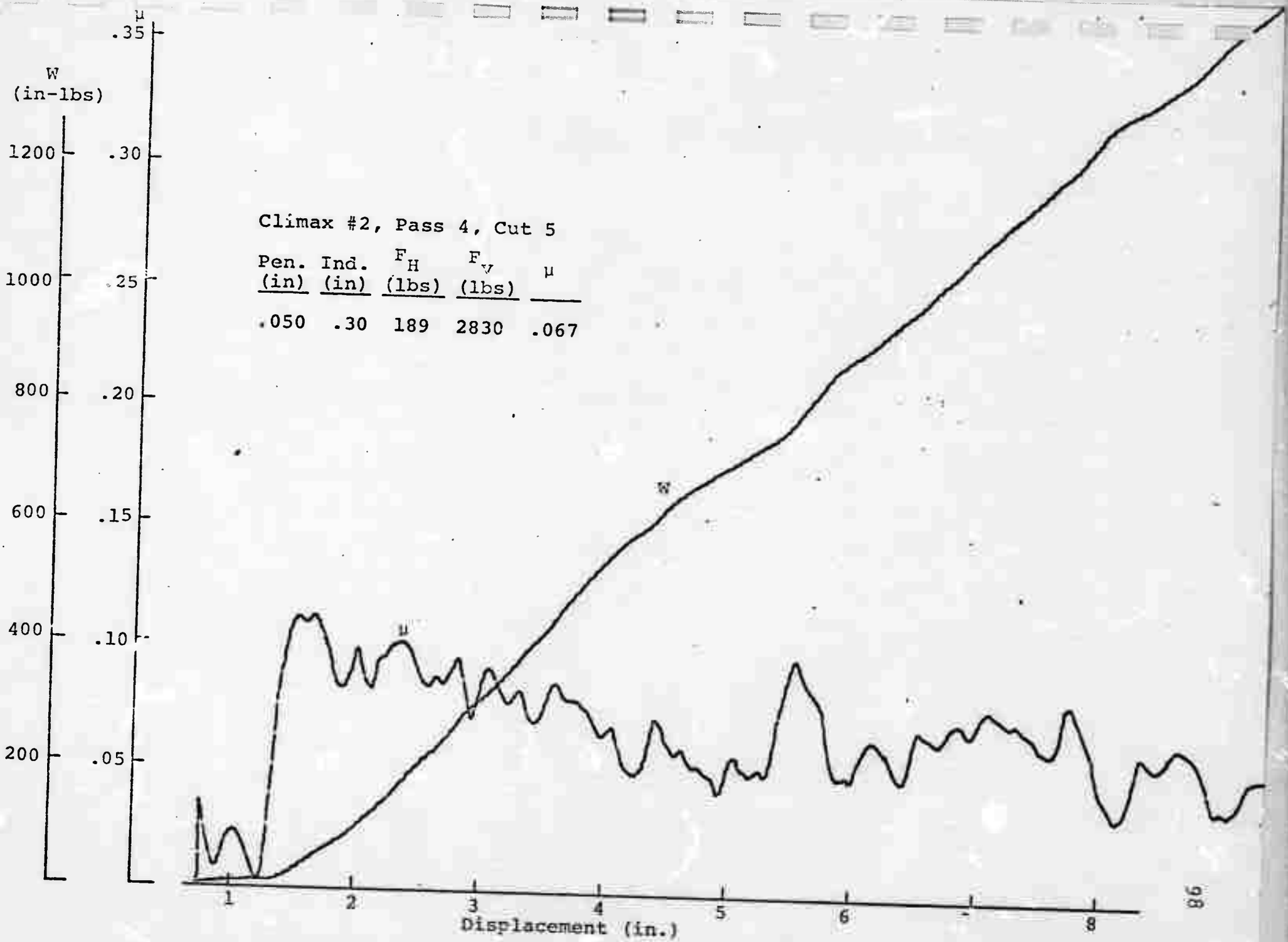
μ
.35
W
(in-lbs)
1200
.30
1000
.25
800
.20
600
.15
400
.10
200
.05
Climax #2, Pass 4, Cut 5
Pen. (in) Ind. (in) F_H (lbs) F_V (lbs) μ
.050 .30 189 2830 .067
W
μ
1
2
3
4
5
6
8
Displacement (in.)
86

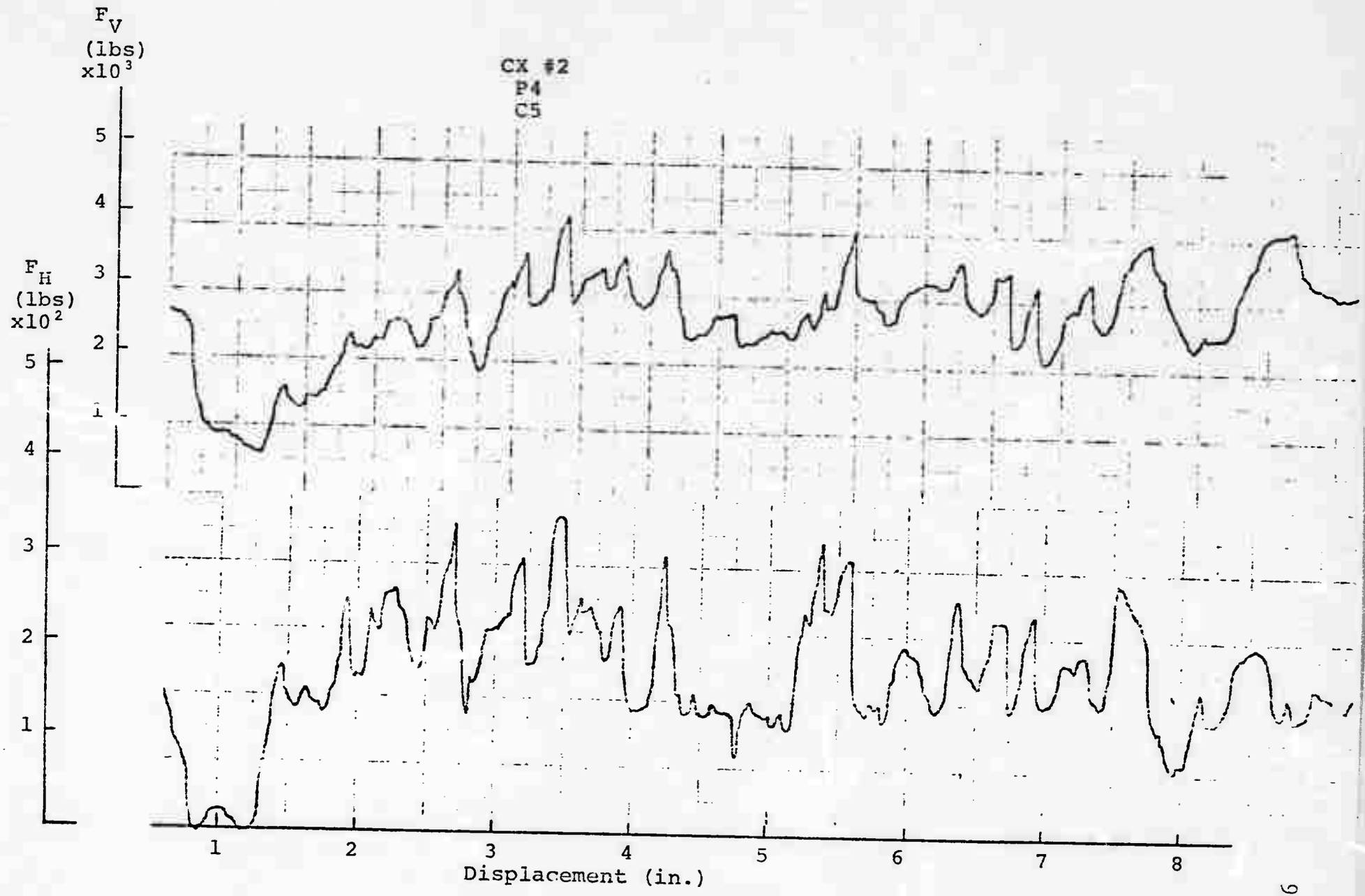
CX #2
P4
C5
F_V (lbs) x10^3
5
4
3
2
1
F_H (lbs) x10^2
5
4
3
2
1
1
2
3
4
5
6
7
8
Displacement (in.)

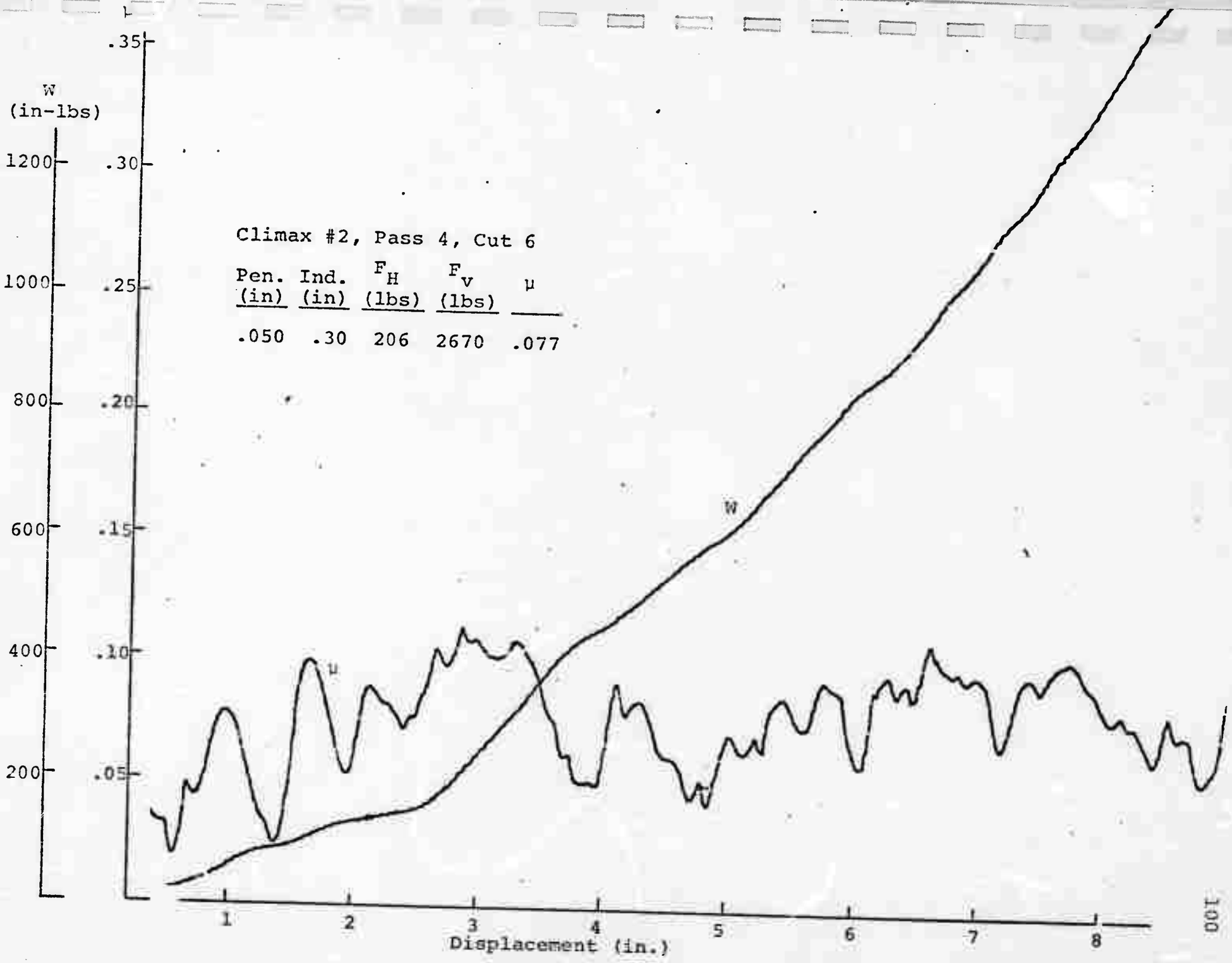
μ
.35
W
(in-lbs)
1200
.30
1000
.25
800
.20
600
.15
400
.10
200
.05
Climax #2, Pass 4, Cut 6
Pen. (in) Ind. (in) F_H (lbs) F_V (lbs) μ
.050 .30 206 2670 .077
W
μ
1
2
3
4
5
6
7
8
Displacement (in.)
100

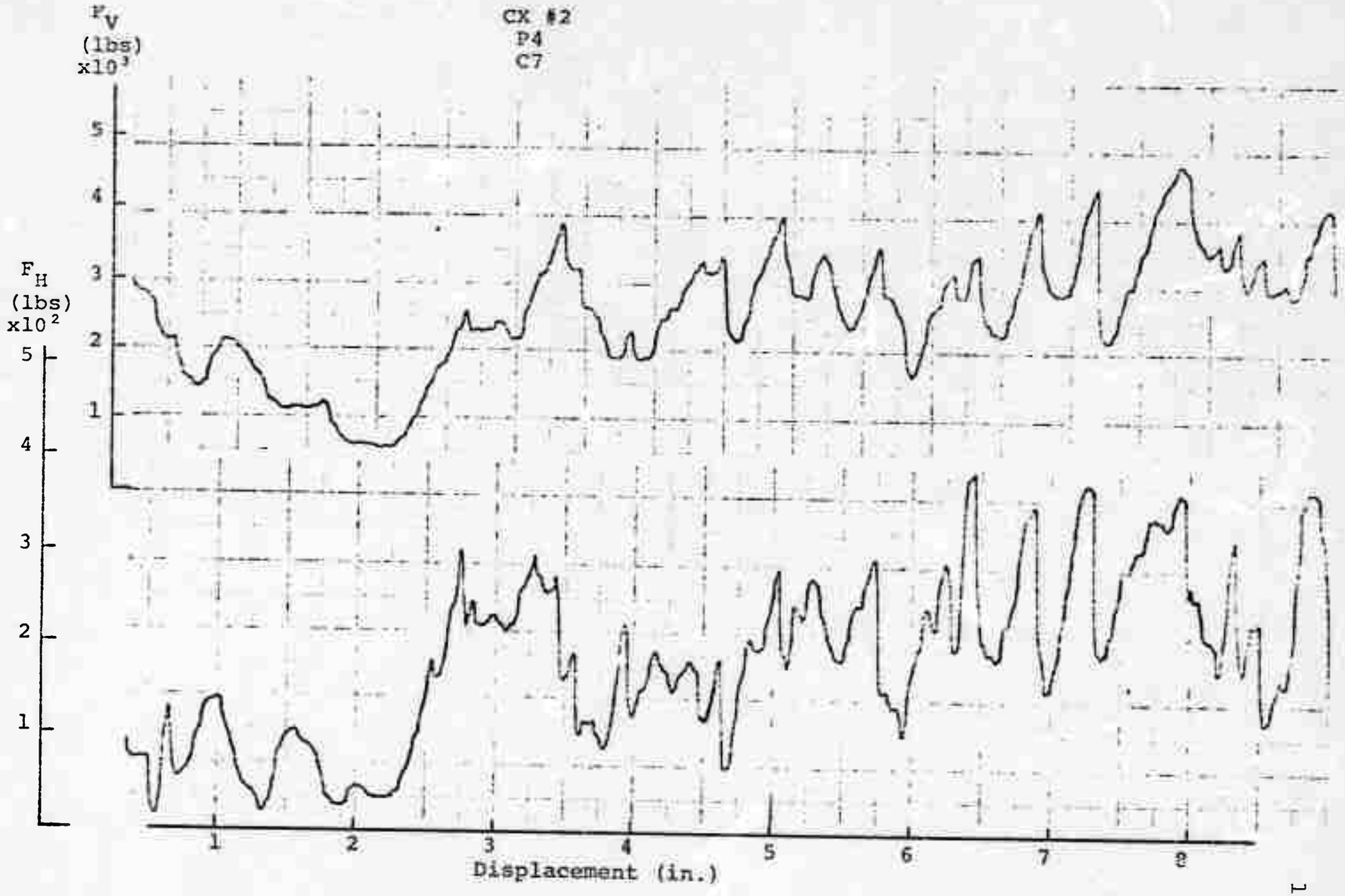
F_V (lbs) x10³
CX #2
P4
C7
5
4
3
2
1
F_H (lbs) x10²
5
4
3
2
1
1
2
3
4
5
6
7
8
Displacement (in.)

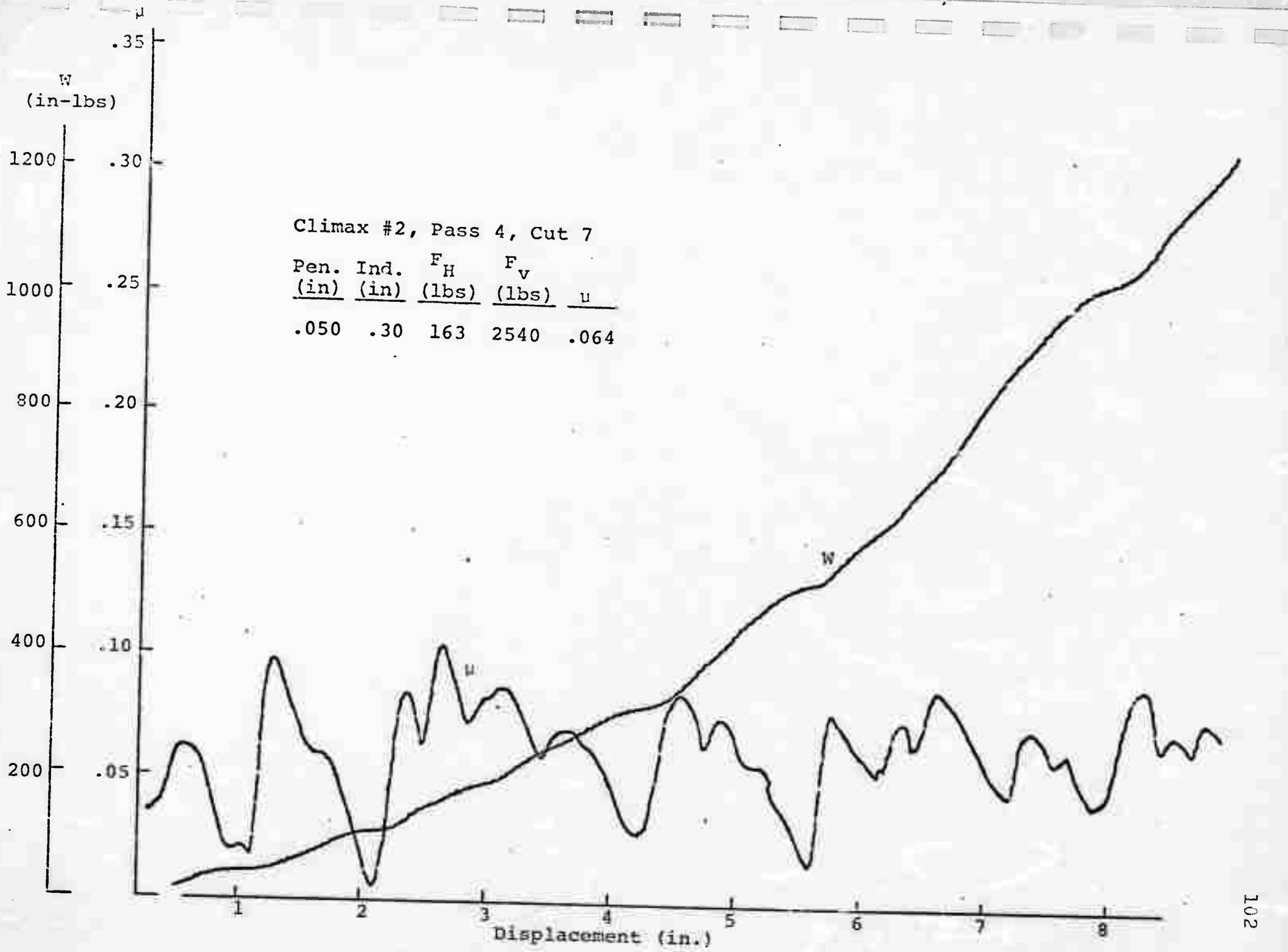
μ
.35
W
(in-lbs)
1200
.30
1000
.25
800
.20
600
.15
400
.10
200
.05
Climax #2, Pass 4, Cut 7
Pen. (in) | Ind. (in) | F_H (lbs) | F_V (lbs) | u
.050 | .30 | 163 | 2540 | .064
W
μ
1
2
3
4
5
6
7
8
Displacement (in.)

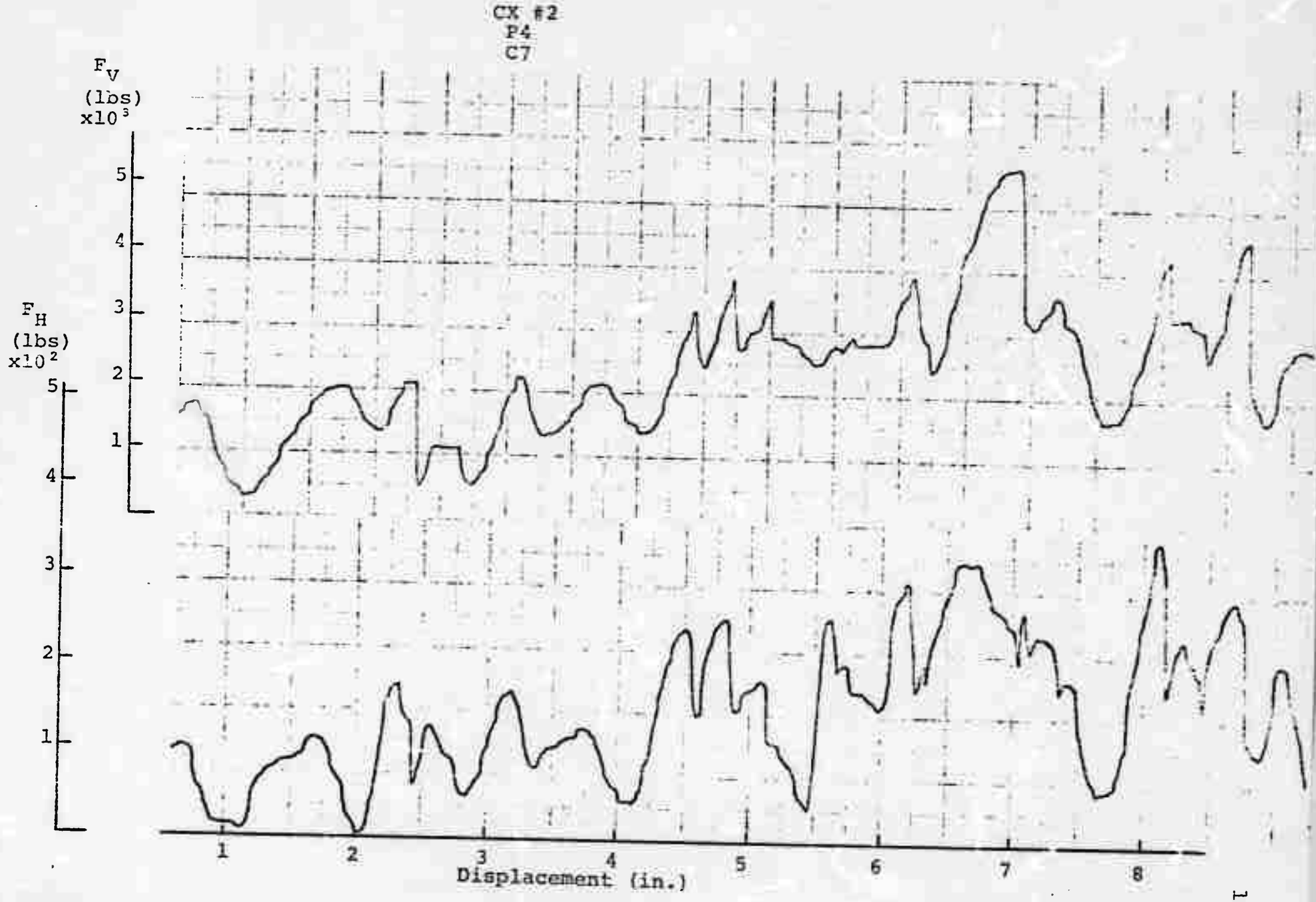
CX #2
P4
C7
F_V (lbs) x10^3
5
4
3
2
1
F_H (lbs) x10^2
5
4
3
2
1
1
2
3
4
5
6
7
8
Displacement (in.)

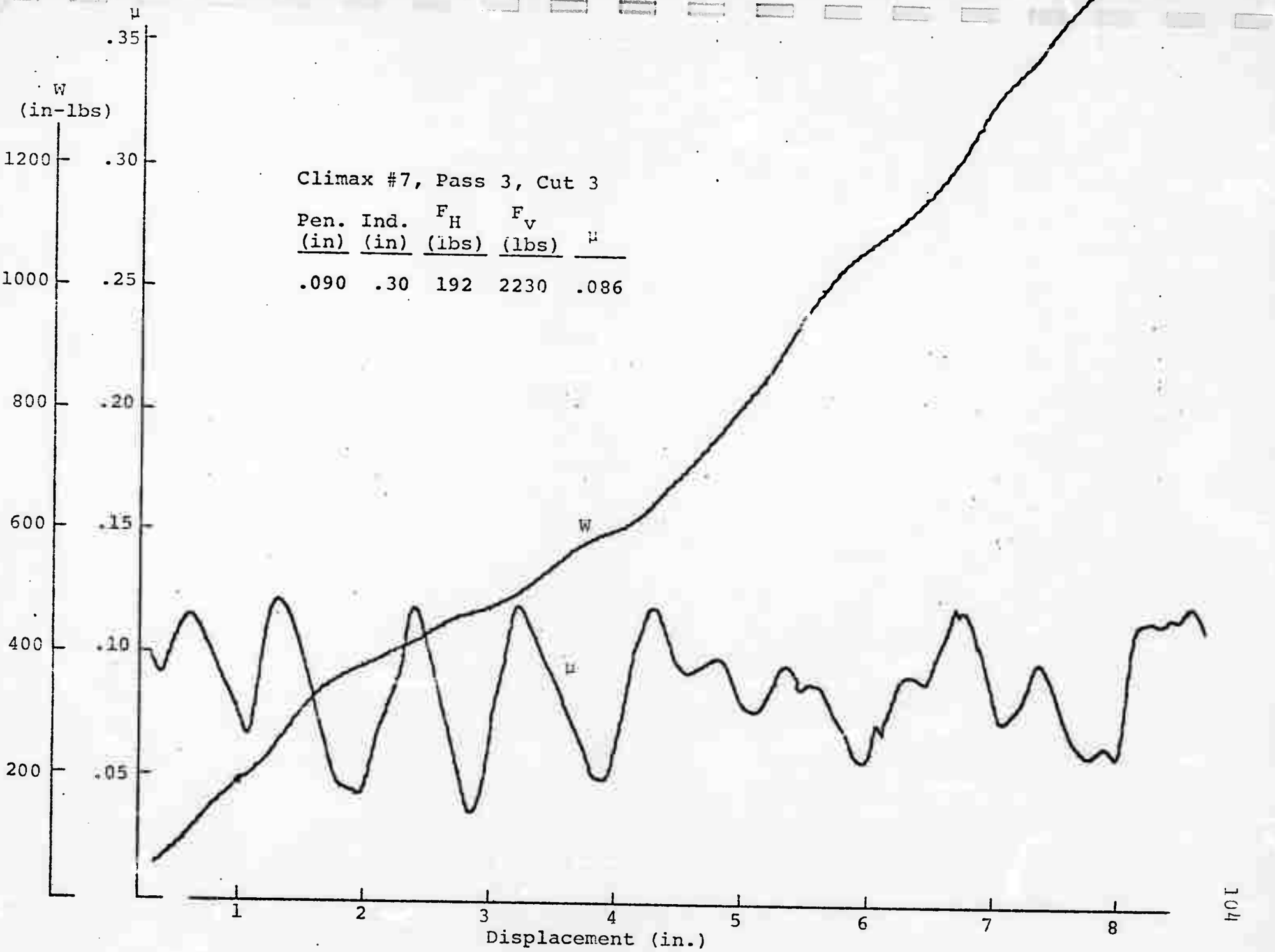

Climax #7, Pass 3, Cut 3

Pen. Ind. (in)	(in)	F_H (lbs)	F_V (lbs)	μ
.090	.30	192	2230	.086

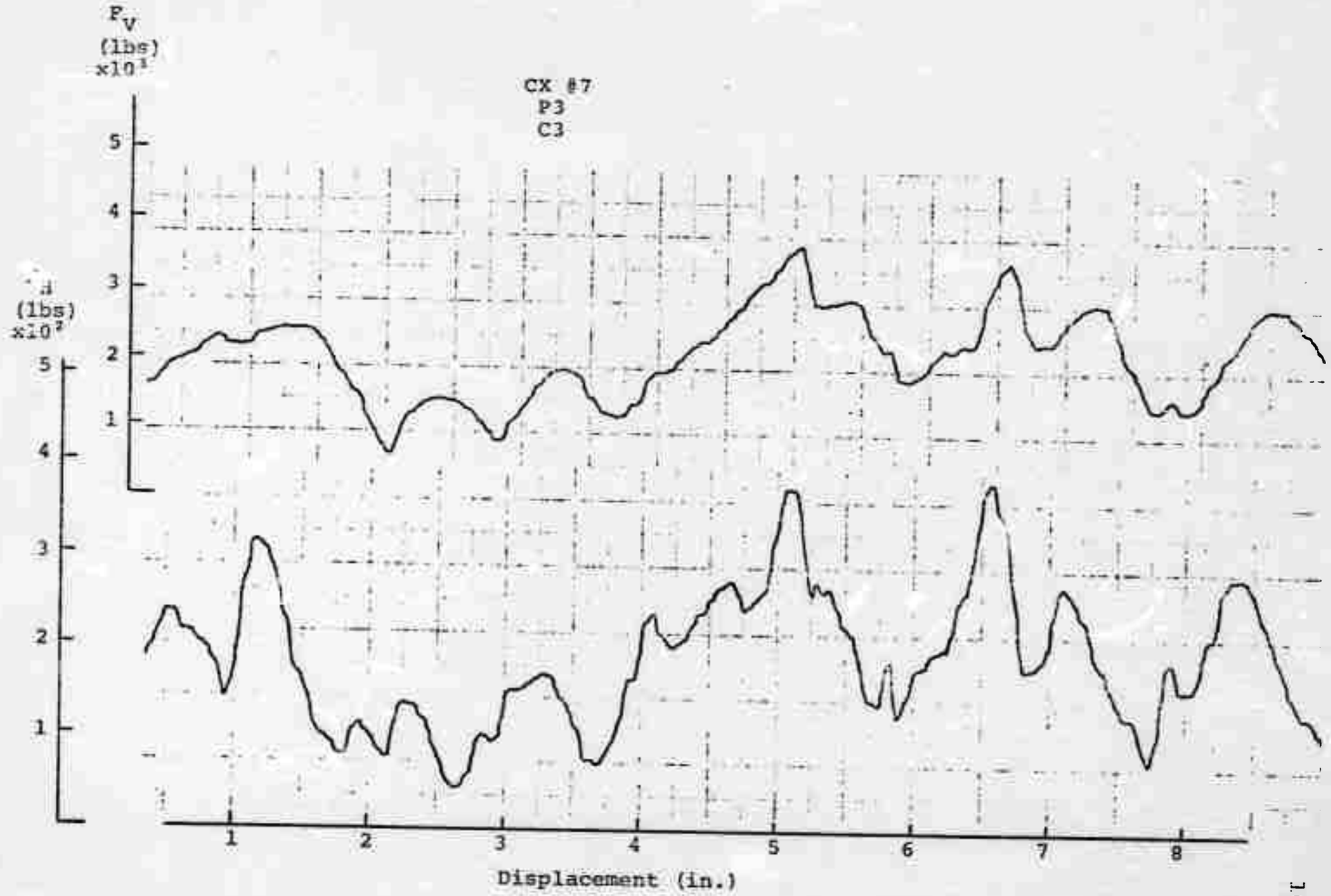
P_V
(lbs)
x10³
CX #7
P3
C3
5
4
3
2
1
(lbs)
x10²
5
4
3
2
1
1
2
3
4
5
6
7
8
Displacement (in.)

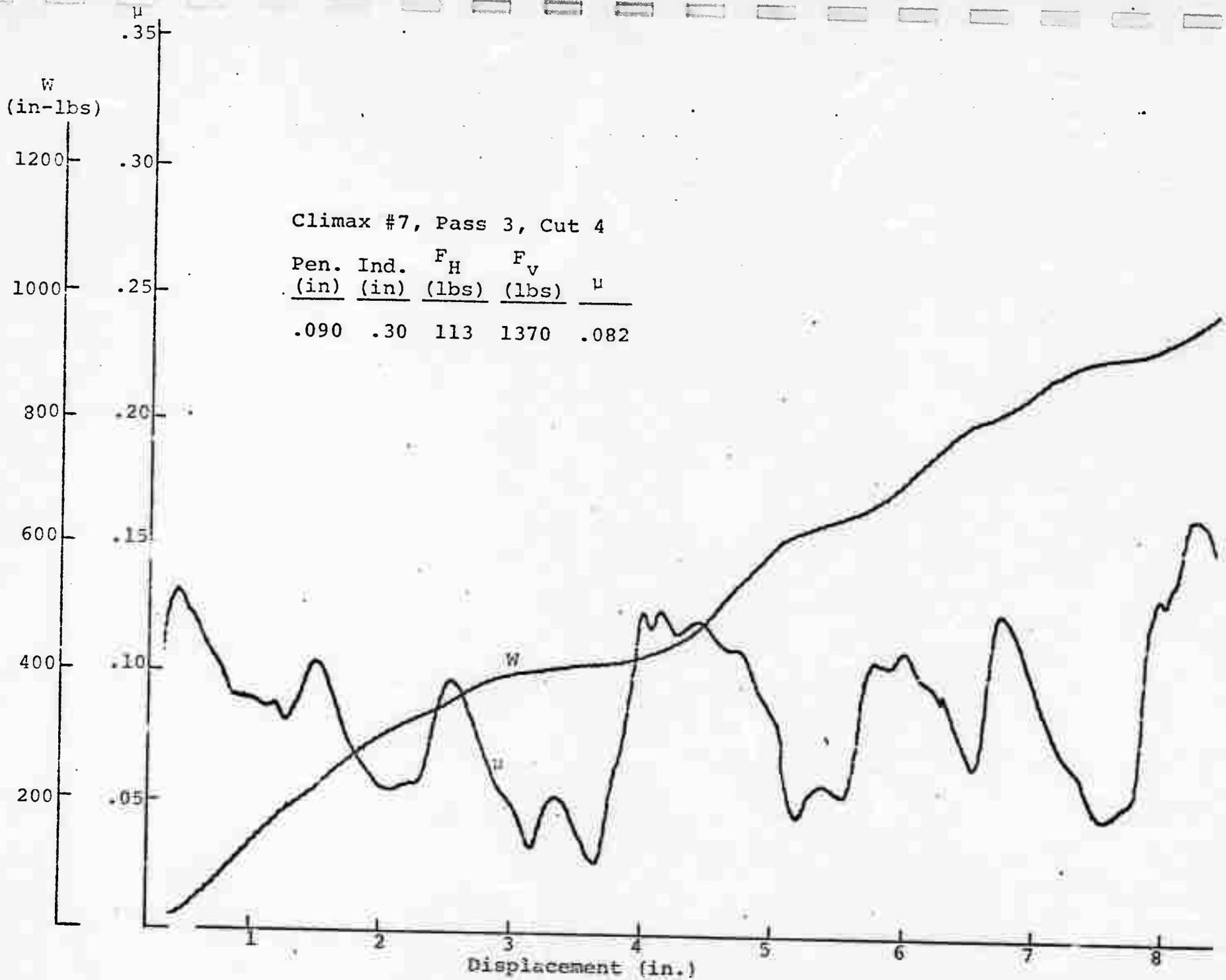

Climax #7, Pass 3, Cut 4

Pen. (in)	Ind. (in)	F_H (lbs)	F_V (lbs)	μ
.090	.30	113	1370	.082

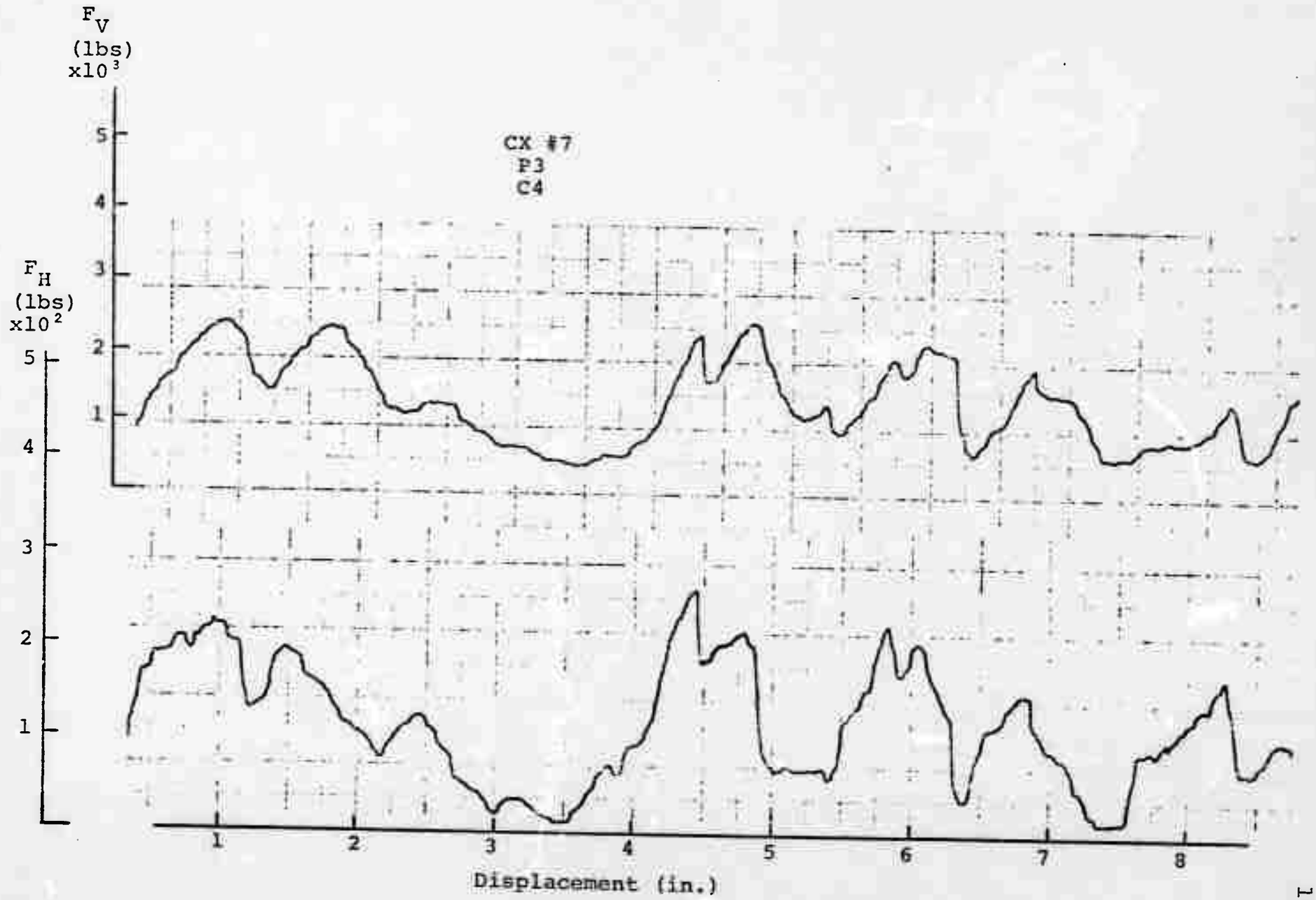
F_V (lbs) x10^3
5
4
3
2
1
CX #7
P3
C4
F_H (lbs) x10^2
5
4
3
2
1
1
2
3
4
5
6
7
8
Displacement (in.)

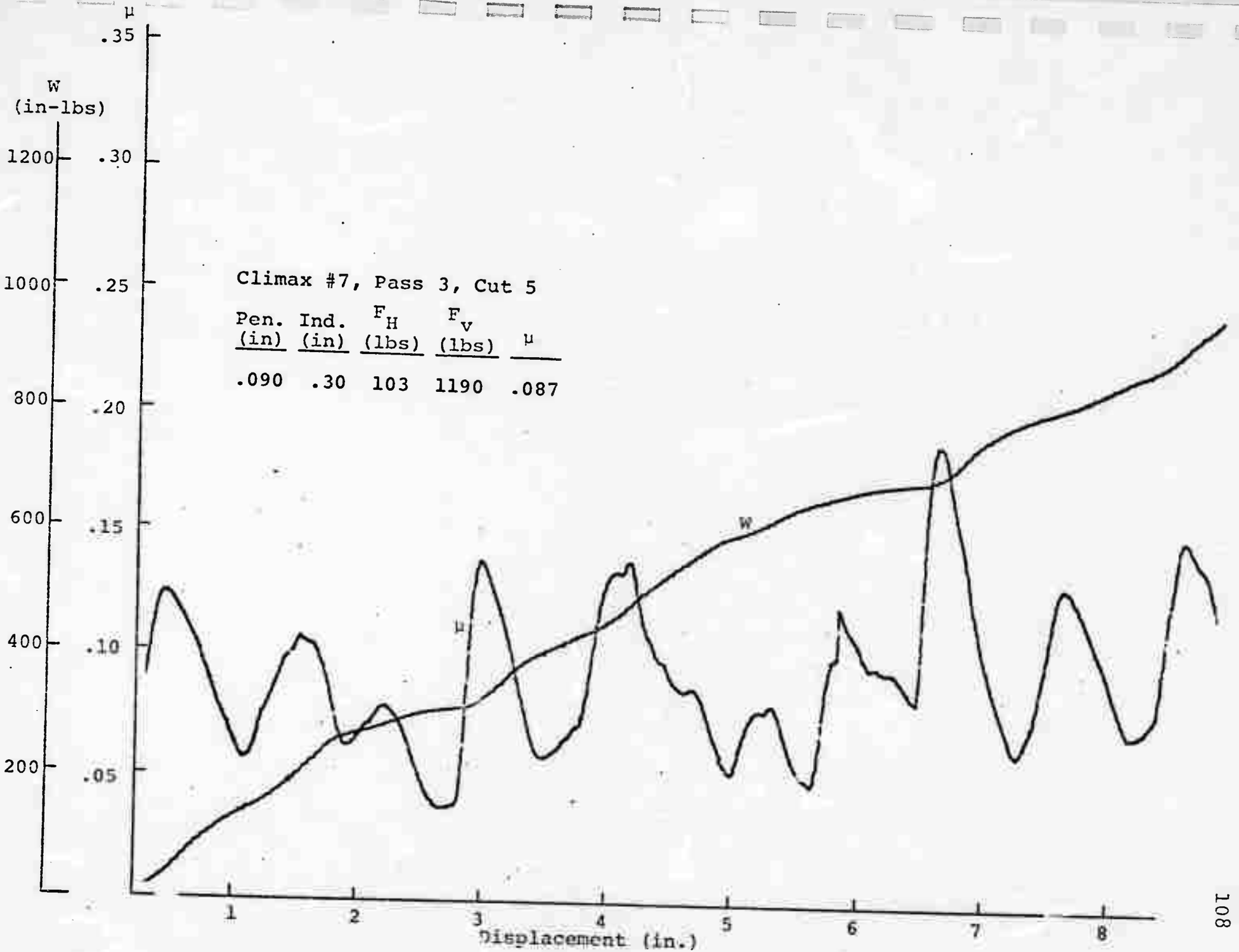
μ
.35
W
(in-lbs)
1200
.30
1000
.25
800
.20
600
.15
400
.10
200
.05
Climax #7, Pass 3, Cut 5
Pen. (in) Ind. (in) F_H (lbs) F_V (lbs) μ
.090 .30 103 1190 .087
W
μ
1
2
3
4
5
6
7
8
Displacement (in.)

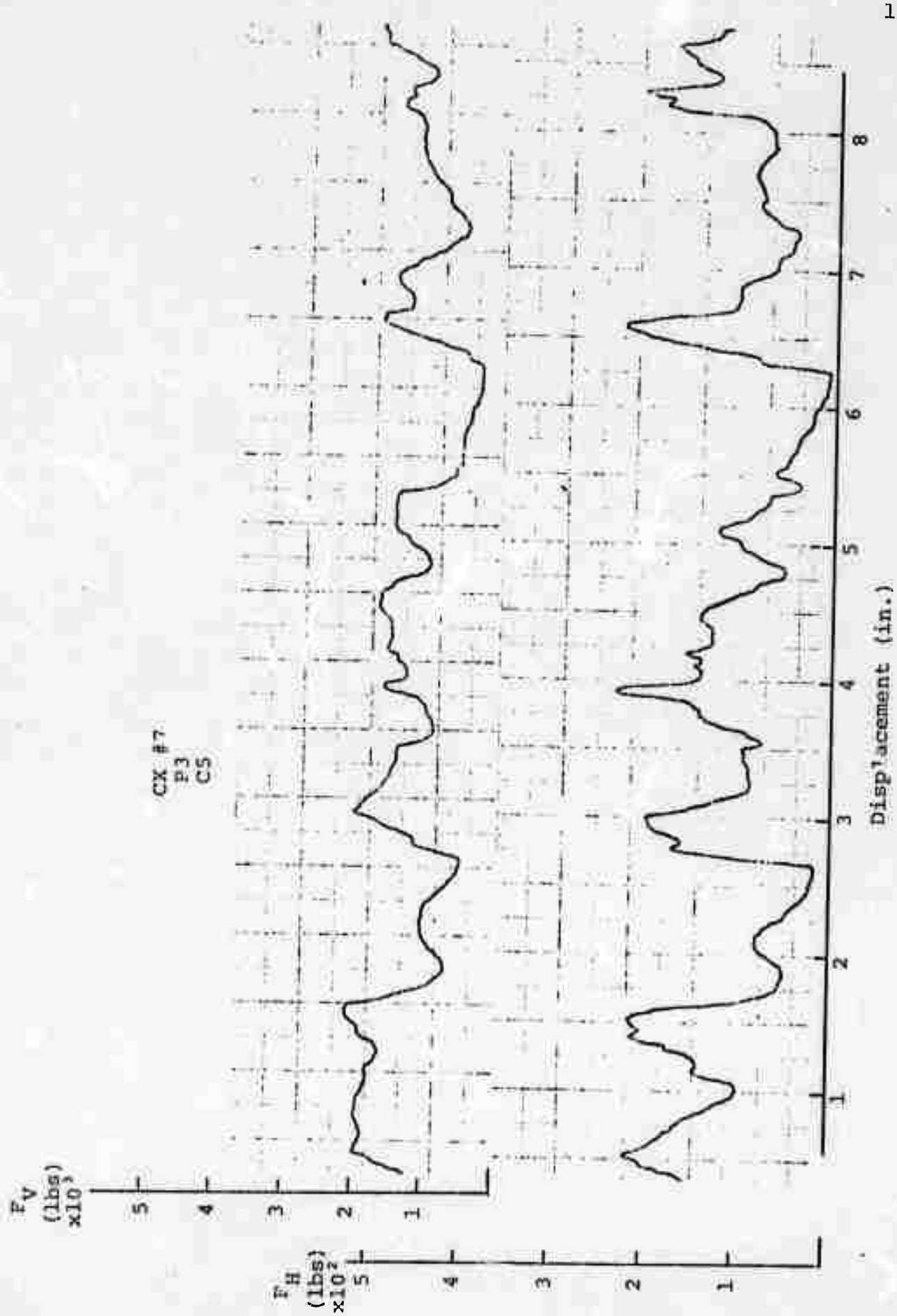
CX #7
P3
C5
F_V (lbs) x10³
F_H (lbs) x10²
Displacement (in.)

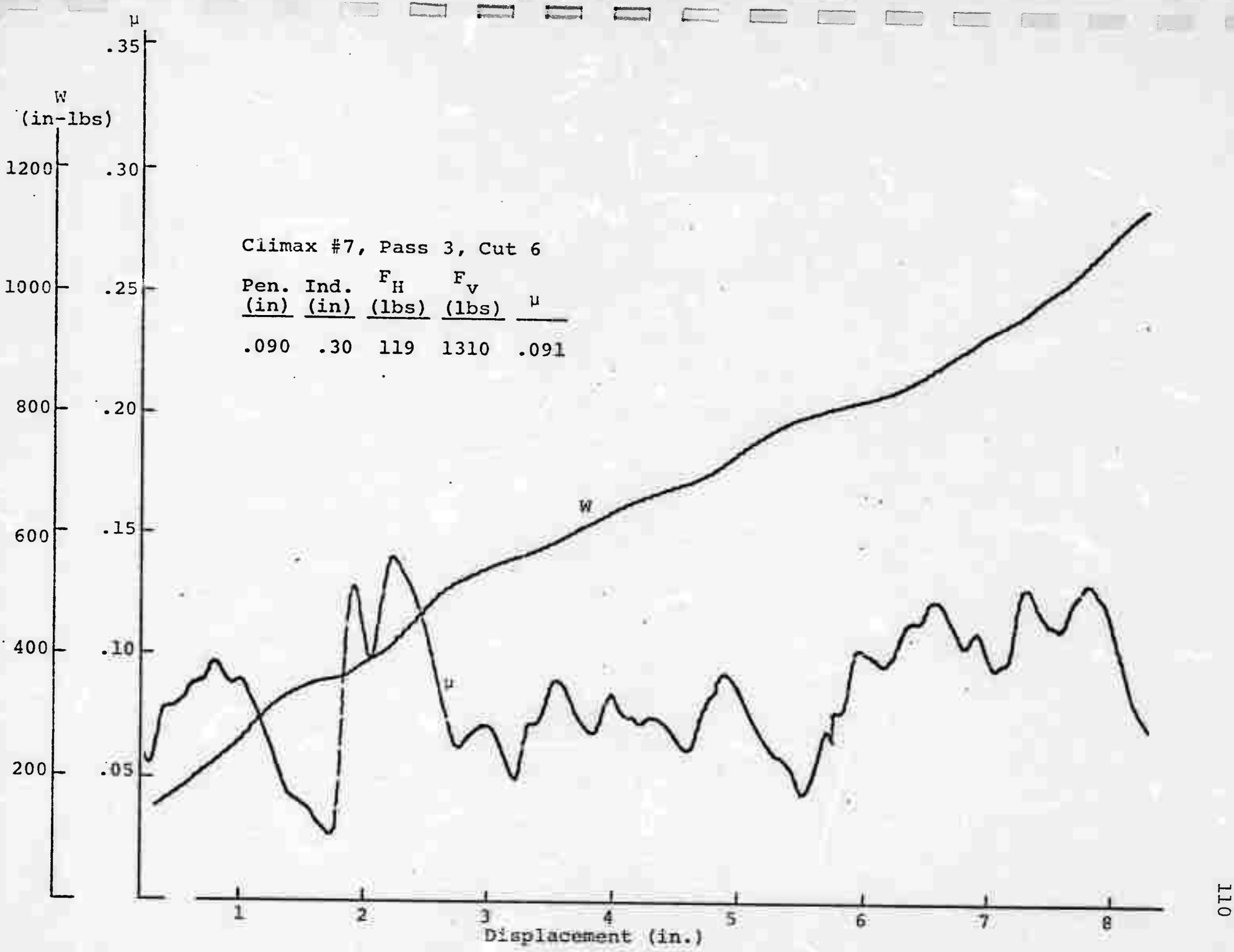
μ
.35
W
(in-lbs)
1200
.30
1000
.25
800
.20
600
.15
400
.10
200
.05
Climax #7, Pass 3, Cut 6
Pen. (in) Ind. (in) F_H (lbs) F_V (lbs) μ
.090 .30 119 1310 .091
W
μ
1 2 3 4 5 6 7 8
Displacement (in.)

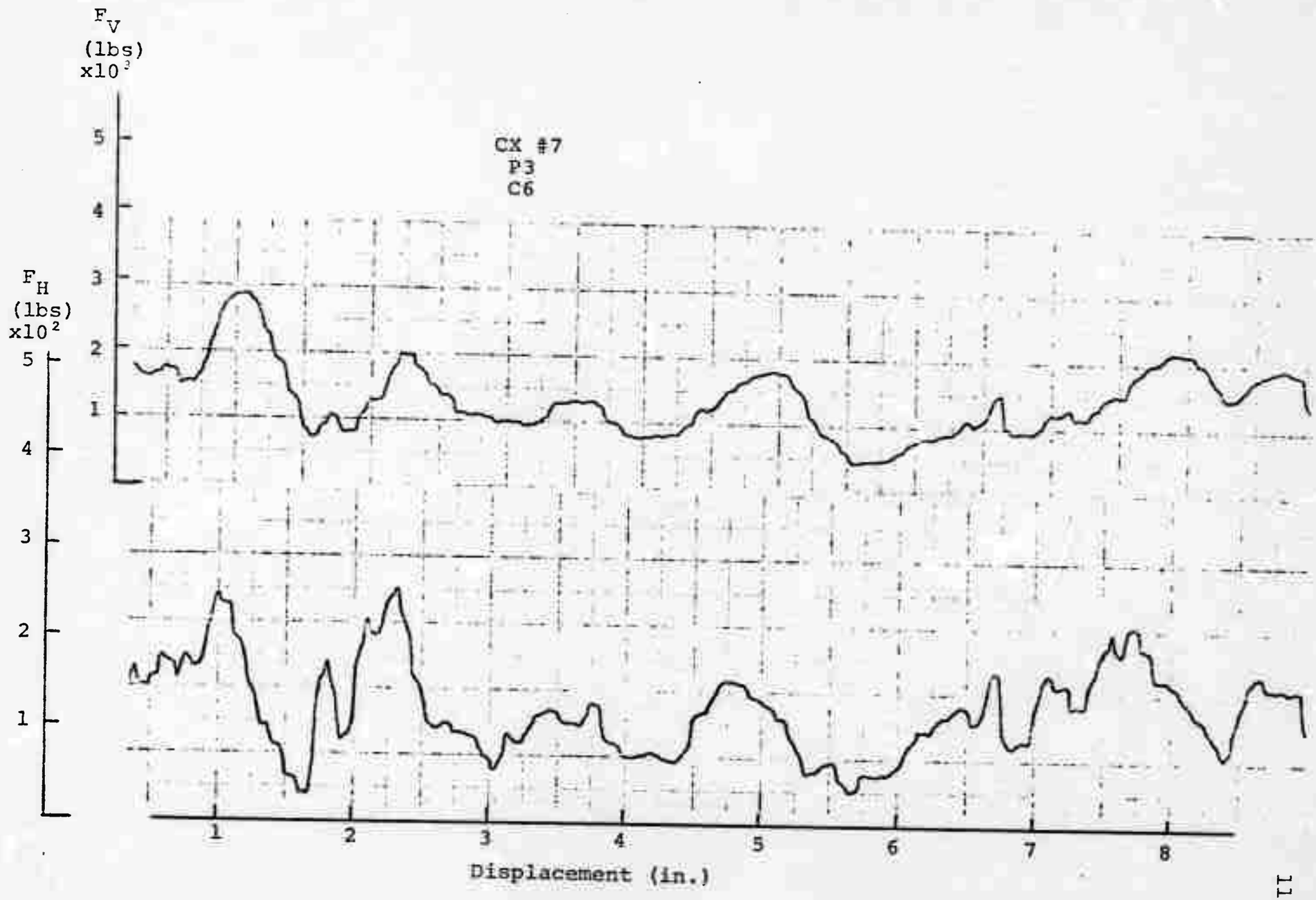
F_V (lbs) x10³
5
4
3
2
1
CX #7
P3
C6
F_H (lbs) x10²
5
4
3
2
1
1
2
3
4
5
6
7
8
Displacement (in.)

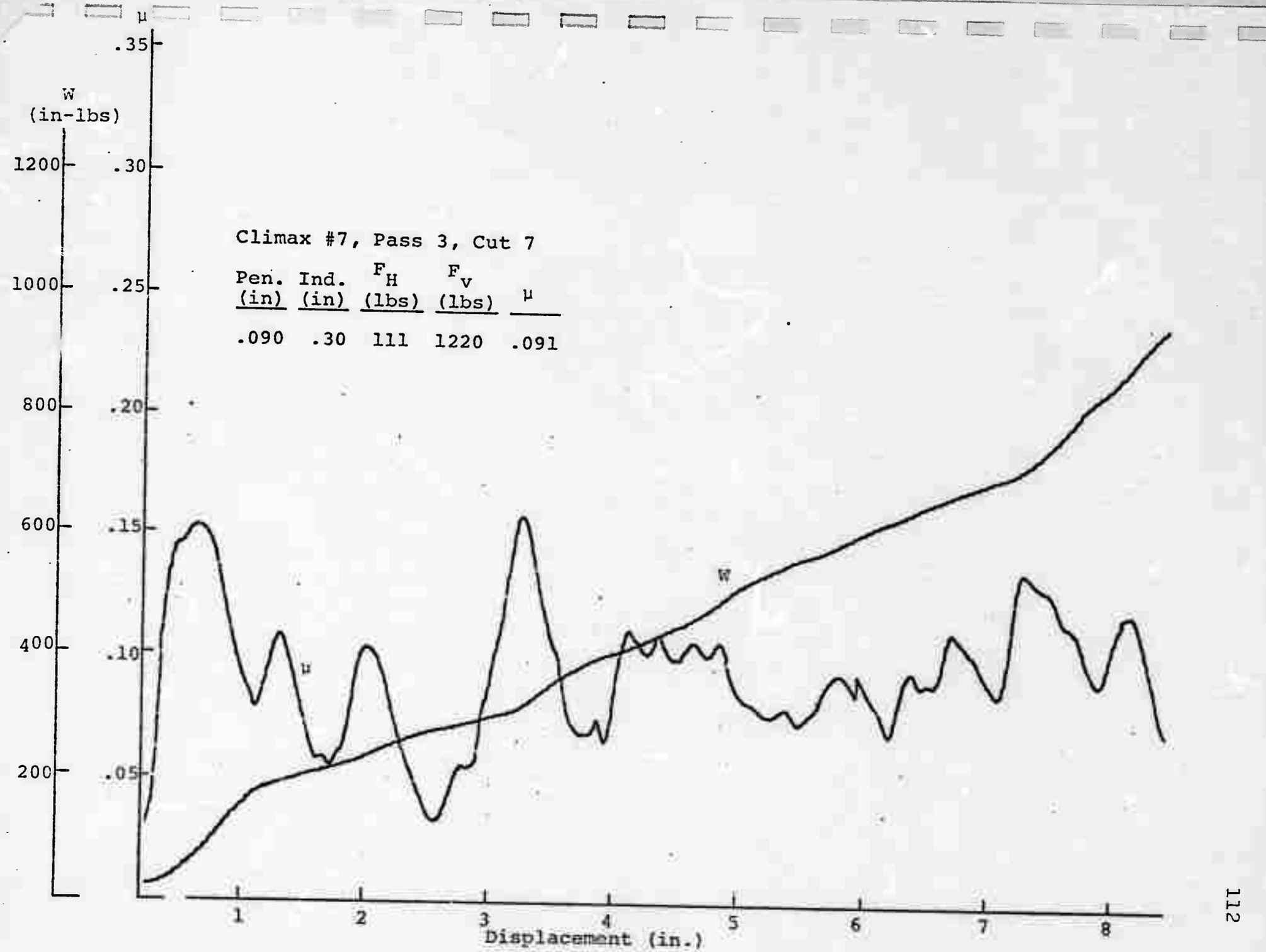

Climax #7, Pass 3, Cut 7

Pen. (in)	Ind. (in)	F_H (lbs)	F_V (lbs)	μ
.090	.30	111	1220	.091

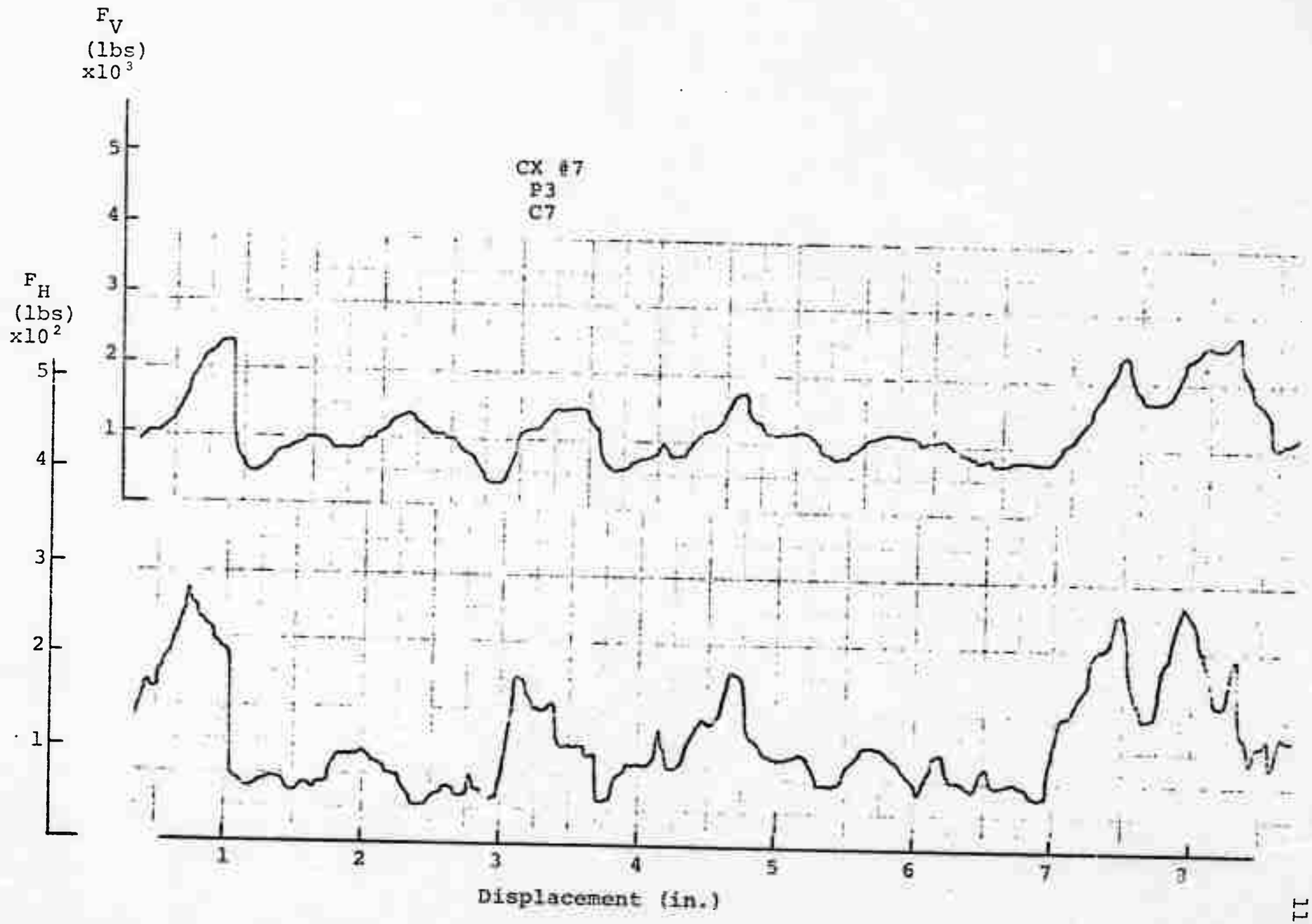
F_V (lbs) x10^3
5
4
3
2
1
CX #7
P3
C7
F_H (lbs) x10^2
5
4
3
2
1
1
2
3
4
5
6
7
8
Displacement (in.)

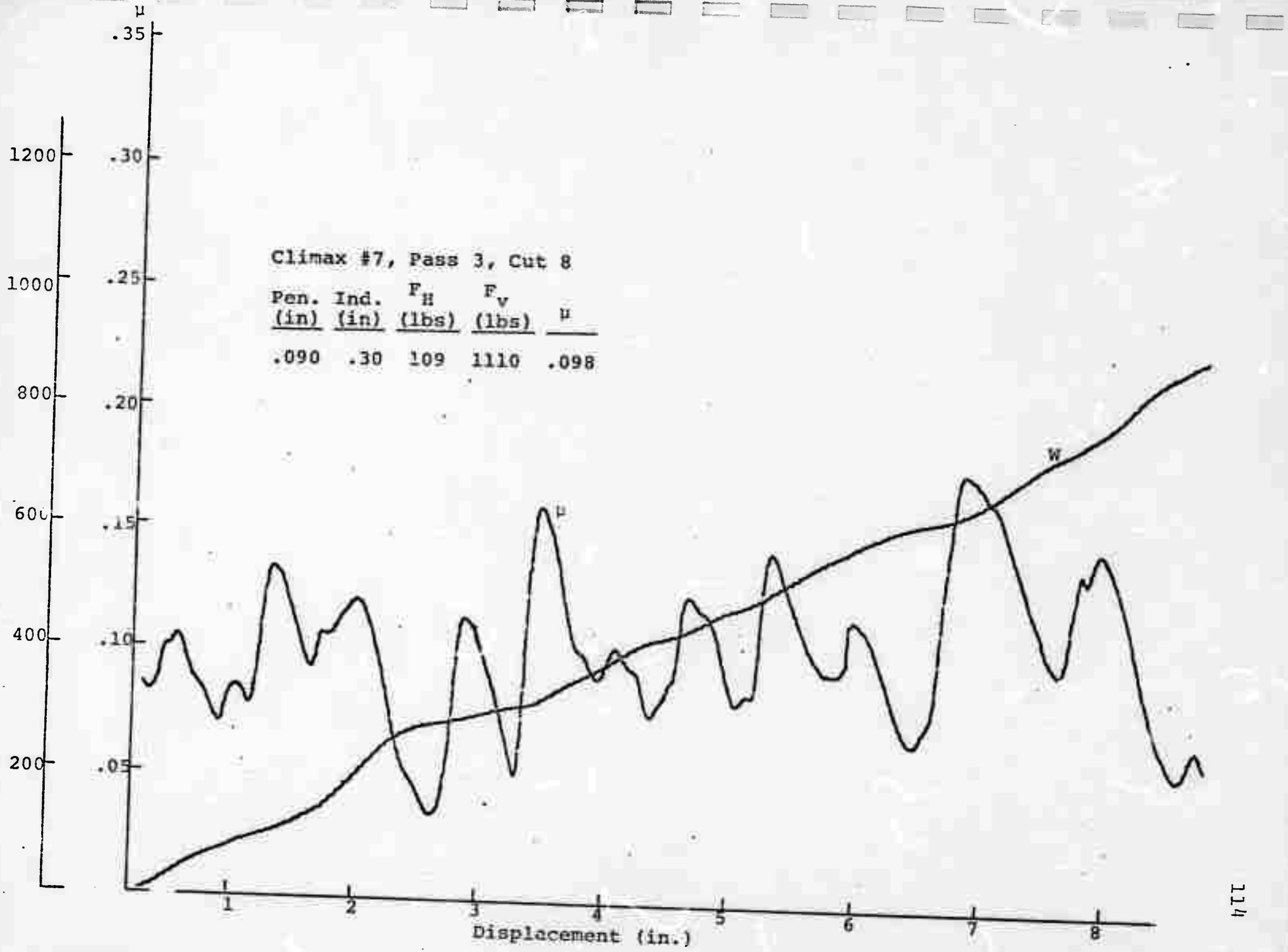
μ
.35
.30
.25
.20
.15
.10
.05
1200
1000
800
600
400
200
Climax #7, Pass 3, Cut 8
Pen. (in) Ind. (in) F_H (lbs) F_V (lbs) μ
.090 .30 109 1110 .098
W
μ
1
2
3
4
5
6
7
8
Displacement (in.)

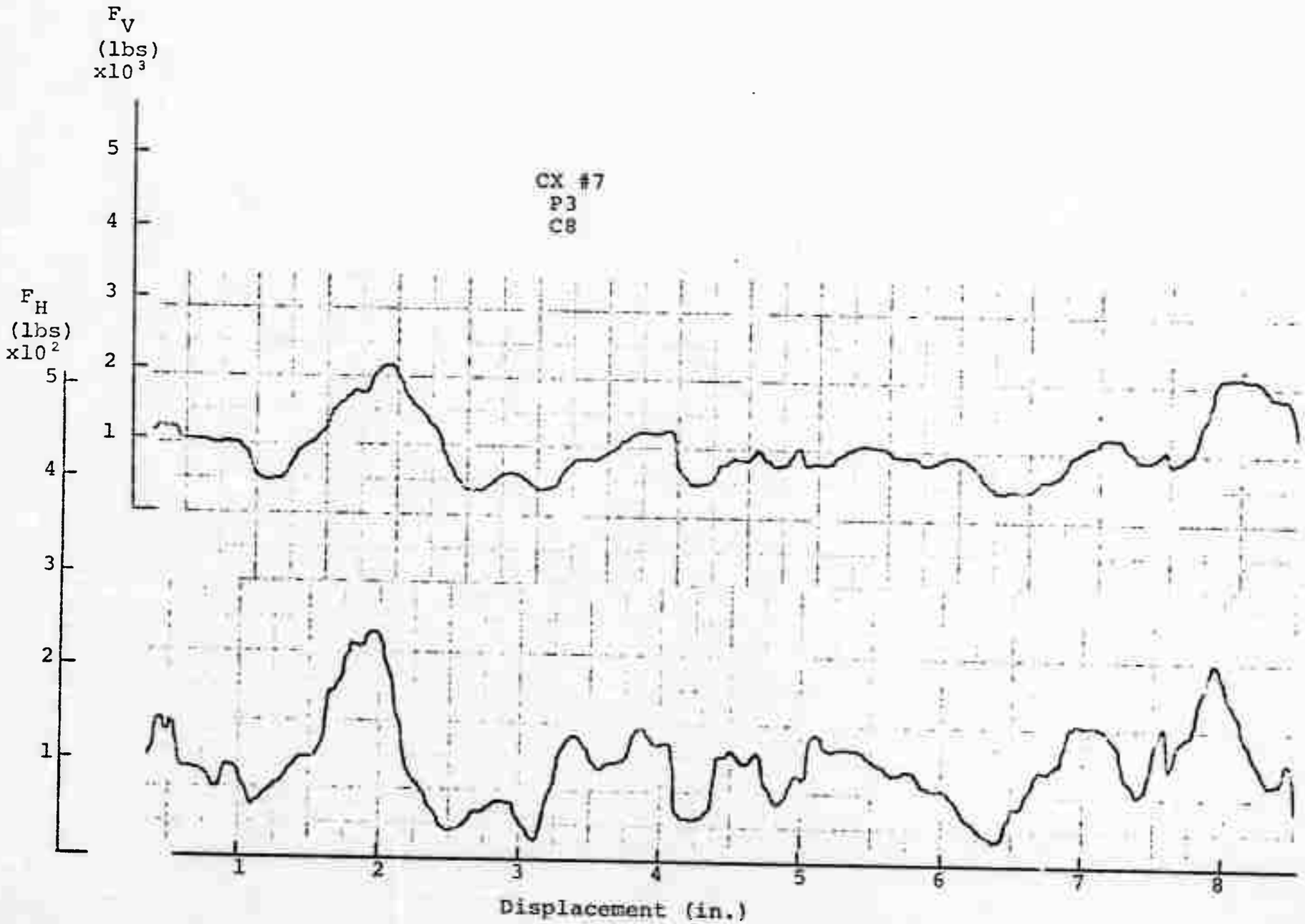
F_V
(lbs)
x10^3
5
4
3
2
1
CX #7
P3
C8
F_H
(lbs)
x10^2
5
4
3
2
1
1
2
3
4
5
6
7
8
Displacement (in.)

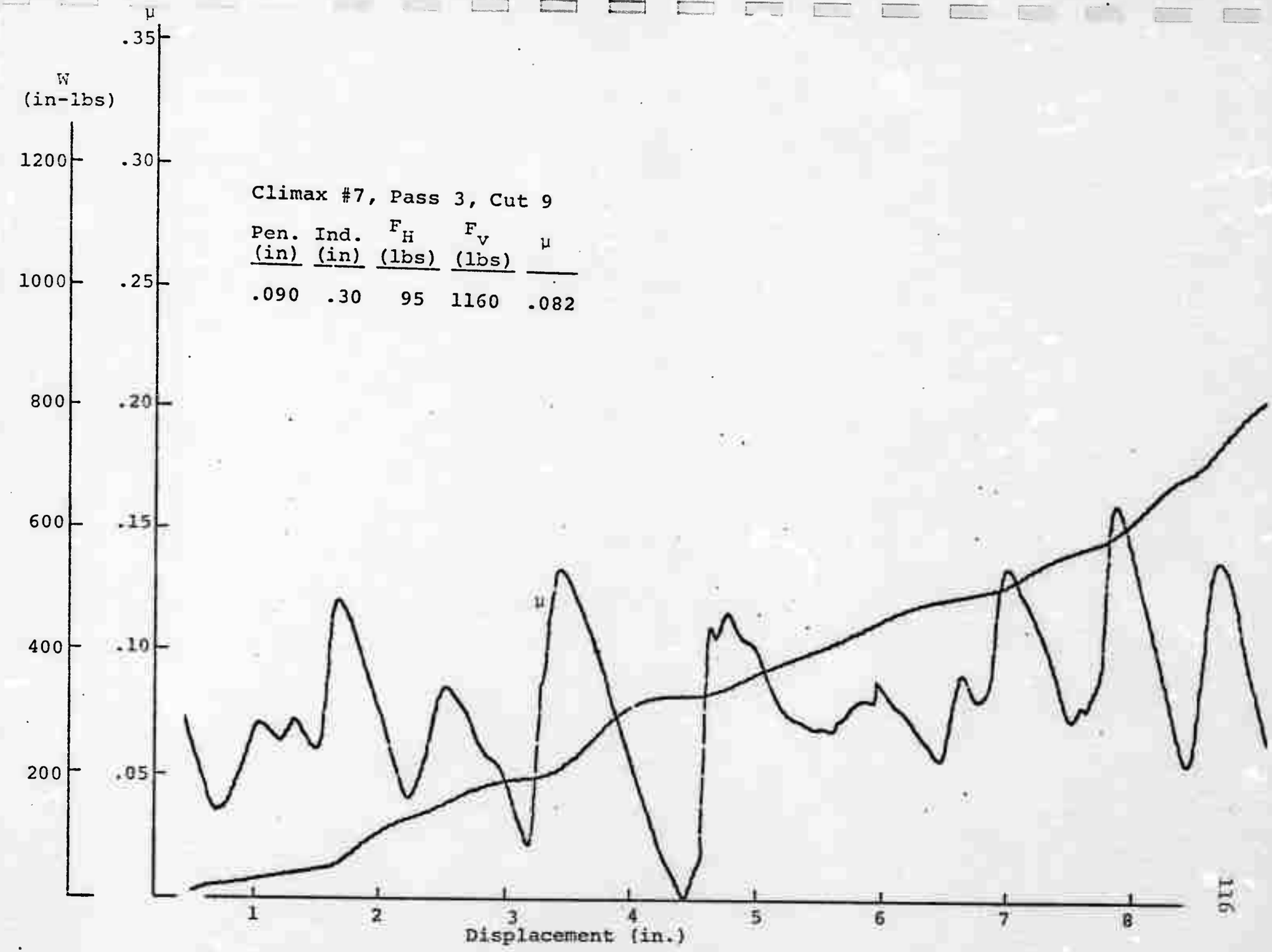

Climax #7, Pass 3, Cut 9

Pen. (in)	Ind. (in)	F_H (lbs)	F_V (lbs)	μ
.090	.30	95	1160	.082

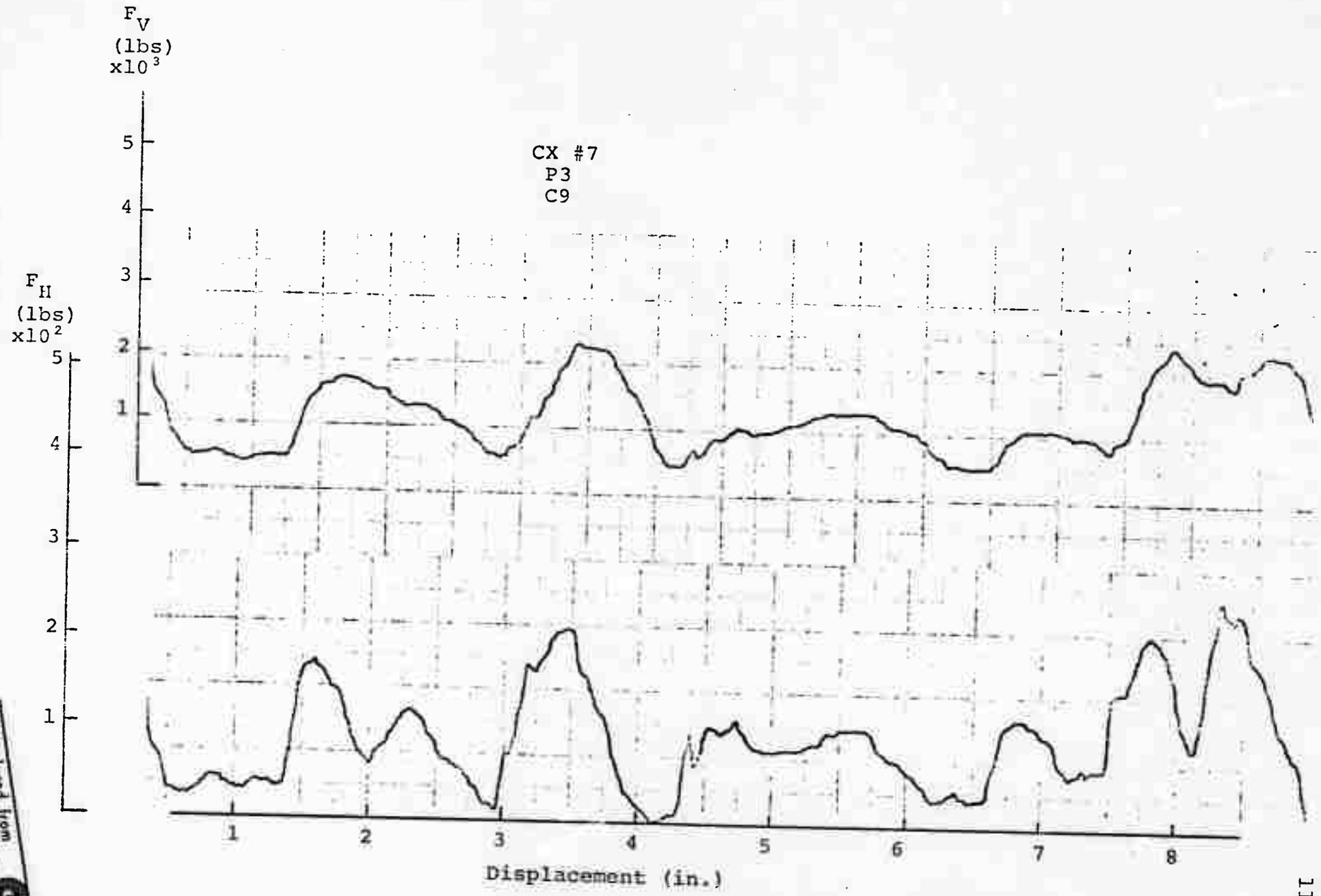

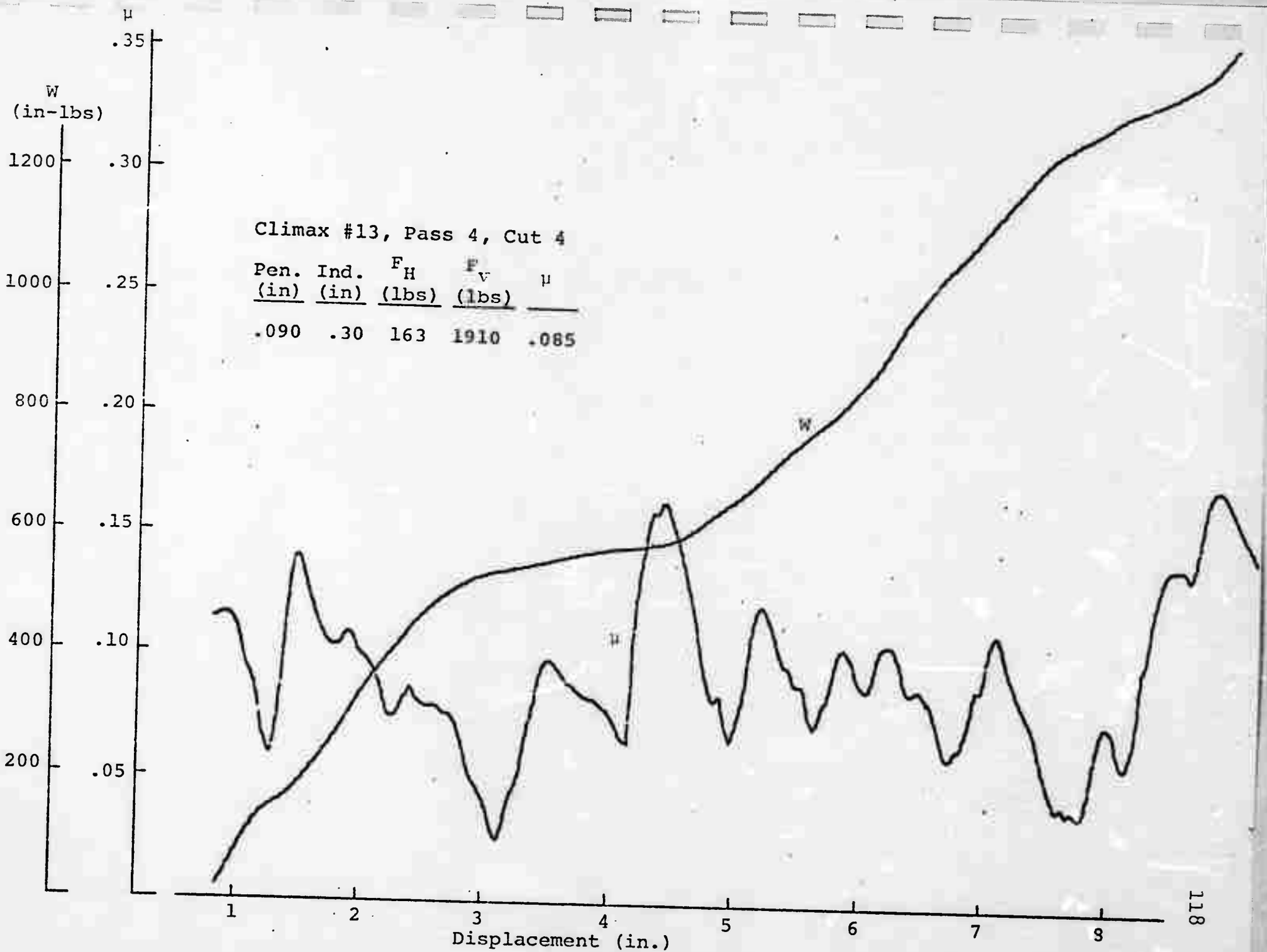
μ
.35
W
(in-lbs)
1200
.30
1000
.25
800
.20
600
.15
400
.10
200
.05
Climax #13, Pass 4, Cut 4
Pen. (in) Ind. (in) F_H (lbs) F_V (lbs) μ
.090 .30 163 1910 .085
W
μ
1
2
3
4
5
6
7
8
Displacement (in.)

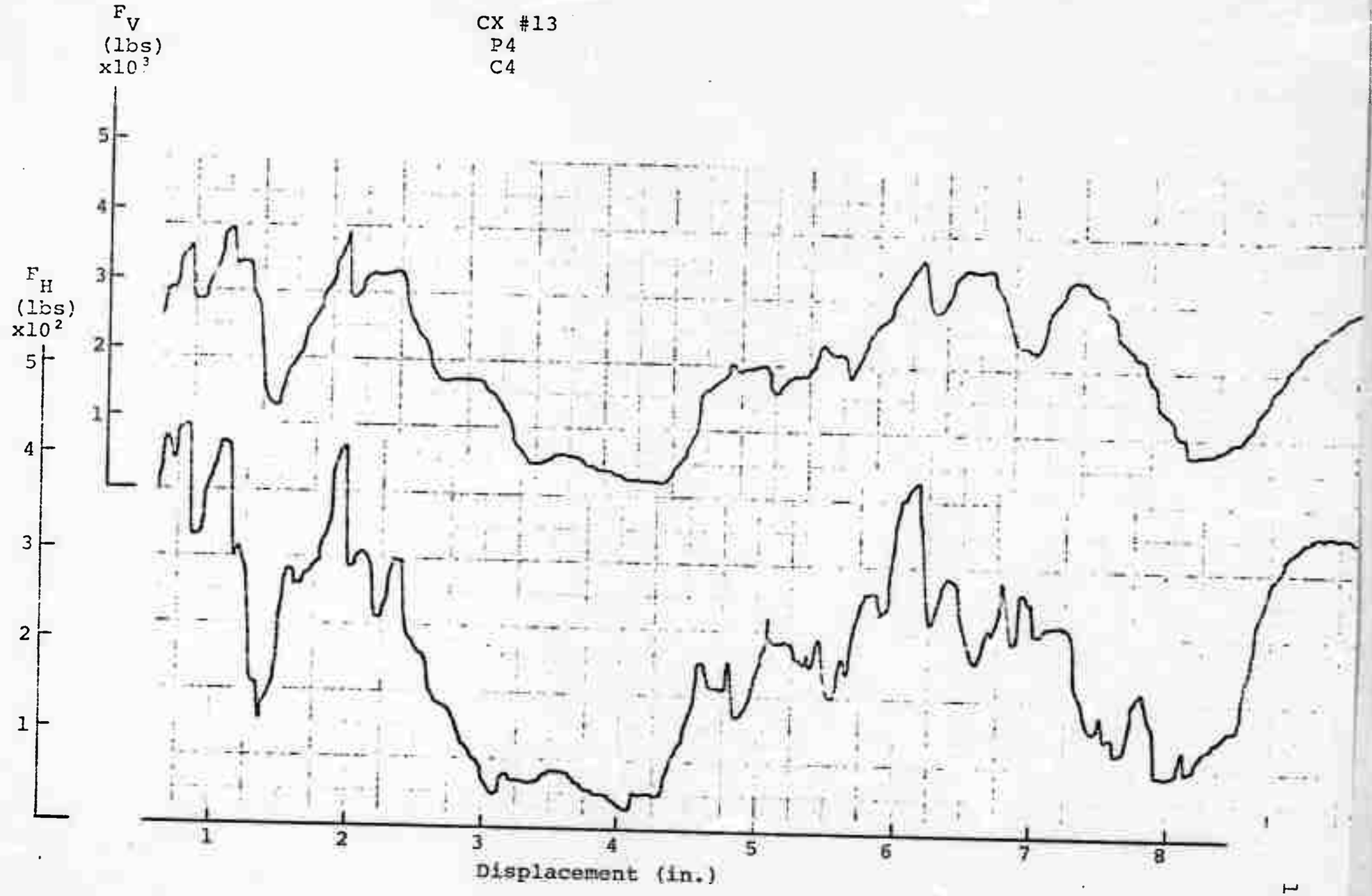
F_V (lbs) x10^3
CX #13
P4
C4
5
4
3
2
1
F_H (lbs) x10^2
5
4
3
2
1
1
2
3
4
5
6
7
8
Displacement (in.)

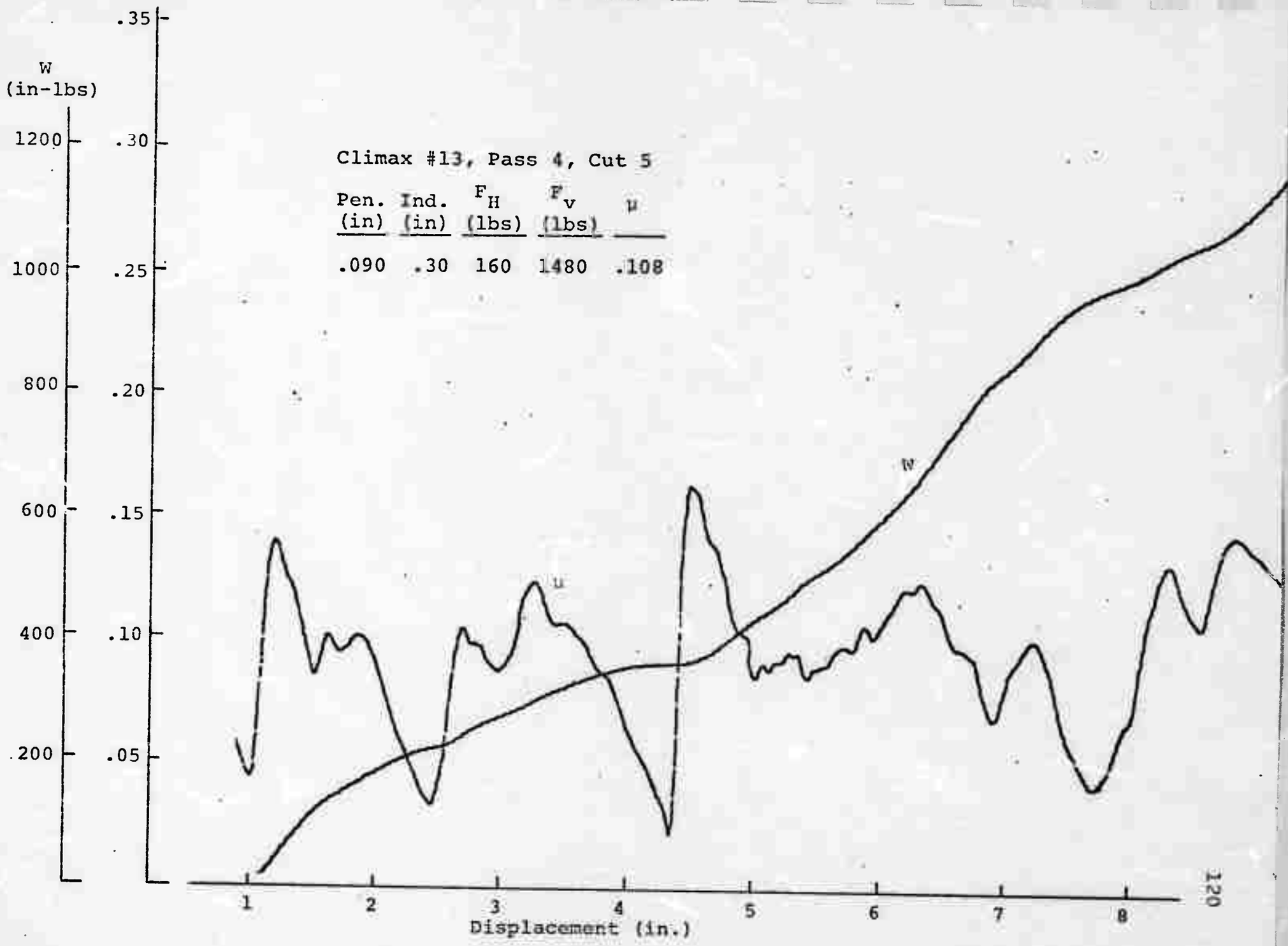
W
(in-lbs)
1200
1000
800
600
400
200
.35
.30
.25
.20
.15
.10
.05
Climax #13, Pass 4, Cut 5
Pen. (in) Ind. (in) F_H (lbs) F_V (lbs) μ
.090 .30 160 1480 .108
W
u
1
2
3
4
5
6
7
8
Displacement (in.)
120

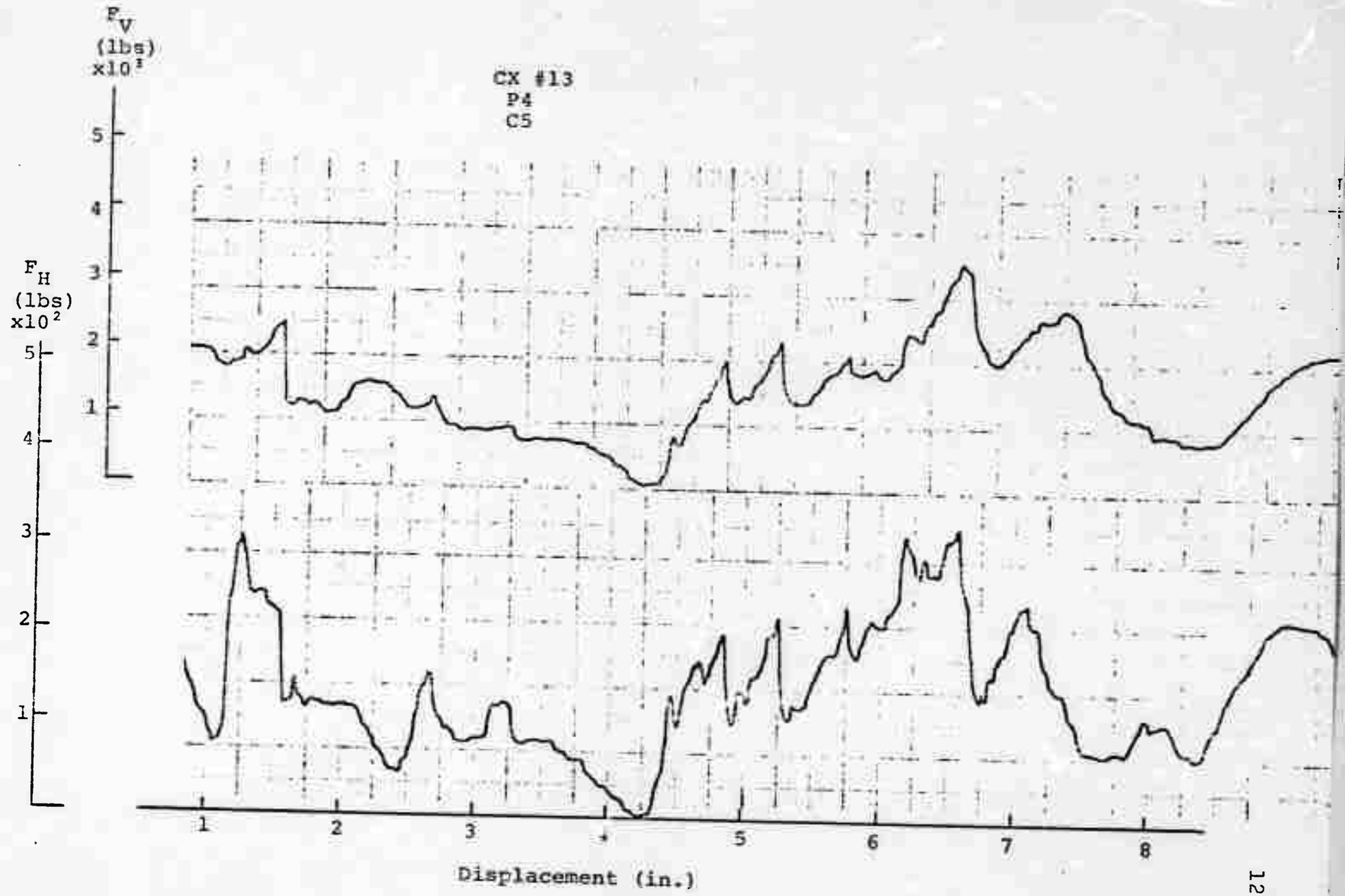
CX #13
P4
C5
F_V (lbs) x10³
5
4
3
2
1
F_H (lbs) x10²
5
4
3
2
1
1
2
3
4
5
6
7
8
Displacement (in.)

Climax #13, Pass 4, Cut 6

Pen. Ind. (in)	F_H (lbs)	F_V (lbs)	μ
.090	.30	120	1230	.098

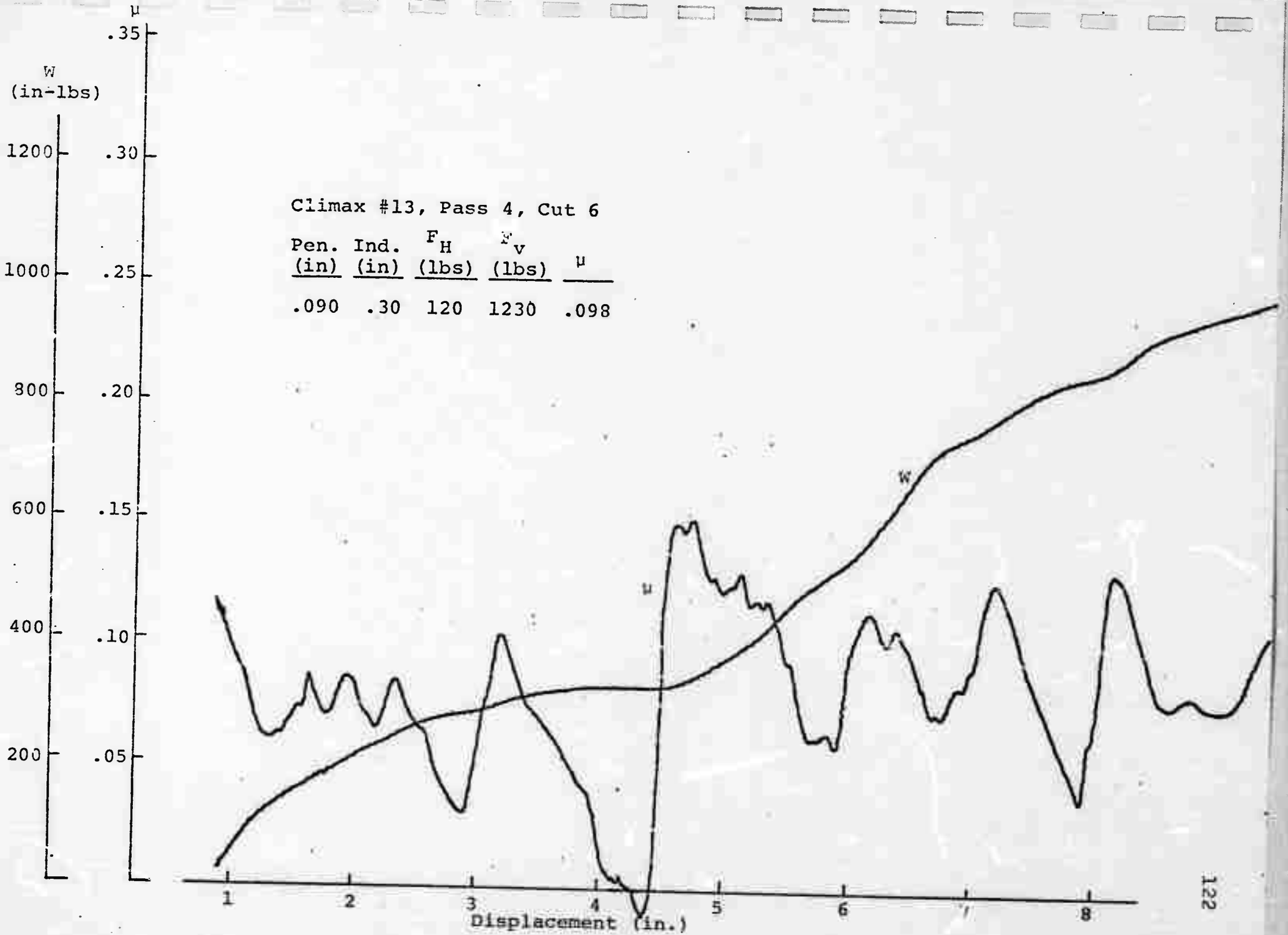

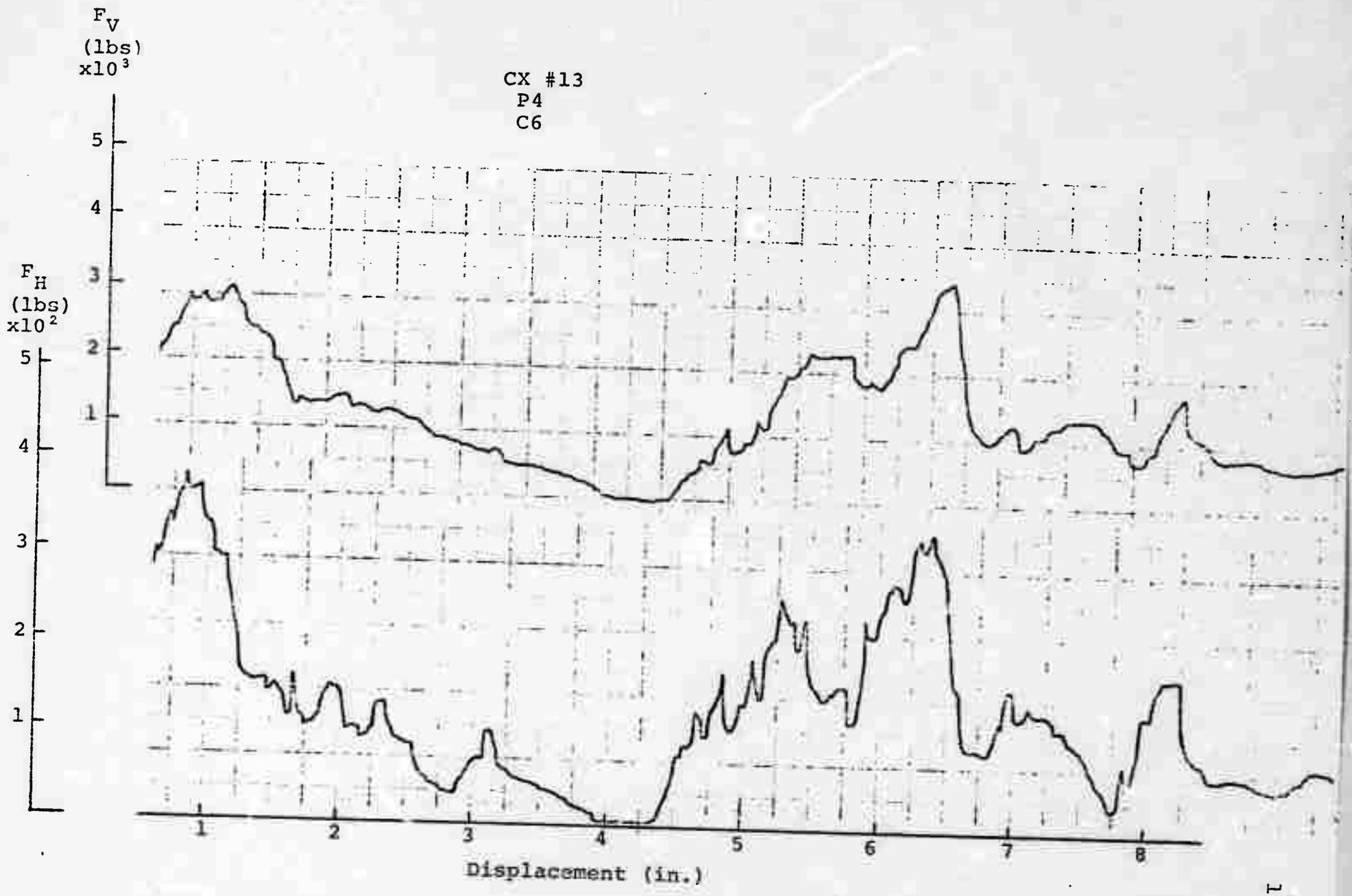
F_V (lbs) x10^3
CX #13
P4
C6
F_H (lbs) x10^2
Displacement (in.)

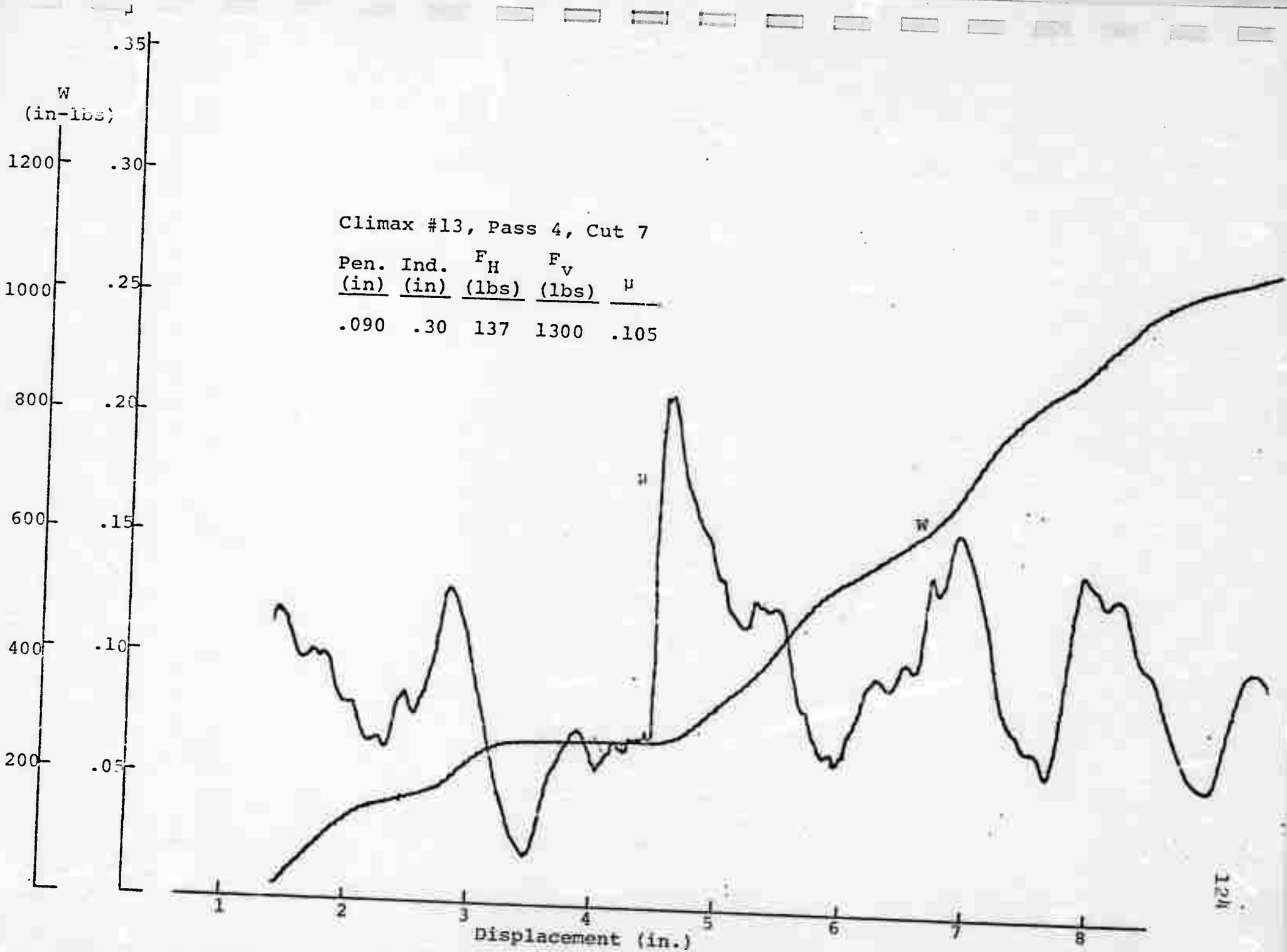
μ
.35
W
(in-lbs)
1200
.30
1000
.25
800
.20
600
.15
400
.10
200
.05
Climax #13, Pass 4, Cut 7
Pen. Ind. F_H F_V
(in) (in) (lbs) (lbs) μ
.090 .30 137 1300 .105
μ
W
1
2
3
4
5
6
7
8
Displacement (in.)
12M

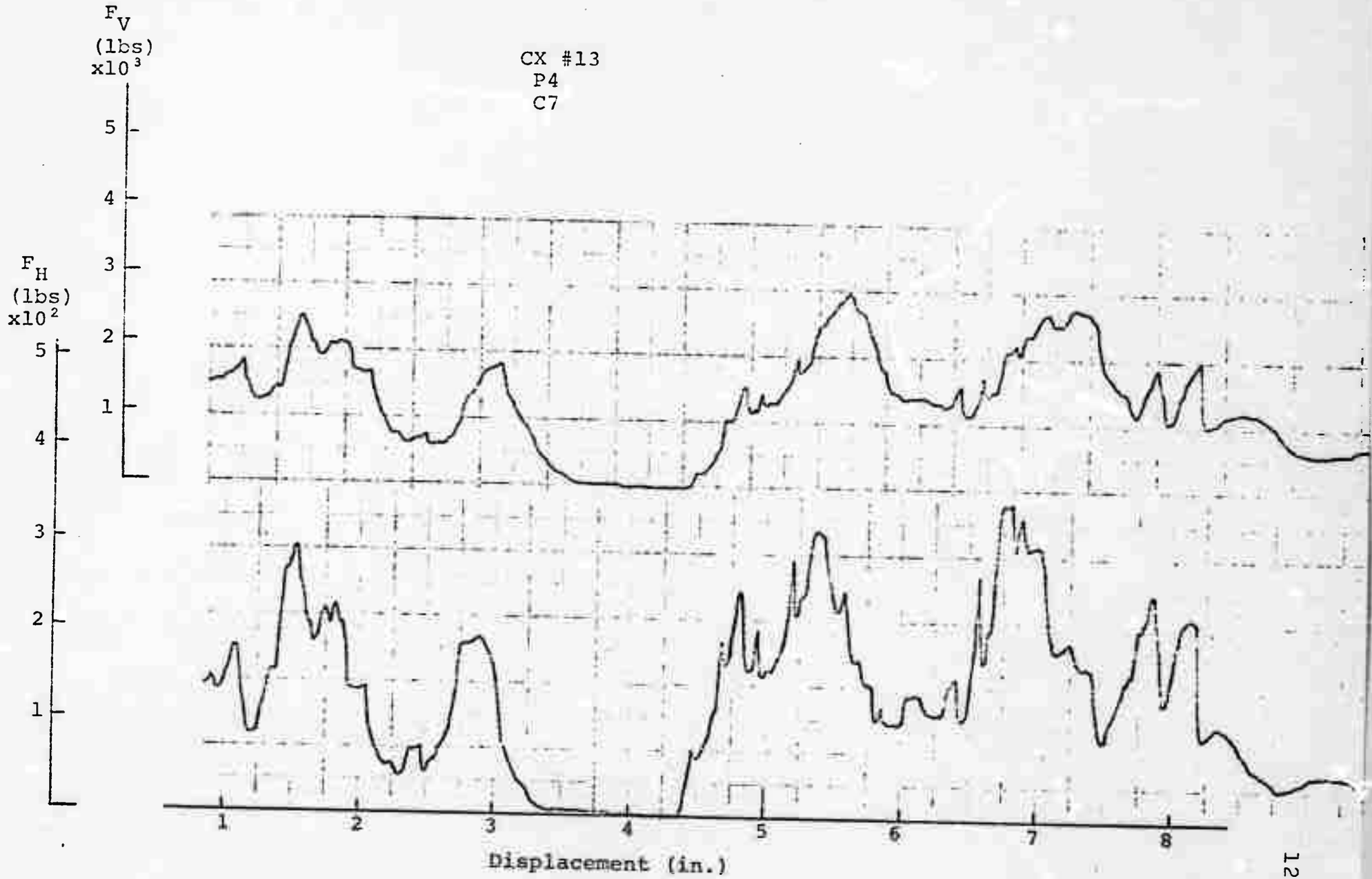
CX #13
P4
C7
F_V (lbs) x10^3
5
4
3
2
1
F_H (lbs) x10^2
5
4
3
2
1
1
2
3
4
5
6
7
8
Displacement (in.)

Climax #13, Pass 4, Cut 8

Pen. Ind. (in)	Ind. (in)	F_H (lbs)	F_V (lbs)	μ
.090	.30	125	1420	.088

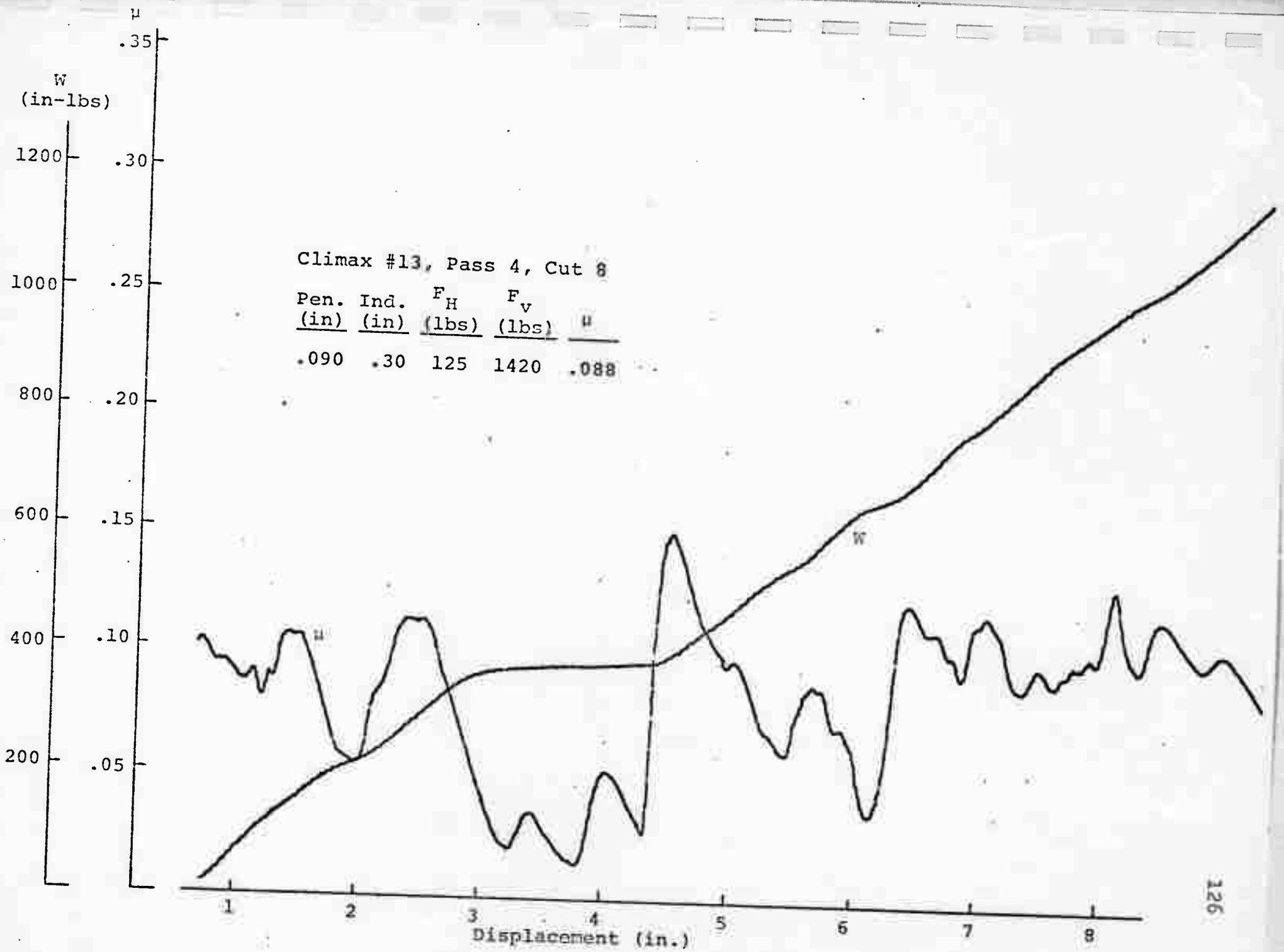

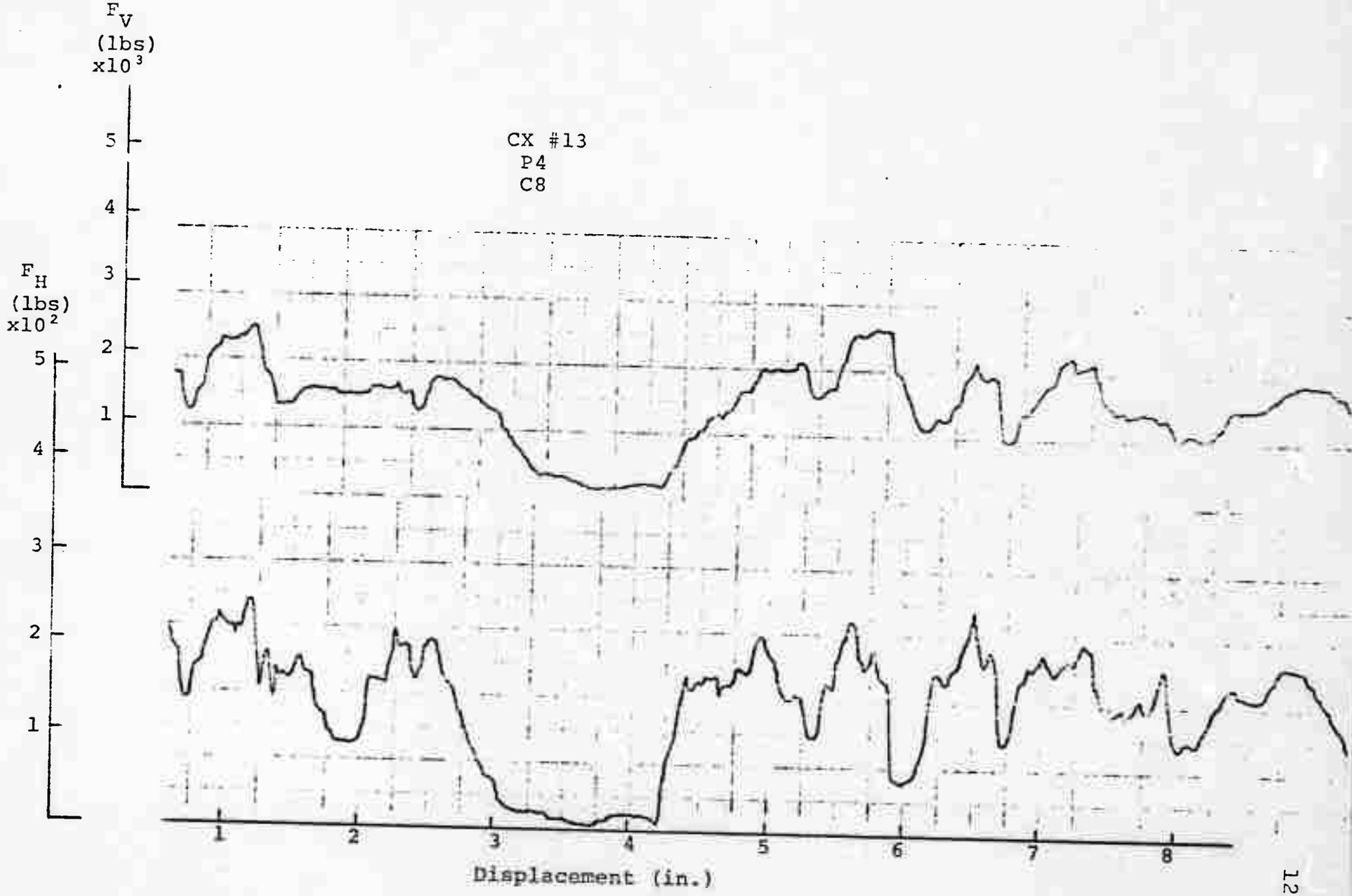
F_V (lbs) x10^3
5
4
3
2
1
CX #13
P4
C8
F_H (lbs) x10^2
5
4
3
2
1
1
2
3
4
5
6
7
8
Displacement (in.)

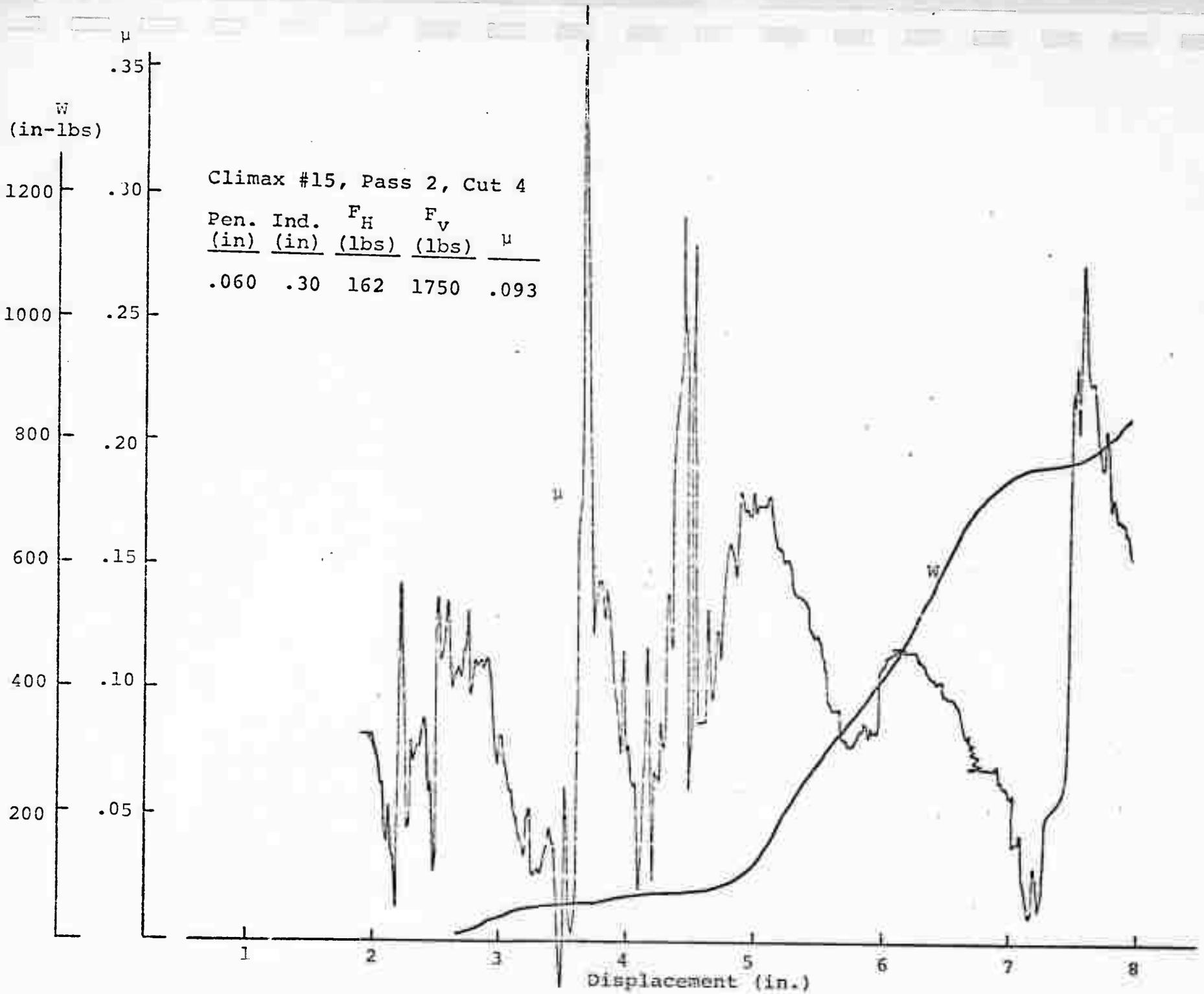
μ
.35
W
(in-lbs)
1200
.30
1000
.25
800
.20
600
.15
400
.10
200
.05
Climax #15, Pass 2, Cut 4
Pen. (in) Ind. (in) F_H (lbs) F_V (lbs) μ
.060 .30 162 1750 .093
μ
W
1
2
3
4
5
6
7
8
Displacement (in.)

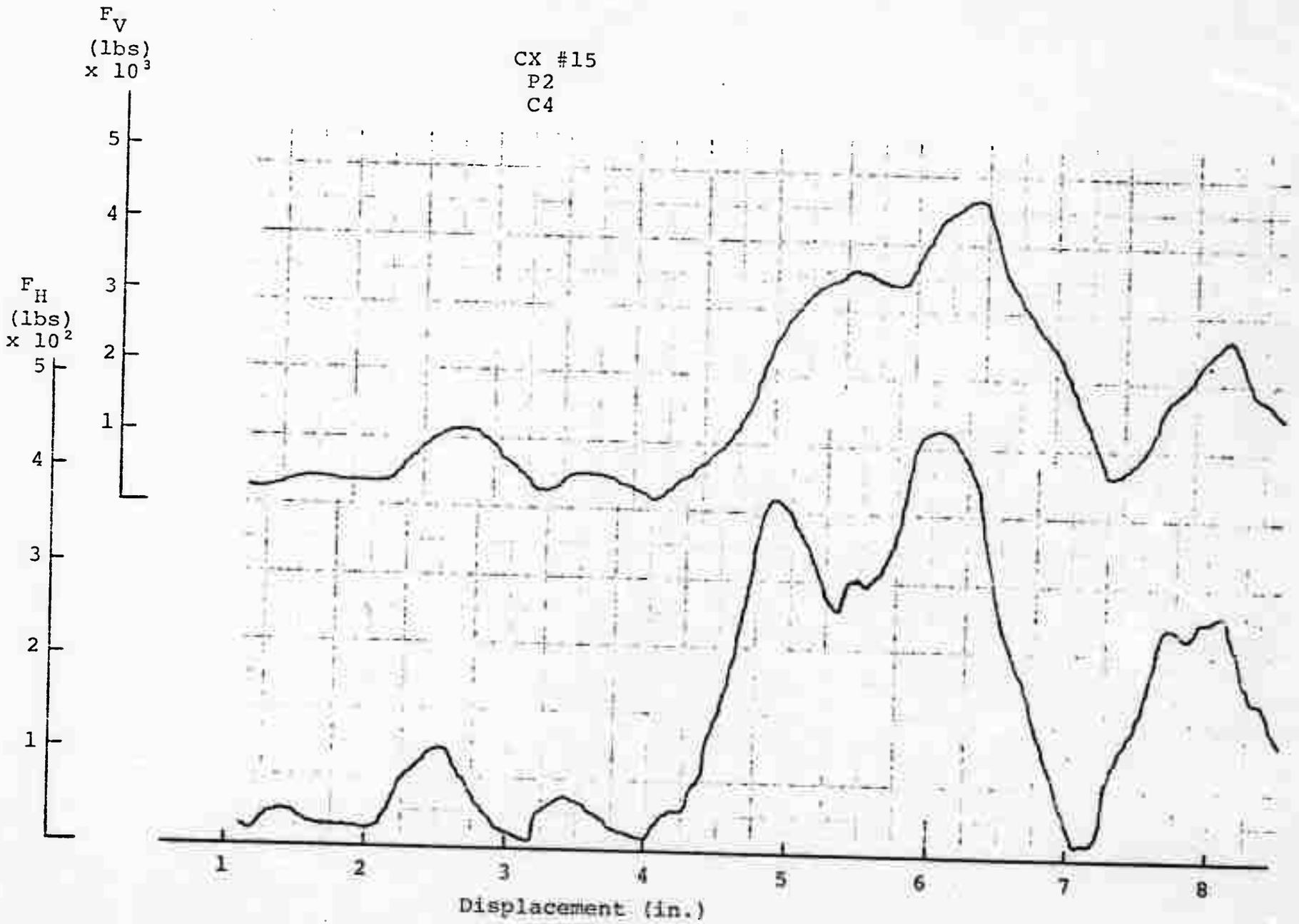
F_V (lbs) x 10^3
5
4
3
2
1
F_H (lbs) x 10^2
5
4
3
2
1
CX #15
P2
C4
1
2
3
4
5
6
7
8
Displacement (in.)

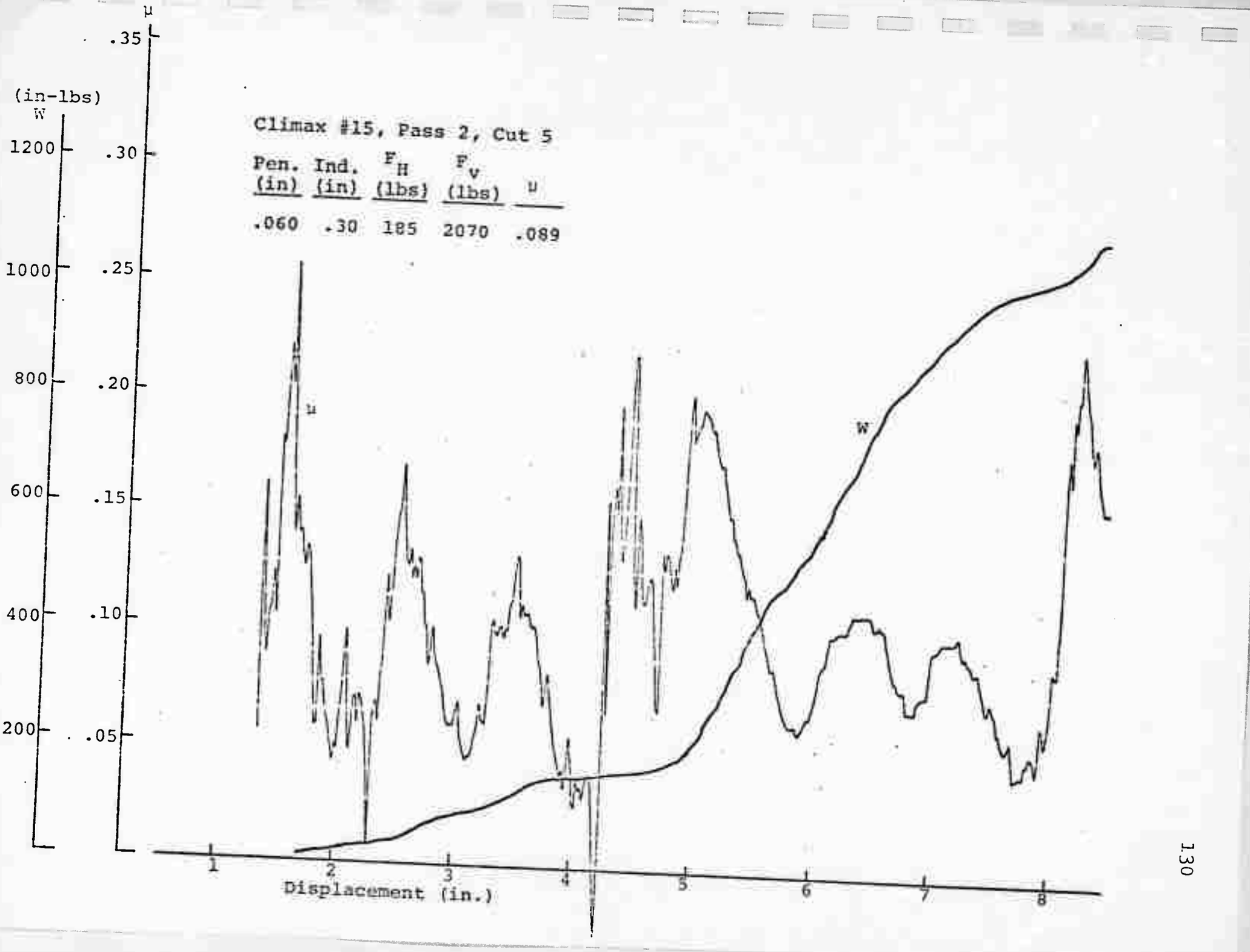
μ
.35
(in-lbs)
W
1200
.30
1000
.25
800
.20
600
.15
400
.10
200
.05
Climax #15, Pass 2, Cut 5
Pen. Ind. (in) (in) F_H (lbs) F_V (lbs) μ
.060 .30 185 2070 .089
μ
W
1 2 3 4 5 6 7 8
Displacement (in.)

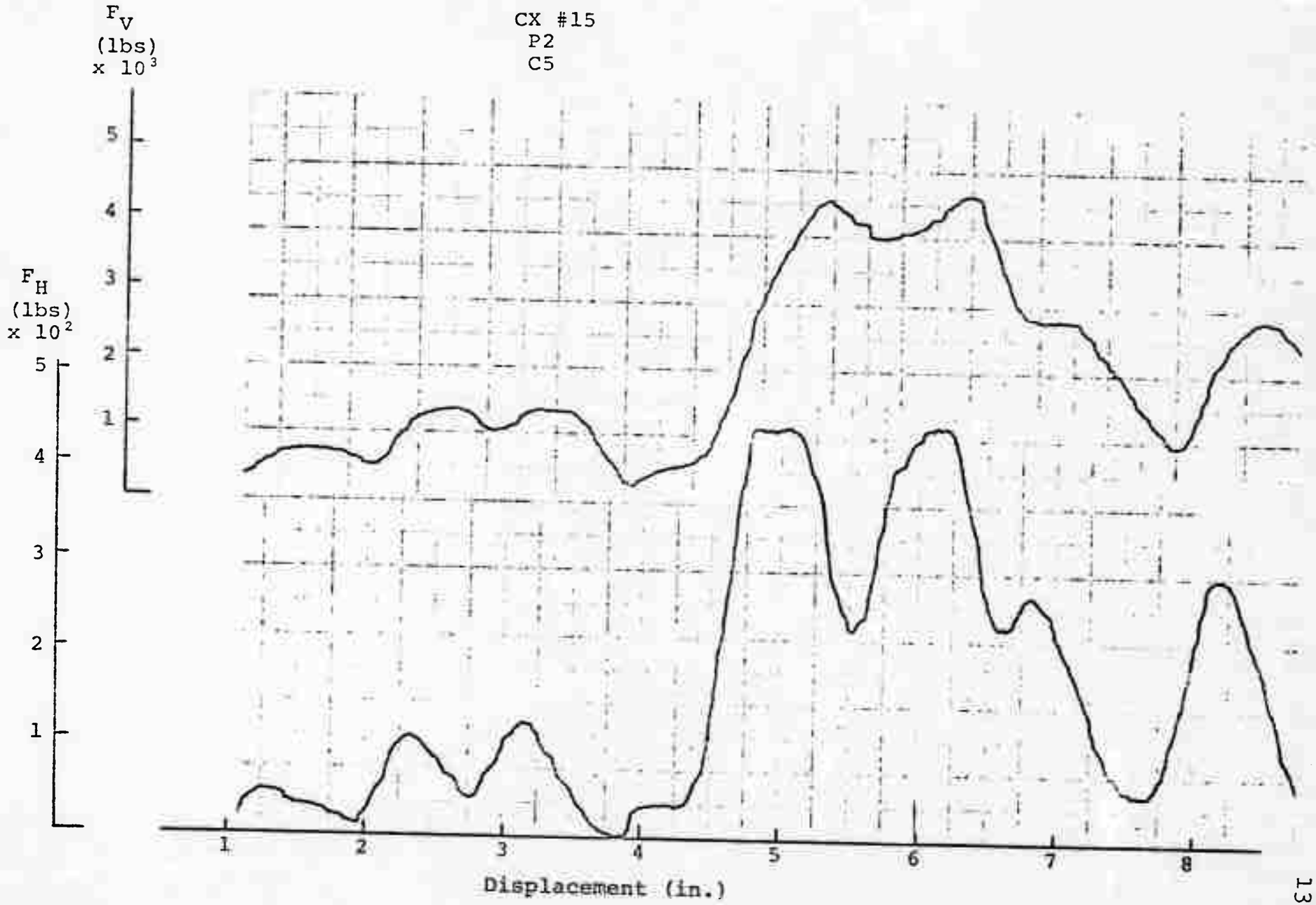
CX #15
P2
C5
F_V (lbs) x 10^3
5
4
3
2
1
F_H (lbs) x 10^2
5
4
3
2
1
1
2
3
4
5
6
7
8
Displacement (in.)

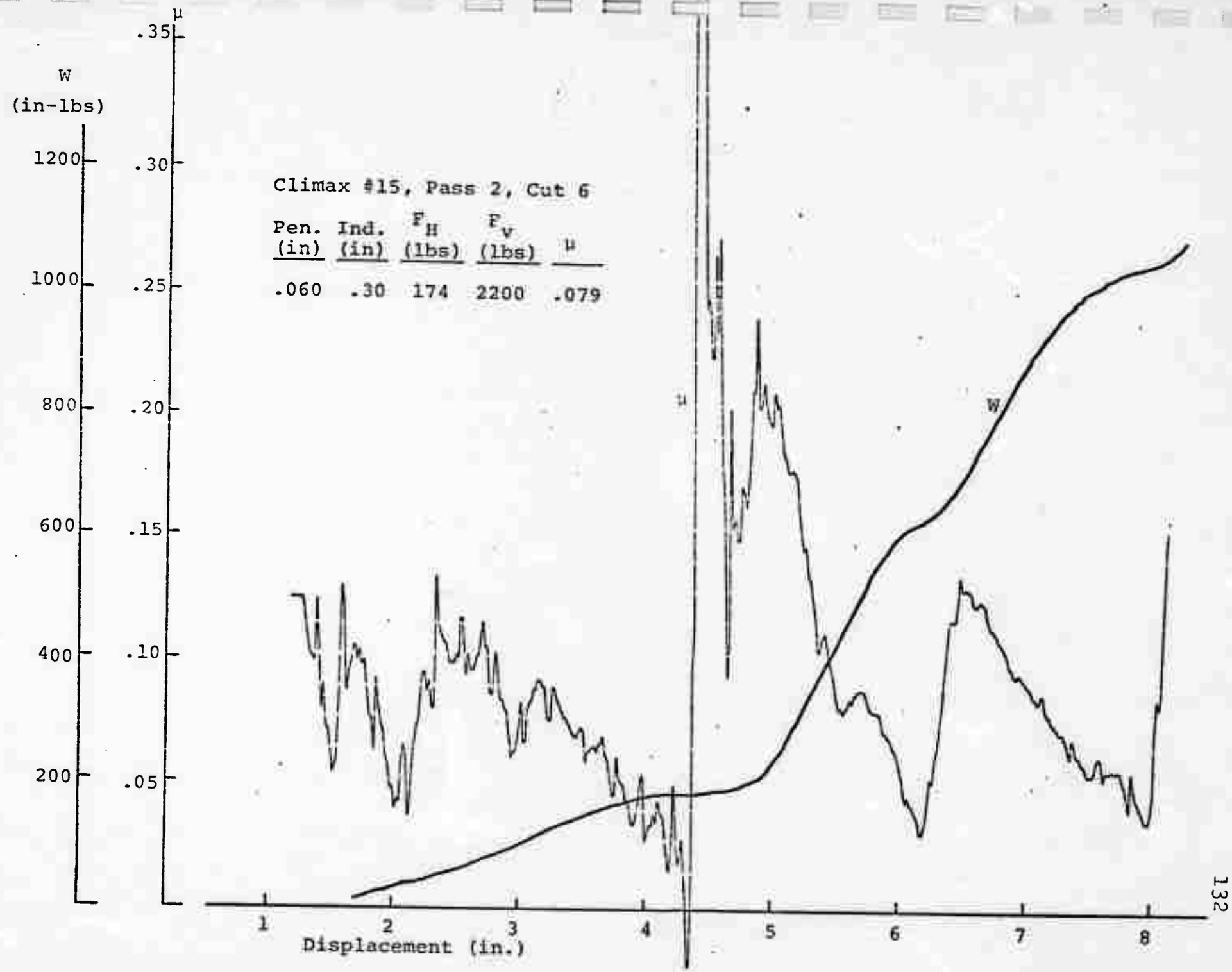
μ
.35
W
(in-lbs)
1200
.30
1000
.25
800
.20
600
.15
400
.10
200
.05
Climax #15, Pass 2, Cut 6
Pen. (in) | Ind. (in) | F_H (lbs) | F_V (lbs) | μ
.060 | .30 | 174 | 2200 | .079
μ
W
1
2
3
4
5
6
7
8
Displacement (in.)

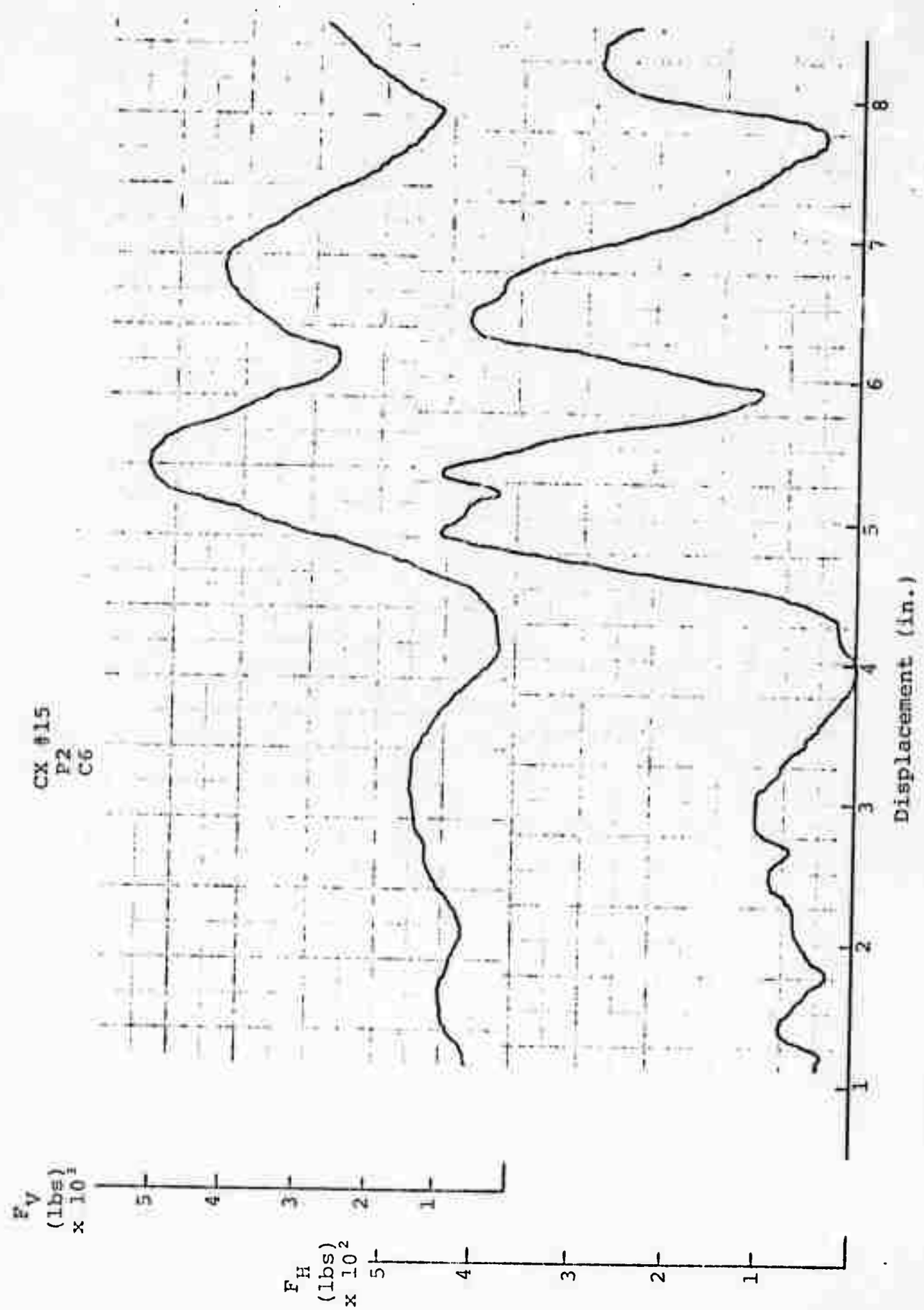
CX #15
P2
C6
F_V (lbs) x 10^3
F_H (lbs) x 10^2
Displacement (in.)

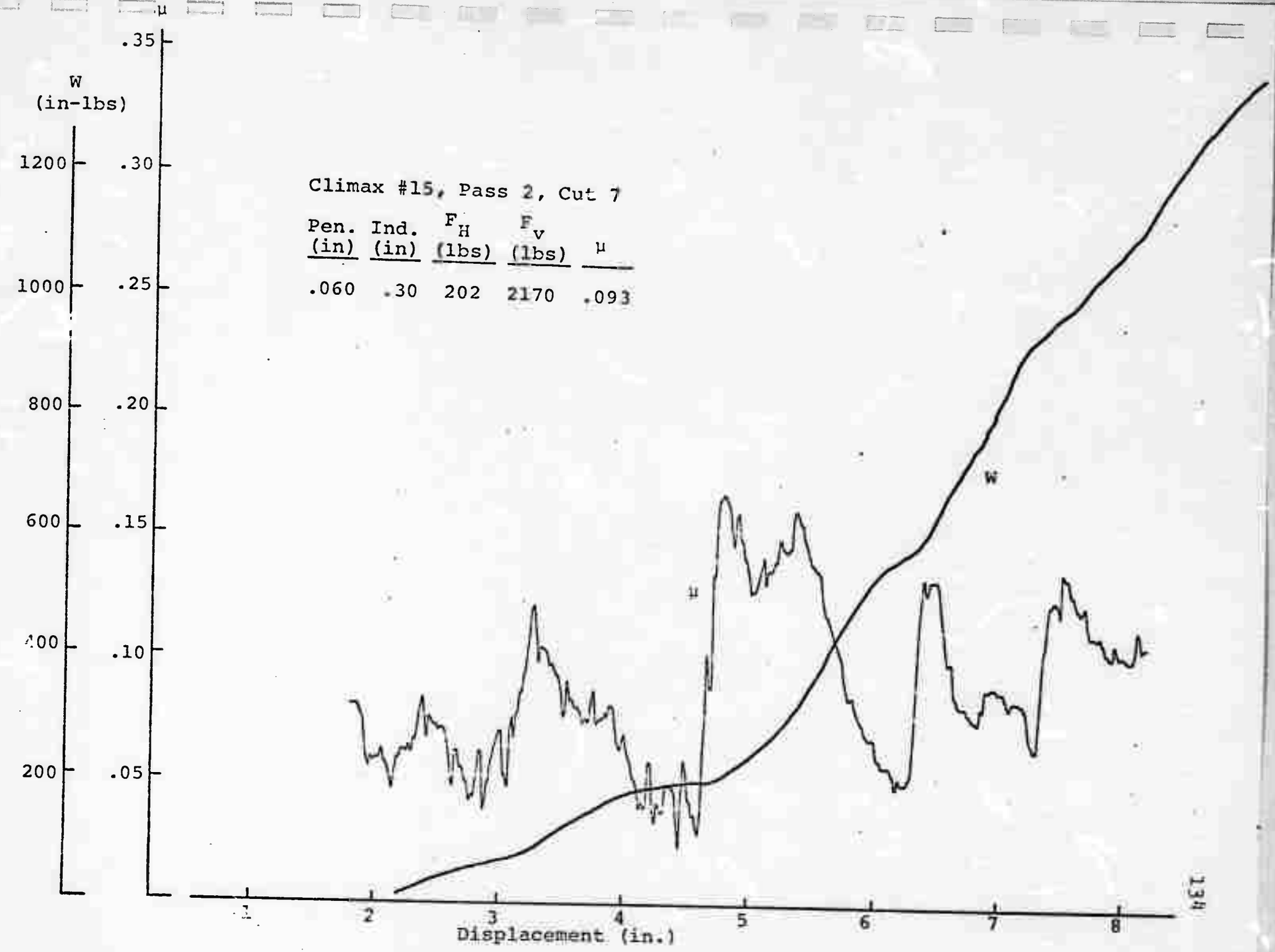
μ
.35
W
(in-lbs)
1200
.30
1000
.25
800
.20
600
.15
400
.10
200
.05
Climax #15, Pass 2, Cut 7
Pen. (in) | Ind. (in) | F_H (lbs) | F_v (lbs) | μ
.060 | .30 | 202 | 2170 | .093
W
μ
1
2
3
4
5
6
7
8
Displacement (in.)

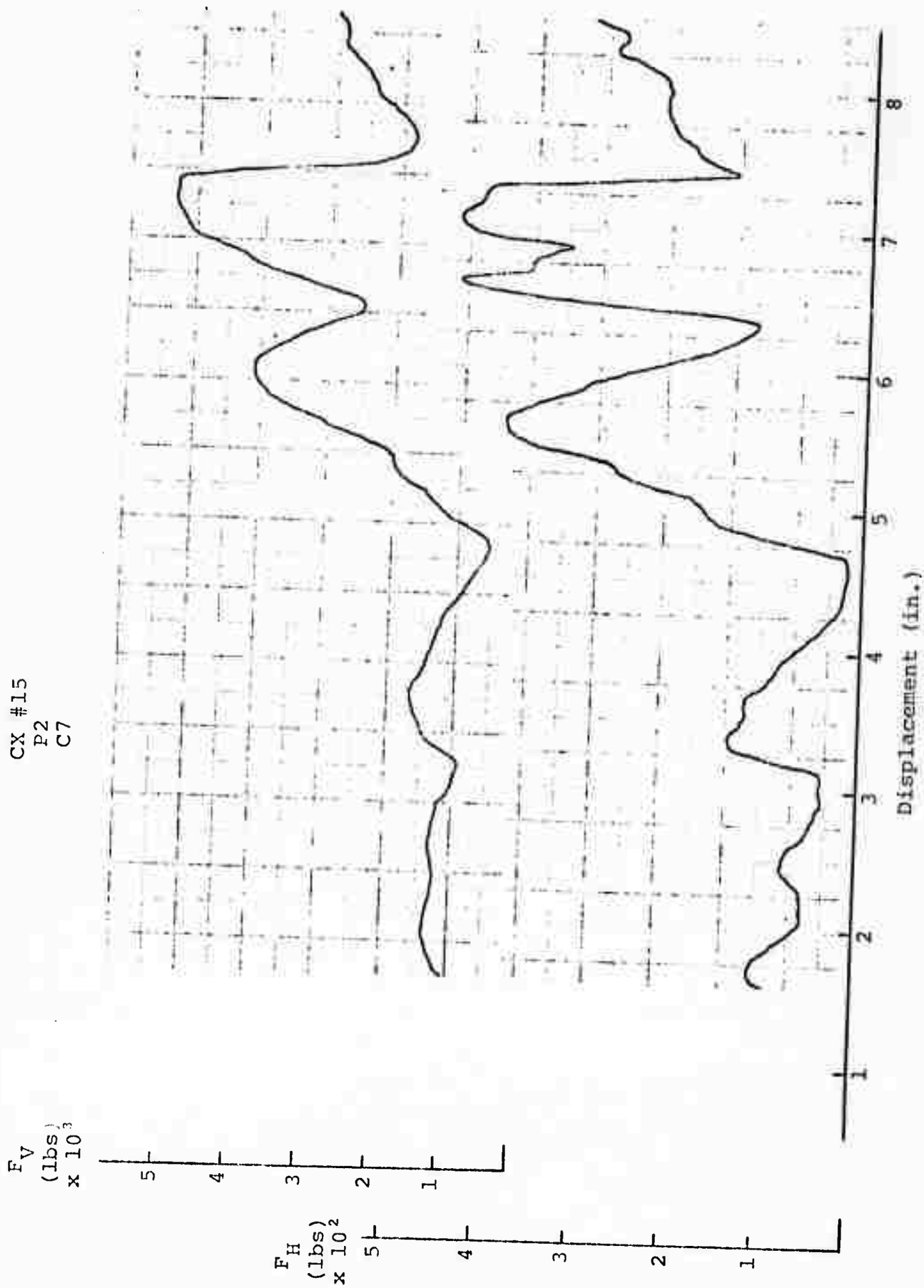
CX #15
P2
C7
F_V (lbs) x 10^3
5
4
3
2
1
F_H (lbs) x 10^2
5
4
3
2
1
1
2
3
4
5
6
7
8
Displacement (in.)

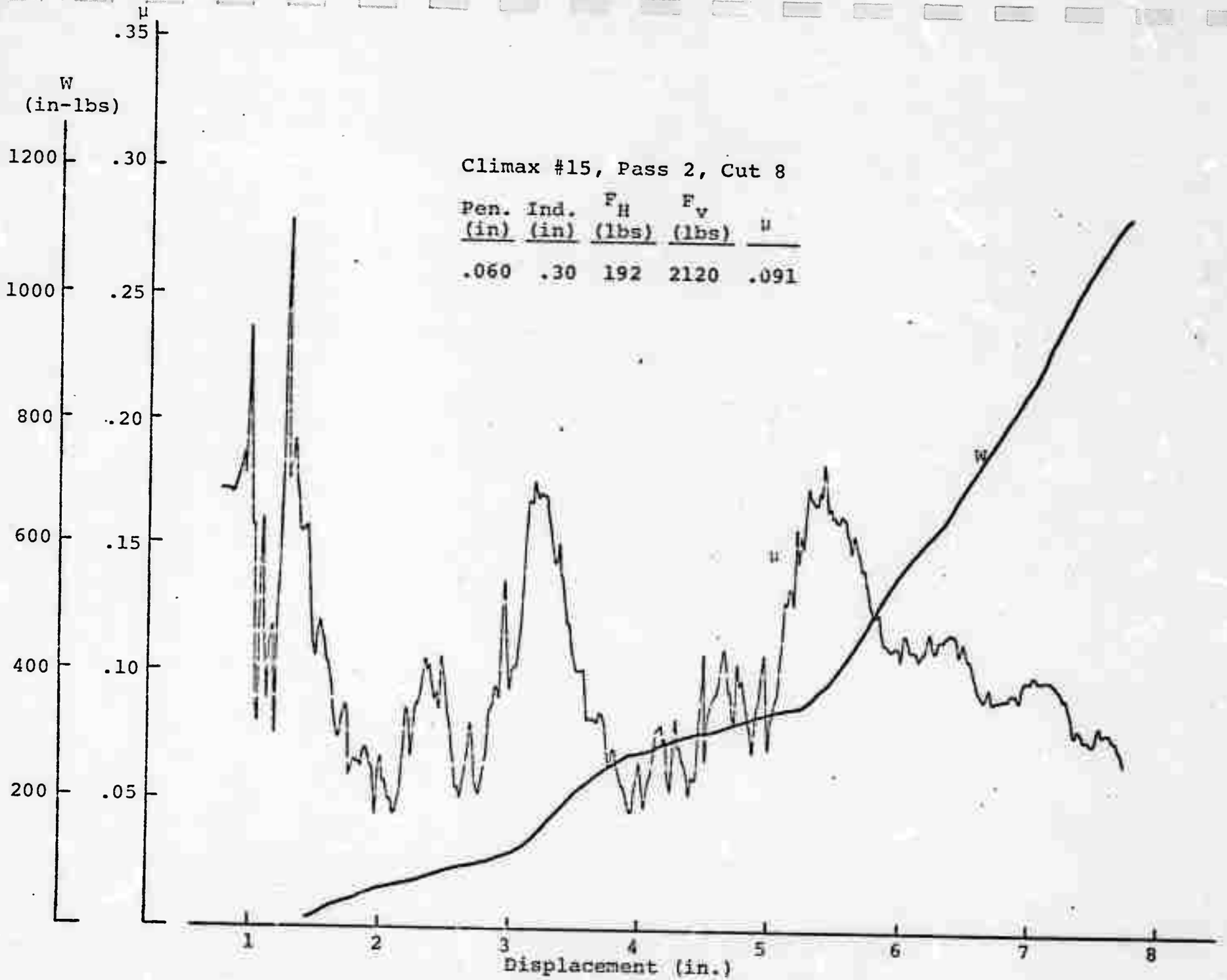
μ
.35
W
(in-lbs)
1200
.30
1000
.25
800
.20
600
.15
400
.10
200
.05
Climax #15, Pass 2, Cut 8
Pen. (in) Ind. (in) F_H (lbs) F_V (lbs) μ
.060 .30 192 2120 .091
W
μ
1
2
3
4
5
6
7
8
Displacement (in.)

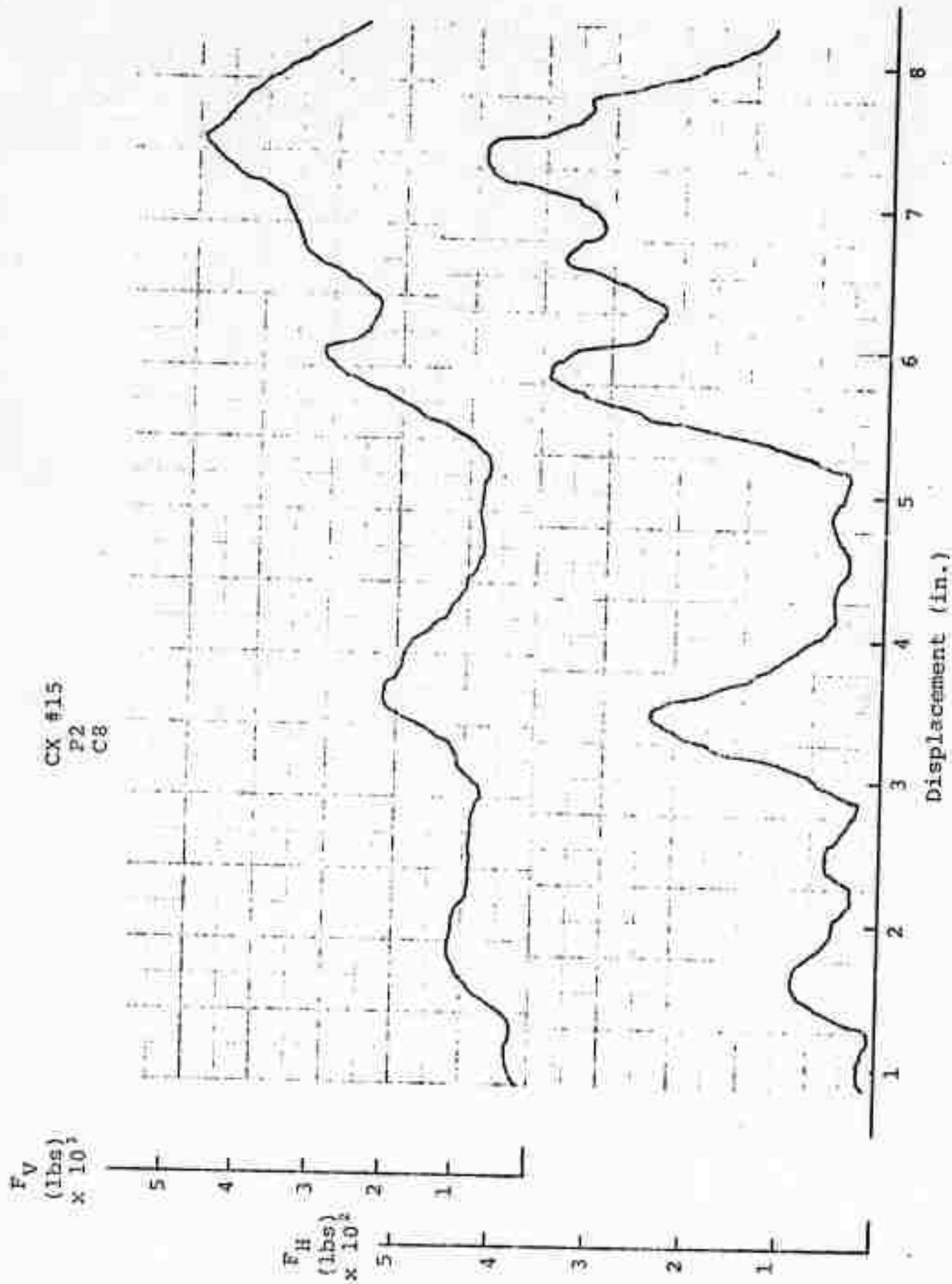
CX #15
P2
C8
F_V (lbs) x 10^3
F_H (lbs) x 10^2
Displacement (in.)

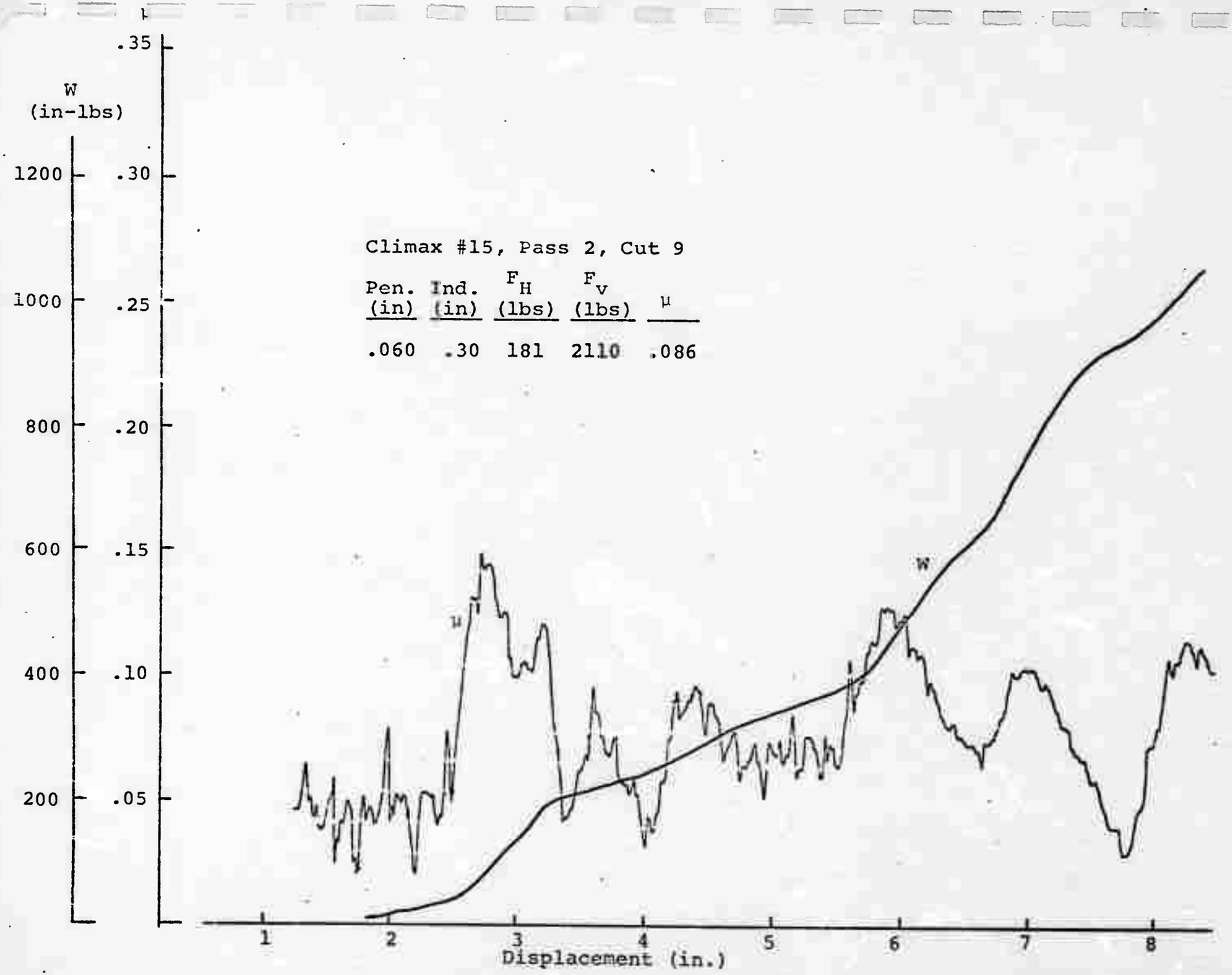
μ
.35
W
(in-lbs)
1200
.30
1000
.25
800
.20
600
.15
400
.10
200
.05
Climax #15, Pass 2, Cut 9
Pen. (in) Ind. (in) F_H (lbs) F_v (lbs) μ
.060 .30 181 2110 .086
μ
W
1
2
3
4
5
6
7
8
Displacement (in.)

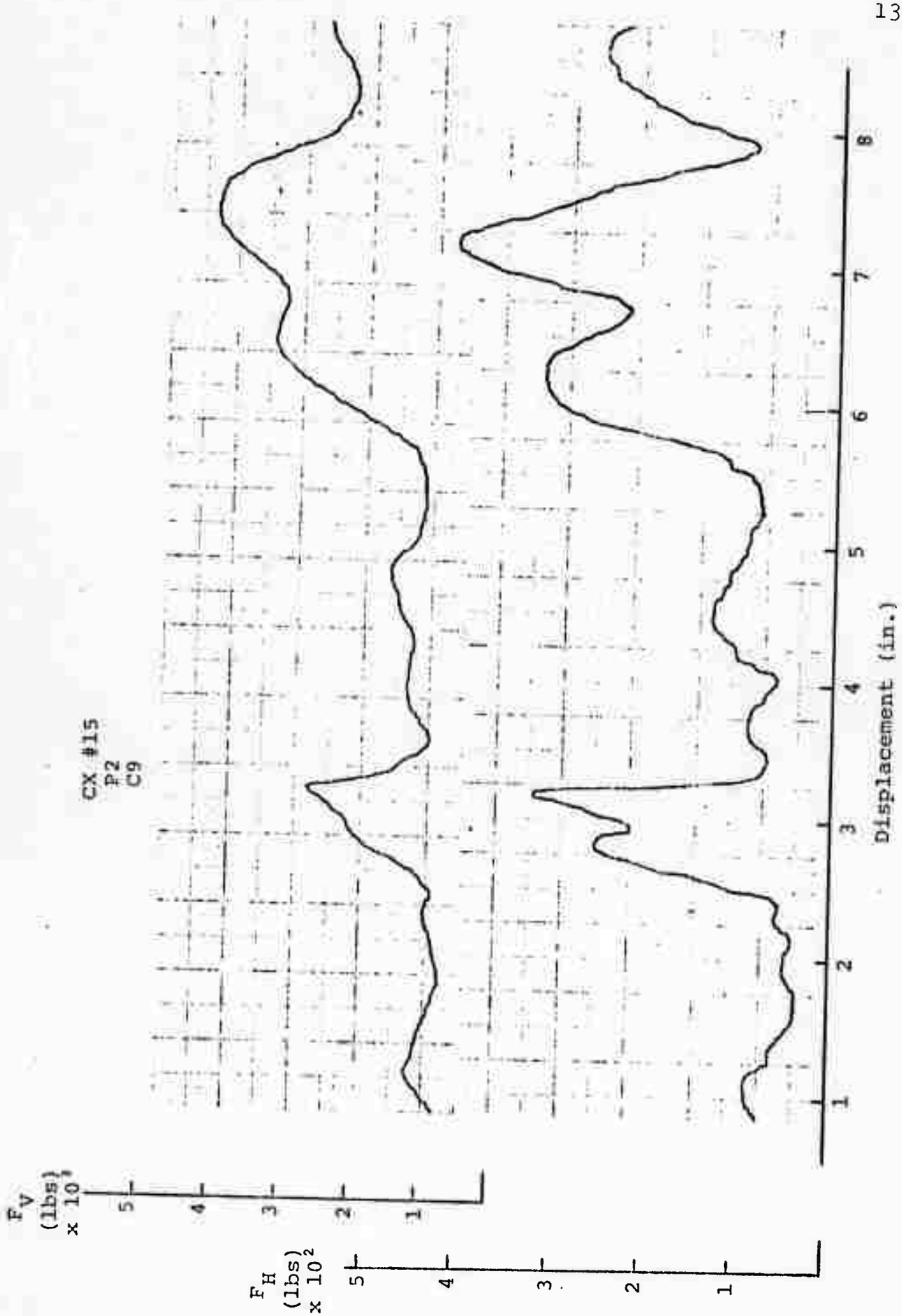
CX #15
P2
C9
Displacement (in.)
1
2
3
4
5
6
7
8
F_V (lbs) x 10^3
F_H (lbs) x 10^2

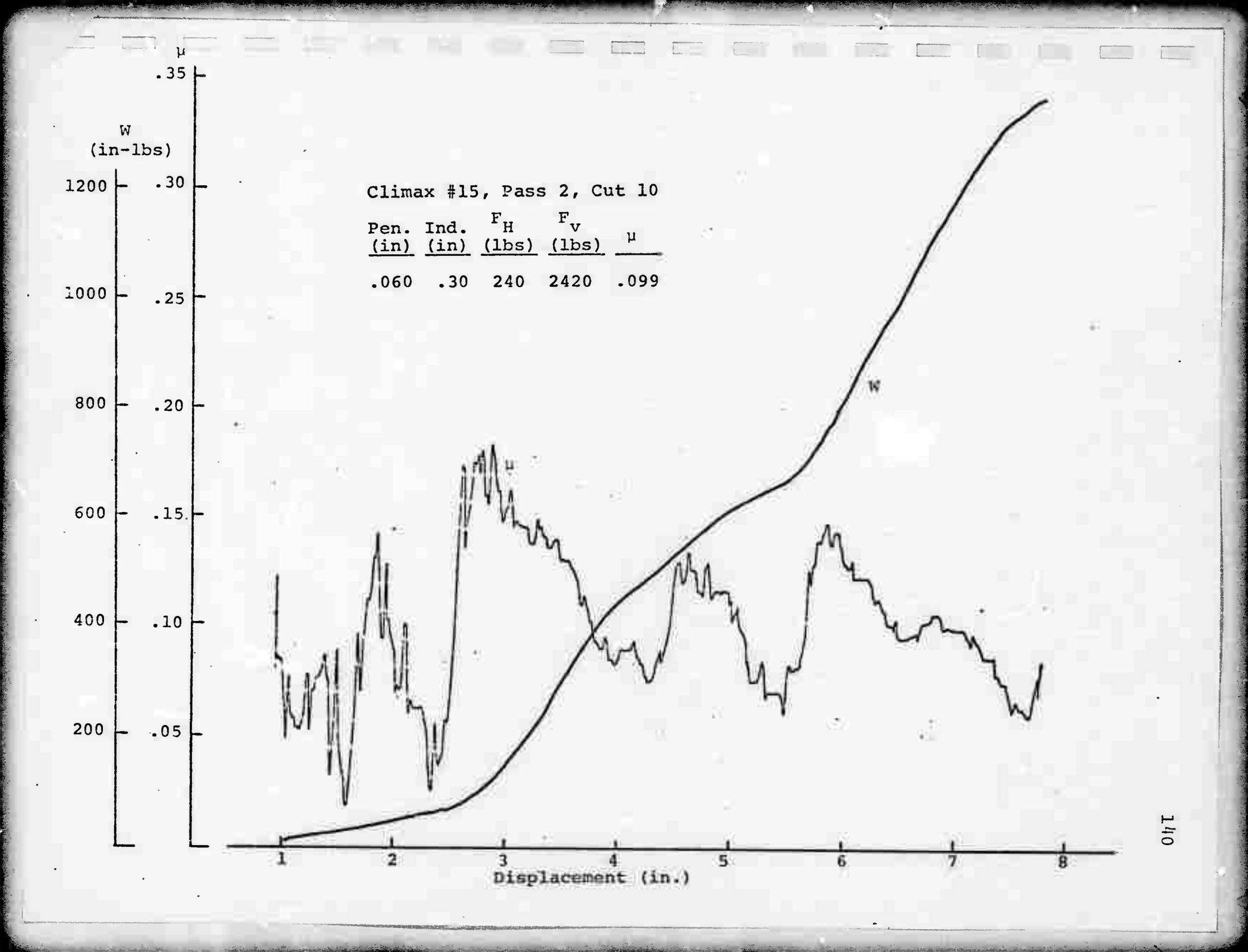
μ
.35
W
(in-lbs)
1200
.30
1000
.25
800
.20
600
.15
400
.10
200
.05
Climax #15, Pass 2, Cut 10
Pen. (in) Ind. (in) F_H (lbs) F_v (lbs) μ
.060 .30 240 2420 .099
W
μ
1 2 3 4 5 6 7 8
Displacement (in.)

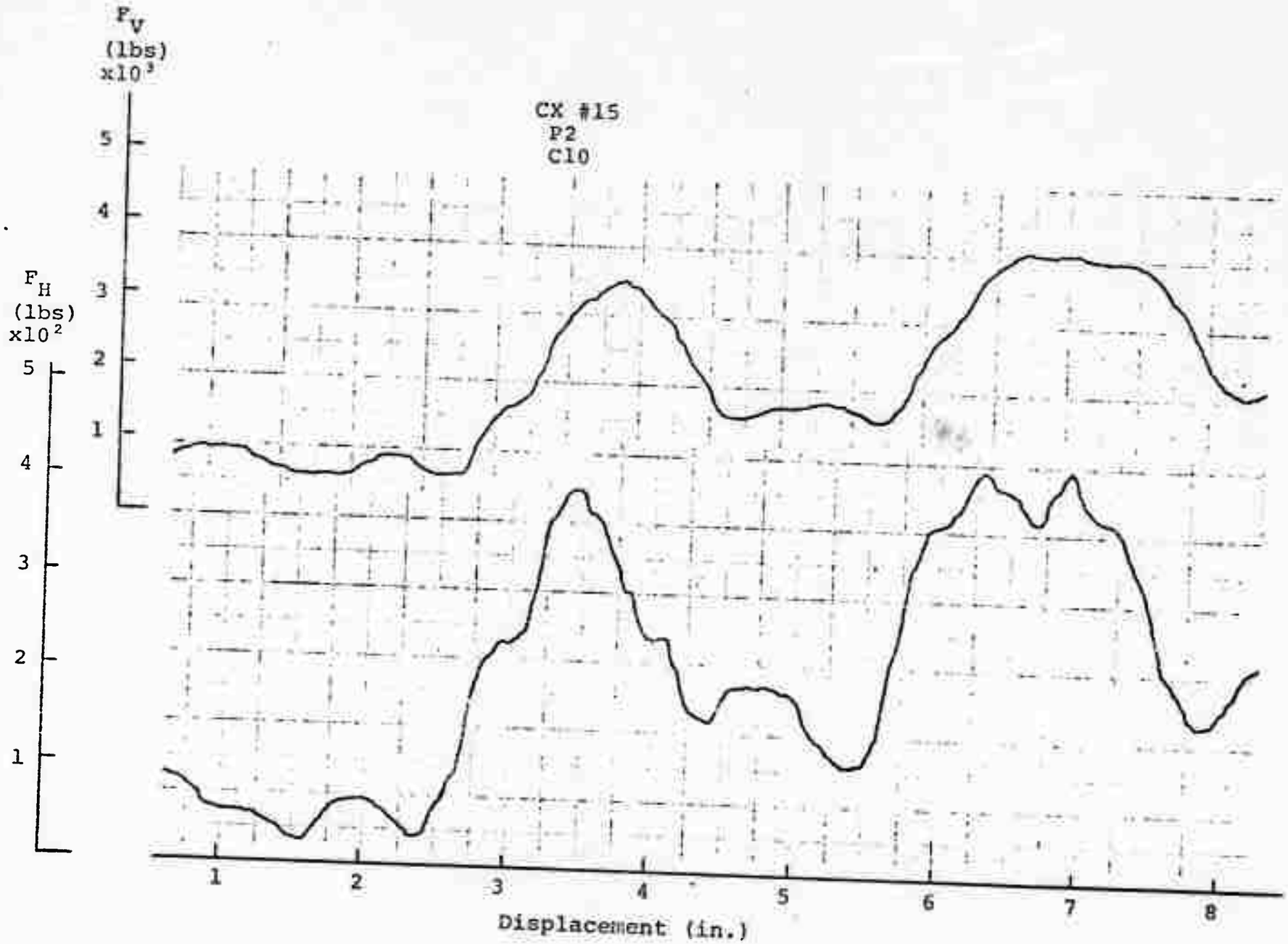
F_V (lbs) x10^3
5
4
3
2
1
CX #15
P2
C10
F_H (lbs) x10^2
5
4
3
2
1
1
2
3
4
5
6
7
8
Displacement (in.)

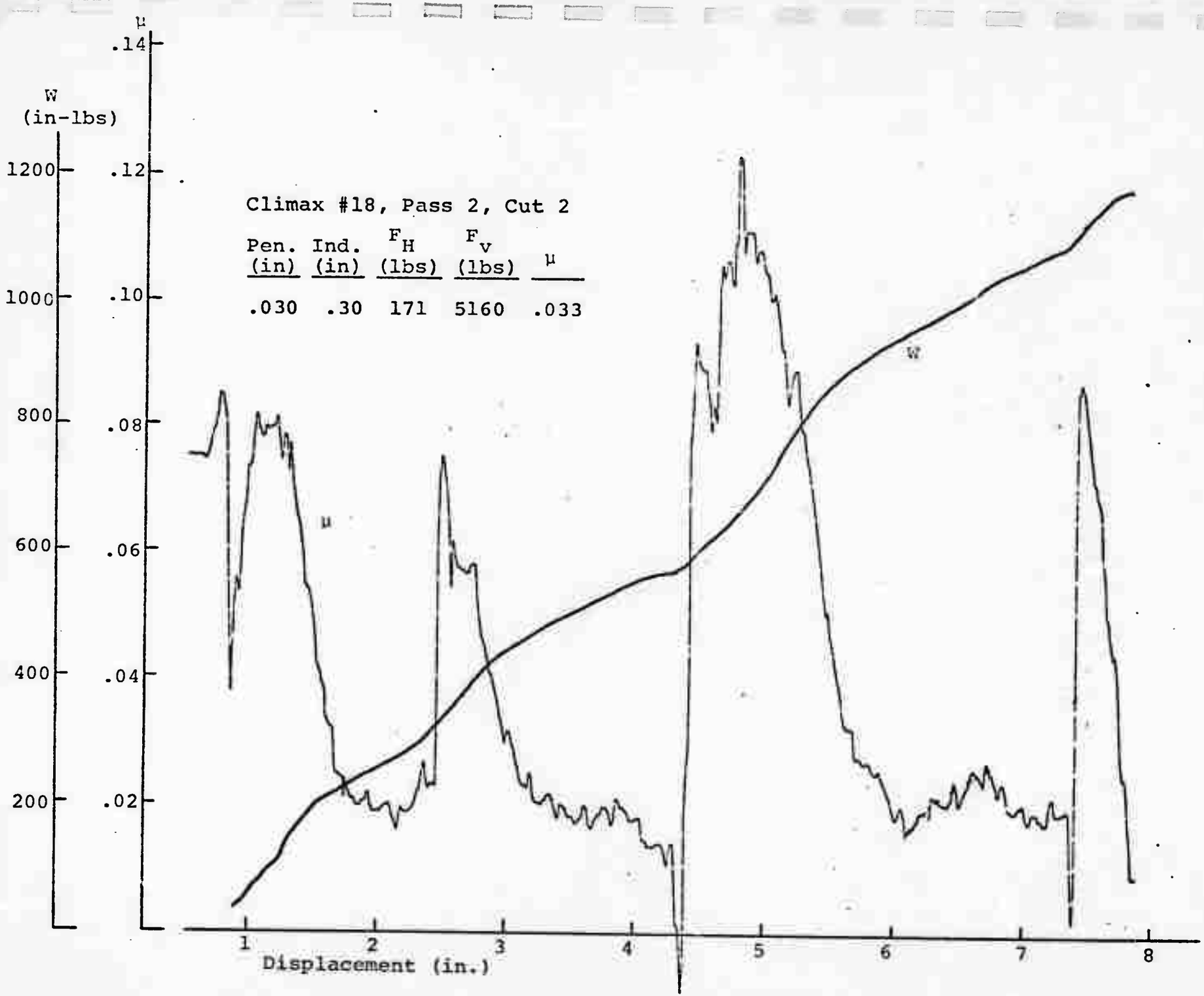
μ
.14
W
(in-lbs)
1200
.12
1000
.10
800
.08
600
.06
400
.04
200
.02
Climax #18, Pass 2, Cut 2
Pen. Ind. F_H F_V
(in) (in) (lbs) (lbs) μ
.030 .30 171 5160 .033
W
μ
1
2
3
4
5
6
7
8
Displacement (in.)

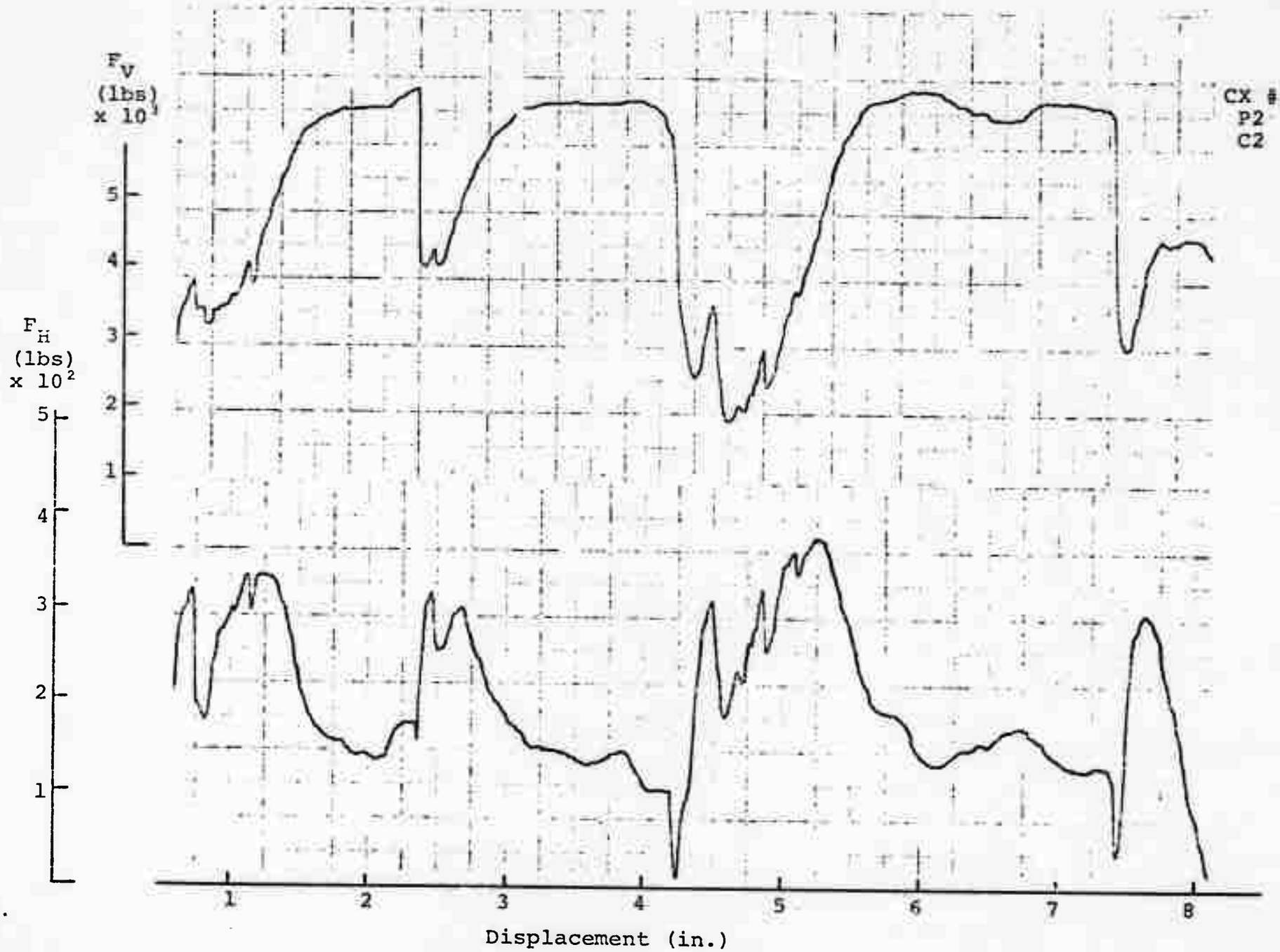
F_V (lbs) x 10^3
5
4
3
2
1
F_H (lbs) x 10^2
5
4
3
2
1
CX #18
P2
C2
1
2
3
4
5
6
7
8
Displacement (in.)

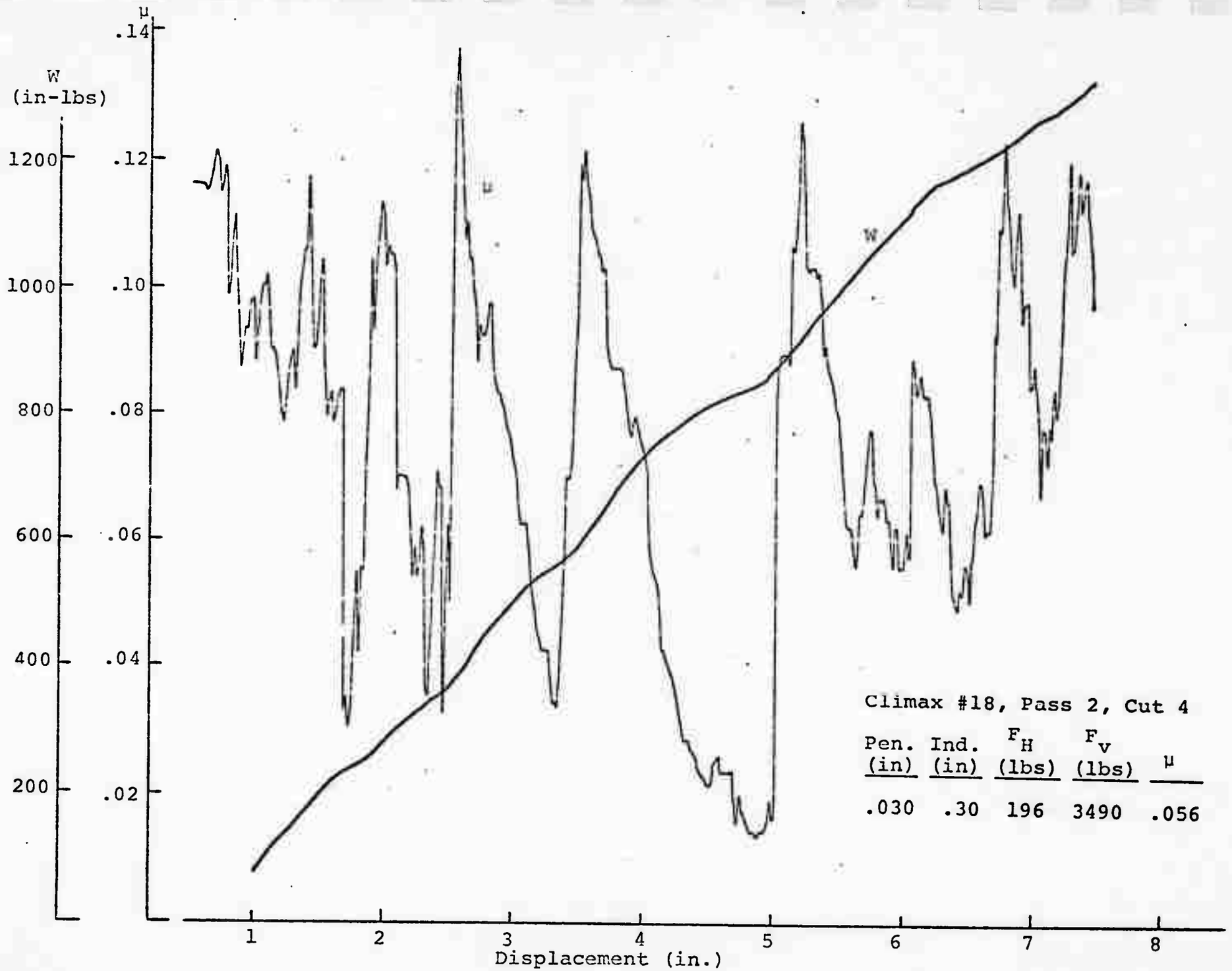

Climax #18, Pass 2, Cut 4

Pen. (in)	Ind. (in)	F_H (lbs)	F_v (lbs)	μ
.030	.30	196	3490	.056

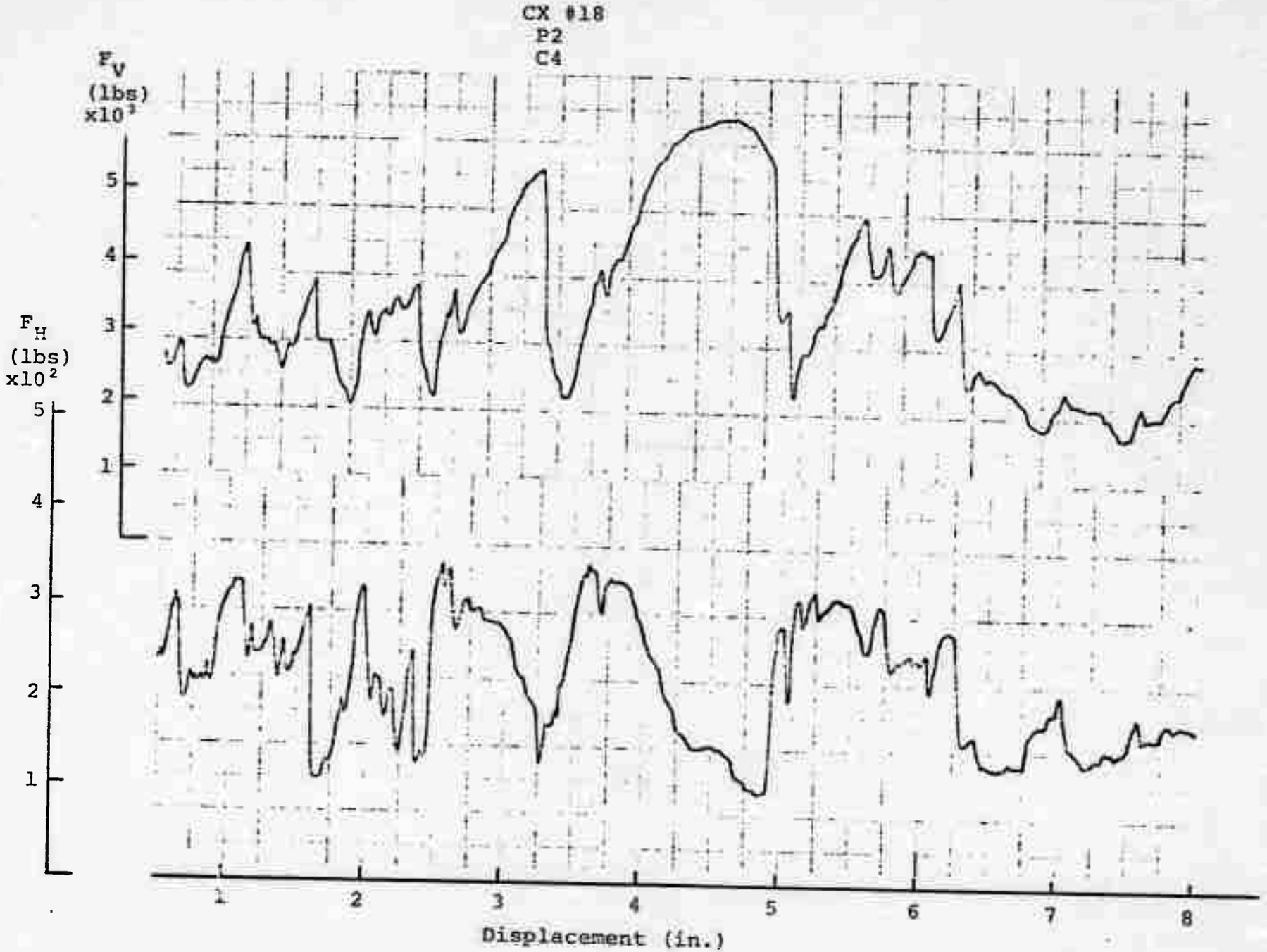
CX #18
P2
C4
F_V (lbs) x10³
5
4
3
2
1
F_H (lbs) x10²
5
4
3
2
1
1
2
3
4
5
6
7
8
Displacement (in.)

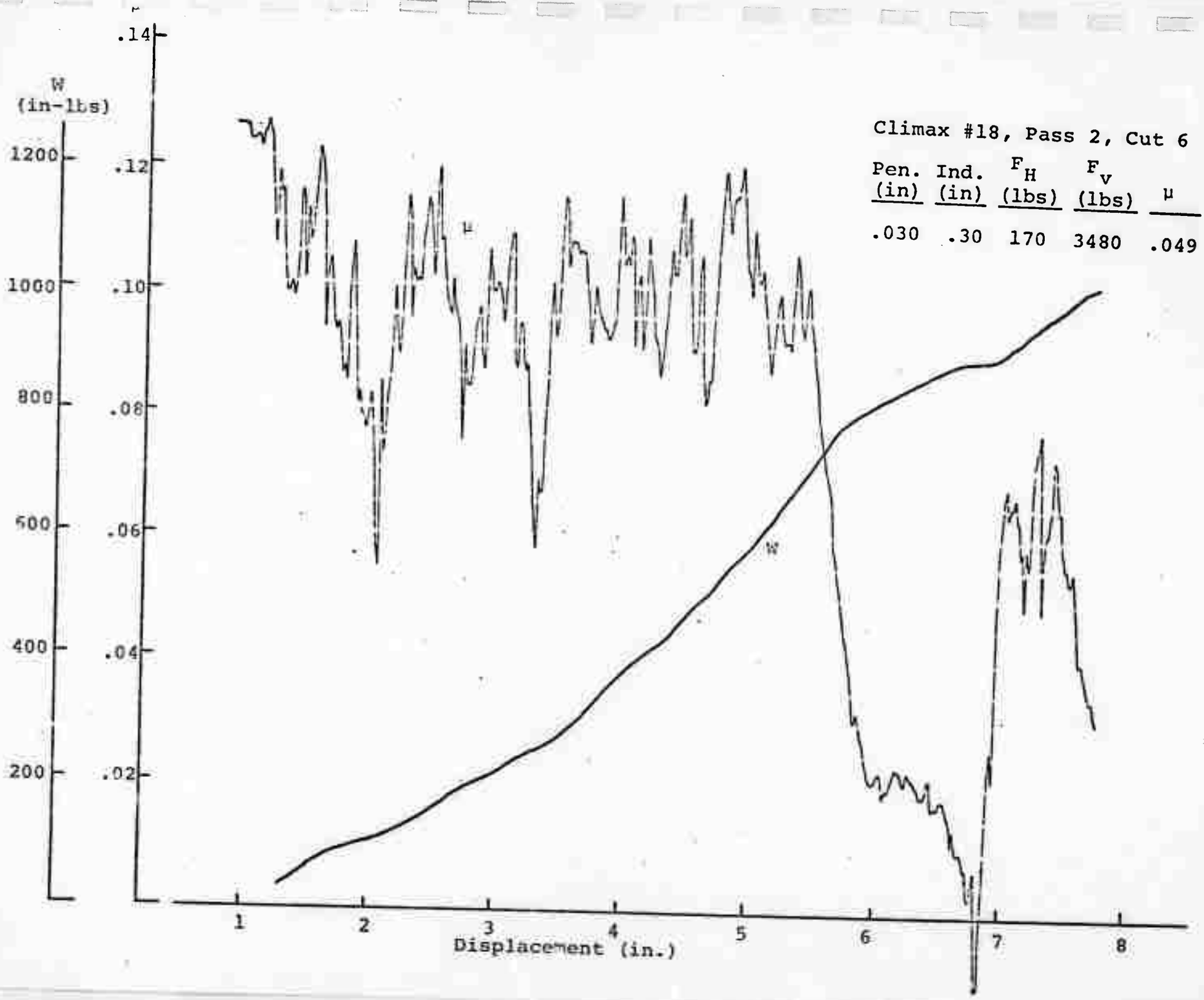

Climax #18, Pass 2, Cut 6

Pen. (in)	Ind. (in)	F_H (lbs)	F_V (lbs)	μ
.030	.30	170	3480	.049

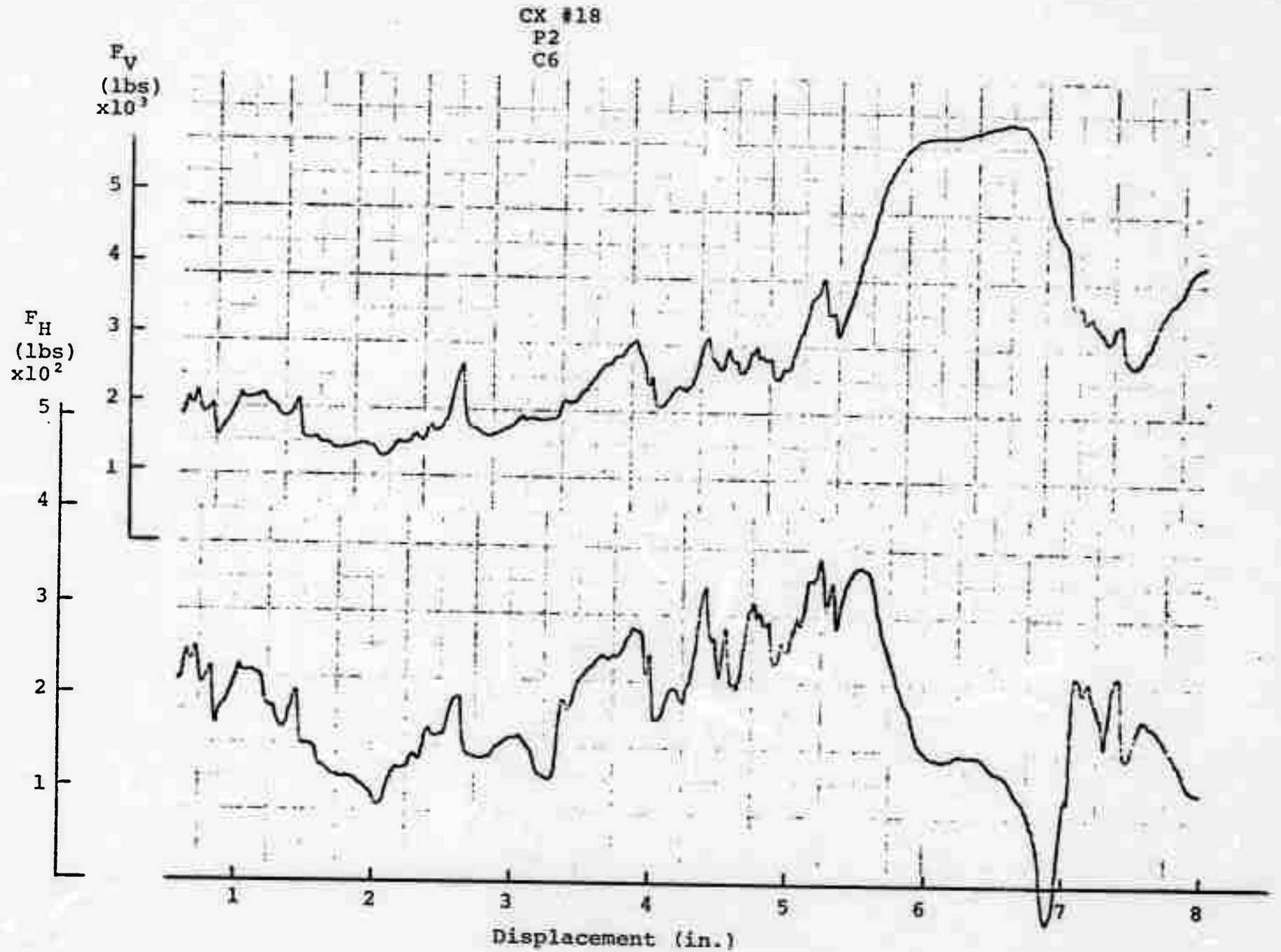
CX #18
P2
C6
F_V (lbs) x10³
5
4
3
2
1
F_H (lbs) x10²
5
4
3
2
1
1
2
3
4
5
6
7
8
Displacement (in.)

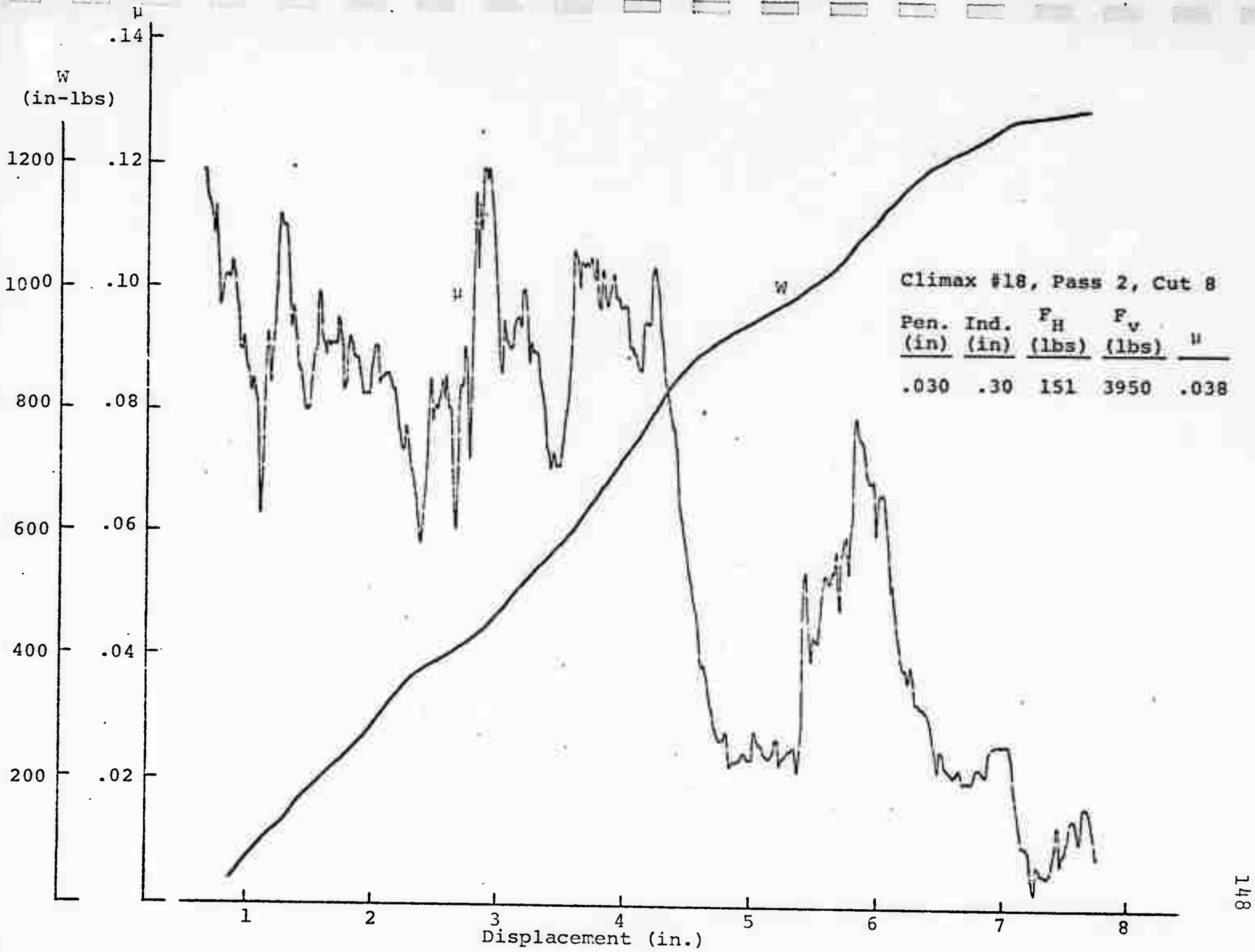
μ
.14
W
(in-lbs)
1200
.12
1000
.10
800
.08
600
.06
400
.04
200
.02
μ
W
Climax #18, Pass 2, Cut 8
Pen. (in) | Ind. (in) | F_H (lbs) | F_V (lbs) | μ
.030 | .30 | 151 | 3950 | .038
1
2
3
4
5
6
7
8
Displacement (in.)

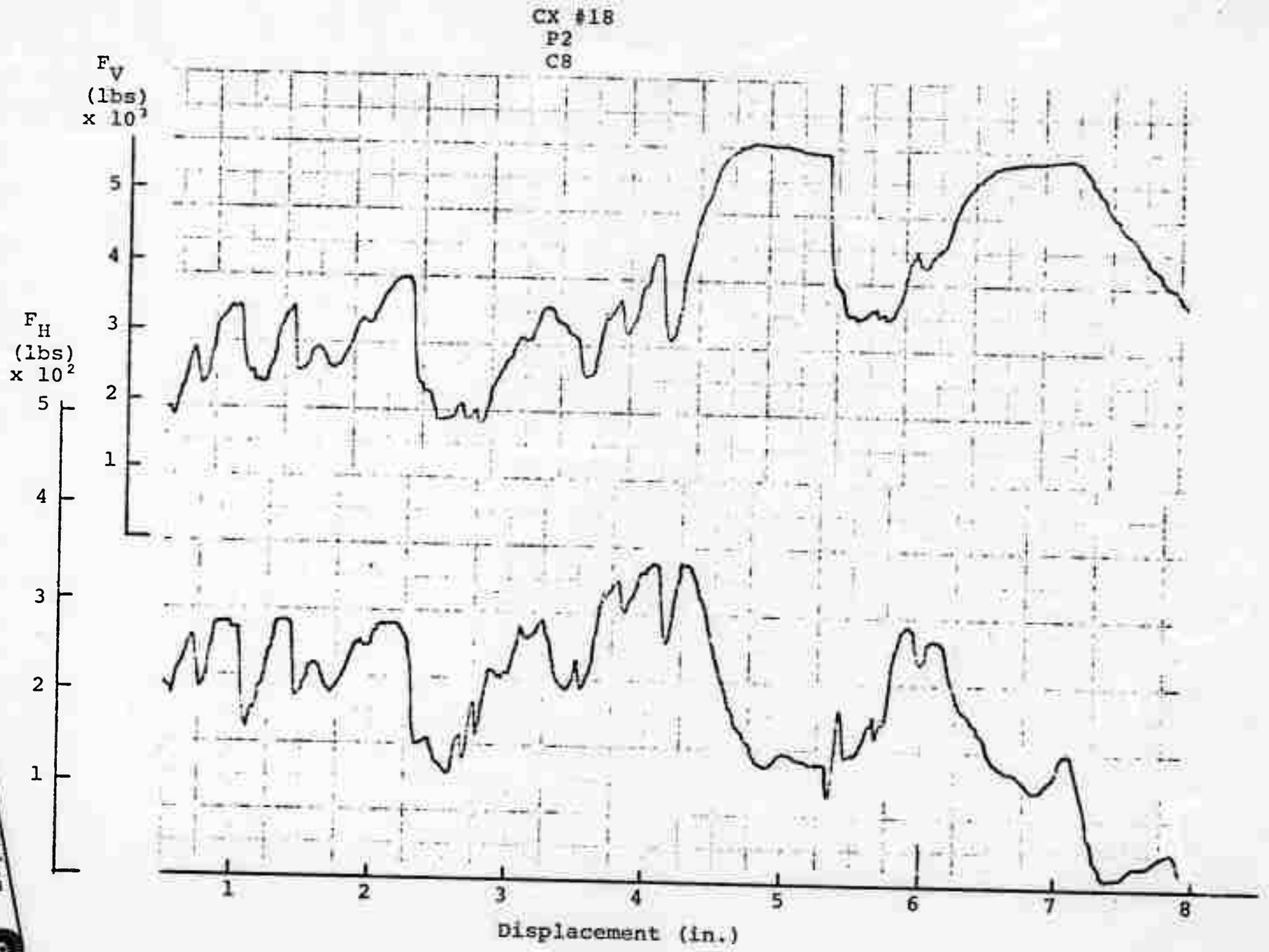

APPENDIX B

THE COMPUTER PROGRAM FOR CALCULATION BY THE HYBRID COMPUTER

```
PROGRAM  ROCK CUT

C       REDUCTION OF ROCK CUTTING DATA
C       * * * MARK II * * * 1/5/72 * * *
C
        DIMENSION FHORIZ[5ØØ],FVERT[5ØØ],DISP[5ØØ],IPAM[2Ø]
        DIMENSION REAL[1ØØ],COMPLX[1ØØ],SCRAT[5ØØ]
        DO 1 I=1,2Ø
    1   ACCEPT TAPE 2,IPAM(I)
    2   FORMAT [A4]
        IMAX = 5ØØ
    3   ACCEPT 4, X,IDENT
    4   FORMAT [F1Ø.0,A4]
        DO 5 I=1,2Ø
        IF [IDENT - IPAM[I]] 5,7,5
    5   CONTINUE
        TYPE 6,IDENT
    6   FORMAT [$NO SUCH NAME AS $,A4]
        GO TO 3
    7   GO TO [8,9,1Ø,11,12,13,14,15,16,3Ø,17,18,19,2Ø,21,22,
        23,24,25,26],I
    8   NSTEP = X
        CALL PLOT 1[Ø,Ø.,1,Ø.,NSTEP]
        GO TO 3
    9   DT = X
        GO TO 3
   1Ø   SHORIZ = X
        GO TO 3
   11   SVERT = X
        GO TO 3
   12   SDISP = X
        GO TO 3
   13   NFROS = X
        GO TO 3
   14   RQIN = X
        GO TO 3
   15   XMAX = X
        GO TO 3
   16   YMAX = X
        GO TO 3
   17   GO TO 3
   18   GO TO 3
   19   GO TO 3
   2Ø   GO TO 3
   21   GO TO 3
   22   GO TO 3
   23   GO TO 3
   24   GO TO 3
   25   GO TO 3
   26   GO TO 3
C
C       * * * RUN MODE SELECTION * * *
```

```
C
 3Ø   CALL PLOT2[X,Ø.]
      CALL PLOT2[Ø.,Ø.]
      TYPE 31
 31   FORMAT [$TYPE 1 FOR SAMPLE, 2 FOR PLOTTINGS$]
      ACCEPT 32, 1
 32   FORMAT [11]
      GO TO [4Ø,33],1
 33   TYPE 34
 34   FORMAT [$TYPE 1 FOR CUTTING COEF., 2 FOR ENERGY, 3 FOR
      FOURIER$]
 35   ACCEPT 32,1
      GO TO [60,80,36],1
 36   TYPE 37
 37   FORMAT [$TYPE 1 FOR FHORIZ PLOT, 2 FOR FHORIZ TTY,
      3 FOR BOTH,...$
      1/3X$4 FOR FVERT PLOT, 5 FOR FVERT TTY, 6 FOR BOTH$]
 38   ACCEPT 32,  IFLAG
      GO TO [1ØØ,1ØØ,1ØØ,14Ø,14Ø,14Ø],IFLAG
C
C     * * * SAMPLING SECTION * * *
C
 4Ø   IF [ITEST[1]] 4Ø,4Ø,5Ø
 5Ø   CALL SIGNAL[Ø]
 41   IF [ITEST[Ø]] 42,42,41
 42   IF [ITEST[Ø]] 42,42,43
 43   CALL ADL [Ø,FHORIZ[I],SHORIZ,FVERT[I],SVERT,DISP[I],SDISP]
      I = I + 1
 44   IF [ITEST[1]] 46,46,45
 45   IF[I - IMAX] 41,41,46
 46   NLAST = I - 1
      CALL SIGNAL[1]
      GO TO 3
C
C     * * * PLOT CUTTING COEFFICIENT * * *
C
 60   X = DISP[1]/XMAX
      Y = FHORIZ[1] / [FVERT[1] * YMAX]
      CALL PLOT2[X,Y]
      PAUSE
      I = 2
 61   X = DISP[I] / XMAX
      Y = FHORIZ[I] / [FVERT[I] * YMAX]
      CALL PLOT2[X,Y]
      I = I + 1
      IF [I - NLAST] 61,61,3
C
C     * * * PLOT ENERGY * * *
C
 80   F1 = FHORIZ[1]
      F2 = FHORIZ[2]
      X1 = DISP[1]
      X2 = DISP[2]
      W = [F1 + F1] / 2. * [X2 - X1]
      I = 3
```

```
      X = X2 / XMAX
      Y = W / YMAX
      CALL PLOT2[X,Y]
      PAUSE
 81   X1 = X2
      F1 = F2
      X2 = DISP[I]
      F2 = FHORIZ[I]
      W = W + [X2 - X1] * [F1 + F2] / 2.
      X = X2 / XMAX
      Y = W / YMAX
      CALI PLOT2[X,Y]
      I = I + 1
      IF [I - NLAST] 81,81,3
C
C     * * * FREQUENCY ANALYSIS OF HORIZONTAL FORCE * * *
C
 1ØØ  NPTS = NLAST
      IF [NLAST - 2 * [NLAST / 2]] 1Ø2,1Ø1,1Ø2
 1Ø1  NPTS = NPTS - 1
 1Ø2  TLWR = Ø
      TUPR = [NPTS - 1] * DT
      CALL FOR INT[FHORIZ,SCRAT,NPTS,TLWR,TUPR,NFRQS,FRQIN,
      REAL,COMPLX]
      GO TO [1Ø5,12Ø,1Ø5],IFLAG
C
C     * * * PLOT FOURIER TRANSFORM * * *
C
 1Ø5  X = Ø
      DB = 2Ø. / [YMAX * ALOG[1Ø.]]
      Y = ABS[REAL[1]] / YMAX
      DX = FRQIN / XMAX
      I = 1
      IF [SENSE SWITCH 1] 11Ø,111
 11Ø  IF [REAL[1]] 112,112,113
 113  Y = DB * ALOG[REAL[1]]
      GO TO 111
 112  Y = -1.
 111  CALL PLOT2[X,Y]
      PAUSE
 1Ø6  X = X + DX
      I = I + 1
      Y = SQRT[REAL[I]*REAL[I] + COMPLX[I]*COMPLX[I]]/YMAX
      IF [SENSE SWITCH 1] 115,118
 115  IF [Y] 116,116,117
 116  Y = -1
      GO TO 118
 117  Y = DB * ALOG[Y*YMAX]
 118  CALL PLOT2[X,Y]
      IF [I - NFRQS] 1Ø6,1Ø7,1Ø7
 1Ø7  GO TO [3,12Ø,12Ø,3,15Ø,15Ø],IFLAG
C
C     * * * PRINT FOURIER TRANSFORM * * *
C
 12Ø  TYPE 121
```

```
 121  FORMAT [///$FOURIER TRANSFORM OF HORIZONTAL FORCE$]
 13Ø  TYPE 122
 122  FORMAT [3X5HFREQ.5X4HREAL5X5HIMAG.]
      I = 1
      X = Ø
 123  TYPE 124, X,REAL[1]
 124  FORMAT [F1Ø.3,F1Ø.5]
 125  I = I + 1
      IF [I - NFRQS] 126,126,3
 126  X = X + FRQIN
      TYPE 127, X,REAL[I],COMPLX[I]
 127  FORMAT [F1Ø.3,2F1Ø.5]
      GO TO 125
C
C     * * * FREQUENCY ANALYSIS OF VERTICAL FORCE * * *
C
 14Ø  NPTS = NLAST
      IF [NLAST - 2 * [NLAST / 2]] 142,141,142
 141  NPTS = NPTS - 1
 142  TLWR = Ø
      TUPR = [NPTS - 1] * DT
      CALL FOR INT [FVERT,SCRAT,NPTS,TLWR,TUPR,NFRQS,FRQIN,
      REAL,COMPLX]
      IF [IFLAG - 5] 1Ø5,15Ø,1Ø5
 15Ø  TYPE 151
 151  FORMAT [///$FOURIER TRANSFORM OF VERTICAL FORCE $]
      GO TO 13Ø
      END
```

APPENDIX C

DATA FROM THE NAST TUNNEL. BORING RATE, SPECIFIC ENERGY, CUTTING COEFFICIENT, TORQUE, AND THRUST ARE GIVEN ALONG THE TUNNEL. DOTS ARE THE VALUES FOR EACH SHIFT, SQUARES ARE THE WEIGHTED AVERAGES OF EACH ONE HUNDRED FEET ADVANCE (TO THE END OF NEAREST SHIFT).

THE GEOLOGICAL CLASSIFICATION IS MARKED ON THE PLOT OF BORING RATE. THE CLASSIFICATION IS MAINLY BASED ON THE STRUCTURAL FEATURES OF ROCK.

X	EXCELLENT
XG, GX	EXCELLENT, GOOD
G	GOOD
GF, FG	GOOD, FAIR
F	FAIR
FP	FAIR, POOR
P	POOR

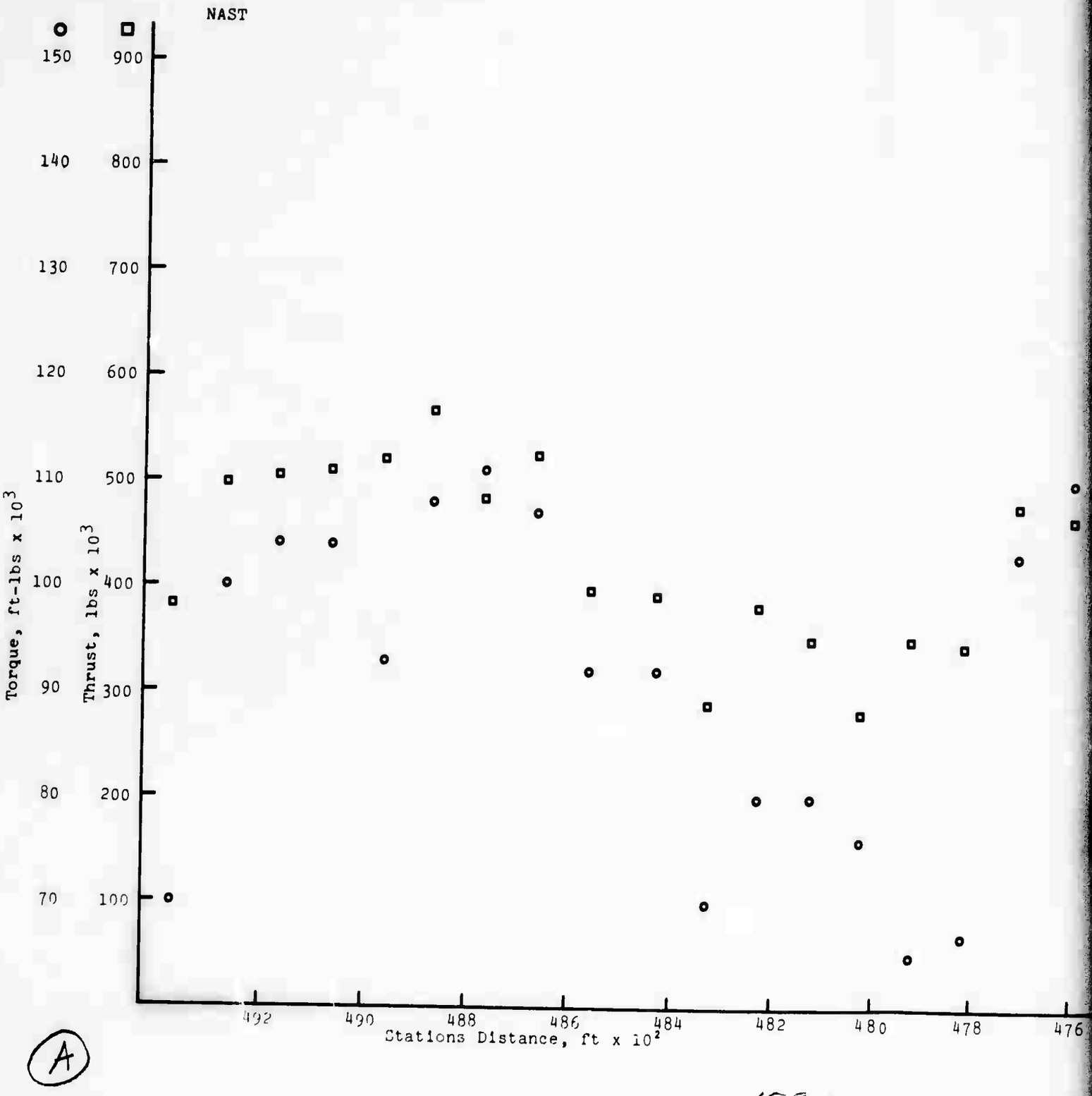
NAST
Torque, ft-lbs x 10^3
Thrust, lbs x 10^3
150
140
130
120
110
100
90
80
70
900
800
700
600
500
400
300
200
100
492
490
488
486
484
482
480
478
476
Stations Distance, ft x 10^2

(A)

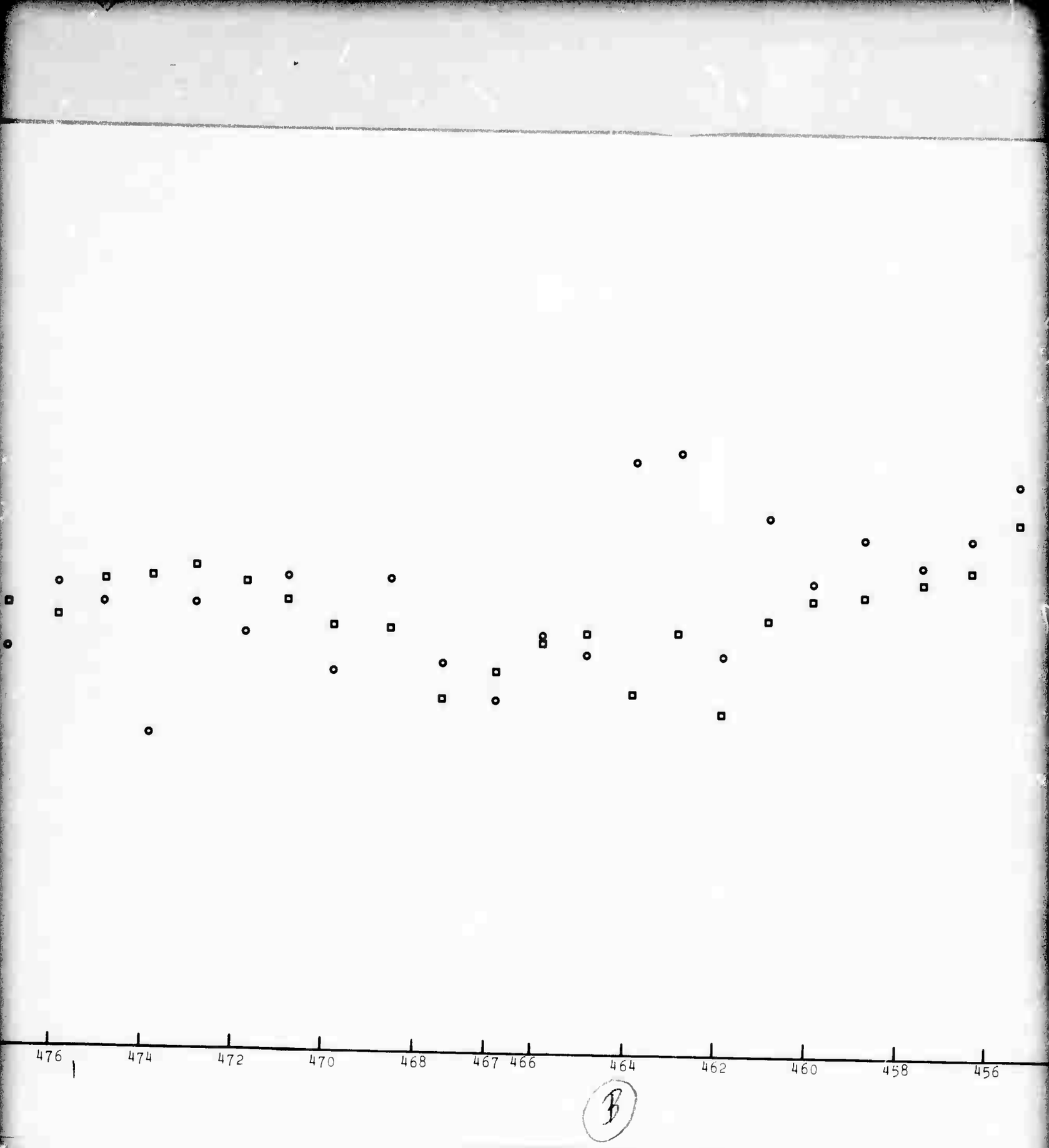

B

(C)

NAST

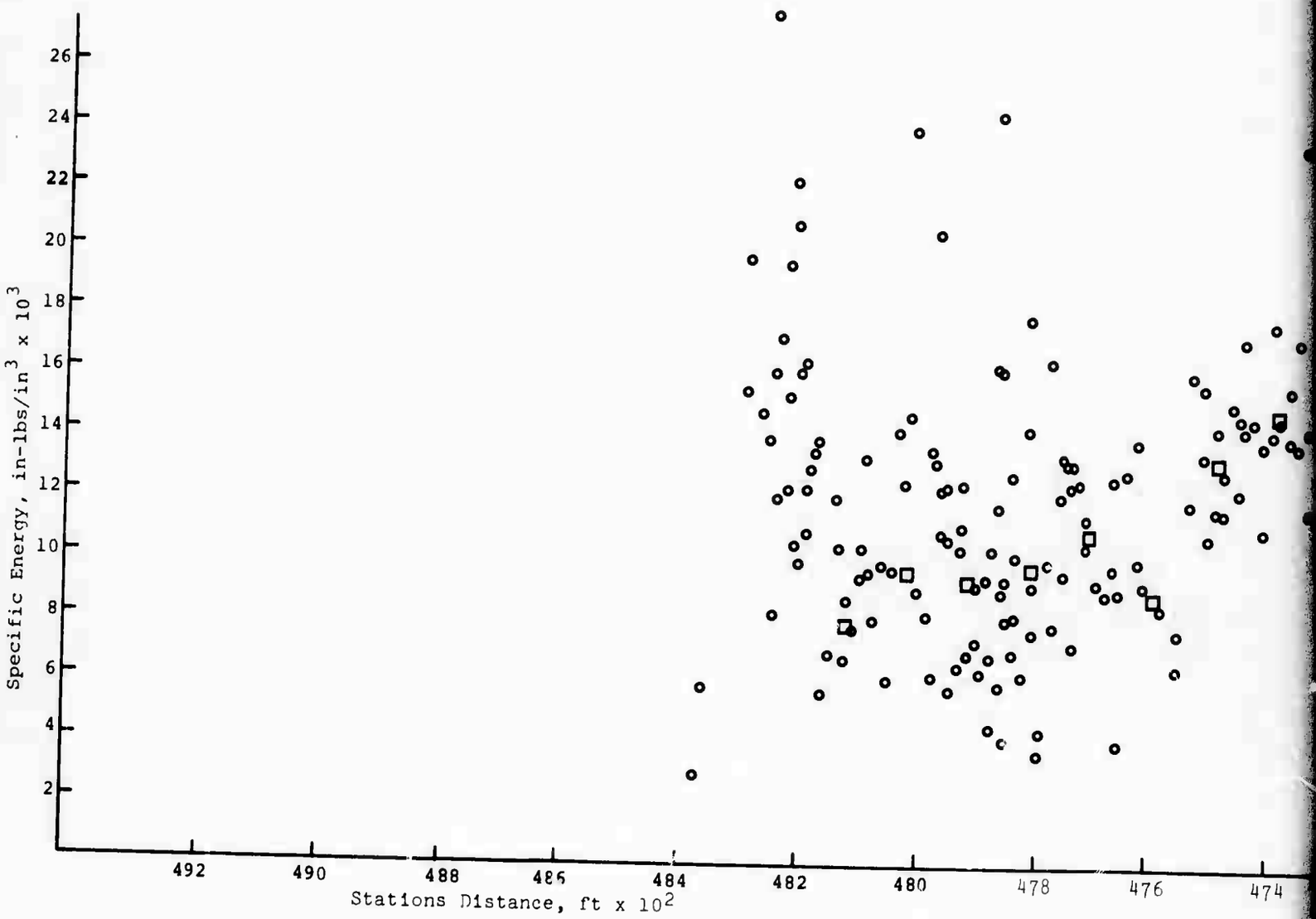
Specific Energy, in-lbs/in^3 x 10^3
26
24
22
20
18
16
14
12
10
8
6
4
2
492
490
488
486
484
482
480
478
476
474
Stations Distance, ft x 10^2

(A)

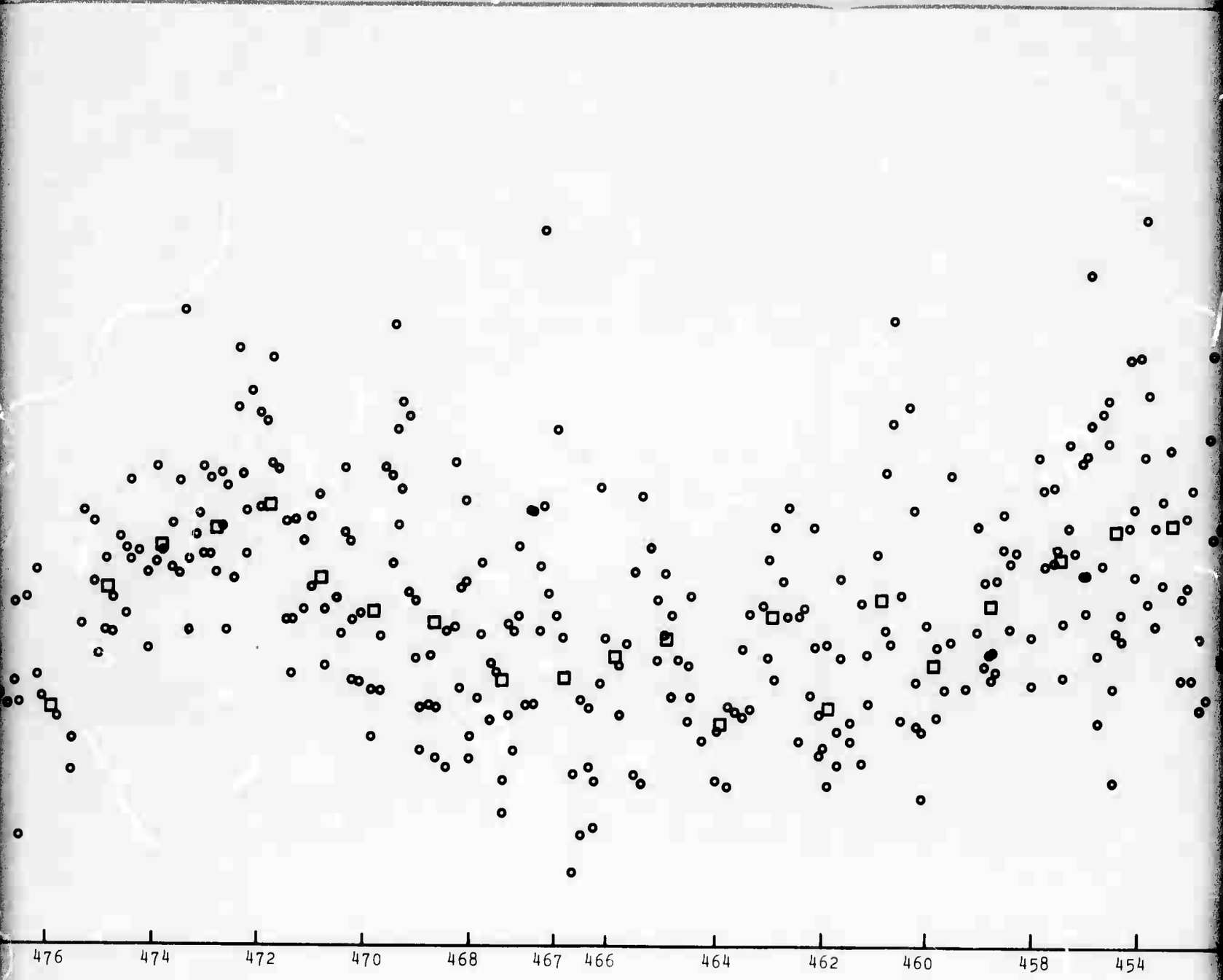

B

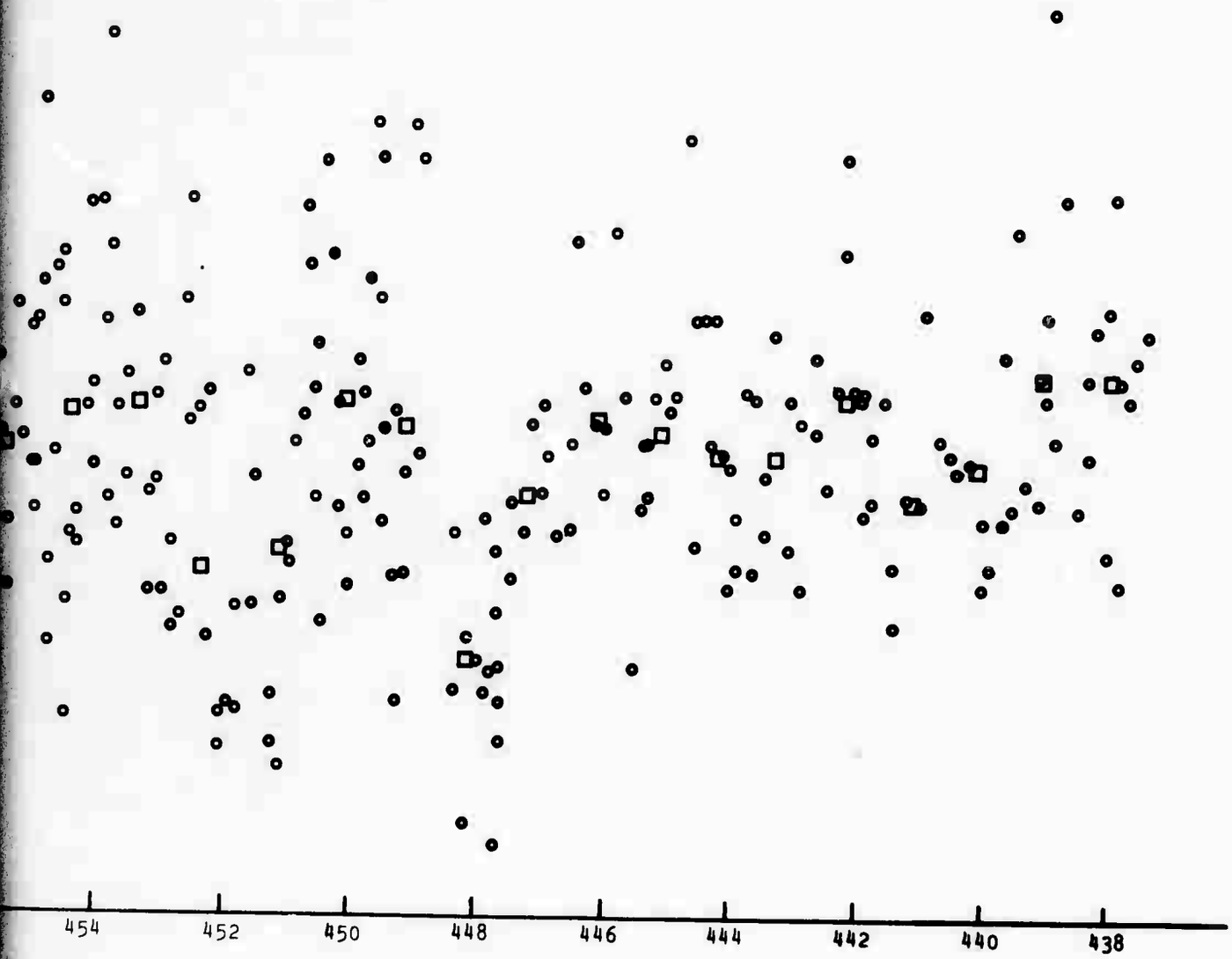

(C)

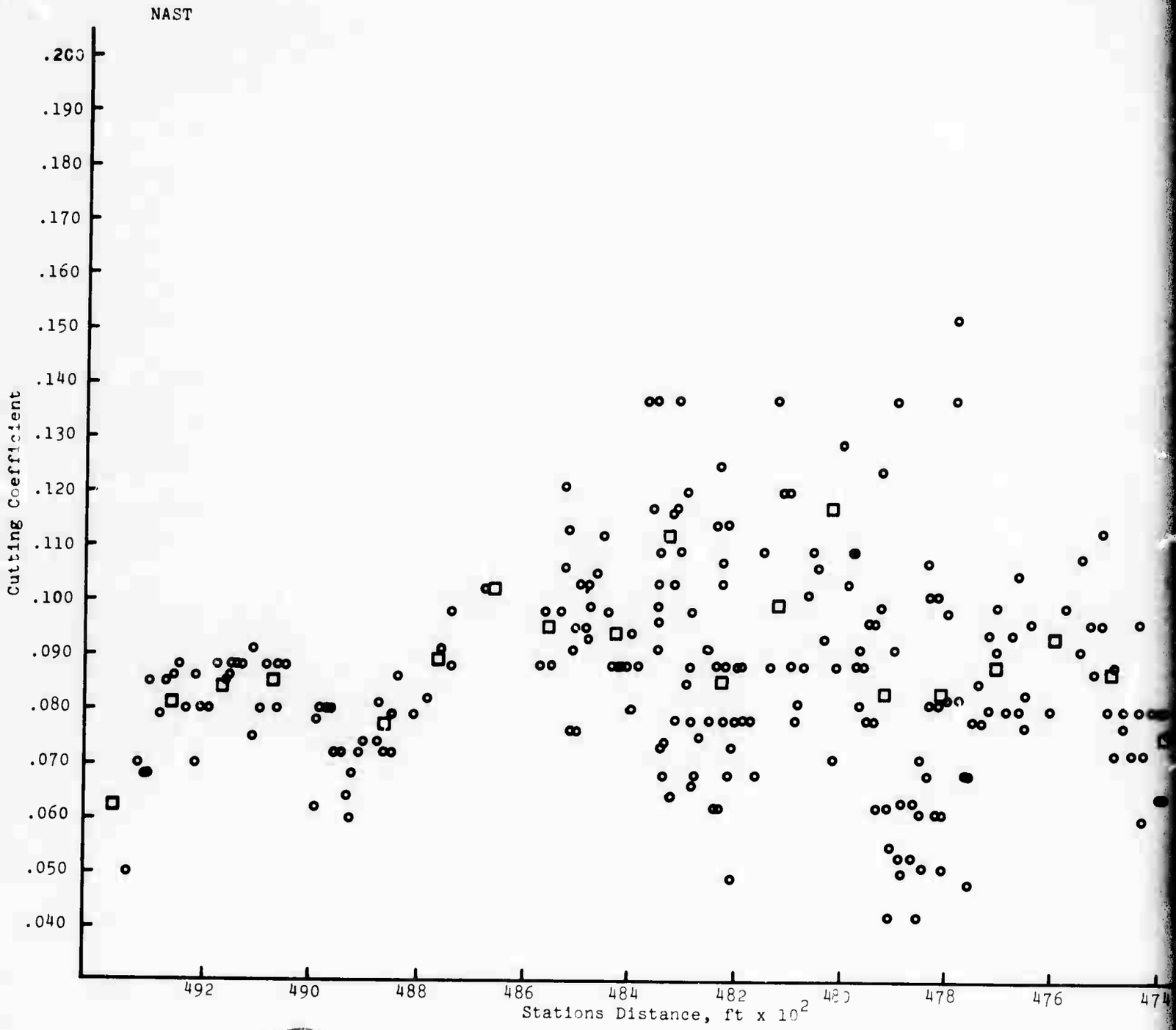
NAST
.200
.190
.180
.170
.160
.150
.140
.130
.120
.110
.100
.090
.080
.070
.060
.050
.040
Cutting Coefficient
492
490
488
486
484
482
480
478
476
474
Stations Distance, ft x 10²

(A)

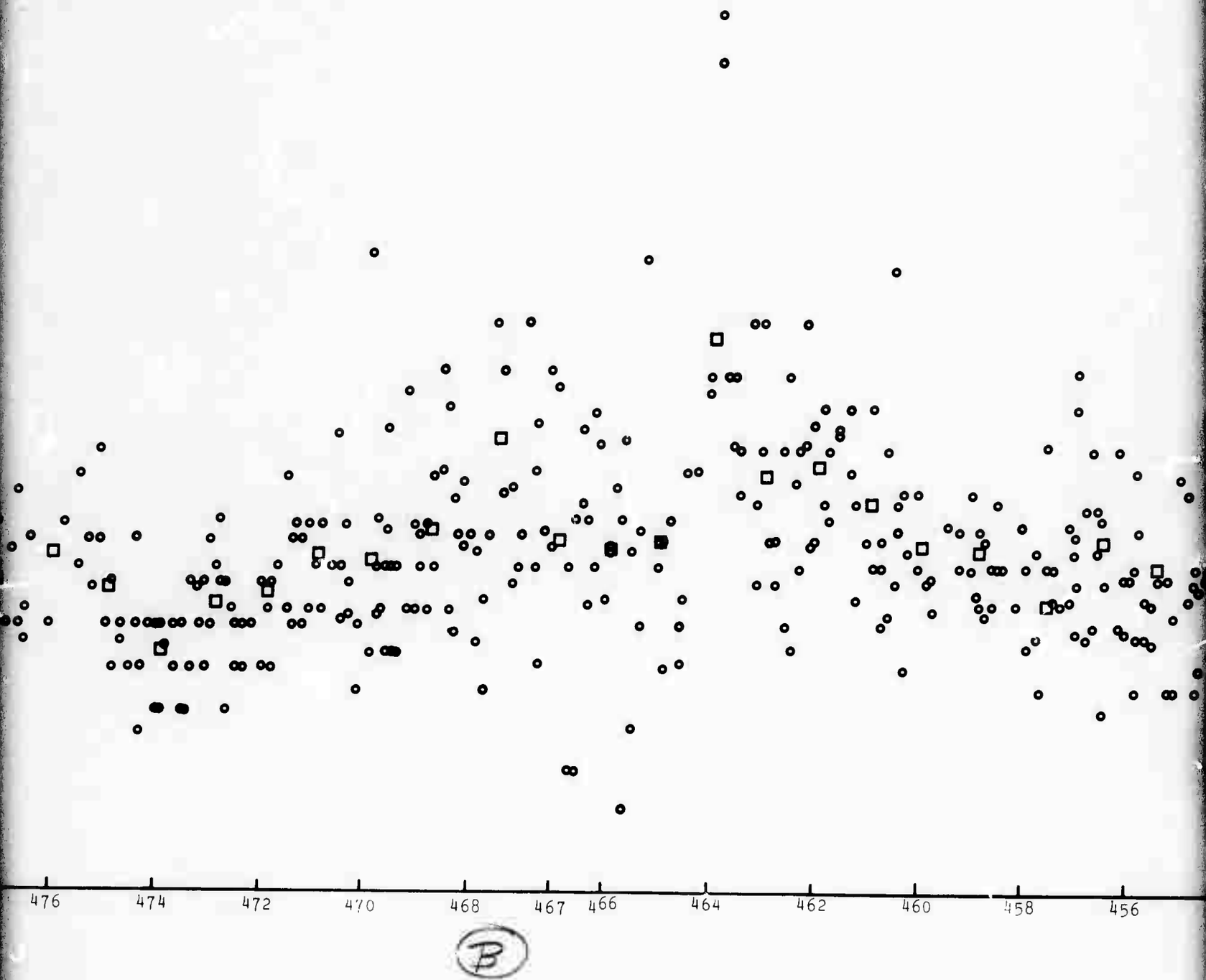

B

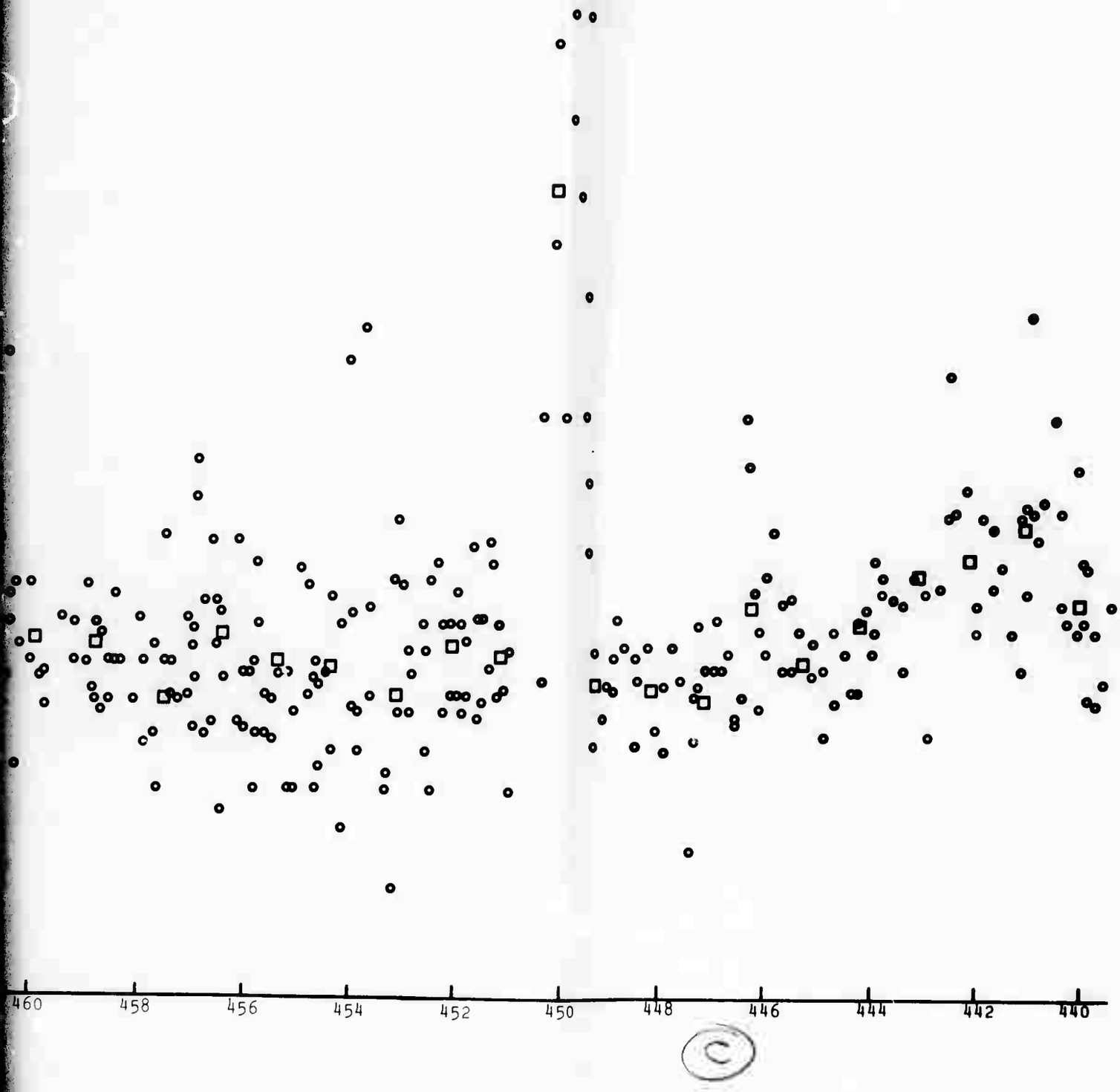
460
458
456
454
452
450
448
446
444
442
440

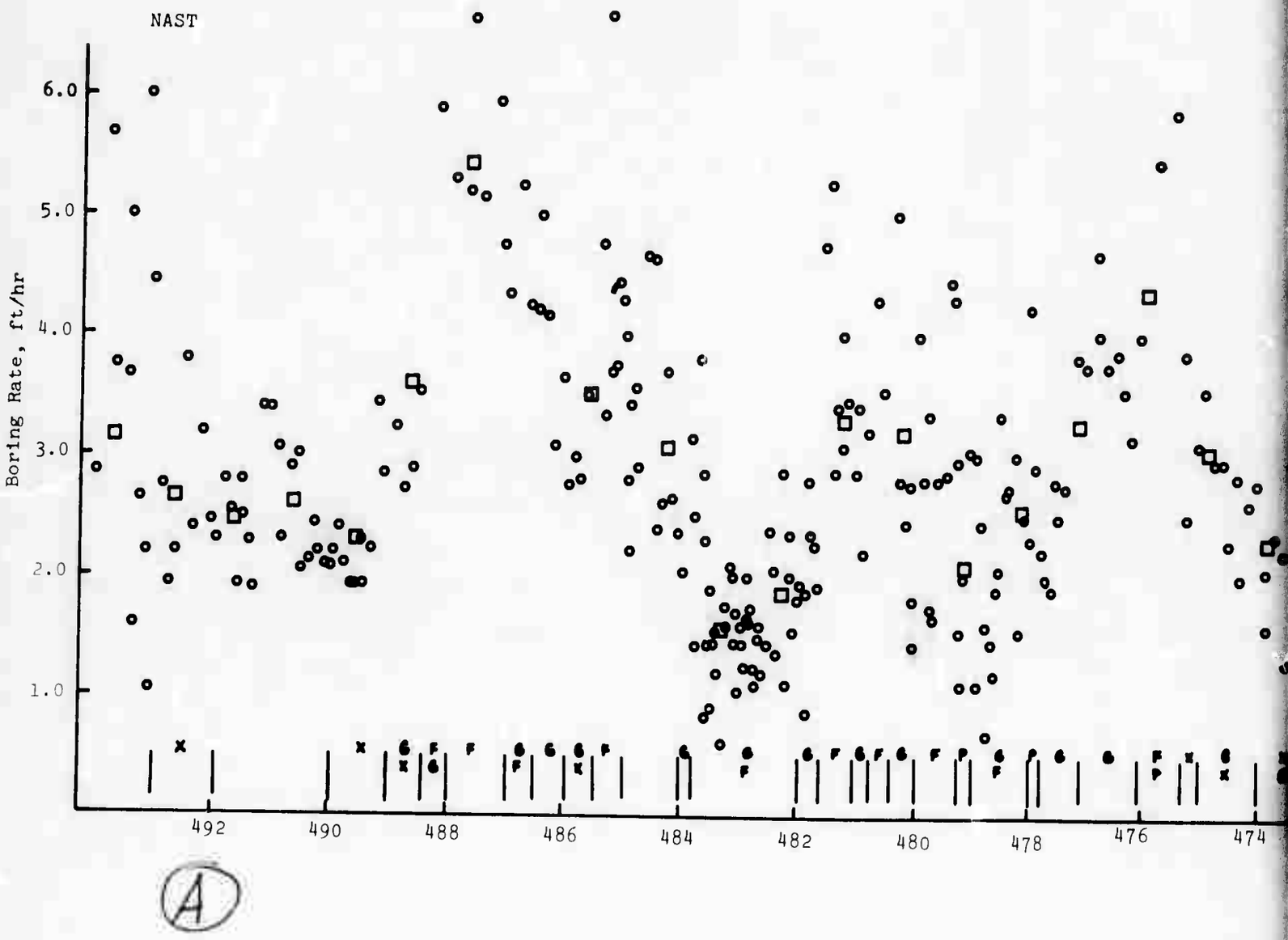
NAST
Boring Rate, ft/hr
6.0
5.0
4.0
3.0
2.0
1.0
492
490
488
486
484
482
480
478
476
474

(A)

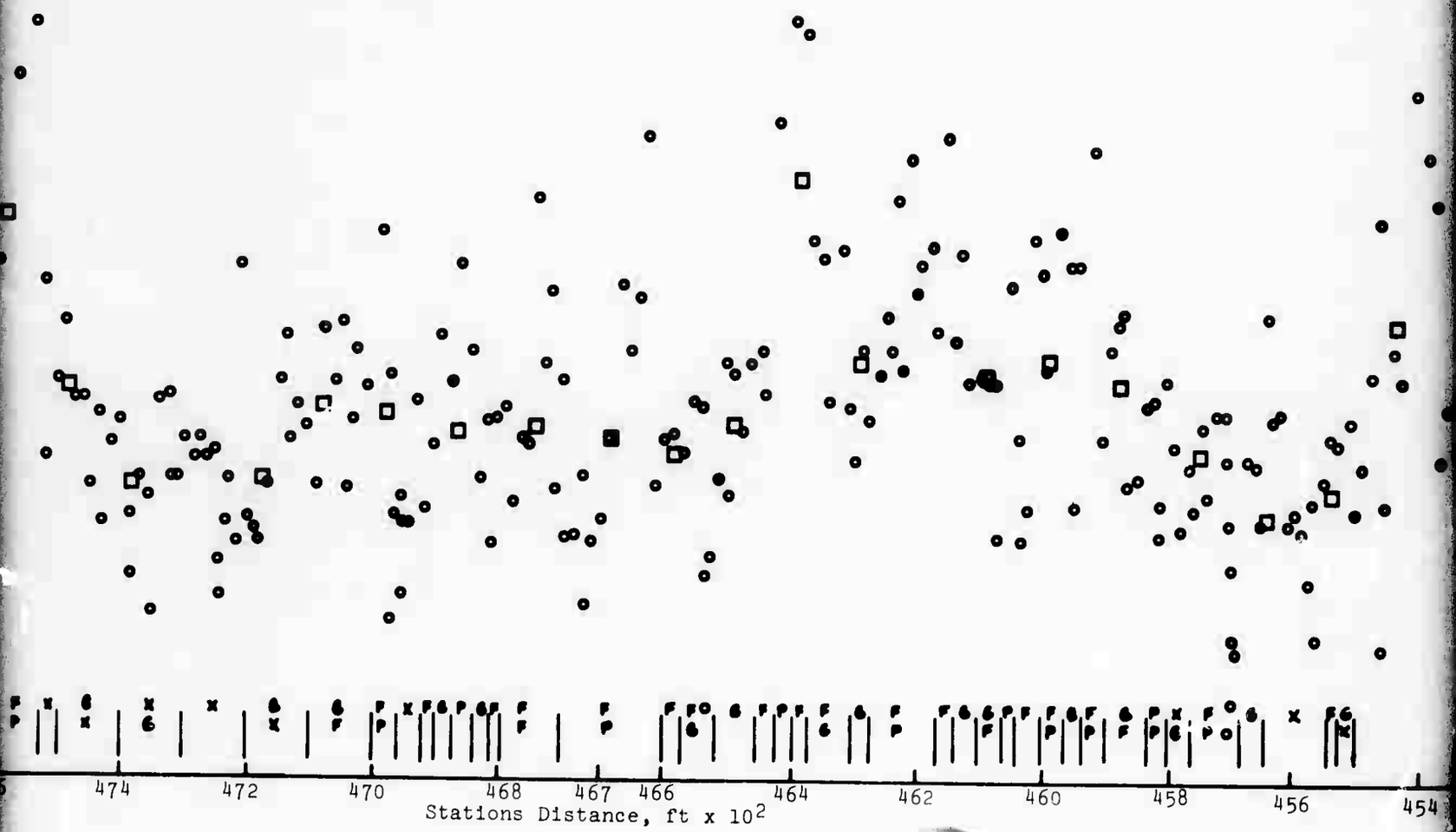
474
472
470
468
467
466
464
462
460
458
456
454
Stations Distance, ft x 10^2

B

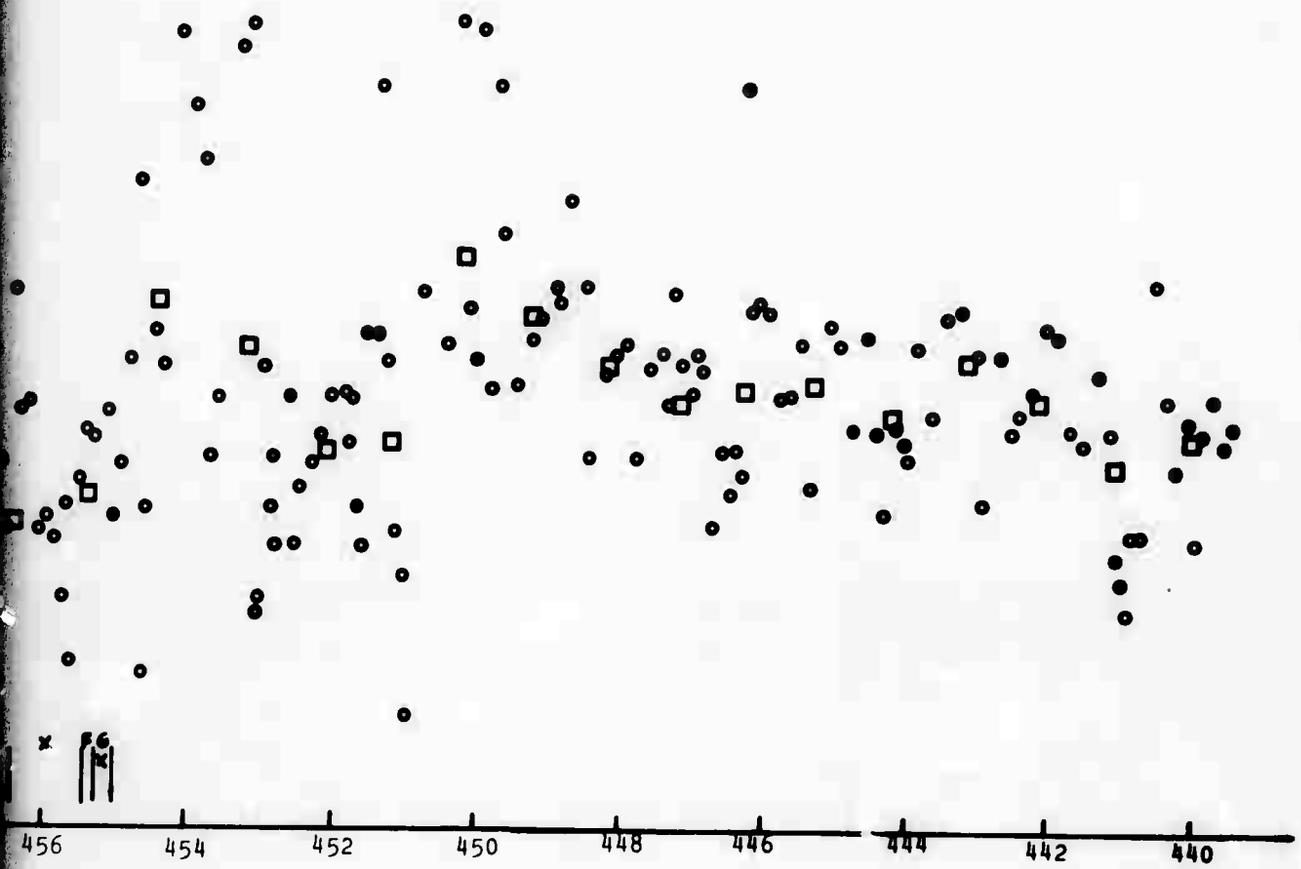

(c)

APPENDIX D

DATA FROM THE LAWRENCE TUNNEL. BORING RATE AND SPECIFIC ENERGY ARE GIVEN FOR THE BORING DURING JULY 1971. DOTS ARE THE VALUES OF EACH SHIFT, SQUARES ARE THE WEIGHTED AVERAGES OF EACH ONE HUNDRED FEET ADVANCE (TO THE END OF NEAREST SHIFT).

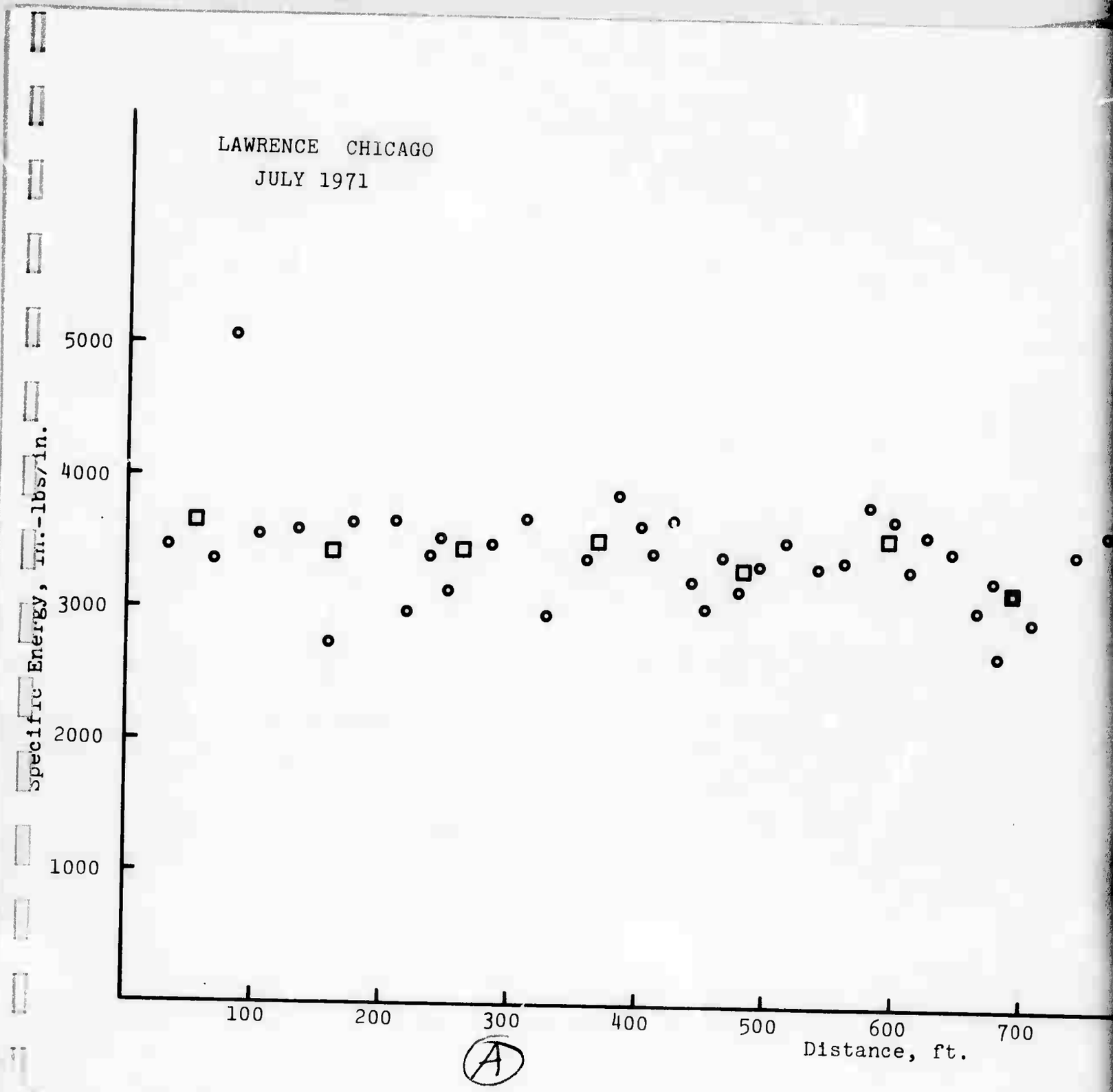
LAWRENCE CHICAGO
JULY 1971
Specific Energy, in.-lbs/in.
5000
4000
3000
2000
1000
100
200
300
400
500
600
700
Distance, ft.

(A)

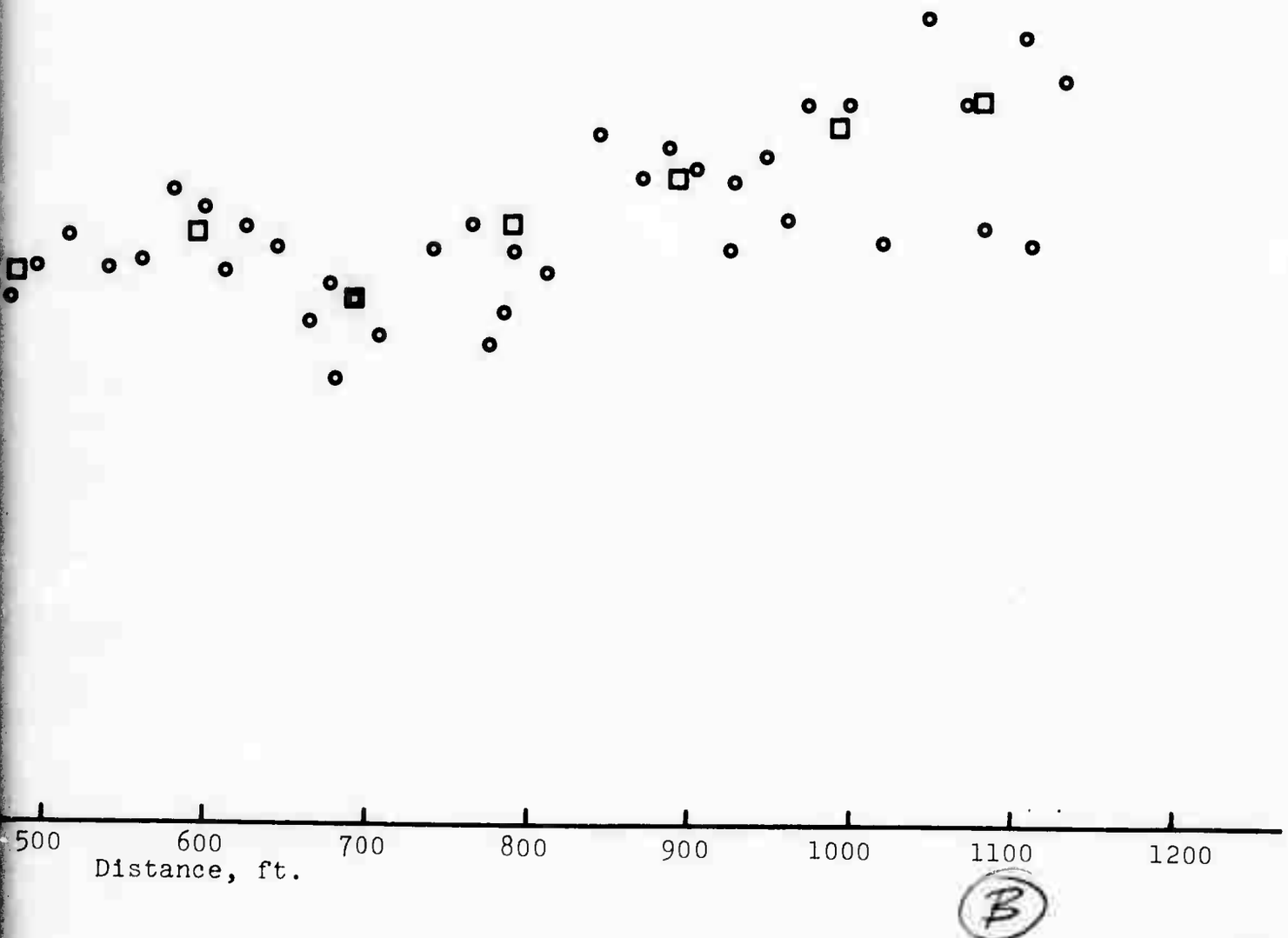

B

163-A

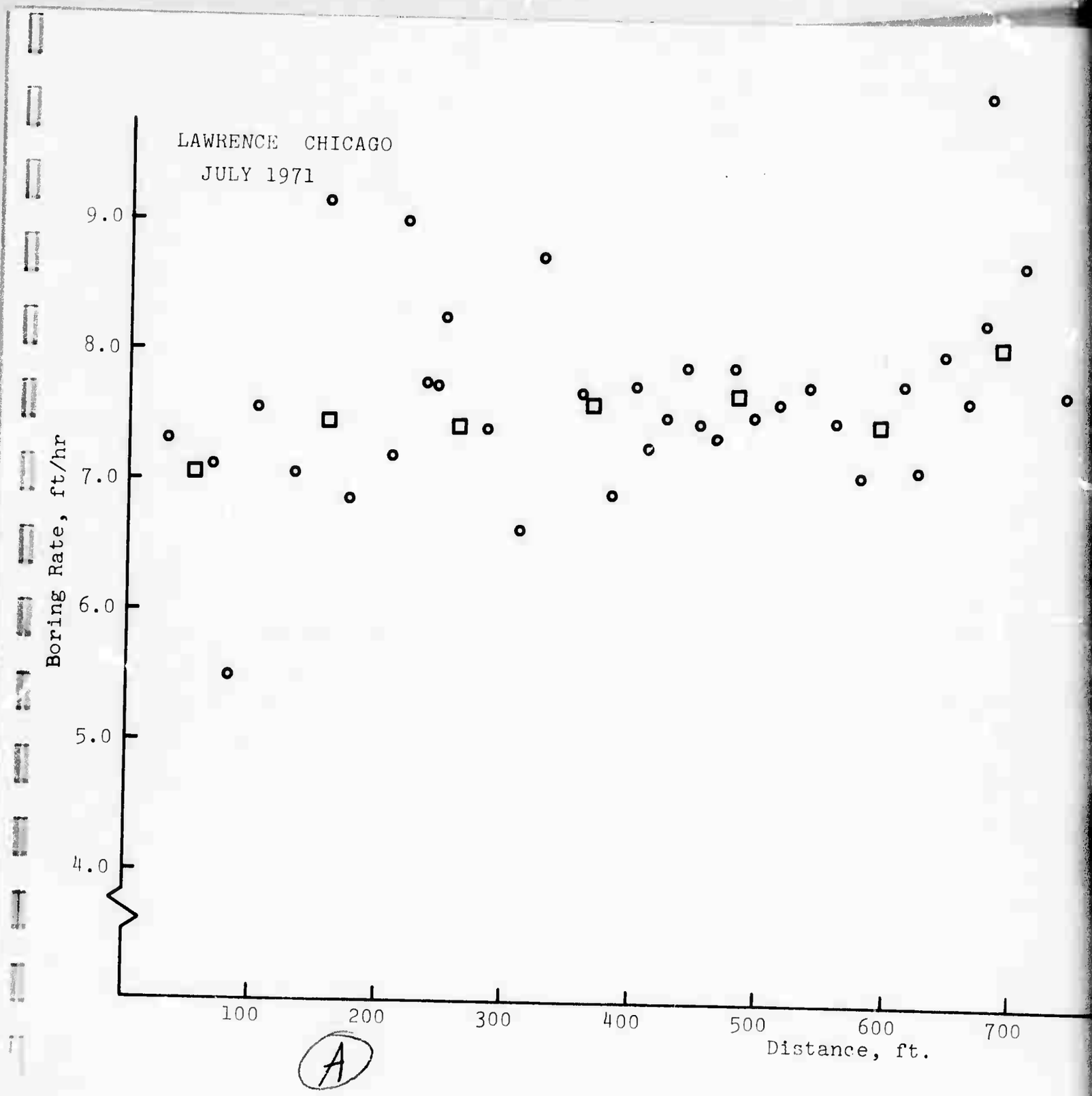
LAWRENCE CHICAGO
JULY 1971
Boring Rate, ft/hr
9.0
8.0
7.0
6.0
5.0
4.0
100
200
300
400
500
600
700
Distance, ft.

A

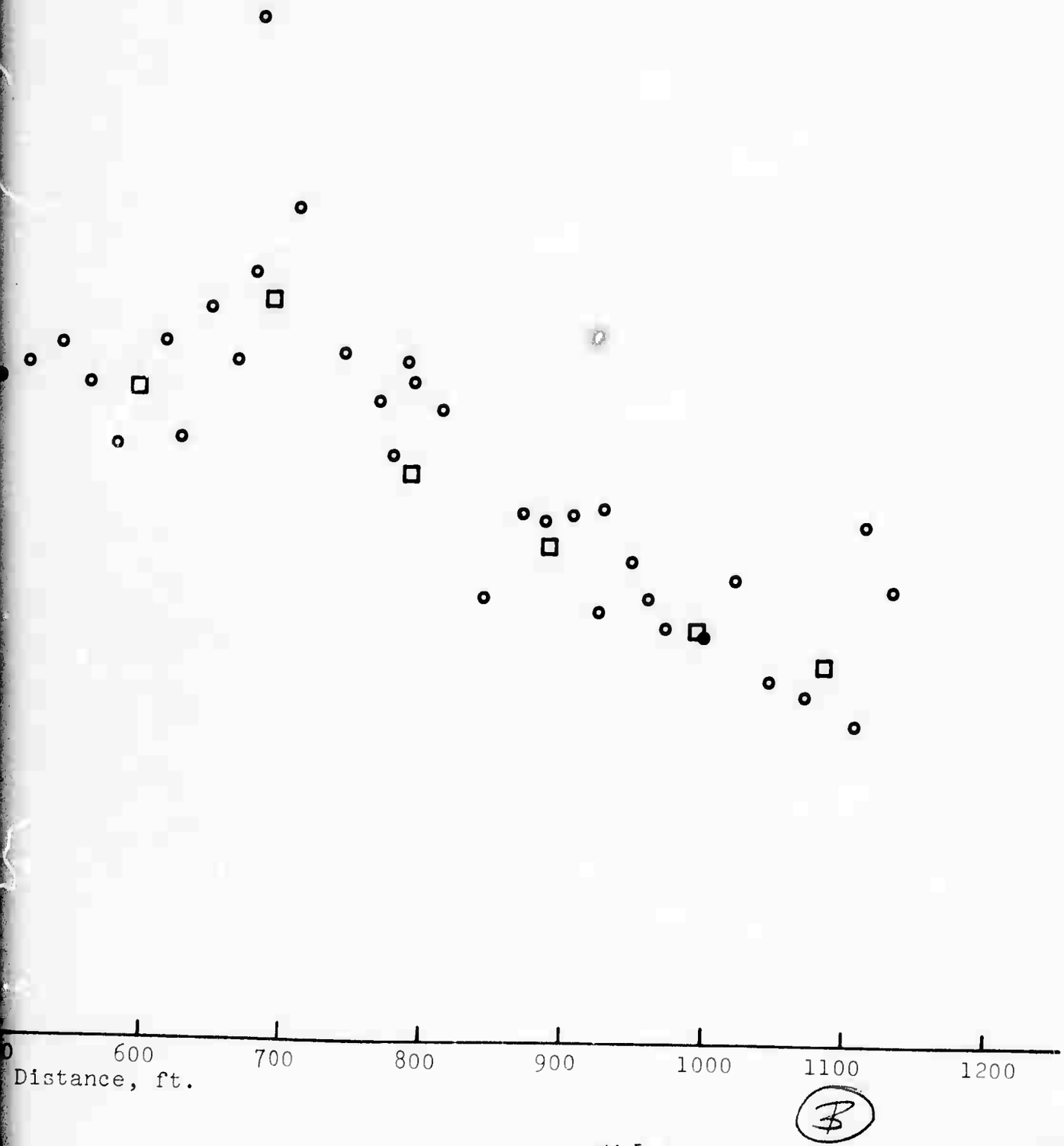

(B)

163-B

APPENDIX E

LABORATORY SAMPLES

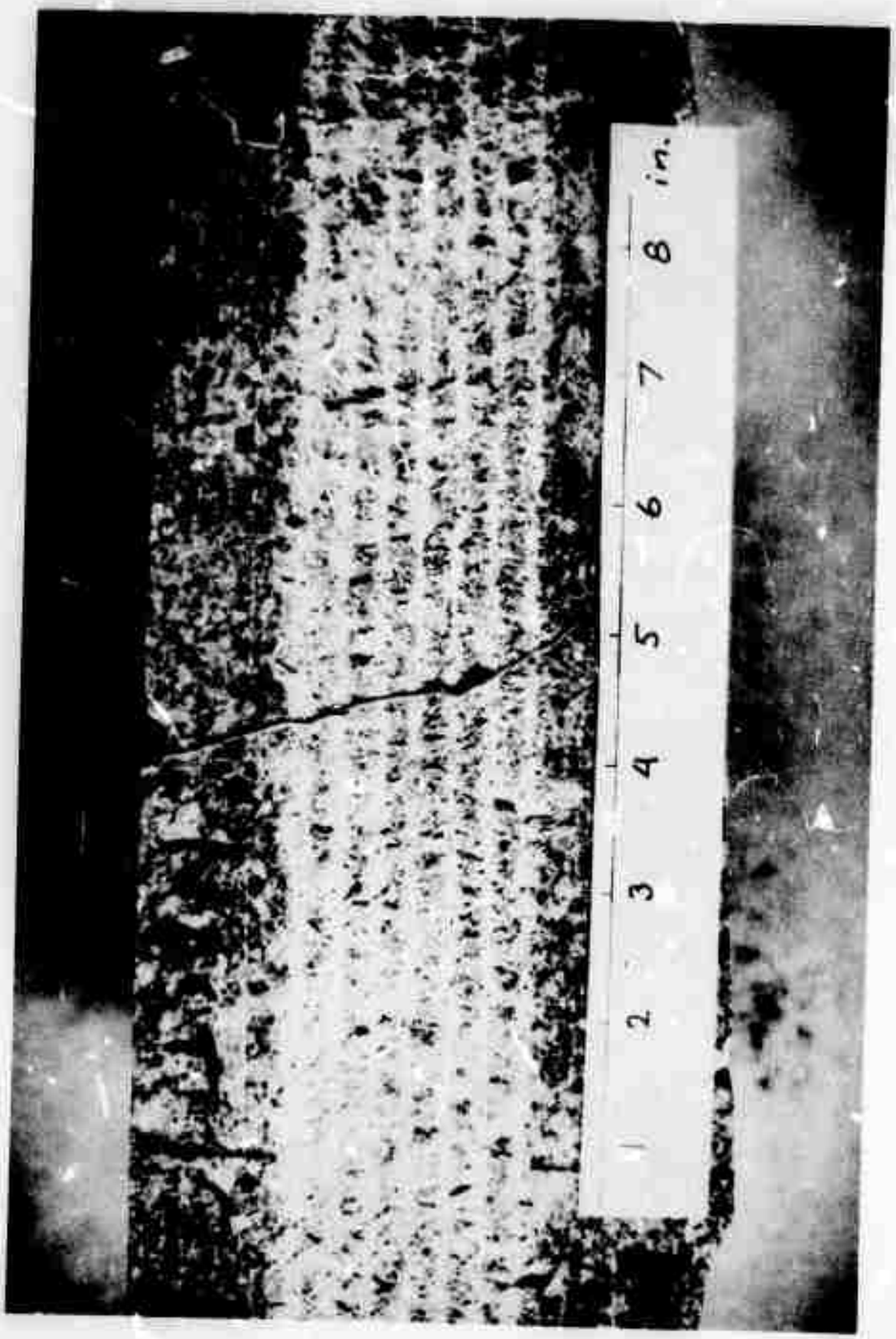

Sample Nast #2 - Specific Gravity 2.64

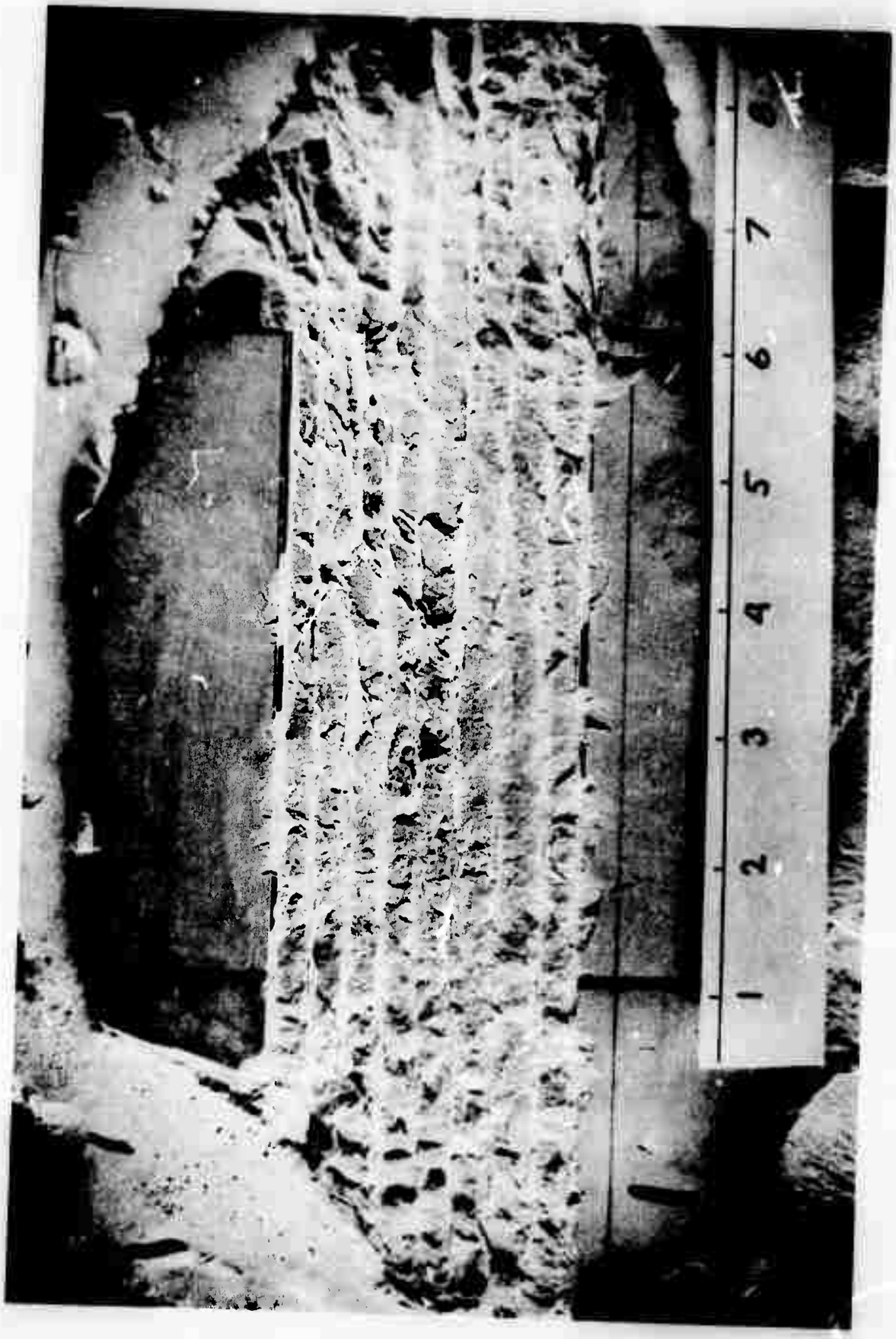

Sample Lawrence #1 - Specific Gravity 2.66

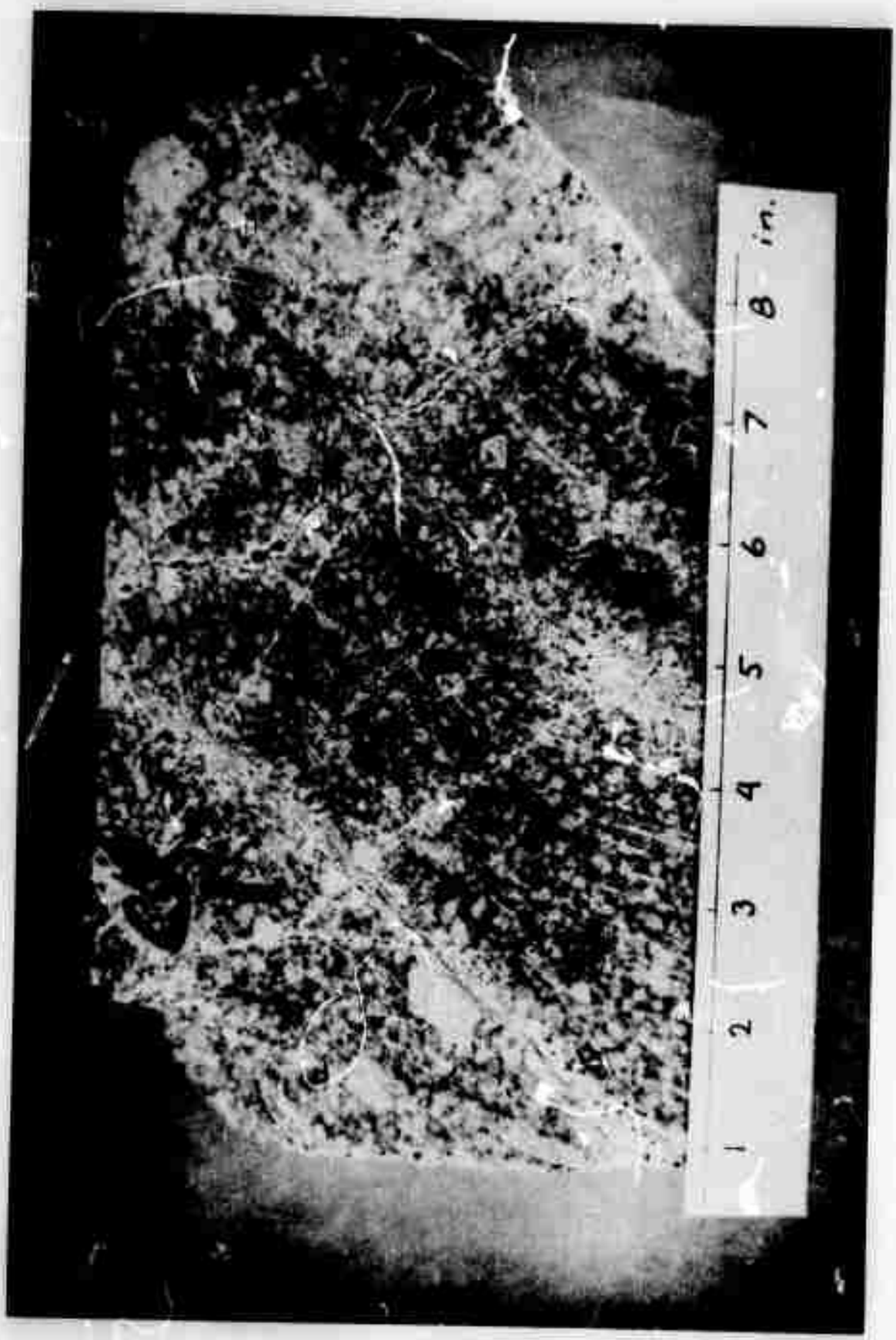

Sample Climax #1 - Specific Gravity 2.64

Sample Climax #2

Sample Climax #7

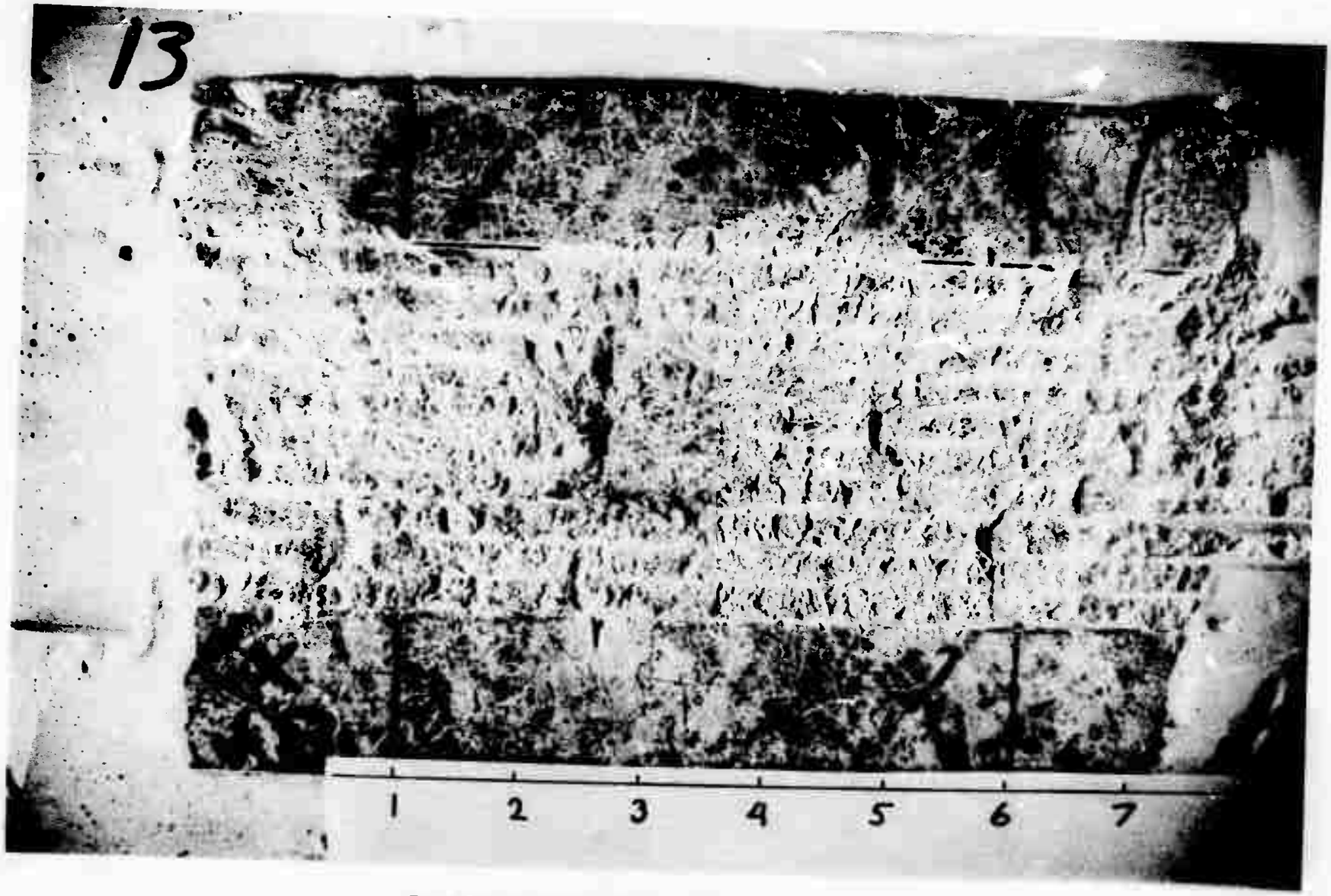

Sample Climax #13 - Specific Gravity 2.55

Sample Climax #15 - Specific Gravity 2.69

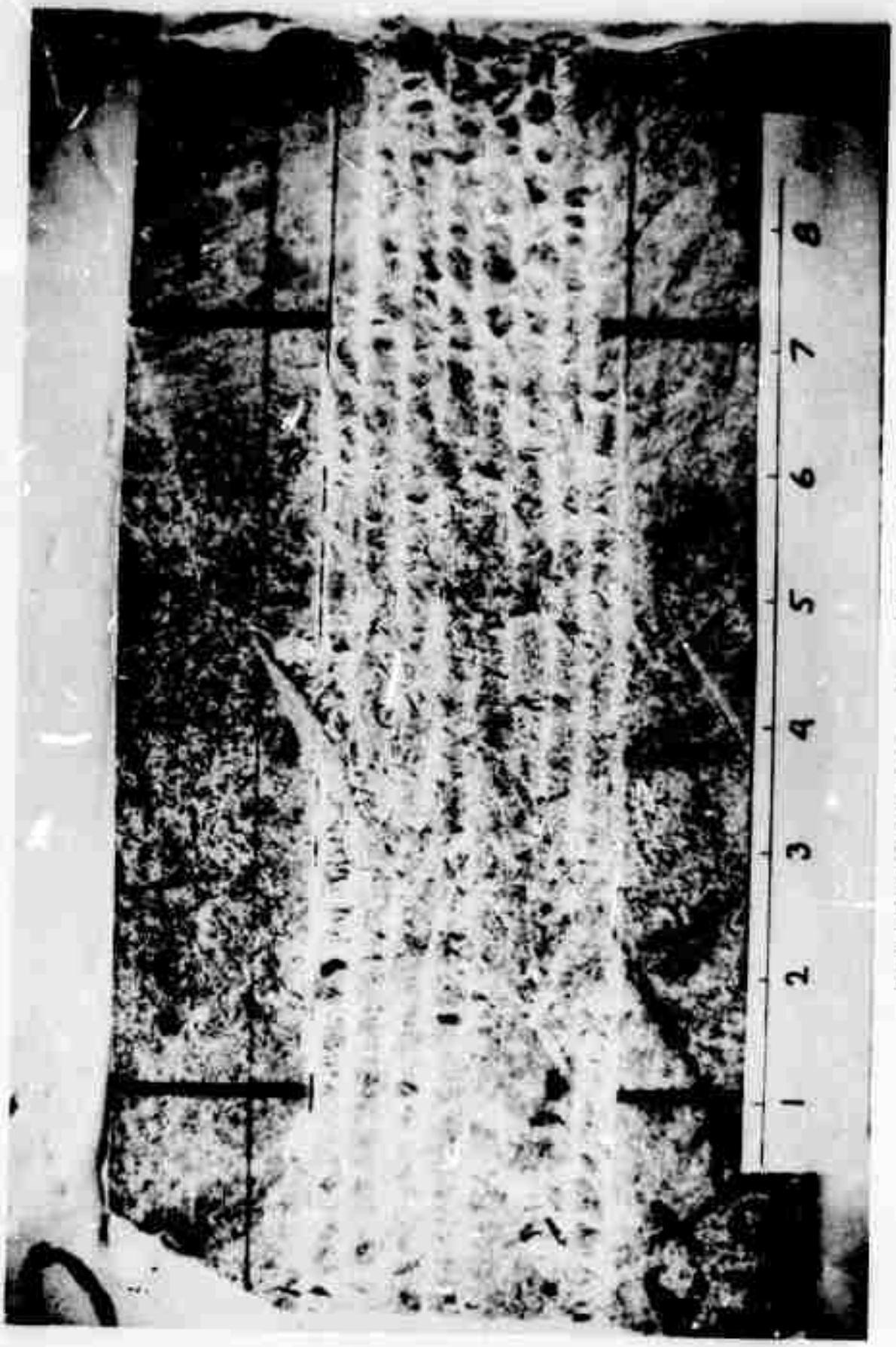

Sample Climax #18 - Specific Gravity 2.64

PART II.

THE DESIGN AND CONSTRUCTION OF THE LARGE LINEAR CUTTER

PART II.

THE DESIGN AND CONSTRUCTION OF THE LARGE LINEAR CUTTER

Introduction

A large linear cutter capable of using full scale cutters has been designed and constructed. Initially this machine will be used to cut man-made rocks containing artificial weakness planes with standard cutters. The effect of the depth of cut and the indexing distance on (1) the specific energy (energy required to remove a unit volume of rock), (2) the vertical force, (3) the horizontal force, (4) the fragment size produced, and (5) the cutting coefficient will be studied. Tests on similar samples using the small linear cutter will also be performed to examine the type of scaling relationships that apply. Later in the program it is planned to perform similar tests on rock samples from actual tunnel sites. A comparison of the results from the small and large linear cutters to those obtained from the full scale machine will be compared. Once these relationships are established, one should be able to (1) predict the performance of present machines based on tests on exploratory samples, (2) recommend the best combination of machine and cutters to be used for that rock, and (3) suggest improved mechanical methods of rock removal. Although tunnel boring machines have been used with success in medium to hard rock, they do not always turn out to be the fastest or most economical method of doing the job. The incorrect selection of such a machine can cause delays

measured in terms of months.

The use of the large linear cutter will allow the testing of many rock type-cutter combinations in a relatively short time. Since it is a full scale machine, recommendations based on results obtained will be more directly translatable into practice than might be possible using a lesser machine. One of the cutter types that will be tried, is the tungsten carbide pick. It is felt that such a cutter can exploit rock weaknesses rather than trying to overcome their strengths. It appears to this author that such improved mechanical methods of removing rock will contribute most to excavation technology in the next 10 years. The design and construction of the large cutter is described in the next section. The design has been predicated upon two basic principles.

1. Since the cutter-rock interaction is of prime interest, special care should be taken to remove or at least minimize the influence of the other parts of the system. This means creating as "stiff" a loading frame as possible.

2. Rock blocks and cutters should be easily changeable and data acquisition should be fairly simple.

It is felt that the machine described below does satisfy these criteria.

Design

The contract specifies that the large linear cutter should be capable of being operated in either a constant force or a constant displacement mode. The constant force mode is accomplished simply by providing the hydraulically powered vertical

force ran with a nitrogen accumulator that maintains a nearly uniform pressure to the ram, thereby maintaining constant force to the cutter as it traverses the rock. This type of operation, however, requires that the depth of cut must then be measured. Thus, one complicates the data collection process at the sake of simplifying the machine construction.

The constant displacement mode is considerably harder to accomplish. One must maintain a uniform depth of cut even with wide variations in vertical force as the cutter passes alternatively over hard and soft sections of the rock. Since the depth of cut is fixed, one need then only measure force variations which is quite easily accomplished using strain gage instrumentation. It is felt, furthermore, that the constant displacement operation better represents the action of an actual boring machine. Ideally, the cutter should be mounted to an infinitely rigid frame, and the rock should rest on an infinitely rigid base. This is, of course, not practical and a maximum allowable deflection must be determined. The linear cutter is then designed to conform to this limit.

For the linear cutter at the Colorado School of Mines, a maximum deflection of 0.01 in. was chosen as a practical limit. Each part of the system must then be designed as rigidly as practically possible.

A 3 ft deep concrete base heavily reinforced with No. 8 and No. 10 steel reinforcing bar was poured in the floor of the Mining Engineering Research Lab to provide a solid base and limit deflections from the anchorage. The slab also provided the means

to keep all forces within the system. The frame for holding the cutter consists of two 36-in. wide-flange columns and a crossbeam consisting of two 18- by 8-in. wide-flange beams and two 18- by 4-in. channels welded together to form an 18- by 24-in. box beam. With the loads to be used, the deflection in each of these members is approximately 0.001 in. The saddle holding the cutter is moved up and down by a 50,000 lb capacity ram. Steel spacers placed between the beam and the saddle are used. To hold the cutter rigidly at a particular depth of cut, the deflection in the cutter mount is comparable to mounts found in commercial use. The vertical ram used on the cutter has a servo-loop control, allowing programming of the vertical load.

Loads on the cutter are measured by load cells similar in concept to stress bolts. The bolts and the strain gages on the bolts are situated to produce maximum output and cancel any bending or torsional effects.

The horizontal translation of the rock under the cutter is accomplished by an MTS servo-controlled hydraulic actuator. The actuator is capable of a stall force of 50,000 lb and a dynamic force of 30,000 lb at full speed. It is designed for operating speeds of from 0 to 40 in. per second. The back of the actuator is mounted on a 3- by 2- by 2-ft concrete block which is in turn anchored 3-ft into the base previously described with two 5-in. wide-flange beams and No. 10 reinforcing bar. The horizontal actuator is controlled by an MTS function generator and controller that provides the full range of requirements for

effective operation. The hydraulic power is supplied by a 20-hp 20-gpm standard MTS power supply. The power supply is equipped with two nitrogen-pre-charged piston accumulators to provide the flow necessary to supply the actuator at high speeds.

The platform upon which the rock is carried was fabricated from 5-in. wide-flange beams and 1/2-in. plate. The platform slides along 3" centerless-ground 60-case-hardened shafts supported every 12 in. to eliminate bending. The bearings consist of a solid block of aluminum having a 3" hole cut to fit the shafts. Four bronze-impregnated teflon rods 3/4 in. in diameter and 8-in. long are situated around the circumference of the 3" hole and are cut to provide a bearing surface and to keep the aluminum out of contact with the shafts. The frame for holding the rock was constructed by stacking 5-in. wide-flange beams horizontally to form a box of inner dimension 3 by 3 1/2 ft. The reason for such heavy construction is to provide the capability of installing flat jacks which would allow the application of a biaxial stress field to the specimen, simulating underground loading. Safety harnesses to prevent runaway of the sliding platform are currently being installed. Shields to deflect chips of rock are presently being designed.

Due to the possible danger of the powerful units involved in the operation of the linear cutter, a special room providing limited access was constructed around the apparatus.

Pictures of the cutting machine are shown in figures 1 through 4.

Fig. 1. Overall view of the cutter showing the frame, the rock carriage and guides, the saddle, and the cutter.

Fig. 2. View showing the cutter head and the rock block mounted in the carriage.

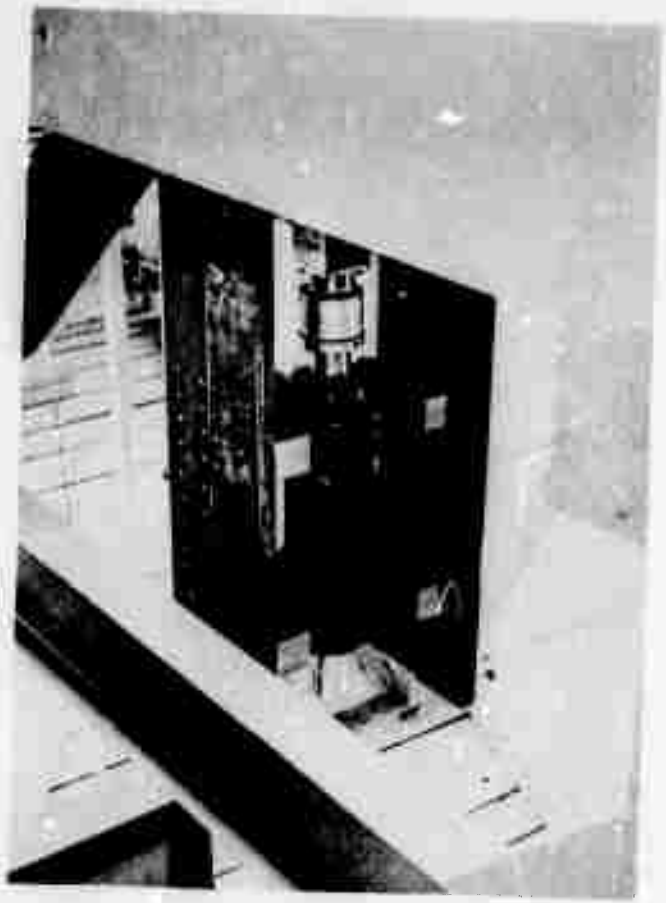

Fig. 3. View of the ram for running the tests in the constant mode.

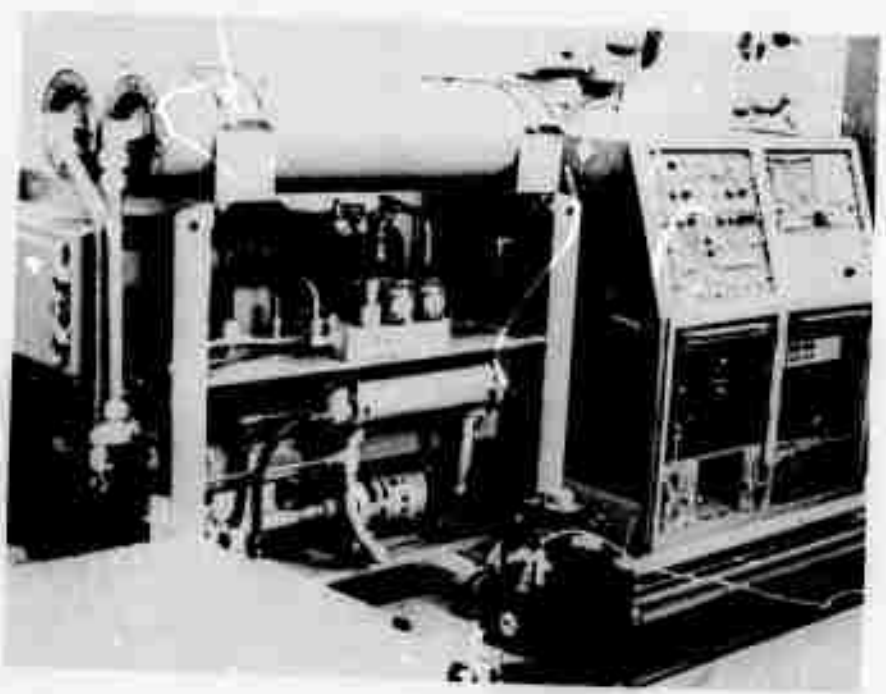

Fig. 4. MTS Power Supply, the servo controller for the vertical ram, the actuator for driving the rock under the cutter.

PART III

TRANSLATIONS OF SOME SIGNIFICANT JAPANESE ARTICLES ON TUNNEL BORING

Three articles on tunnel boring research performed in Japan some time ago have been translated as part of this contract. An analysis of the work is being made and will be included in a later report.

STUDIES ON THE CUTTING OF ROCK BY ROTARY CUTTERS - PART 1*: ROCK CUTTING BY DISC CUTTERS

by S. Takaoka[1], H. Hayamizu[2], and S. Misawa[2] - Translated from Japanese by Y. Kojima[3] and W. Hustrulid[4].

ABSTRACT

The cutting resistance using disc cutters was observed experimentally. In these experiments, straight cuts were made on smooth rock surfaces with disc cutters; the distance between adjacent cuts being kept sufficiently large so that no interaction occurred. The normal and tangential components of the cutting resistance was measured.

Experimental results show that the cutting resistance increases the depth of cut, the compressive strength of the rock and the cutting angle of the disc cutter. The tangential component increases more drastically with the depth of the groove than the normal component. It should be emphasized that in an actual rock boring operation in which a cutter head having a series of disc cutters is used, the application of increased torque to the cutter head is an important factor for increasing the rate of penetration.

---

*Originally Published in the Journal of The Mining & Metallurgical Institute of Japan, v. 84, no. 960, 1968-9, pp. 427-432.

[1]Dr. of Engineering, Dept. of Mining & Preservation of Safety, National Research Institute of Polution & Resources, Saitama, Japan.

[2]Dept. of Mining & Preservation of Safety, National Research Institute of Polution & Resources, Saitama, Japan.

[3]Graduate Student, Colorado School of Mines, Golden, Colo. 80401

[4]Associate Professor, Department of Mining, Colorado School of Mines, Golden, Colorado 80401.

1. Introduction

Recently continuous boring by machine has replaced the more conventional drilling and blasting methods in driving drifts and tunnels in some metal and coal mines. In mechanical boring, the type of cutters used on the head has a large effect on the boring efficiency. This study describes the rock cutting process using disc cutters (one of cutter types commonly used on boring machines).

Each disc cutter makes a continuous groove in the tunnel face partly by pushing and partly by rolling the outer edge of the cutter into the rock surface. Since many disc cutters are attached to the head, the rock is cut in concentric rings. The rock removal process is affected by the presence of these adjacent cutter paths and in actual boring these effects cannot be neglected.

In this fundamental study, the disc cutter was used to make independent, straight cuts in various rocks. The shape of the cut and the resistance to cutting was measured.

2. The Apparatus and Experimental Methods

2.1 Apparatus

A sketch of the cutting apparatus is shown in fig. 1. The cutter is mounted at the end of the piston on bearings so that it can rotate freely. When compressed air is supplied to the thrust cylinder, the cutter is pushed into the rock surface. The sample is fixed to a screw-driven carriage. As the screw is rotated by a motor, the rock moves at a constant speed beneath the cutter causing a groove to be cut in the rock surface.

A tension meter (load cell) forms part of the horizontal arm which is attached to the axis of the disc-cutter through bearings. The other end of the horizontal arm is pinned to the frame in such a manner that it can be freely adjusted up and down. The upper end of the thrust cylinder is attached to the frame so that it can rotate freely. Therefore, the horizontal force which reacts to the disc-cutter can be measured by the tension meter. In this experiment the rock sample rather than the disc-cutter moves. Although this is the opposite of actual machine behavior, the force acting on the tension meter is the same as the tractive force which rotates the disc-cutter on the rock surface.

In this experiment, the axial line of the tension meter should be parallel to the rock surface, and perpendicular to the piston rod attached to the disc-cutter. However, for slight deviations, the measured values do not seem to be greatly affected. The disc-cutter used in this experiment is shown in fig. 2. It has a diameter of 200 mm, a tip hardness of Rockwell C 60, and tip angles of 60°, 70°, 80°, and 90°. Although the cutting speed is an important factor, it was treated as a constant in these experiments. The effect of changing the tip angle on rock fracture was the only variable studied.

2.2 Rock Samples

Properties of the 3 rock types used in this experiment (Fukushima Andesite, Kofu Andesite, and Sawairi Granite) are given in Table 1. The compressive strength values were determined from tests on cubic samples having a side length of 5 cm. The tensile strengths shown for reference were determined from the indirect

tensile strength test using cylindrical samples having diameters of 22 mm and lengths of 22 mm.

Table 1. Properties of the Rock Types Used

Rock Name	Avg. Shore Hardness	Compressive Strength (kg/cm^2)	Tensile Strength (kg/cm^2)	Place of Production
Fukushima Andesite	65	780	50	Fukushima, Japan
Kofu Andesite	82	1,680	127	Yamanashi, Japan
Sawairi Granite	88	1,370	92	Gunma, Japan

2.3 Experimental Methods

The surface of the sample was polished and the block attached to the rock carriage so that the top surface would be horizontal. The disc-cutter was pressed into the surface of the sample and the block translated at a constant speed of about 30 cm/min. The width and depth (the maximum depth at each cross section) of the cut were measured using a scale and dial depth gage, respectively at 10 points selected at random along the groove. The horizontal force acting on the disc-cutter was recorded using an oscillograph connected to the tension meter. As was the case for the depth of groove, ten (10) points were selected at random as the measuring places.

3. The Experimental Results

Figures 3, 4, and 5 show the results of the depth of cut

*The cutting velocity is considered to be an important factor influencing both the cutting resistance of the rock and the shape of the groove. This will be considered further in a future report.

experiments. To reduce the complexity of the diagrams, the experimental points were deleted in figs. 3 and 4. The experimental points are shown in fig. 6.

Fig. 3 shows the relationship between the depth of cut and the vertical (normal) force applied to the disc-cutter. As can be seen, the vertical force increases with the depth of cut for all three rocks. The rate of increase, however, decreases as the depth of the cut increases.

Fig. 4 shows that the tractive force applied to the disc-cutter increases as the depth of cut increases. The rate of increase increases as the depth of cut increases. This behavior is just the opposite of that observed for the thrust.

In actual tunnel boring, the vertical and tractive forces are thought to be the same as the thrust force and the rotary force, respectively, applied to the boring head. The experimental results suggest that the boring rate can be increased, even if thrust force is not large, by choosing a disc cutter that allows the rotary power to increase rapidly. An examination of the results of figs. 3 and 4 reveals that to get the same depth of cut by as small a normal force and tractive force as possible, one should use the disc-cutter which has the smallest tip angle.

Fig. 5 shows the relationship between the width and depth of cut. The relationship appears to be independent of the disc-cutter tip angle for all rock types. The rate of increase of the width with depth of cut increases with increasing depth. It appears that when one cuts the rock using the disc-cutter, the rock which is right beneath the tip is fractured to a certain depth by compression, and the rock on both sides of the cut is fractured by tensile and shear forces due to bending type of

deformations.

The above result suggests that the width of cut is obtained by shear and tensile forces with almost no influence of the tip angle of the disc cutter. The fracture width is determined by the depth of fracture only; the width increasing more rapidly than linearly with increasing depth.

4. Cutting Resistance

As already mentioned, when the rock is cut by the disc-cutter, both vertical and tractive forces act on the cutter. In addition, a resisting force to cutting and a friction force act as distributed forces on the contact surface between the disc-cutter and the rock.

Because of the cutting mechanism of the disc, these distributed forces are symmetrical with respect to the cutting edge. Since the line of action of the resultant force on each side passes through the tip of the cutter, the components normal to the surface of the cutter cancel each other.* Therefore, the distributed forces are thought to be on the line of the tip of the disc-cutter.

Fig. 7 shows the forces acting on the disc-cutter. The arc $\overset{\frown}{ab}$ is the line of contact of the rock and the tip of the disc-cutter. As mentioned above, the distributed forces are considered to be distributed on the arc $\overset{\frown}{ab}$. Also, R_n and R_t are the vertical and horizontal components respectively of the resultant (R) of the distributed forces (R will be called the cutting resistance). The vertical component R_n balances the vertical force W, and the horizontal component R_t balances the tractive

*Actually the distributed forces are not necessarily symmetrical. There can exist a component normal to the plane of the cutter. However, this component has no direct relationship with either the normal or tractive forces.

force T. Because of the design of the apparatus, the vertical force W and the tractive force T act on the center of the axis of the disc-cutter, and as the total moment around the axis is actually zero, the line of action of the cutting resistance R must go through the axis of the disc-cutter and intersect arc $\overset{\frown}{ab}$.* Therefore, the angle (θ) between the cutting resistance R and the perpendicular line is always less than the center angle ϕ of the arc $\overset{\frown}{ab}$, i.e., $\phi \geq \theta$.

5. The Influence of the Depth of Groove to Cutting Resistance

Comparing figs. 5 and 4, one can observe that the ratio of the tractive to the vertical force, that is, the horizontal to the vertical component, is generally very small. The value of cutting resistance can be considered to be almost the same as the vertical component of the force, and so the relationship between the depth of the cut and the cutting resistance is similar to that of fig. 3. That is, the rate of increase of the cutting resistance with depth of the cut decreases as the depth of the cut becomes larger. Therefore, the greater the depth of cut, the larger is the increase in depth for a given increase in vertical force. The relationship between the depth of groove d, the arc length $\overset{\frown}{ab}$ of the contact of the disc-cutter and the rock, the radius of the disc cutter r, and the central angle ϕ (radians), is given by

$$\overset{\frown}{ab} = r\,\phi = r \cos^{-1}\left(1 - \frac{d}{r}\right)$$

*In this experiment the point of intersection cannot be determined.

The rate of change of arc length $\overset{\frown}{ab}$ to the change of depth of cut becomes smaller as d increases. Because of the way it's defined, the value of the cutting resistance depends upon the length of the arc $\overset{\frown}{ab}$ and the average distributed forces on this arc.

Fig. 8 shows the relationship between the length of the arc ab and the cutting resistance as calculated from the results given in figs. 3 and 4 for each depth of cut. As can be seen, the cutting resistance increases with the length of the arc. This means that the net force on the arc $\overset{\frown}{ab}$ increases with the depth of the cut. Therefore, if the depth of cut and the length of the arc $\overset{\frown}{ab}$ are proportional, the cutting resistance can be represented by a curve like that shown in fig. 4. This is the opposite of that shown in fig. 3, even though the average value of the distributed forces increases with depth of cut. Because of the geometry of the disc-cutter, the ratio of the depth of cut to the arc length $\overset{\frown}{ab}$ is small, and in general the ratio of the cutting resistance to the depth of the groove increases slowly. This is one of the merits of the disc-cutters.

A similar analysis can be done using the vertical force component. Since the length of arc $\overset{\frown}{ab}$ is related to the radius r of the cutter, by changing r the cutting resistance can be changed. The relationship between the direction of the line of action, θ (which is another factor of the cutting resistance) and the depth of the groove, was obtained from the experimental results. As seen in fig. 9, θ increases with the depth of cut, eventually tending toward a horizontal inclination. The reason for this is that the inclination near the point a of arc $\overset{\frown}{ab}$ increases with

the depth of the cut, and thus the direction of the distributed forces in this part tends toward the horizontal. The inclination near the point a, i.e., the angle ϕ between the tangent and the rock surface at a, at a certain depth of cut (d) is given by

$$\phi = \cos^{-1}\left(1 - \frac{d}{r}\right)$$

Therefore, by changing the diameter of the cutter, the inclination at the point 'a' can be changed.

6. The Influence of the Tip Angle on the Cutting Resistance

As is clear from figures 3 and 4, in each rock the tip angle of the disc cutter influences both the vertical and horizontal components of force. An increase in the tip angle makes each component and therefore the cutting resistance increase. As the rock is cut, the sides of the cutter tip contact the rock. Removal is considered to be by a wedge-like action. It is very interesting that the ratio of the depth to the width of the groove shows almost no dependence on the tip angle.

Fig. 10 shows the relationship between the direction of the line of action of the cutting resistance and the tip angle. When the depth of the cut is small, Θ is small. Although the general relationship appears fairly complex, the changes with angle are not very large. From this it can be concluded that the cutter tip angle does influence the value of the cutting resistance, but not the direction of the line of action.

7. The Influence of the Compressive Strength of Rock on Cutting Resistance

As already mentioned, when the rock is cut by a disc-cutter, the rock which is immediately beneath the tip is fractured in compression, and the rock on both sides of it is fractured in shear. It may not therefore be appropriate to attempt to find a relationship between the compressive strength and the cutting resistance. However, assuming that the strength of the rock can be represented by the compressive strength, its relationship with the vertical component and horizontal force components is shown in figs. 11 and 12. As the experimental results were derived for only 3 rock types, it is, of course, dangerous to make general conclusions regarding the influence of the compressive strength. However, as far as the results of this experiment are concerned, the compressive strength can be considered to have a larger influence on the horizontal component than on the vertical component. This means that when the compressive strength of rock increases, not only will the cutting resistance increase, but the direction of the line of action will also tend towards the horizontal. Fig. 13 shows an example of the variation of the direction of the line of action. Fig. 5 reveals that at a certain depth of cut the ratio of the width to the depth of cut increases as the compressive strength of rock increases. From this and the results of fig. 13, an increase in the compressive strength of the rock can be considered to have a similar influence as an increase in the depth of cut.

8. The Relationship Between the Vertical Force and the Tracting Force

These studies have mainly considered the influence of the depth of cut, the tip angle of the cutter, the compressive strength of rock, etc., on the value and the direction of the cutting resistance. One can now develop the relationship between the power and the thrust force on the boring head needed when designing a boring machine.

Generally, the boring head is covered by many disc-cutters, and the total torque delivered by the drive shaft is related to the horizontal component of force acting on each disc-cutter and the radius of the point of application. The thrust on the boring head is determined by the sum of the vertical components of the forces acting on each disc cutter. Therefore, if the positions of the disc-cutters are fixed, the torque and the thrust on the boring head are related to the vertical and the horizontal components of force which act on the disc cutters. Fig. 14 shows the relationship between the vertical and the horizontal components of force derived from the experimental results. From the figure, it is seen that the horizontal component of force increases rapidly with an increase in the vertical component. It is clearly necessary that the torque on the boring head be increased according to the increase in thrust. Also, from the figure, the smaller the tip angle of the cutter, the larger the horizontal component of force necessary at each vertical force level. This is true since, as the tip angle becomes smaller, the depth of cut becomes larger for the same vertical component of force. Therefore, if the angle of tip is decreased, the ratio of the torque to the thrust should be increased.

9. Conclusions

In this fundamental study of rock cutting by disc cutters, experiments were performed in which straight cuts were made on the rock surface. Measurements were made of the cutting resistance of rock, the friction force between the cutter and the rock, etc. As a result, it was found that the cutting resistance of rock can be considered as a vector which has magnitude and direction. The magnitude of the cutting resistance is influenced by the depth of cut, the tip angle of the cutter, the compressive strength of rock, etc. The angle of cutting resistance (θ) is influenced by the depth of cut, the compressive strength of rock, etc. The tip angle, however, has little influence on θ.

The increase in the magnitude of the cutting resistance (or the increase of the vertical component of force) with an increase in the depth of cut is comparatively low, and this is one of the merits of rock cutting by the disc-cutter. The horizontal component of the cutting resistance is influenced by the direction of the cutting resistance. It increases rapidly when high thrusts are applied and therefore the drilling power is increased rapidly.

Under a constant vertical force, when the tip angle of the disc-cutter is small, a large tracting force is necessary. Thus, if the boring head is equipped with this kind of cutter, a large torque is required. This result is for the case of the straight cut made by a single cutter. The diameter of the disc-cutter is presumed to influence the rock fracturing. Also, the rotating speed of cutter, and the radius of the circle through which the cutter rotates, may have an influence on the rock fracturing; therefore, we are considering continuing these experiments.

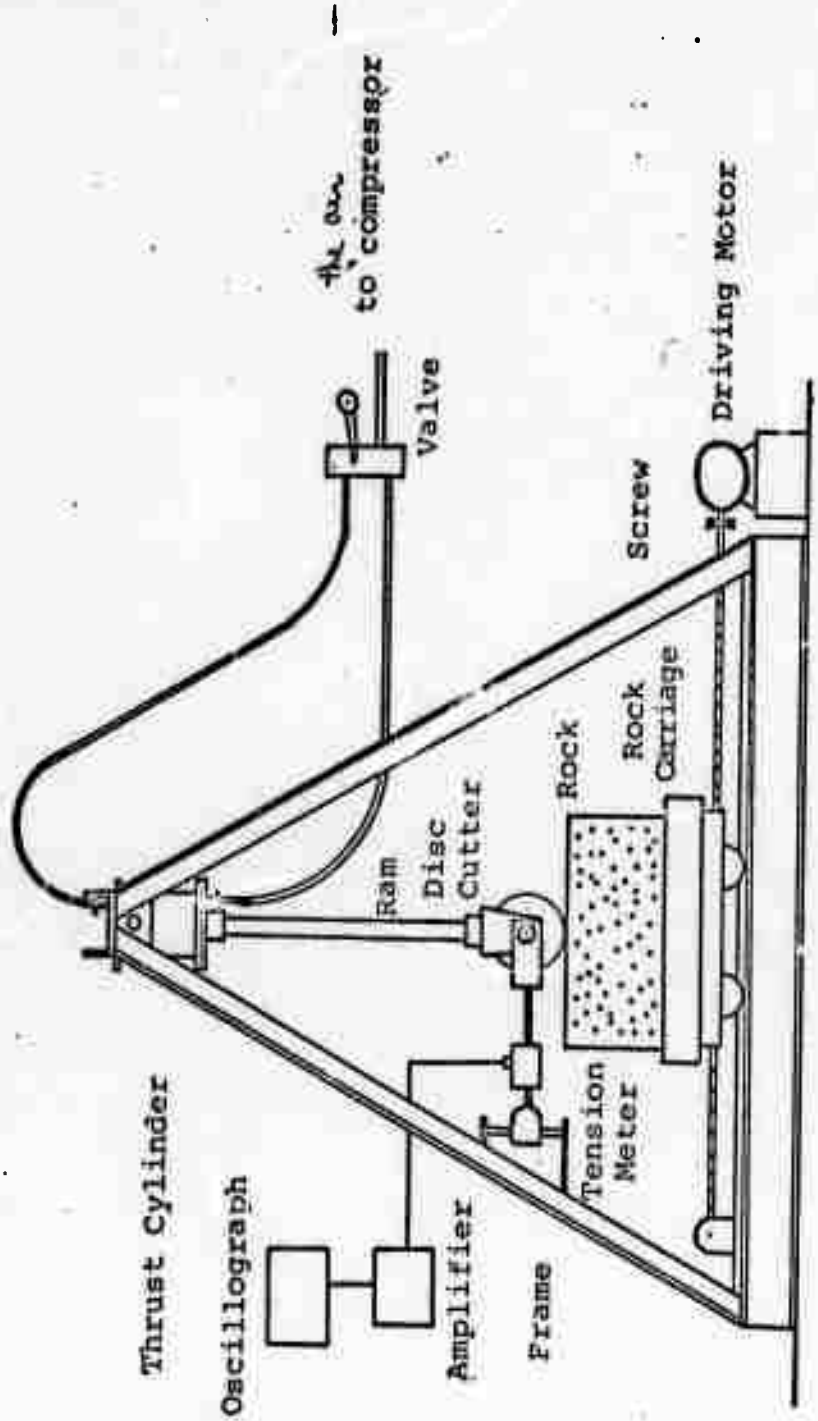

Figure 1. Diagrammatic Representation of the Experimental Apparatus.

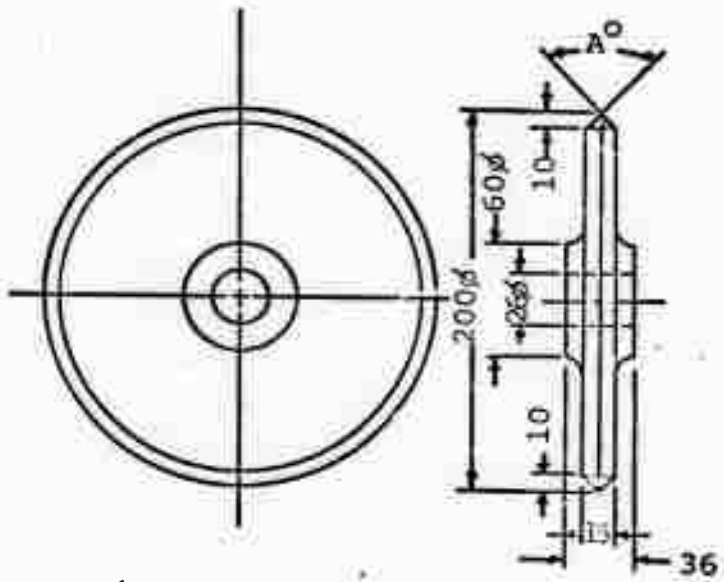

Tip Angle = 60°, 70°, 80°, 90°

Material = Tool Steel #7

Hardness of the Cutting Edge = Rockwell C 60

Fig. 2. A Diagrammatic Representation of the Disc Cutter.

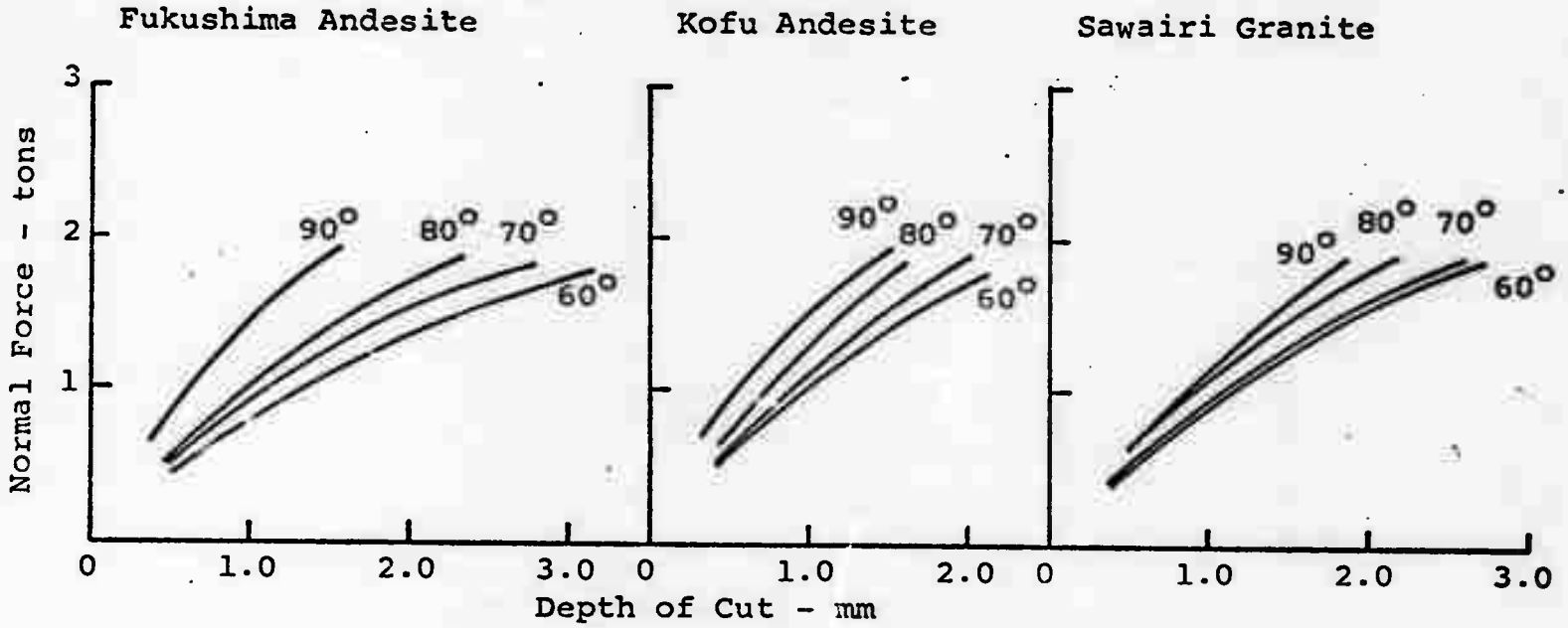

Figure 3. The Relationship Between the Normal Force and the Depth of Cut as a Function of Tip Angle.

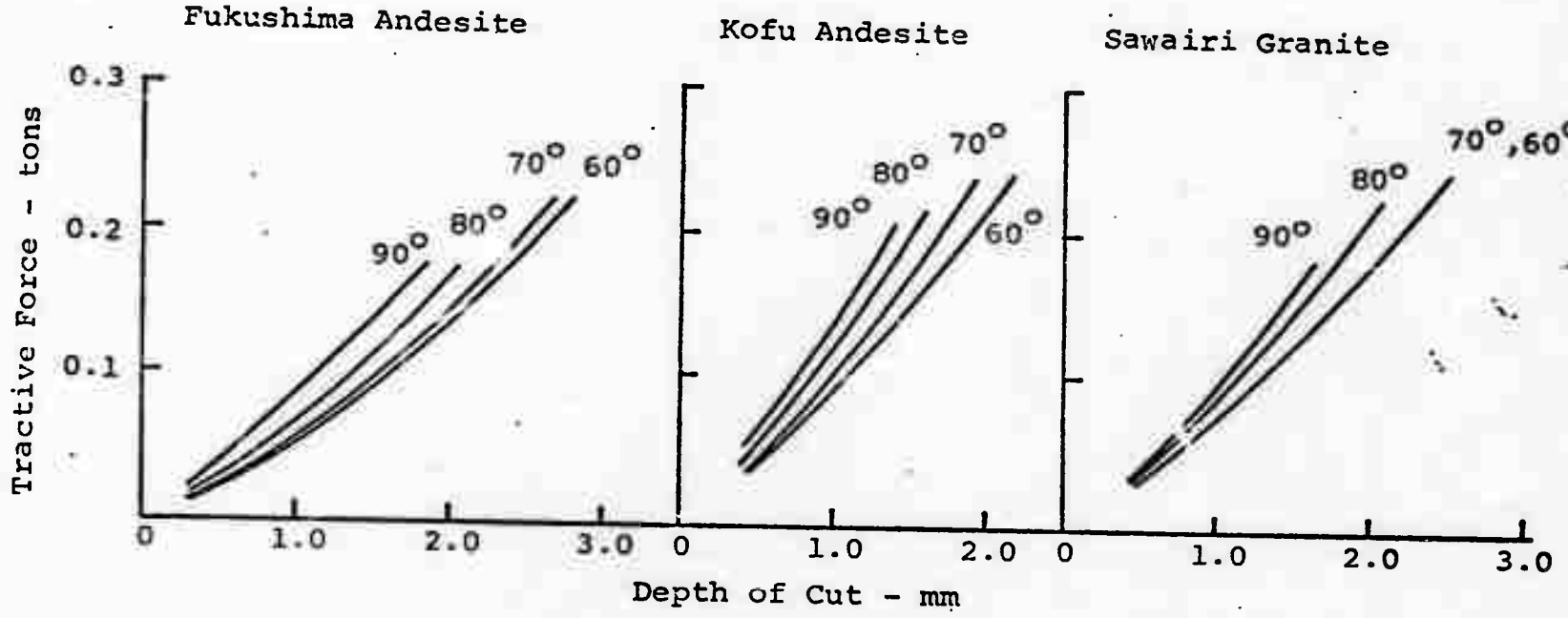

Figure 4. The Relationship Between the Tractive Force and the Depth of Cut as a Function of Tip Angle.

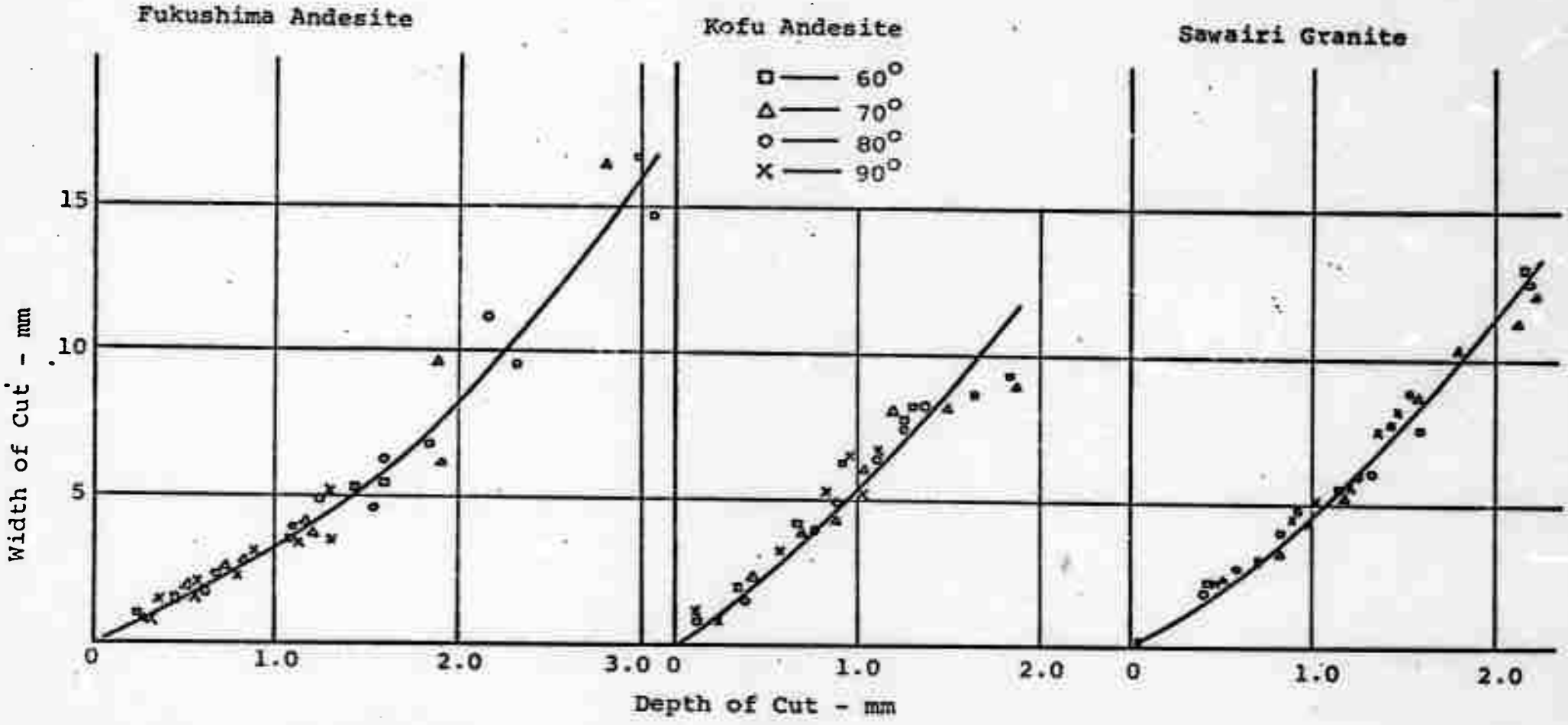

Figure 5. The Relationship Between the Width and Depth of Cut.

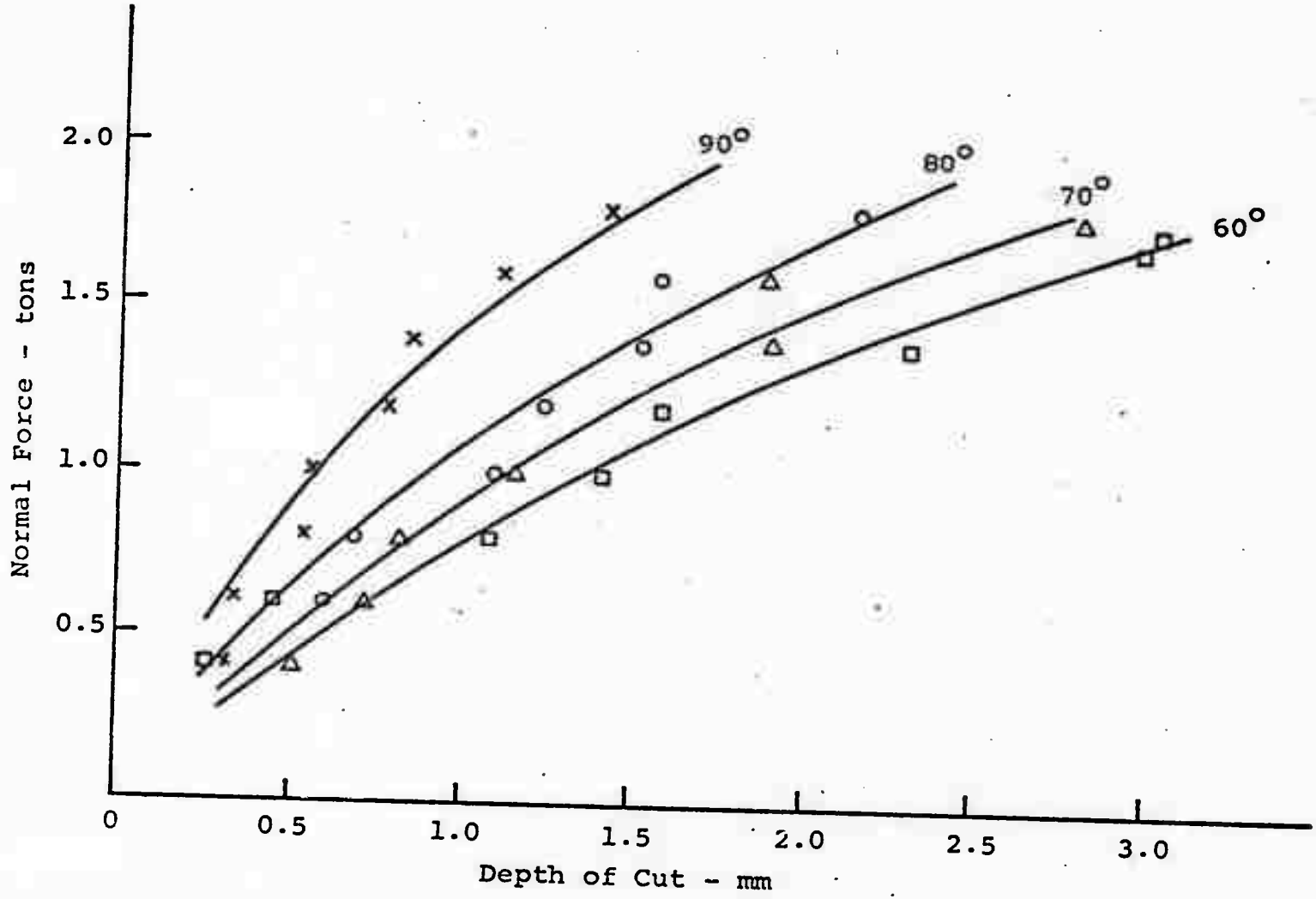

Figure 6. The Relationship Between the Normal Force and the Depth of Cut for Fukushima Andesite.

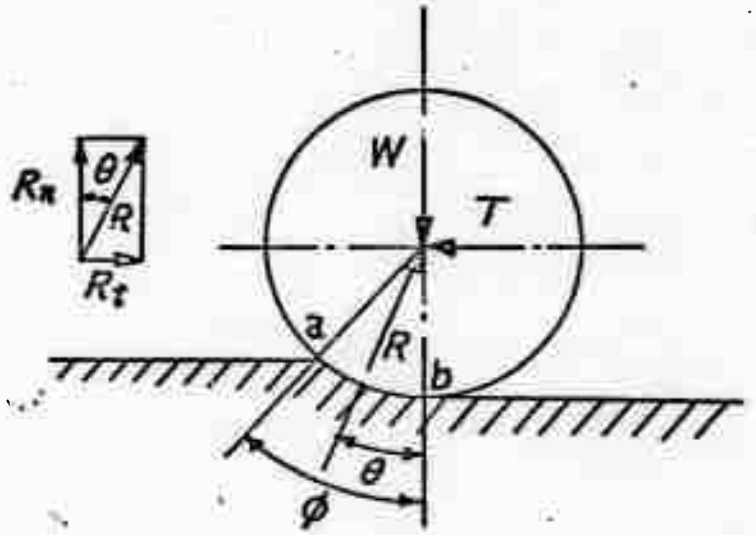

Figure 7. Equilibrium of Forces Acting on the Disc Cutter.

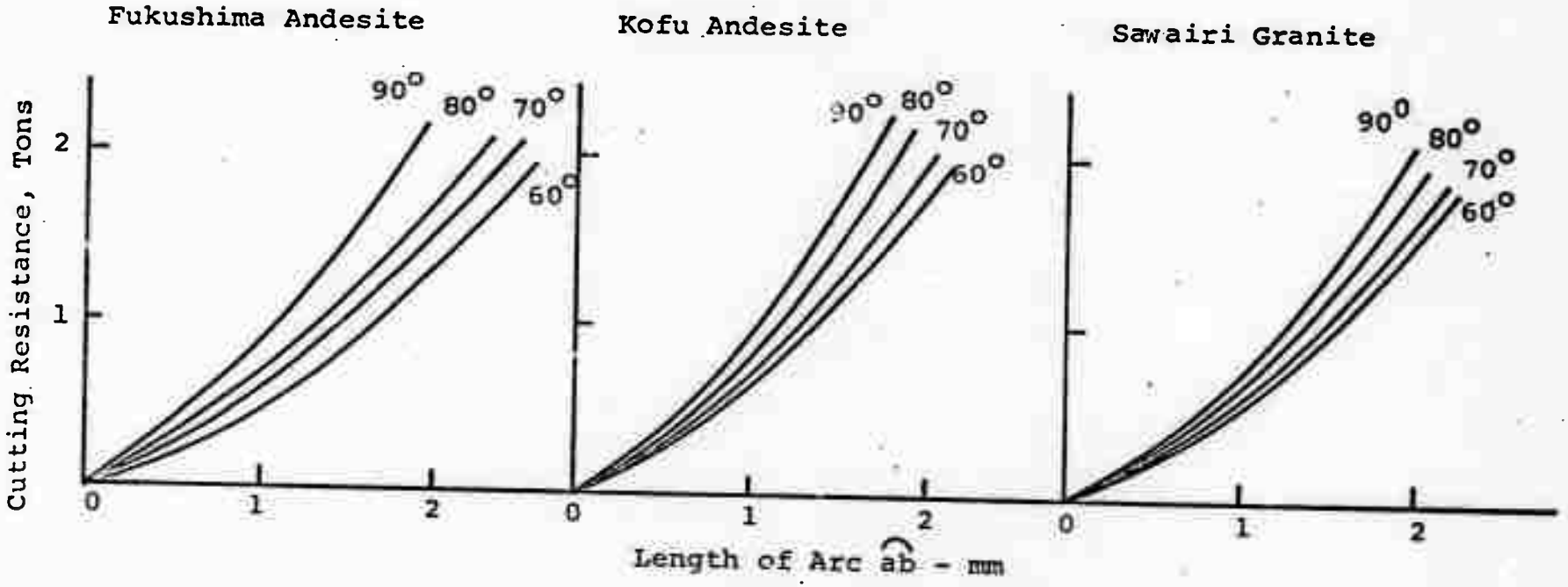

Figure 8. The relationship Between the Cutting Resistance (Assumed to be the same as the Normal Force) and the Tip Contact Length for Various Tip Angles.

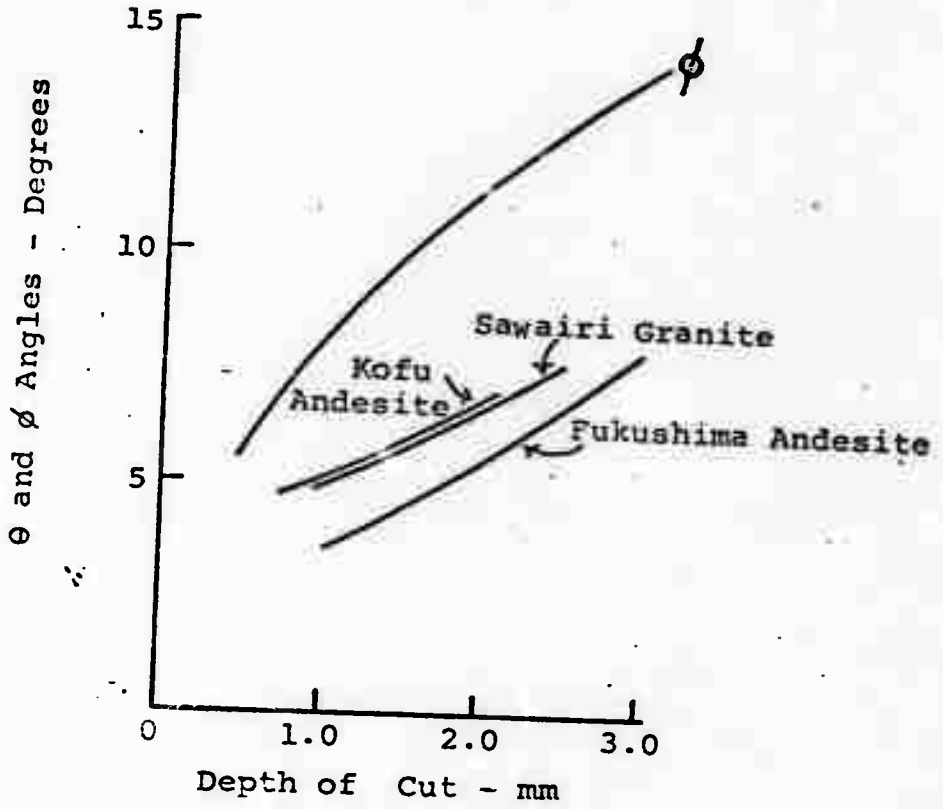

Figure 9. The Relationship Between the Angle of Action (θ) of the Cutting Resistance and the Depth of Cut for a Tip Angle of 60°. Shown Also is the Center Angle ϕ of the Contact Arc.

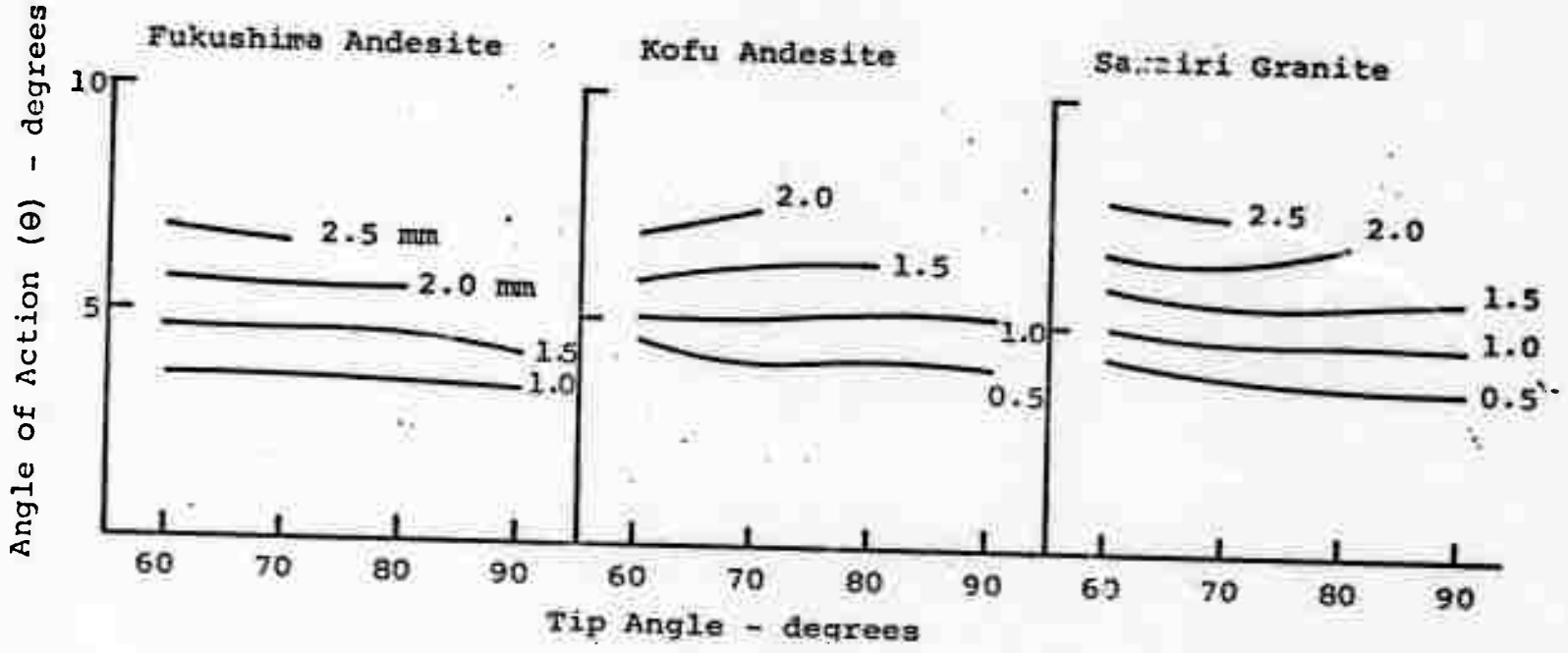

Figure 10. The Relationship Between the Angle of Action of the Cutting Resistance and the Tip Angle for Various Cutting Depths.

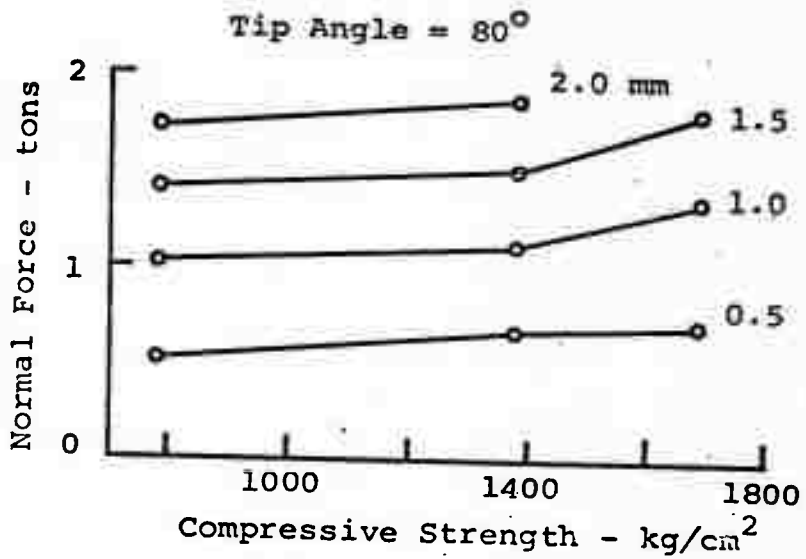

Fig. 11. The Relationship Between the Normal Force and the Compressive Strength as a Function of Depth of Cut.

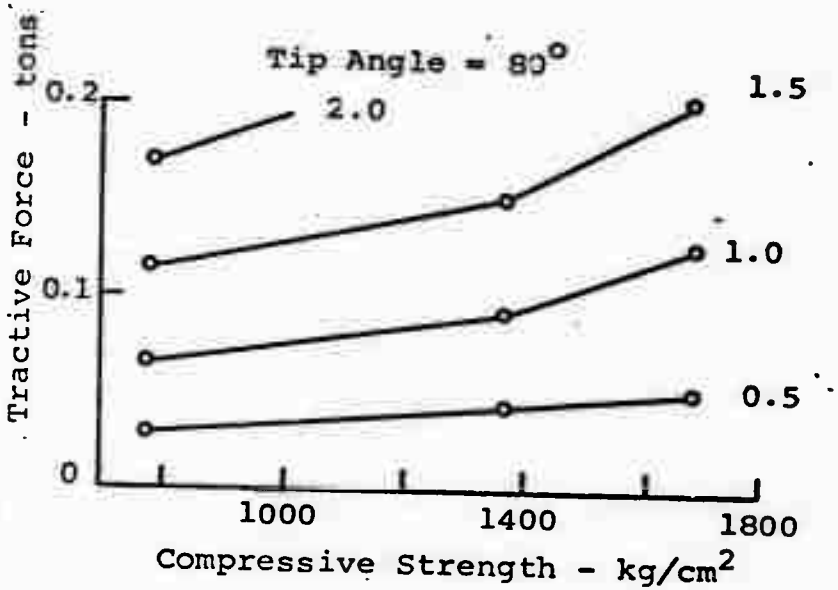

Fig. 12. The Relationship Between the Tractive Force and the Compressive Strength as a Function of Depth of Cut.

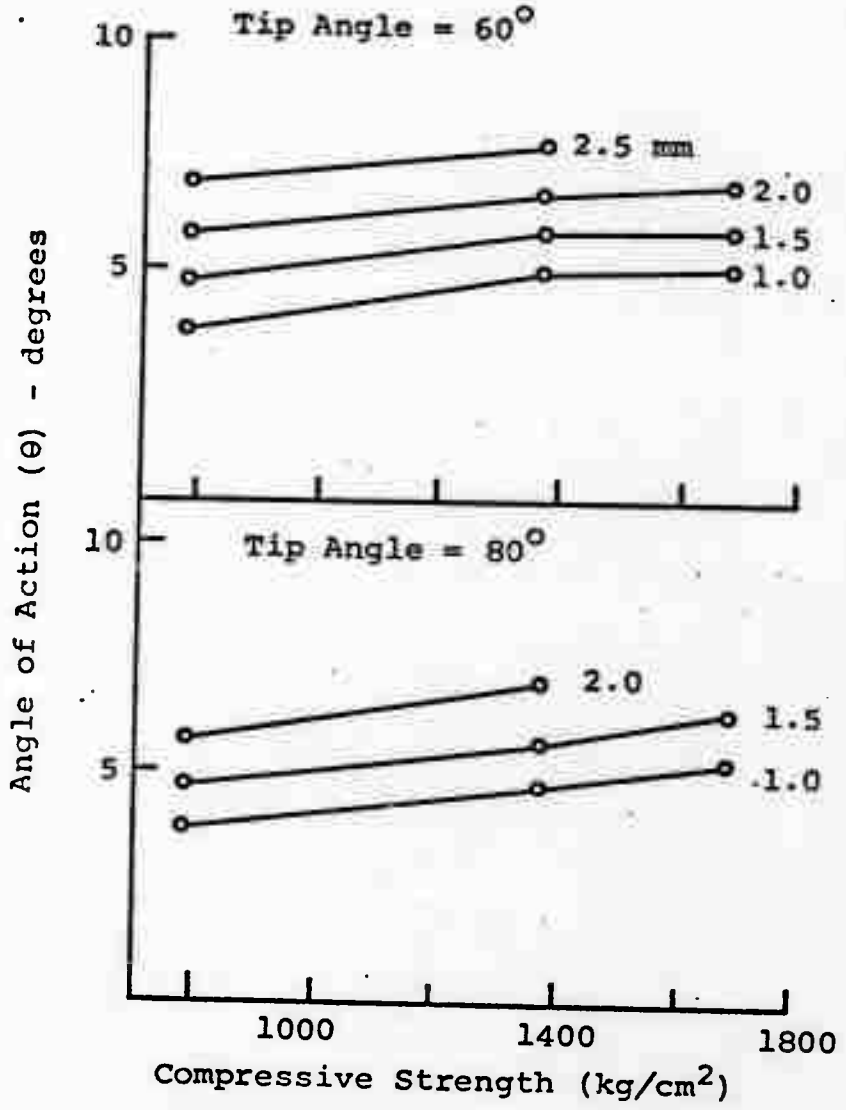

Figure 13. The Relationship Between the Angle of Action of the Cutting Resistance and the Compressive Strength as a Function of Depth of Cut.

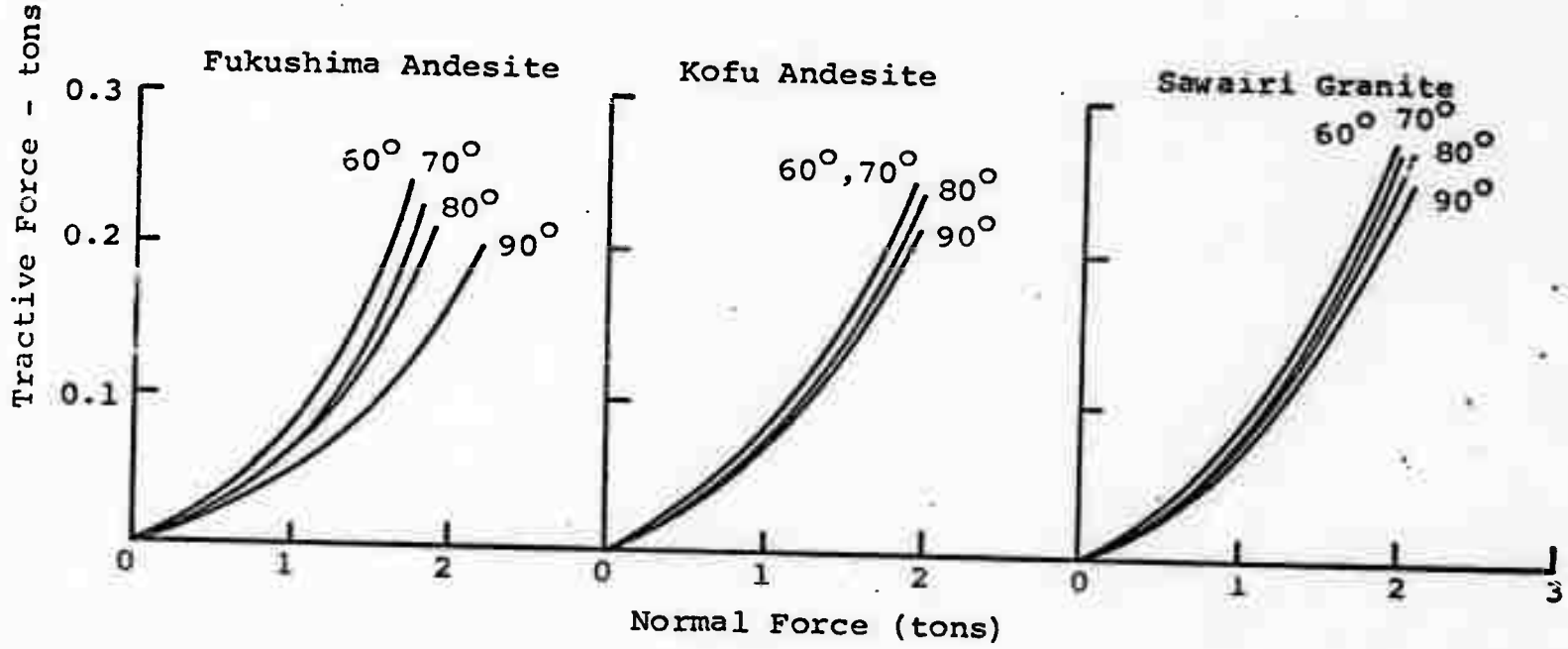

Figure 14. The Relationship Between the Tractive and Normal Force Components as a Function of Tip Angle.

STUDIES ON THE CUTTING OF ROCK BY ROTARY CUTTERS - PART 2*: CUTTING USING A SPHERICAL CHIP AND A MILLED TOOTH CUTTER

by S. Takaoka[1], H. Hayamizu[2], S. Misawa[2], and M. Kuriyagawa[2] - Translated from Japanese by Y. Kojima[3] and W. Hustrulid[4].

ABSTRACT

Fundamental experiments on the cutting of rocks by spherical chip and milled tooth cutters were carried out as part of a tunnel boring research program. The following results were obtained:

(1) The depth and width of the cut increases with the pitch of the milled tooth cutter. A similar result was not observed for the spherical chip cutter since apparently the range of pitch used wasn't large enough.

(2) The volume fractured decreases with the pitch.

(3) A larger traction force is required when the pitch is large. The difference between the maximum and minimum values of traction force is also large.

(4) The relationship between the depth and width of cut depends on the rock properties rather than on the pitch.

(5) The moment which produced results because of the friction between the cutter and its rotating axis has large influence on the friction force.

---

*Originally Published in the Journal of the Mining and Metallurgical Institute of Japan, v. 85, no. 975, July 1969, pp. 491-6.

[1]Dr. of Engineering, Dept. of Mining & Preservation of Safety, National Research Institute of Polution & Resources, Saitama, Japan.

[2]Dept. of Mining & Preservation of Safety, National Research Institute of Polution & Resources, Saitama, Japan.

[3]Graduate Student, Colorado School of Mines, Golden, Colo. 80401

[4]Associate Professor, Department of Mining, Colorado School of Mines, Golden, Colorado 80401.

1. Introduction

Recently, in driving a drift or tunnel in a metal or coal mine, where rapid advance is desired, the possibility of mechanical boring is attracting more and more attention. This method uses the full face boring machine for continuous rock removal. Remarkable advances have been made in this technique, and several boring machines are now being used in actual operation in Japan.

The efficiency of mechanical boring is influenced largely by the type of rock cutting tool equipped to the drilling head.

Since there are various possible cutter types which can be used on the head, it is very important to determine the best cutter for the rock being bored.

As one of several studies on the ability of various cutters to cut hard rock, we have done experiments using the disc cutter, the spherical cutter, and the gear cutter. In this paper we report the results of rock cutting experiments using a spherical cutter and a gear cutter.

2. The Rock Samples and the Cutter Description

2.1 The Rock Samples

The rock samples used in this experiment were Samairi Granite, Kofu Andesite, and Fukushima Andesite. These were the same types as used in the cutting experiments with the disc cutter.

2.2 The Cutter Description

(1) The Spherical Cutter

The spherical cutter used in the experiment is shown in fig. 1. A disc of carbon steel having a thickness of 20 mm (the thickness

at the shaft section is 36 mm) and a diameter of 200 mm is used. Tips of tungsten carbide with various pitches are inserted into the circumference of the cutter. The tip of the insert is a hemisphere having a radius of 3 mm. Four tip pitches (12, 15, 18, and 20 mm) were used.

(2) The Gear Cutter

As shown in fig. 1, tungsten carbide is also used for the gear parts of the gear cutter. The diameter of the cutter is 200 mm, the thickness is 15 mm, and the tip pitch used were 10, 20, and 30 mm.

3. The Experimental Apparatus and the Experimental Method

The apparatus and the experimental method used is the same as described earlier in the study of rock cutting by the disc cutter (Part 1). However, the volume of the cut was determined by injecting liquid paraffin from a graduated syringe into the cut.

4. The Experimental Conditions

Cutting experiments were done on each of the above rock samples using vertical force values of 1.0, 1.5, 2.0, 2.5, and 3.0 tons.

In the case of the actual tunnel boring machine, many spherical chip cutters or gear cutters are attached to the boring head. The cuts are made on concentric circular paths, and the adjacent cuts will, in general, affect one another.

When the rock is cut by the above cutters, the mutual effect of the cutters, the effect of the distance of the cutters

from the axis, and the cutting velocity of the cutter, etc. cannot be neglected. However, in these experiments, linear, independent cuts were made at a constant cutting velocity of 30 cm/min.

5. The Experimental Results

The following results were obtained from rock cutting experiments using the above methods and experimental conditions. Since the experimental results for each rock type are similar, only one example is reported.

5.1 The Vertical Force and Depth of Cut

The depth of cut made in the rock surface by the rotary cutter is an important factor which has a direct relationship with the boring rate of the actual tunneling machine. We studied the relationship of this variable with the vertical (thrust) force. The depth of cut directly beneath one tip and that between adjacent tips is generally different. Therefore, we recommend that both depths be measured (fig. 2). In fig. 3, the solid line shows the average depth of the cut which is directly beneath the tip, and the dotted line shows the average depth of the cut which is between adjacent tips. Now, considering the solid line in the case of both the spherical cutter and the gear cutter, the depth of cut increases as the vertical force increases. In the case of the gear cutter, the larger the pitch (distance between adjacent tips) the larger the depth of cut becomes for the same vertical force.

In the case of the spherical cutter, the effect of pitch on the depth of cut for each value of vertical force is not as clear. This is because the variation in pitch was only 3 mm,

whereas in the case of the gear cutter the variation was as large as 10 mm. For both cutters, the rate of increase in the depth of cut has a tendency to decrease as the vertical force becomes larger.

Next, considering the dotted line, the depth of cut clearly increases as the vertical force increases. For a constant vertical force, the smaller the pitch, the larger the depth of cut. This is just the opposite of that observed for the depth of cut directly beneath the tip. The reason for this is easily seen since if the pitch is small, the adjacent indentations are easily connected to each other. In the case of the 30 mm pitch of the gear cutter and 21 mm pitch of the spherical cutter, the connection of the two indentations could not be seen.

5.2 The Vertical Force and Width of Cut

Fig. 4 shows the relationship between the vertical force and the width of the cut. When the rock is cut by the spherical cutter, the shape of each indentation on the rock surface is not true circle. The width of the indentation was assumed to be the average of the length in the direction of the movement of cutter and in the direction perpendicular to this. In the case of the gear cutter, we recorded the length in the direction of the movement of the cutter and the lateral width (see Fig. 2).

As is clear from fig. 4, in the case of both cutters, the width of the indentation (groove) increases as the vertical force increases; however, the rate of increase decreases as the vertical force increases. In the case of the gear cutter, for the same vertical force, the indentation dimensions, both longitudinal and lateral, clearly become larger, as the pitch becomes larger.

However, in the case of the spherical cutter, for the reasons given in section 5.1, the width of indentation for the same vertical force is apparently not influenced by the pitch. In the experimental results using the gear cutter, for the cutter of 10 mm pitch, the length of each indentation for vertical loads of more than 1.5 tons was not recorded since the indentations were connected. The dotted line of fig. 4 shows that the width of groove between two tips also increases as the pressing force increases. However, in the case of the same vertical force, the width of groove increases as the pitch of the tip becomes smaller. In the case of the spherical cutter having a 12 mm pitch, and a gear cutter having a 10 mm pitch, when the pressing force is nearly 3 tons, the width of the groove between two tips is almost the same as the width right beneath each tip. This means that the indentations made on the rock surface have connected to the same width, but the depth of groove directly beneath the tip is deep, whereas the intermediate region is shallow. From fig. 3, in the case of the spherical cutter whose pitch is 12 mm, the depth directly beneath the tip and that between the two tips is about the same when the vertical force is increased to 4.0 tons. In the case of the gear cutter whose pitch is 10 mm, the depth directly beneath the tip and that between the two tips is about the same when the vertical force is about 3.5 tons. A completely connected groove is presumed to be made.

5.3 The Vertical Force and the Volume of Groove

Fig. 5 shows the relationship between the vertical force and the volume of groove per unit length. For both the spherical and the gear cutter, the volume of groove increases as the ver-

gear cutter, for the same vertical force, the larger the pitch of the tip, the larger the tracting force becomes. However, as mentioned in section 5.1, in the case of the spherical cutter, the influence of the pitch is not as clear as in the case of the gear cutter. As far as this experiment is concerned, the value of the tracting force is shown to be about 1/50 to 1/100 of the value of the vertical force. Contrary to the results for the maximum tracting force, the minimum tracting force (the average of the minimum values) increased for the same pressing force, as the pitch becomes smaller. From the above results, when the pitch of the cutter is large, the difference between the maximum and minimum values of the tracting force is very large, and therefore the variation of the torque acting on the boring axis is presumed to be large.

5.5 The Depth of Groove and Width of Groove

Fig. 8 shows the relationship between the depth and the width of the groove derived from figs. 3 and 4. In the case of both cutters, the width of indentation at a point directly above the maximum tip indentation was used. It is seen that the width of groove increases irrespective of the pitch of tip as the depth of groove increases. This relation is observed in other methods of rock cutting too, and it is considered to be part of the nature of the rock cutting process.

6. The Tracting Forces

6.1 The Equilibrium of Forces When the Rock is Grooved by the Gear Cutter

We showed in section 5.4 that the variation in tracting

tical force increases. For a constant vertical force, the volume of groove increases as the pitch decreases. This is just the opposite of that observed for the depth and width of groove. This means that if the pitch is small, the number of indentations per unit length is large, and the rock between adjacent indentations is broken. The pitch, in the case of the spherical cutter, had very little influence on the results given in sections 5.1 and 5.2. Here, however, the influence of the pitch is seen comparatively clearly.

5.4 The Vertical Force and Tracting Force

When rock is cut, the tracting force which must be applied to the cutter is related to the rotary resistance acting on the boring axis. When a boring machine is designed, it is necessary to decide the relationship between the torque on the drive shaft and the driving force (thrust) on boring head, and therefore this problem is of concern. Fig. 6 shows an example of the tracting force on the cutter measured by the tension meter, and recorded by the oscillograph. As is clear from the diagram, the variation in tracting force has a period which almost coincides with the pitch of the cutter. However, when the pitch is small, so that two or three tips are in contact with the rock at the same time, the period-like nature does not appear. The value of the tracting force is taken as the average of the maximum and minimum values shown in Fig. 6.

Fig. 7 shows the relationship between the vertical force and the tracting force obtained from the experimental results. If the vertical force is increased, the maximum tracting force (the average of the maximum values) increases also. In the case of the

force has almost the same period as the pitch of the cutter. This was studied in detail using the gear cutter as an example. Fig. 9 shows the explanatory diagram of the equilibrium of the forces when the rock is being cut.

First, consider the equilibrium of forces acting when the cutter rotates on the surface of the rock rather than indenting it. The situation shown as the solid line is the state when two tips of the cutter are in contact with the rock surface at the same time. If the rock moves to the right, the tip of the right side separates from the rock surface and the tracting force becomes a maximum. As the rock moves further to the right, the tracting force becomes smaller and smaller, and when the tip of the left side becomes vertical (shown by the dotted line), the tracting force becomes zero. If the cutter moves to the right still further, the tracting force of the reverse direction occurs; however, as the tension meter used in this experiment is not sensitive to a compressive tracting force, the force as shown on the oscillograph in this interval is zero. According to the movement of the cutter, when the next tip comes into the position of the solid line, the tracting force returns to the original situation, and after this, the cutter continues to rotate on the rock surface. Since the cutter does not actually cut the rock, the small variation of distance between the axis of the cutter and the rock surface can be neglected. Although the cutter has been assumed to rotate at a constant velocity, the actual interval in which the cutter rotates at a constant velocity in the diagram is only between the position of the left tip shown in the dotted line. Since the tension meter

used in this experiment does not react to a compressive force, after the tip passes the vertical position shown in the dotted line, the rotation of the cutter accelerates.

i) Torque Acting on the Cutter

The torques which act on the cutter are (1) the counter-clockwise moment, shown by the product of $r\sin\theta$ and R_t, (2) the horizontal component of R which acts between the rock and the cutter, and (3) the clockwise moment of the frictional resistance, M. For the cutter to continue the uniform motion, the forces must balance, and so,

$$R_t r\sin\theta - M = I\frac{d^2\theta}{dt^2} = 0 \qquad (1)$$

$$\therefore R_t r\sin\theta = M \qquad (2)$$

ii) The Condition That the Piston Applying the Force Does Not Rotate Around the Axis of the Cutter

The condition that the piston applying the vertical force does not rotate around the axis of the cutter, requires that the two moments, i.e., the clockwise moment shown by the product of the reaction P acting on the fulcrum of the rod of length l, and the counter-clockwise moment of the frictional resistance acting on the axis of the cutter must balance. Therefore:

$$M - Pl = 0 \qquad (3)$$

$$\therefore P = \frac{M}{l} \qquad (4)$$

iii) The Condition that the Axis of the Cutter Does Not Move

Finally, we consider the equilibrium of the forces such that the axis of the cutter does not move. First for the case

when the axis of the cutter is not accelerated up or down, the load W, added to the cutter and the reaction R_{rn}, acting on the cutter from the rock must balance. Therefore,

$$R_{rn} = W \tag{5}$$

$$R_{rt} = R_{rn}\cot\theta = W\cot\theta \tag{6}$$

Next, when the axis of cutter does not move to the right or left, R_t (the force acting between the rock and the cutter), R_{rt} (the horizontal component of the grooving resistance R_r), P (the reaction acting on the fulcrum of rod), and T (the tracting force acting on the tension meter) must balance. Therefore,

$$R_t + R_{rt} - T + P = 0 \tag{7}$$

Rearranging one obtains

$$R_t + P = T - R_{rt} \tag{8}$$

Combining equations (2) and (4) and substituting into (8), one finds that

$$R_t \left(1 + \frac{r}{l}\sin\theta\right) = T - R_{rt} \tag{9}$$

The expression for R_t then becomes

$$R_t = \frac{T - R_{rt}}{1 + \frac{r}{l}\sin\theta} \tag{10}$$

which upon comparing with equation (2)

$$M = \frac{T - R_{rt}}{1 + \frac{r}{l}\sin\theta} r\sin\theta \tag{11}$$

provides the desired result,

$$\therefore T - R_t = \frac{M\left(1+\frac{r}{l}\sin\theta\right)}{r\sin\theta} \tag{12}$$

That is, the difference between T (which is recorded on the tension meter) and R_{rt}, is just the traction needed to overcome the moment of the frictional resistance, M, and to rotate the cutter. In the case of rock cutting using the same experimental apparatus, as the moment of frictional resistance is considered to be influenced only by the load, the value of $(T-R_{rt})$ is considered to be a constant. Therefore, by obtaining R_{rt} by measuring T when the rock is cut. Since $F = T - R_{rt}$ is considered to be the resistance due to the friction produced by rotation of the cutter, we call this for convenience the frictional resistance. The angle of rotation, Θ, of the cutter shown in the solid line of fig. 9, is given by the complementary angle of $\phi/2$, where the pitch angle is ϕ. Furthermore, for the situation shown in fig. 10, when the rock is grooved to the depth h, the angle of rotation Θ is given by the complementary angle of ϕ_1. Here, ϕ_1 is

$$\phi_1 = \sin^{-1} \frac{h}{r\sqrt{(\cos\phi-1)^2+\sin^2\phi}} - \tan^{-1} \frac{\cos\phi-1}{\sin\phi} \qquad (13)$$

where h is the depth of groove given by the experiment.

6.2 An Example of the Traction Analysis

Fig. 11 shows an example of the tractive force recorded on the oscillograph when cutting Kofu Andesite using a gear cutter whose pitch is 30 mm. The diagram on the left shows the case in which the vertical force is 1.0T and the rock is not cut. The right side shows the case in which the rock is cut by the vertical force of 3.0T. The diagrams include the time interval during which the two cutter tips are in contact with the rock surface and the time at which the tip on the left side reaches the position of the original right side tip (see figs. 9 and 10).

Now, in the left diagram, the curve drawn in the solid line shows the traction T, actually recorded on the oscillograph. The curve shown as the dotted line is R_{rt}, calculated by equation (6). The difference between these curves is the frictional resistance F. Its value depends on the experimental apparatus, and is determined by the vertical force only.

In the diagram to the right, if the rock is not cut, a record like that shown as the fine solid line should be expected. The curve of R_{rt} would then be like the fine dotted line. Moreover, as the difference of the two is decided by the vertical force only, even if the rock is cut, the difference is considered to be constant. Therefore, when the rock is cut, R_{rt} is shown by the thick dotted line.

6.3 The Influence of the Moment of the Frictional Resistance on the Traction

As mentioned above, the moment of the frictional resistance principally influences the traction. Fig. 12 shows the relationship between the vertical force and the frictional resistance F, when the gear cutter whose pitch is 20 mm is used. As can be seen, regardless of the type of rock, the frictional resistance clearly increases as the vertical force increases. Therefore, to get the true traction, R_{rt}, without any influence of the moment of frictional resistance, we can subtract the value shown in fig. 12 from the traction T recorded on the oscillograph. This value is determined by the radius of the cutter r, the length of piston l, and the moment of frictional resistance M, existing between the cutter and the shaft. If the contact surface between the cutter

and the shaft is constant, the value is considered to be applicable not only to the gear cutter, but also to the disc and the spherical cutter. For the results shown in fig. 7, the above correction is not required at all.

7. Conclusions

In these fundamental rock cutting experiments, spherical and gear type cutters were used to make single straight cuts in a rock surface. The shape of the rock groove was measured and the relationships existing between various factors based on the vertical force studied. In the case of the gear cutter, the equilibrium of the forces when the rock is grooved, and the influence on the traction caused by the frictional resistance acting on the shaft of the cutter were studied. In summary:

(1) For both cutters, the depth and the width of groove were observed to increase as the vertical force was increased. The rate of the increase, however, decreased as the vertical force increased. In the case of the spherical cutter, since the range through which the pitch could be varied was small, the influence of pitch could not be determined. In the case of the gear cutter, it was determined that the larger the pitch, the larger the depth and width of the groove for the same vertical force.

(2) For both cutters, the volume of cut increases as the vertical force increases. For the same vertical force, the volume of cut increases as the pitch decreases. For small values of pitch, the rock remaining between the indentations is essentially broken.

(3) The traction of the cutter increases as the vertical force increases. For the same vertical force, the traction

increases as the pitch of tip increases. The difference between the maximum and the minimum values of the traction increases as the pitch of tip increases. From this, it can be concluded that when the rock is actually bored by a rotary cutter, if a cutter of large pitch is used, it is necessary to take under consideration the variation of torque acting on the shaft.

(4) The relationship between the depth and the width of groove is not influenced by the pitch. For a given rock, the width of groove was observed to increase as the depth of groove increases. Finally, as a result of the study of the forces acting when the rock is cut by the gear cutter, the traction was determined to be larger than the true traction because of the frictional resistance acting on the cutter shaft. The traction which was found in this experiment is about 40% larger than the true traction because of this frictional resistance. Therefore, when the actual boring head is designed, it is considered to be important to try and reduce the needed rotary power by reducing the moment of frictional resistance of the axis of the cutter.

The above results apply to the case of a straight-cut made by a single rotary cutter. It is hoped to continue these experiments on rock cutting using the rotary cutter. The rotational speed of the cutter, the radius of the circle through which the cutter moves, etc., will be considered.

Milled Tooth Cutter

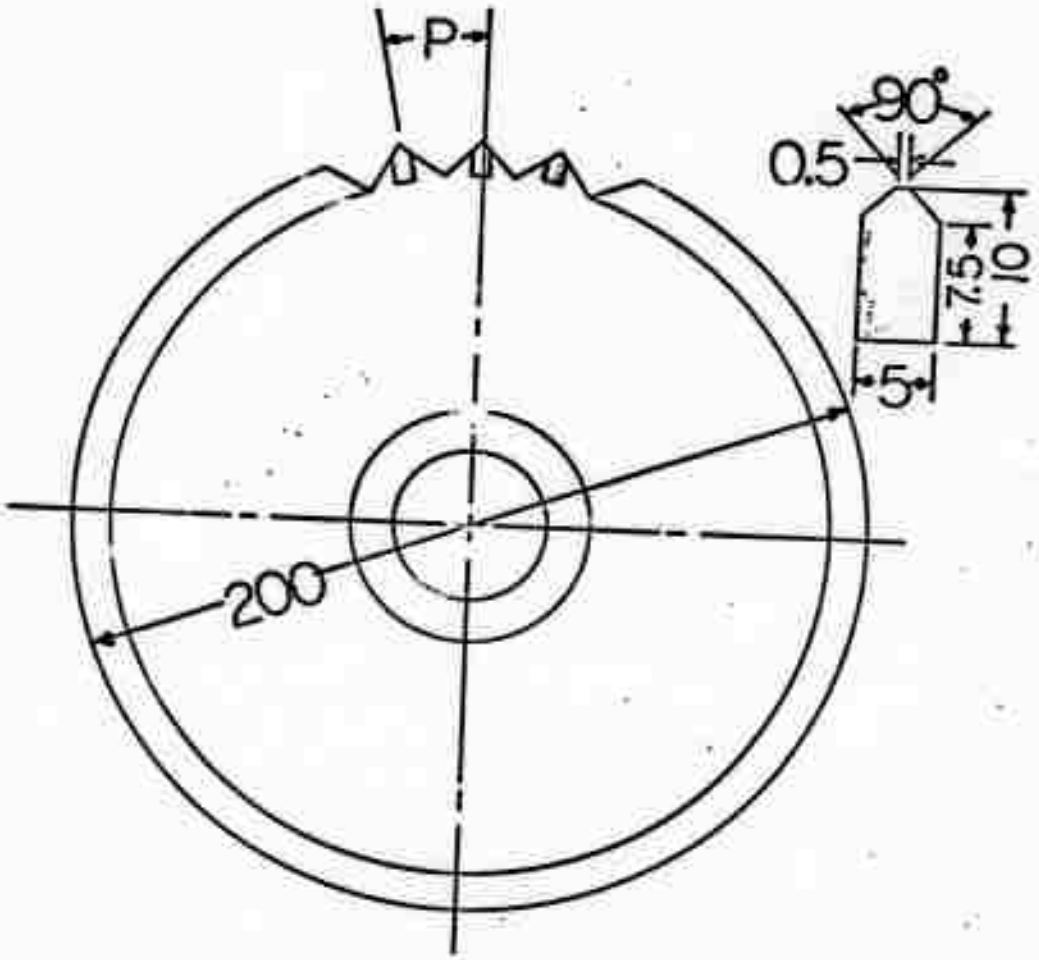

Spherical Chip Cutter

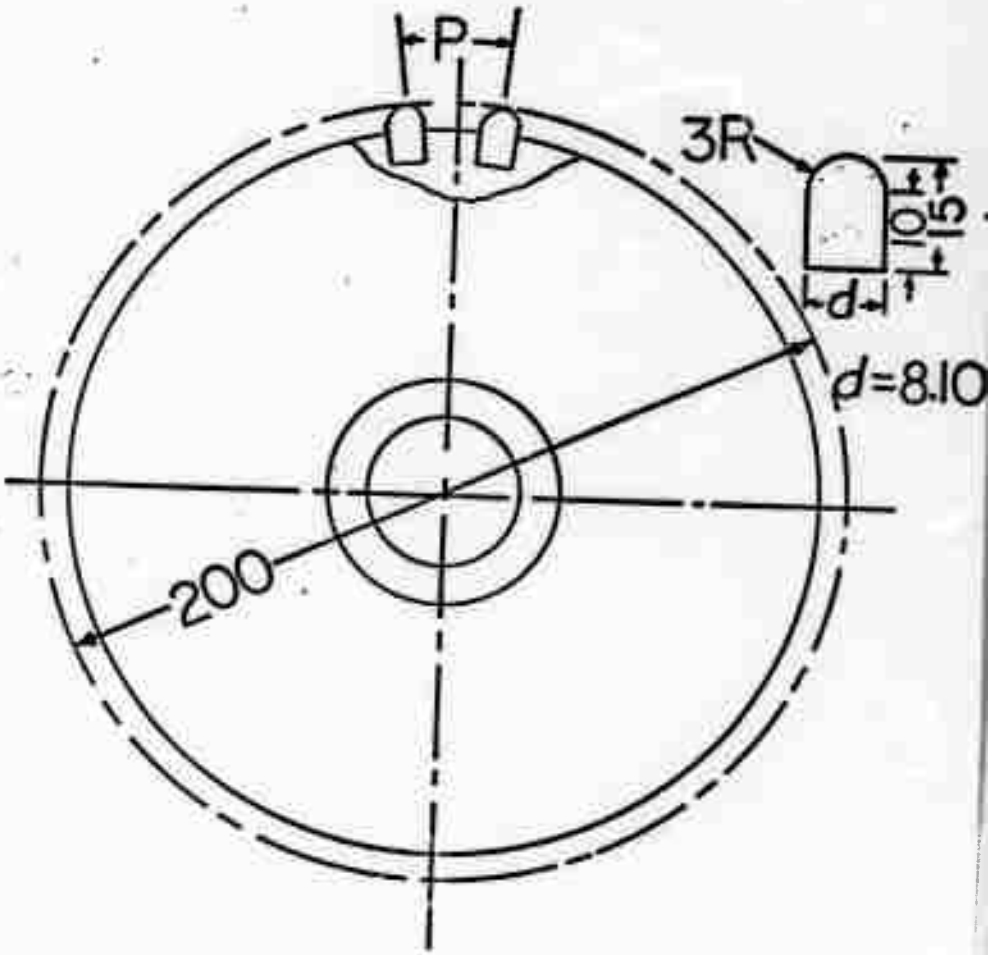

Figure 1. A Diagrammatic Representation of the Cutters Used.

$$w_2 = \frac{w_{21}+w_{22}+w_{23}}{3}$$

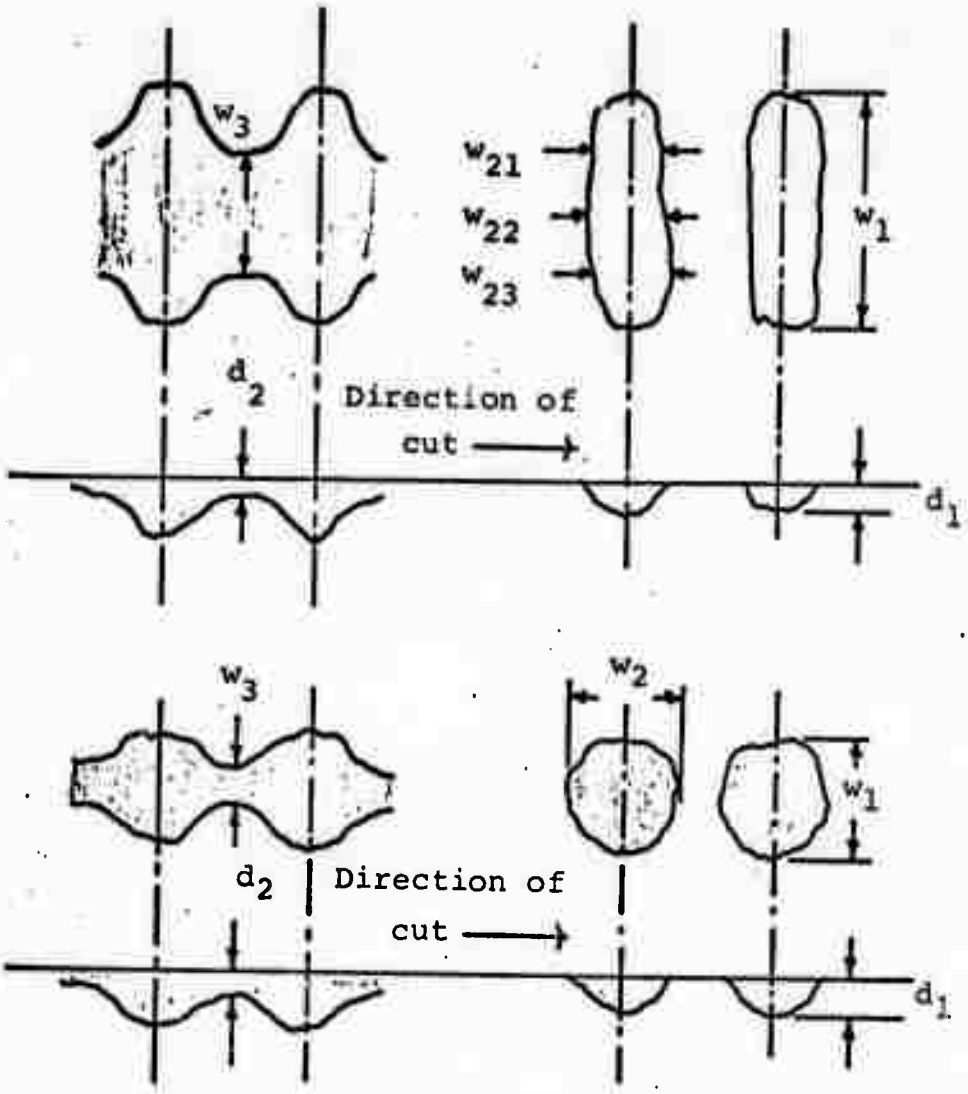

w_1 = the width of cut which is directly beneath the tip and perpendicular to the cutting direction.

w_2 = the width of cut which is directly beneath the tip and in the cutting direction.

w_3 = the width of the cut between adjacent tips perpendicular to the cutting direction.

d_1 = the depth of the cut directly beneath the tip.

d_2 = the depth of the cut between adjacent tips.

Figure 2. Diagrammatic Representation of the Shape of the Cut.

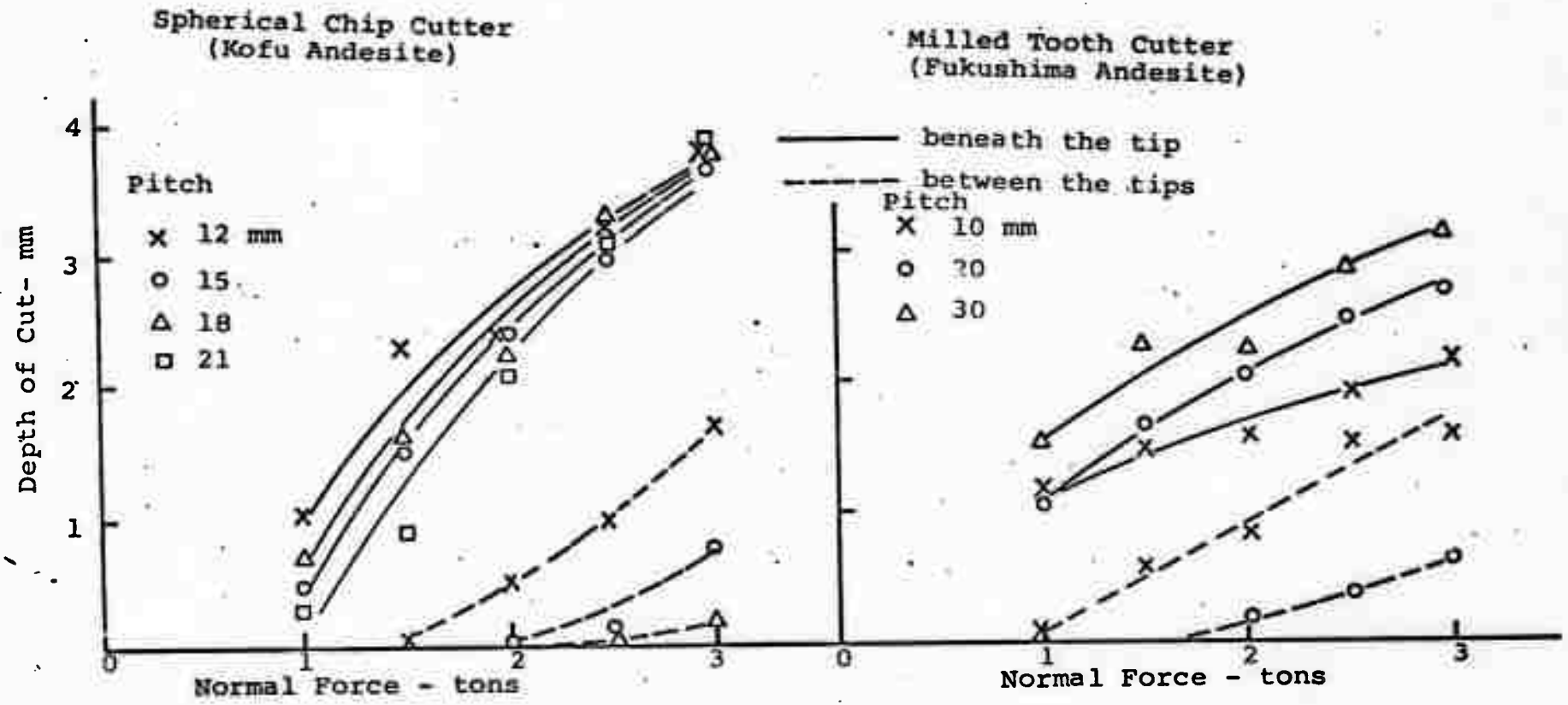

Figure 3. The Relationship Between the Normal Force and the Depth of Cut.

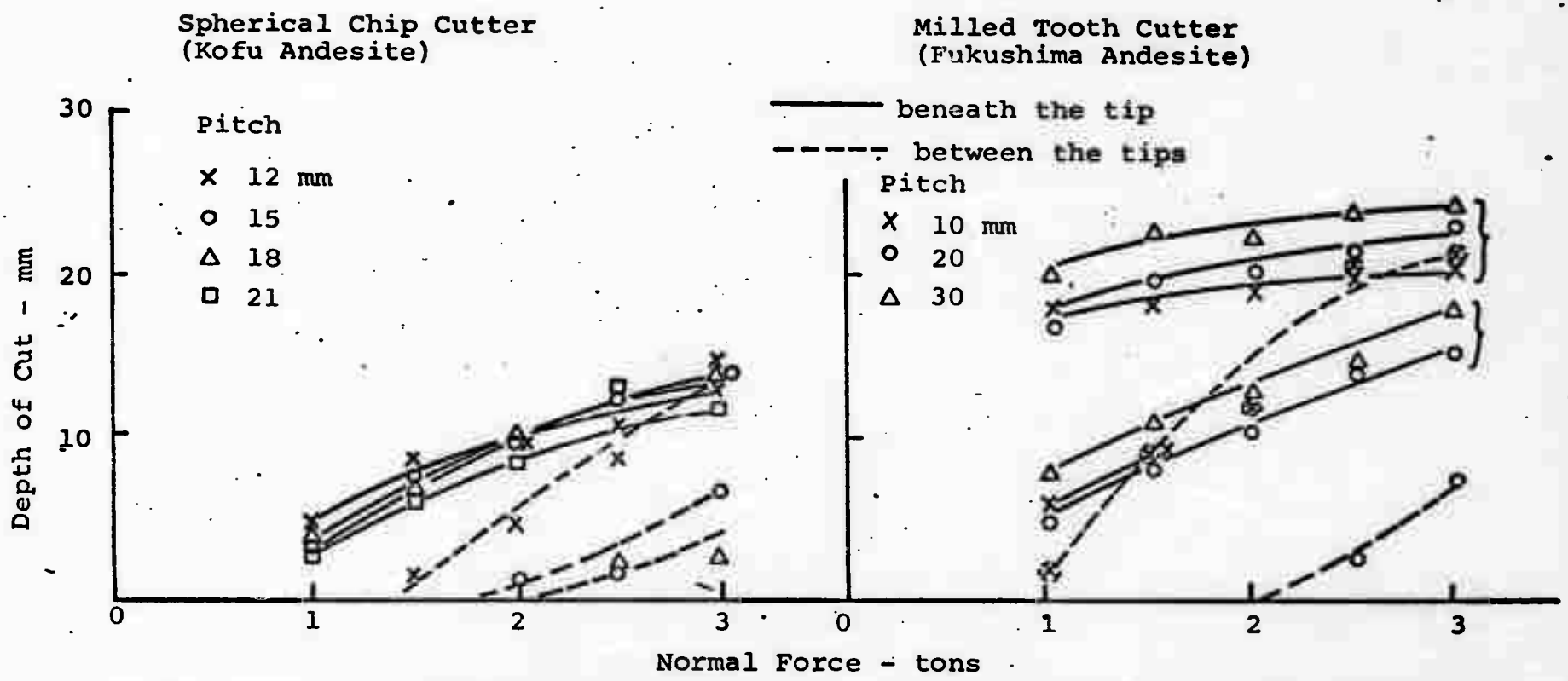

1) The Width Perpendicular to the Cutting Direction

2) The Width in the Cutting Direction

Figure 4. The Relationship Between the Width of Cut and the Normal Force.

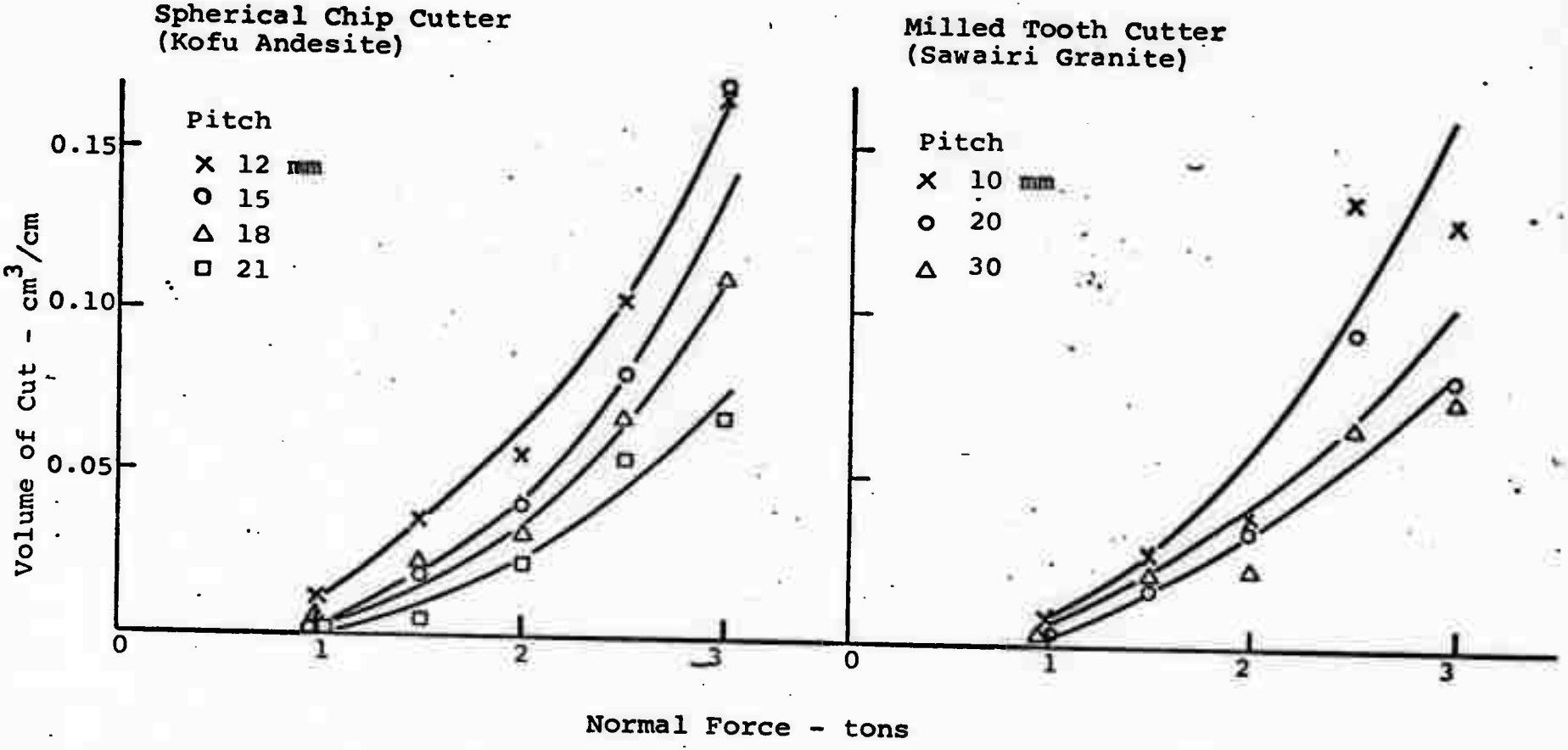

Figure 5. The Relationship Between the Cut Volume and the Normal Force.

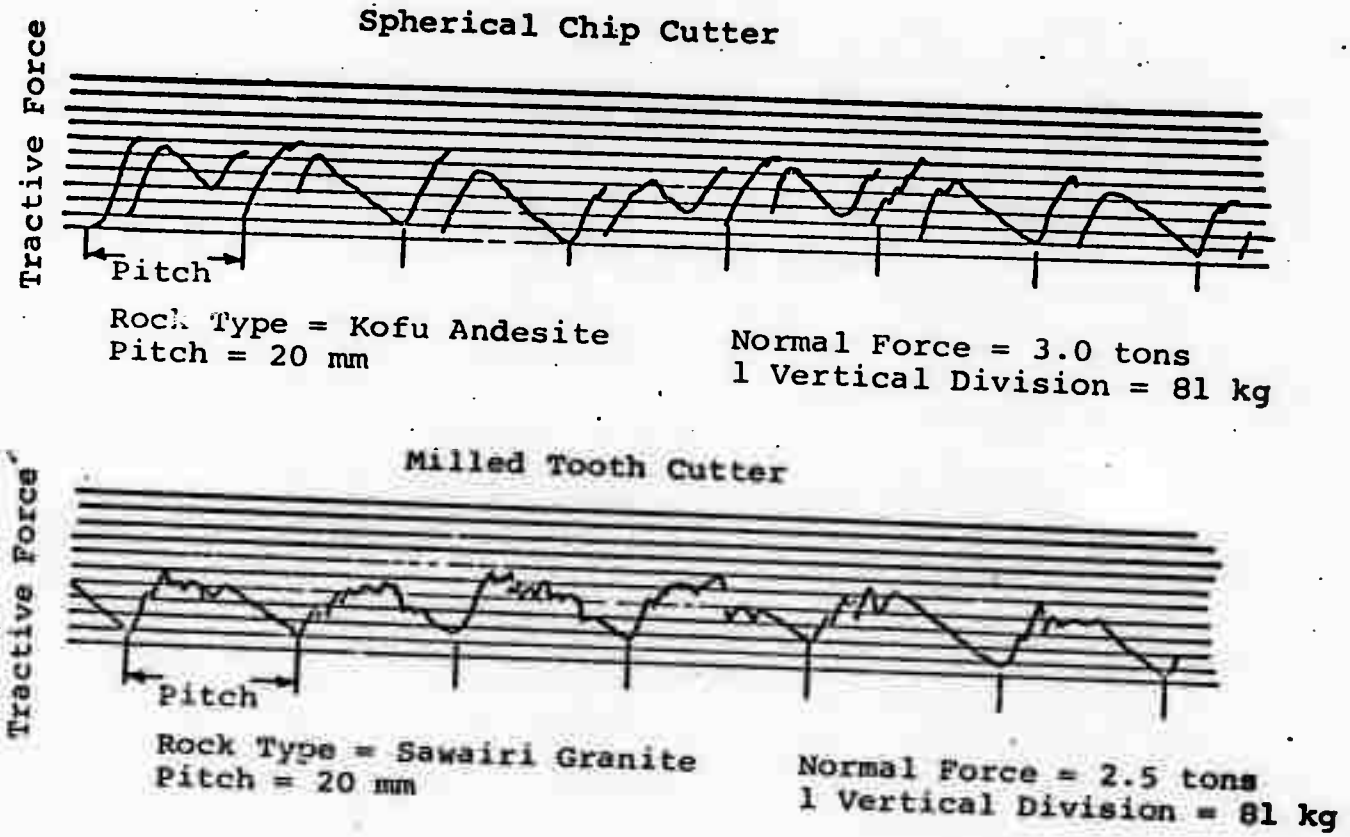

Figure 6. Typical Examples of the Tractive Force Records from the Oscillograph.

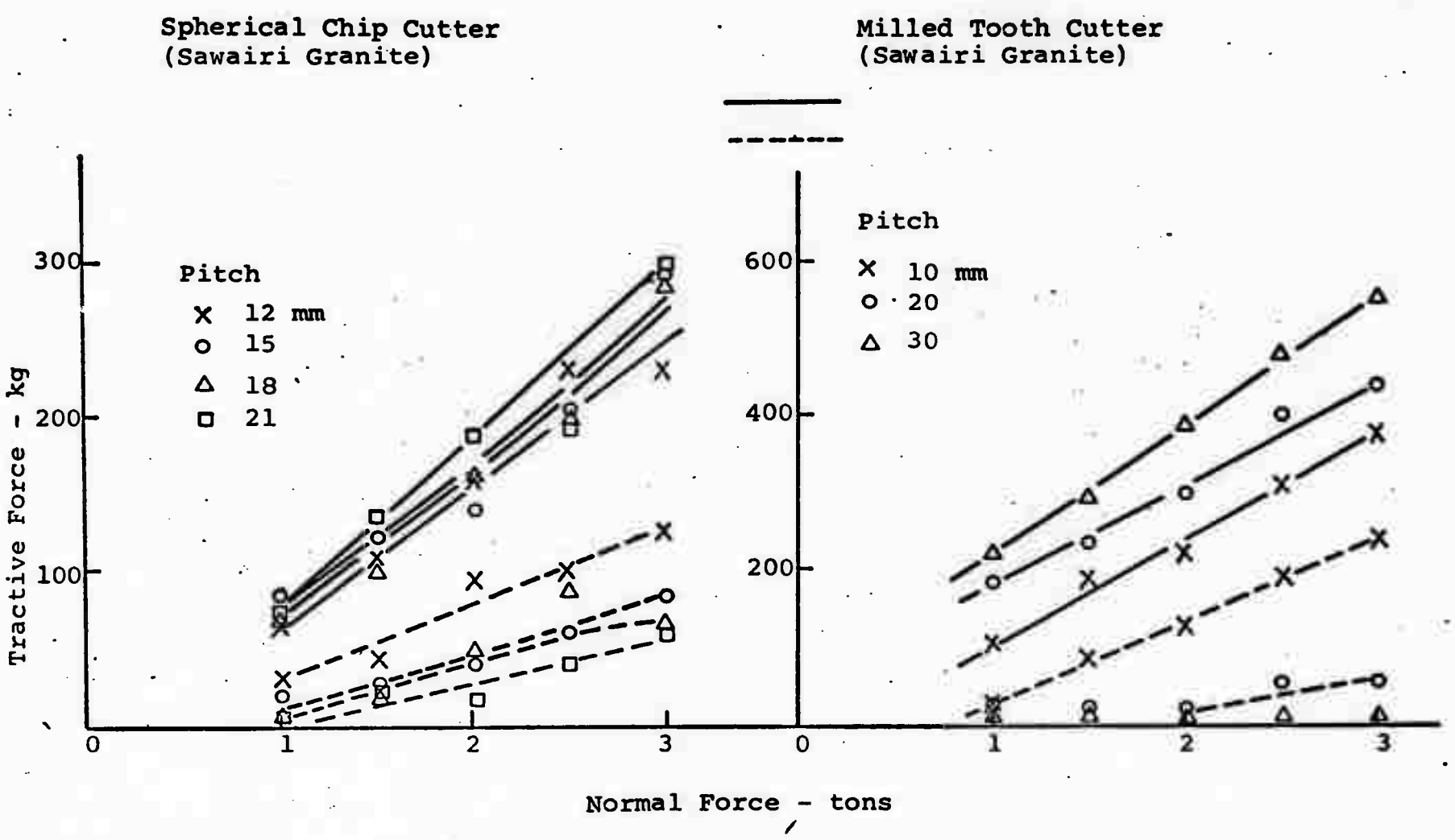

Figure 7. The Relationship Between the Tractive and Normal Forces for Various Pitches.

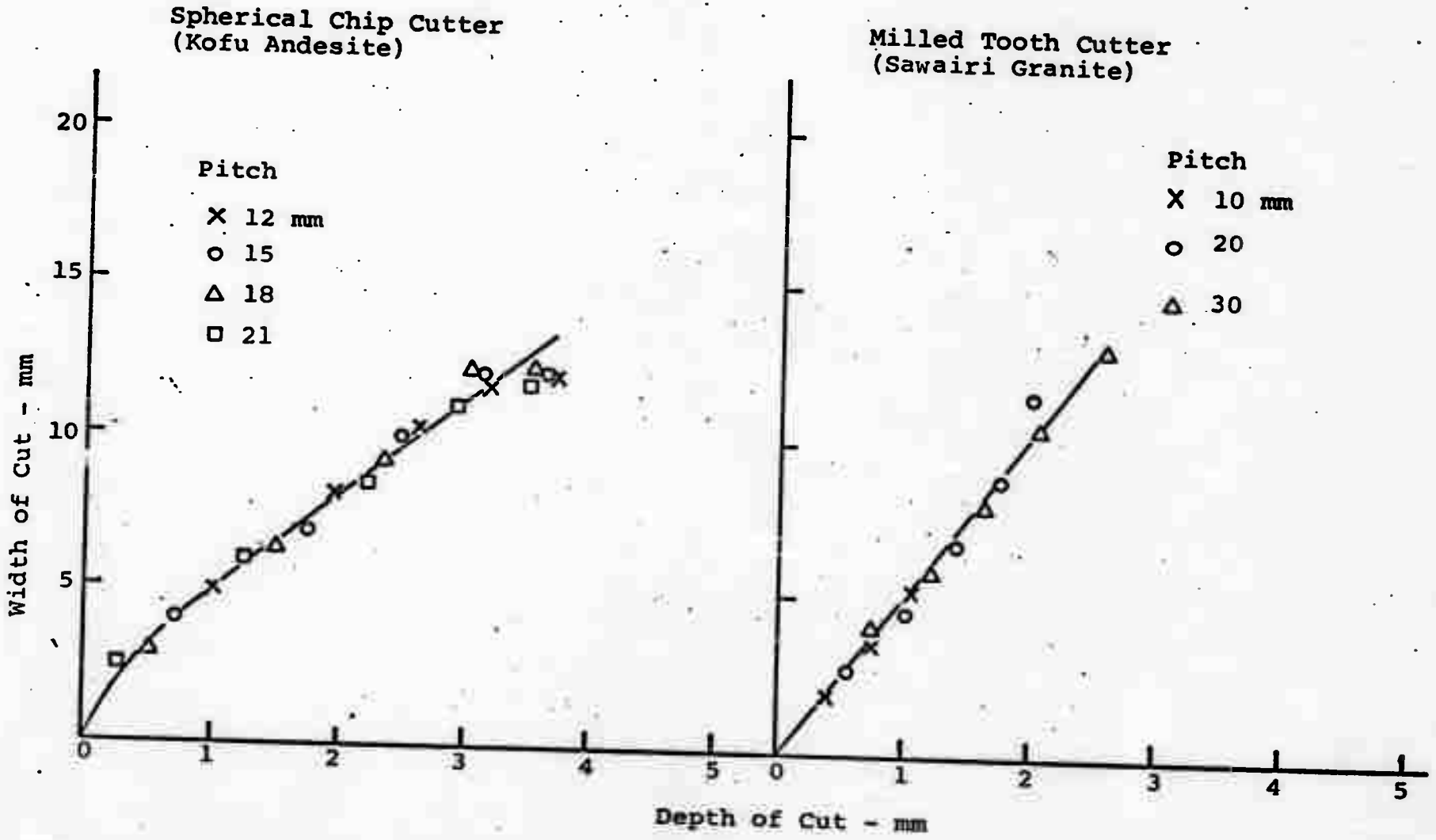

Figure 8. The Relationship Between the Width and the Depth of the Cut.

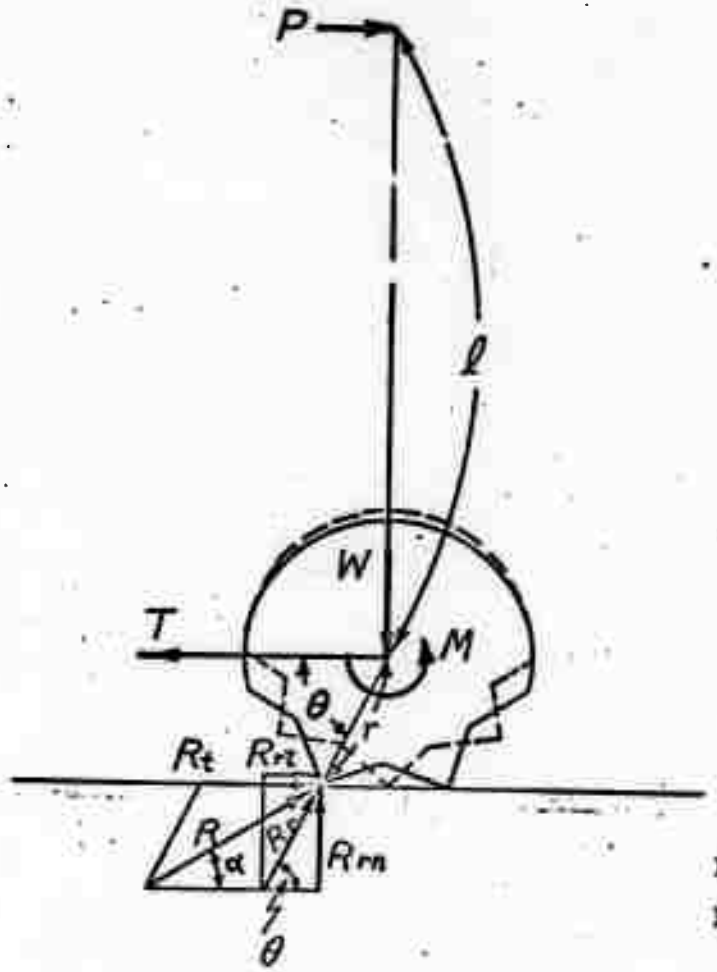

r = radius of the cutter

ℓ = length of piston

w = load

θ = angle of rotation of the cutter

M = moment of frictional resistance acting on the axis of the cutter

-M = moment of frictional resistance acting on the cutter

R = force acting between the cutter and the rock

T = tractive force acting on the tension meter

P = reaction acting on the fulcrum of the piston

R_t = horizontal component of R

R_r = component of R in the direction of the radius of the cutter

R_{rt} = horizontal component of R_r

R_{rn} = vertical component of R_r

Figure 9. The Force Equilibrium Diagram when the Rock is Cut by the Milled Tooth Cutter.

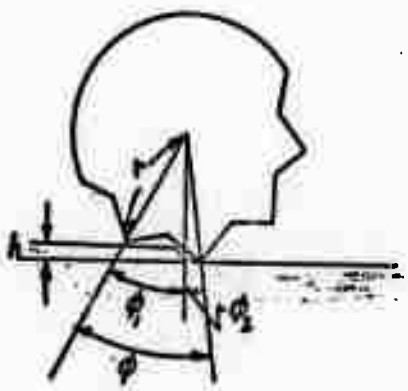

Figure 10. Diagrammatic Representation of the Contact Situation When the Rock Surface is Cut by the Milled Tooth Cutter.

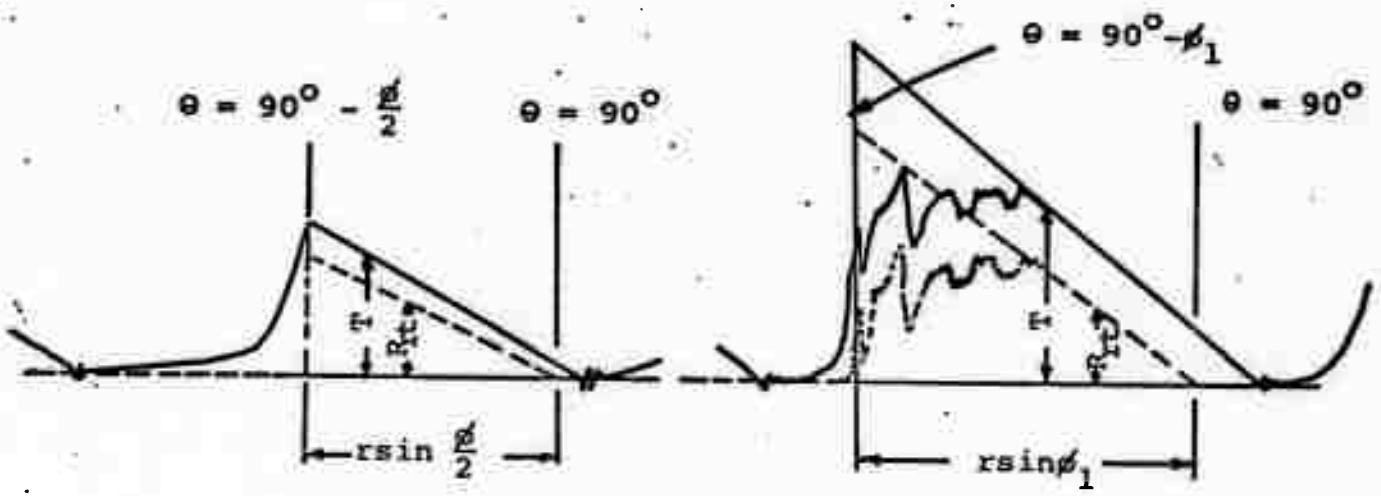

Normal Force = 1.0 tons.
(Rock is not cut)

Normal Force = 3.0 tons
(Rock is cut)

Figure 11. A Comparison of the Theoretical and Experimental Tractive Force Records for the Milled Tooth Cutter, Kofu Andesite, Pitch = 30 mm.

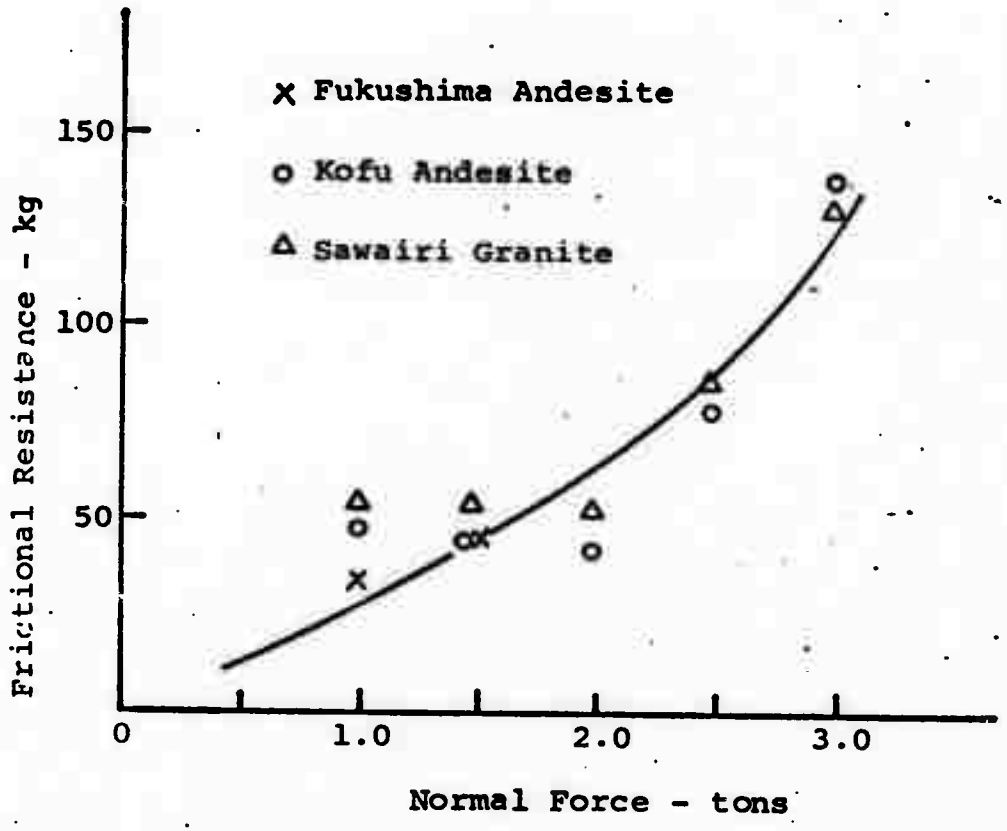

Figure 12. The Influence of the Normal Force on the Frictional Resistance for the Milled Tooth Cutter Having a Pitch of 20 mm.

STUDIES ON THE CUTTING RESISTANCE OF ROCK*

by K. Sasaki[1], N. Yamakado[2], Z. Siohara[2], and M. Tobe[2] - Translated from Japanese by Y. Kojima[3] and W. Hustrulid[4].

ABSTRACT

A rotary bit penetrates the rock along a helical path under the action of an axial thrust force and a rotary torque. The action of the cutting tip is one of planing. It seems reasonable to assume, therefore, that a study of the planing action of a tool on rock would reveal much information pertinent to rotary drilling or boring.

We have studied the following problems using a rock planing apparatus with which we are able to measure the horizontal and vertical components of the cutting resistance of rock: 1) the effect of depth of cut, 2) the effect of the number of free surfaces, 3) the effect of width of the cutting tip, 4) the effect of wear of the cutting tip, etc.

---

*Originally Published in the Journal of the Mining and Metallurgical Institute of Japan, v. 77, no. 881, Nov. 1961, p. 975-980.

[1] Chief, Mining and Safety Division, Agency of Industrial Science and Technology, National Research Institute for Pollution and Resources, Tokyo, Japan.

[2] Agency of Industrial Science and Technology, National Research Institute for Pollution and Resources, Tokyo, Japan.

[3] Graduate Student, Colorado School of Mines, Golden, Colo. 80401.

[4] Associate Professor, Department of Mining, Colorado School of Mines, Golden, Colorado 80401.

1. Introduction

When rock is drilled or bored using a rotary system, many shapes of bits are used. For example, rotary drilling using an auger type bit, diamond drilling using a metal core bit, tunnel boring in which cutters are applied to a rotating head, etc. Even though the type of bit used is different, the objective of each of these drilling methods is to cut rock. Therefore, if the basic cutting mechanism for rock could be clarified, the drilling mechanism of the above machines could also be clarified. This would lead to better drilling efficiency through improved design of these machines. As for this cutting mechanism, there are many studies pertaining to coal cutting (Hobel, etc.), but few regarding rock.

2. The Apparatus and the Method of the Experiment

The apparatus which was used in this experiment consists of the cutting machine and the measuring apparatus. The basic machine used in the cutting studies is a shaper. The bit is held in a special chuck which allows one to measure the cutting resistance. Fig. 1 shows the chuck and the system used for measuring the cutting resistance and the speed. The horizontal and vertical components of the cutting force are monitored by means of strain gages attached to the chuck. The gages are connected to a strain meter through a D.C. amplifier. The signals are recorded automatically on an oscillograph. The cutting speed is monitored by the closing of contact for every 20 mm of cut length. This signal is also recorded automatically.

The cutting speed can be set at one of four values (5, 8, 12, 18 cm/sec) and the maximum cutting length is 55 cm.

The bit used (see fig. 2) was chosen on the basis of strength and cutting resistance considerations. The tip of the cutting edge is tungsten carbide. The shape of the tip is constant, but four widths were used (5, 9, 15, and 20 mm).

In the experiments the material to be tested is set in a concrete slab, and the slab is then bolted to the fixed base plate. The surface of the material is then cut and smoothed using the bit. Once this has been done the rock is cut by charging the cutting position, the depth, and the speed of cut. For each test the cutting resistance is recorded automatically on the oscillograph.

As the cutting resistance of rock is far more variable than that of metal, etc., we recorded the change of cutting resistance of the rock, as well as the mean cutting resistance through a capacitance-resistance circuit.

Fig. 3 shows an example of a cutting resistance record. Because of the structure of the chuck the values recorded are not the pure horizontal or vertical components of force. The horizontal component of the force also includes the vertical component. Thus to obtain the true cutting resistance one needs to adjust these records by calculation.

3. The Discussion of the Results

Rock cannot be cut as smoothly as metal. Fig. 4 shows an example of fine grained marble cut by a coal cutter bit. In general, when cutting rock, even if the shape of the bit or

the depth of cut is changed, one can represent the cutting process in this manner.

Fig. 3 shows the variation of cutting resistance with travel. When only cutting occurs (as shown in frames 1 through 4 of fig. 4) the variation in cutting resistance is small. When the rock is primarily removed by chipping such as shown in frame 5, the variation is large. However, when the bit continues to advance after the rock has chipped, the variation again becomes small. Later, when the rock chips once again (such as shown in frame 7), the variation becomes a maximum. The fact that the constituents of a rock are not uniform is one of the reasons for the variation in cutting resistance. However, even if the components are uniform, the cutting resistance varies and the surface becomes rough as mentioned above.

This tendency is most prominent for larger depths of cut and harder rocks. Fig. 5 shows clearly the roughness of the cutting plane of andesite. Fig. 6 shows the cutting resistance R which can be replaced by the horizontal component R_H and the vertical component R_V.

The cutting force works in the opposite direction to the cutting resistance R. This seems to be the reason why the cutting plane is chipped as seen in frame 7 of fig. 4. The horizontal component of the cutting resistance is called the main cutting resistance or main force component, and the vertical component the minor force component. The horizontal component corresponds to the torque force in rotary drilling, and the vertical component corresponds to the thrust. The depth of cut corresponds to the drilling speed. Therefore, if

we know the relationship between the depth of cut and the horizontal and vertical components of force, we can deduct the relationship between drilling speed, thrust, and torque. Furthermore, the cutting resistance varies according to the type of rock, the shape of the bit, the depth of cut, the cutting position, and the number of free surfaces present.

3.1 The Relationship Between the Cutting Position and the Cutting Resistance

The cutting resistance measured at the rock surface and at a certain depth into the rock is different.

3.1.1 Variation of Cutting Resistance at the Rock Surface. Fig. 7 shows the relationship between the depth of cut and the cutting resistance. The width of bit is 20 mm, the cutting speed is 5 cm/sec and the shore hardness of each sample is given below:

	Soft, fine grained SS	Soft, med. grained SS	Concrete	Hard, med. grained SS
Shore hardness	15.7	21.7	26.6	76.7

From the results of fig. 7, when the depth of cut becomes a certain value, both the horizontal and vertical components of the cutting resistance increase in proportion to the depth of cut. Generally speaking, the horizontal component R_H (the main cutting resistance) is larger than vertical component R_V (the minor component). However, the value of R_V of hard sandstone is larger than R_H when the depth of cut is small.

Fig. 8 shows the relationship between the depth of cut and the ratio R_H/R_V. Initially, the values of R_H/R_V increase with the depth of cut. However, eventually the ratio approaches a

constant value.

3.1.2. The Variation of Cutting Resistance When Cutting is Done in a Preexisting Cut. When the rock surface is cut, the rock at both sides of bit is broken (see fig. 9a) and it is impossible to cut the same width as the bit (see fig. 5). This degree of overbreak depends on the type of rock and the depth of cut. The softer the rock, and the smaller the depth of cut, the smaller the overbreak. If a cut having the same width as the bit is made, and then the bottom of the groove is cut, the situation of breakage of rock is as shown in fig. 9b. When the depth of the previous groove d is small, both sides of the bit are chipped off as in fig. 9b. When d is large enough no chipping at the groove sides occurs. This is shown in fig. 9c.

When rock is cut, the situation for breakage on each of the sides of the bit is different according to the cutting position. The cutting resistance is also different. As an example, fig. 10 shows the relationship between the depth of the groove d and the cutting resistance of limestone for each depth of cut t.

The width of the tip of the bit in this experiment is 9 mm and the cutting speed is 5 cm/sec. It was found that as the depth of groove d increased, even if the depth of cut t is constant, both the horizontal and vertical components of the cutting resistance increase. As d is further increased they approach a constant value k.

The value of d_k (that is the value of d at which the constant value k is obtained) is approximately proportional to the

depth of cut t. The variation in the horizontal component of the cutting resistance with depth d is larger than for the vertical component. If the initial rock surface (d = 0) is cut using a depth of cut t equal to 1 mm, both the horizontal and vertical components are equal to 56 kg. If d is increased to the point where a constant value k is obtained, the vertical component is 82 kg and the horizontal component is 130 kg.

3.2 The Relationship Between the Number of Free Surfaces and the Cutting Resistance

In rotary drilling the hole volume is removed in various ways depending on the shape of the bit. Fig. 11a illustrates the cutting geometry when a bit having a single continuous cutting edge (such as a metal drill bit) is used. Figure 11b illustrates the situation for bits having tips arranged in several lines of concentric circles at various levels, and fig. 11c the situation when the intermediate tip cuts the rock between the 2 outer lines of tips which preceded it. The number of free surfaces shown in figures 11a, b, and c is 1, 2, and 3 respectively. Therefore, even if the tip width and the depth of cut are constant, but the number of free surfaces is different, the condition at the bit tip and the cutting resistance is different.

Fig. 12 shows the relationship between the depth of cut and the cutting resistance for various numbers of free surfaces when soft sandstone is cut by bit having a tip width of 20 mm. From these results, when the depth of cut is larger than a certain value, both the horizontal and vertical components of cutting resistance increase in proportion to the depth of cut. However,

the fewer the number of free surfaces, the larger the cutting resistance. Fig. 13 shows the relationship between the number of free surfaces and the cutting resistance for various depths of cut. The larger the depth of cut, the greater the effect of the free surfaces. The differences in the 1 and 2 free surface results represents the cutting resistance of one side of the bit to the wall. The difference in the 1 and 3 free surfaces results represents the cutting resistance for both sides of the bit to the hole wall. From the experiments the differences in cutting resistances between 1 and 3 free surfaces is approximately twice the difference observed between 1 and 2 surfaces.

3.3 The Relationship Between the Width of Bit Tip and the Cutting Resistance

Fig. 14 shows the relationship between the cutting resistance and the bit tip width for soft sandstone having various numbers of free surfaces and at several cutting depths. For each depth of cut the cutting resistance is approximately proportional to the width of the tip. For small tip widths, however, the change in cutting resistance with width is somewhat smaller than for wider tips. For a particular depth of cut, the relationship between the cutting resistance (both the vertical and horizontal components) and the tip width is nearly independent of the number of free surfaces. The reason for this is that as long as the depth of cut is constant, even if the width of blade changes, the cutting resistance on both sides of the bit (the cutting resistance on the walls) does not change.

3.4 The Relationship Between the Wear of the Cutter Tip and the Cutting Resistance

To determine the effect of tip wear on the cutting resistance, we cut samples of andesite. The depth of cut was kept constant. Fig. 15 shows the relationship between tip wear and the cutting resistance. The width of the tip is 9 mm and the cutting speed is 5 cm/sec. It was found that when the depth of cut is constant and the tip wear large enough, both the horizontal and vertical components of the cutting resistance increase in proportion to the width of wear of the tip.

Fig. 16 shows the relationship between the cutting resistance and the depth of cut for each width of tip wear, as derived from the data of fig. 15. From fig. 16 we can see that both the horizontal and vertical components of cutting resistance increase in proportion to the depth of cut for each tip wear width in the range of the experiment.

3.5 The Relationship Between the Length of Cut and the Bit Wear

After quite a long length of material has been cut, the tip is observed to wear gradually. The andesite was cut by a bit whose tip width was 9 mm, with the depth of cut being kept constant. Fig. 17 shows the experimental relationship between the length of cut L and the width of wear of the tip. The cutting speed is 5 cm/sec and the tip material is tungsten carbide of type G-2 (hardness R_A 89).

As can be seen, at the beginning of cut the wear proceeds rapidly following the relationship $B \propto L^m$ ($m<1$). When the cutting distance becomes large, the relationship becomes nearly $B \propto L$. Furthermore, in the experimental range covered, the slope of

the tip wear width-cutting distance curve is almost constant (independent of the depth of cut). However, the larger the depth of cut, the larger the wear becomes. As an example, for a cut having a length of 5 m, if the depth of cut is 0.1 mm, the width of wear of tip is about 0.18 mm, and if the depth of cut is 0.5 mm, the wear is about 0.24 mm.

The length of cut before the wear reaches 0.25 mm is 9.5 m for a depth of cut of 0.1 mm, 7.2 m for a depth of 0.3 mm, and 5.4 mm for a depth of 0.5 mm. That is, when we cut a constant length, the width of wear of the tip increases in proportion to the depth of cut. The length to produce the same wear of tip decreases in proportion to the increasing depth of cut. From this it would appear that to reduce wear the depth of cut should be reduced. However, in rotary drilling the advance is proportional to the product of the depth of cut and the cutting resistance (i.e. to the volume of cut). Therefore, assuming the volume of cut necessary to produce a tip wear of 0.25 mm to be 1 for a depth of 0.1 mm and 0.5 mm respectively. Hence the deeper the depth of cut, the less wear on a volume basis.

3.6 The Relationship Between the Cutting Speed and Bit Wear

To determine the effect of the cutting speed on the wear of the bit tip, we cut andesite at a constant depth of cut (0.2 mm) at various cutting speeds. Fig. 18 shows the relationship between the cutting distance and the wear flat width. In this case, the tip had a width of 9 mm and was made from tungsten carbide (type G-2) having a hardness a little less than the material used in the test described in section 3.5.

The same type of relationship described in section 3.5 was found between the width of the wear flat and the cutting distance for each cutting speed. However, for the same length of cut the tip wear increased with cutting speed. When metal is cut, the relationship between the wear and the cutting speed is generally a power function. In this experiment, as relationship between the cutting speed and the wear is not as clear. However, when we cut 5 m, for example, the wear flat width is about 0.24, 0.28, and 0.32 mm for cutting speeds of 5, 12, and 18 cm/sec respectively. Therefore, it is presumed that there is a relationship between the cutting speed V and the width of wear B such as $B \propto V^n$.

4. Conclusions

Except for the roller bit most of the methods used in rotary drilling remove the rock by a cutting action. Therefore, it seems that if the cutting mechanism and the cutting resistance between bit and rock can be explained, the technique of rotary drilling will be advanced, and the design and further improvement of these machines will be easier. Rock cutting experiments were done in which cutting conditions such as bit shape, position, and depth of cut and the cutting speed were varied and the effects on the cutting resistance, bit wear, etc. were noted.

For the range of our experimental data the following conclusions appear to apply:

1) The cutting resistance measured when cutting the initial rock surface and that observed for cuts below the

initial surface were different. When the surface of rock is cut, both the horizontal and vertical components of the cutting resistance increase almost in proportion to the depth cut. The cutting resistance increases gradually as the cutting position increases beneath the original surfaces. If the position is deeper than a certain value, the cutting resistance is nearly constant for each successive cut.

2) If the depth of cut is larger than a certain value, the cutting resistance increases in proportion to the depth of cut independent of the number of free surfaces. When the number of free surfaces is 3, the cutting resistance is the smallest.

3) If the tip width is larger than a certain value, the cutting resistance for each depth of cut increases almost in proportion to the width of tip. The ratio of cutting resistance to the width of tip becomes larger as the depth of cut is increased.

4) If the depth of cut is constant, the cutting resistance increases almost in proportion to the width of wear of the tip. For a constant wear width of the tip, the cutting resistance increases almost in proportion to the depth of cut.

5) When the depth of cut is constant, the increase in tip wear width with cutting distance is extremely large at the beginning of the cut. As the cutting distance becomes large, the ratio becomes nearly constant. The increasing ratio of the wear to the cutting distance becomes larger as the depth of cut becomes larger. When the same distance is cut, the tip wear increases almost in proportion to the depth of cut. However,

the rate of increase of the wear to the cutting volume is smaller as the depth of cut becomes larger.

6) When the depth of cut is constant, the rate of tip wear increases as the cutting speed becomes larger.

Acknowledgments

In this study, we received the help of Prof. Mizuta and Prof. Shimomura, both of Tokyo University, and of Mr. Suzuki, the manager of the 6th Department of the Resource and Technical Research Institute. In regard to the experimental equipment, we received the kind cooperation of the Geological Department of the Mitsui Mining Co. to whom we express our deepest thanks.

References

1) M. J. O'Doghery, E. W. Inett, and R. Shepard: "Laboratory and Field Investigation of Coal Ploughing," Trans. Inst. Eng., 118, 1.

2) Mikumo, Aida, Okamoto;
Relation between the hardness of coal and the cutting resistance (1), (2).

3) Masao Kogure;
The life of very hard bits and its experiment, p. 141.

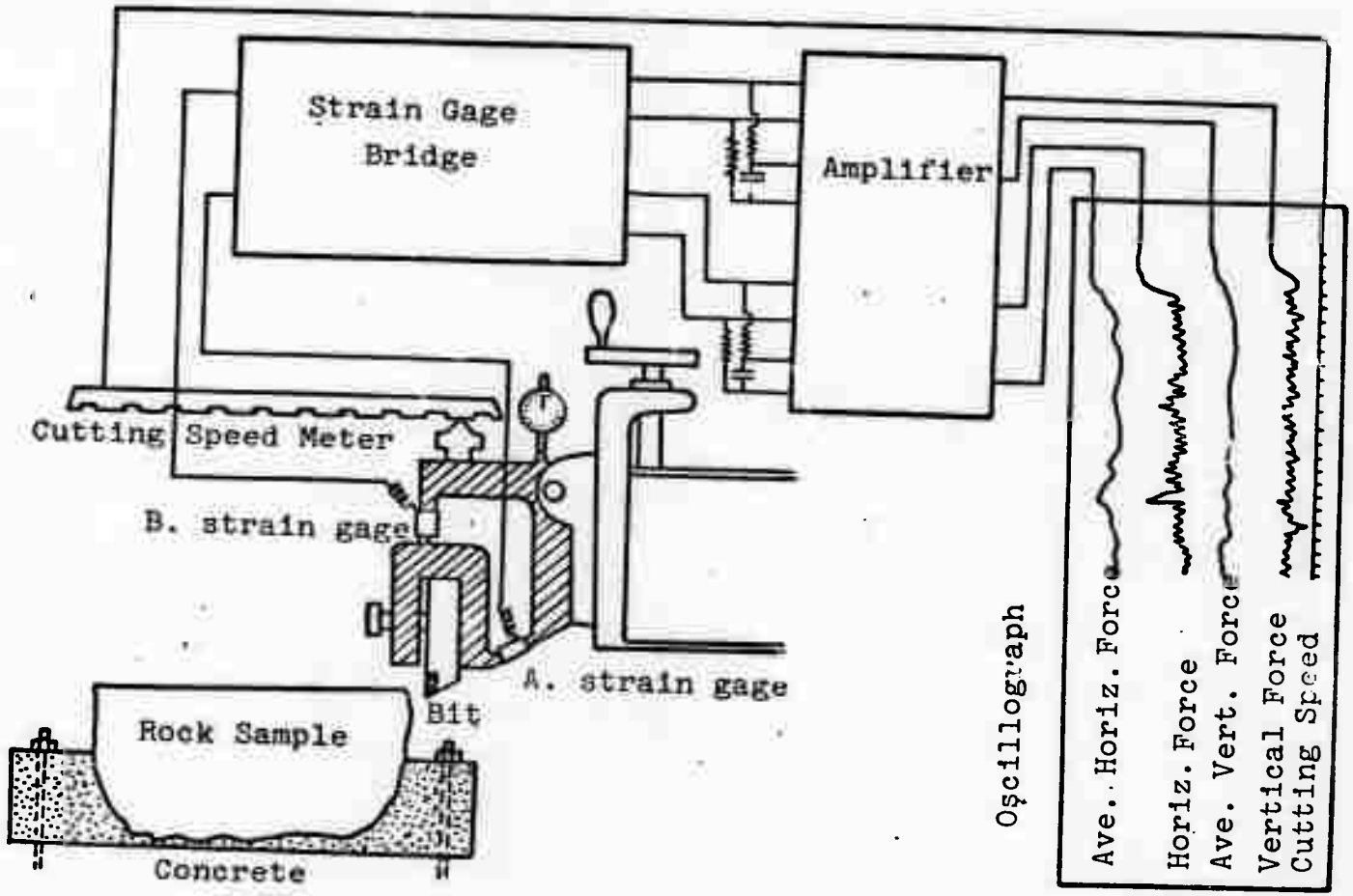

Figure 1. Diagrammatic representation of the experimental apparatus and the measurement system used in the testing.

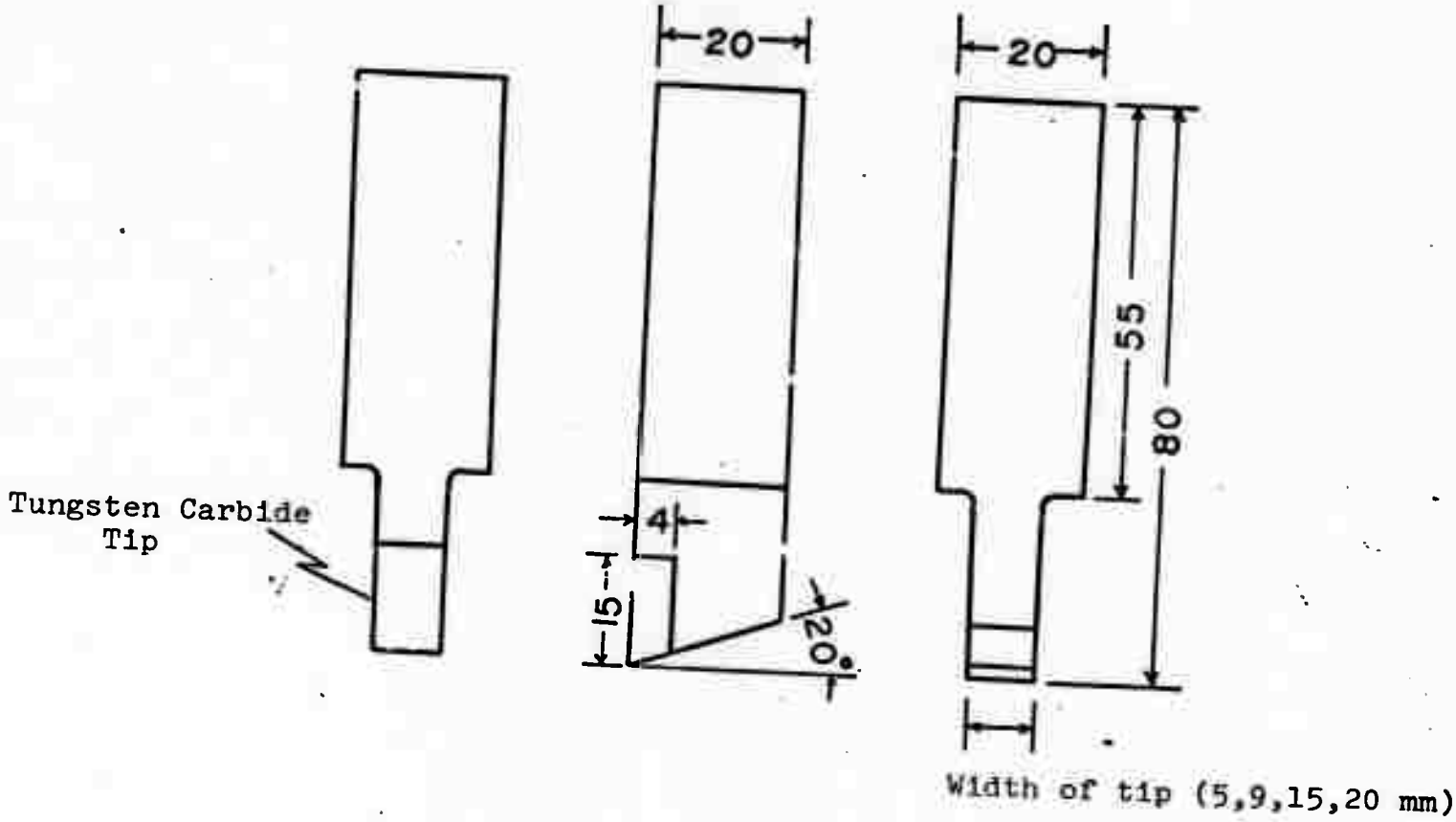

Fig. 2. Diagrammatic representation of the bit used for the cutting tests.

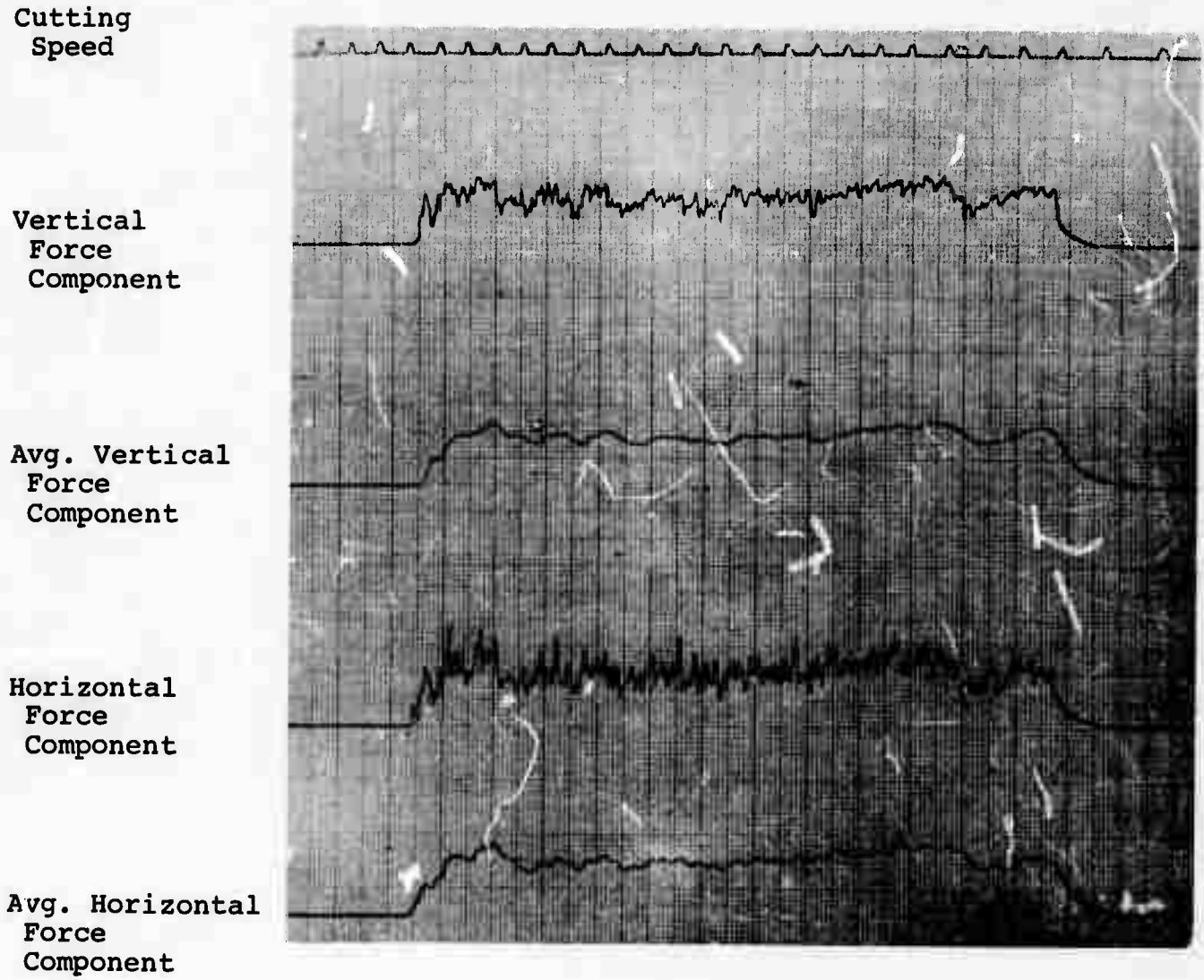

Figure 3. An example of the oscillograph records of the cutting process. Limestone sample, 1.5 mm cutting depth, using a bit having a width of 9 mm.

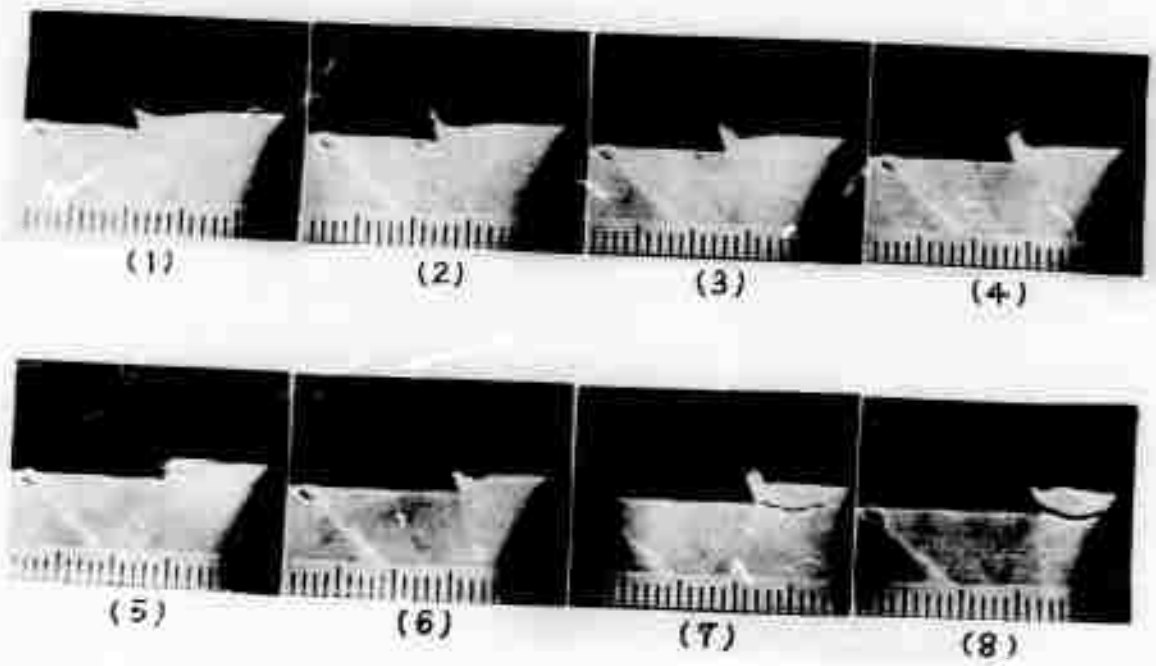

Figure 4. Sequence of Pictures Depicting the Cutting Process.

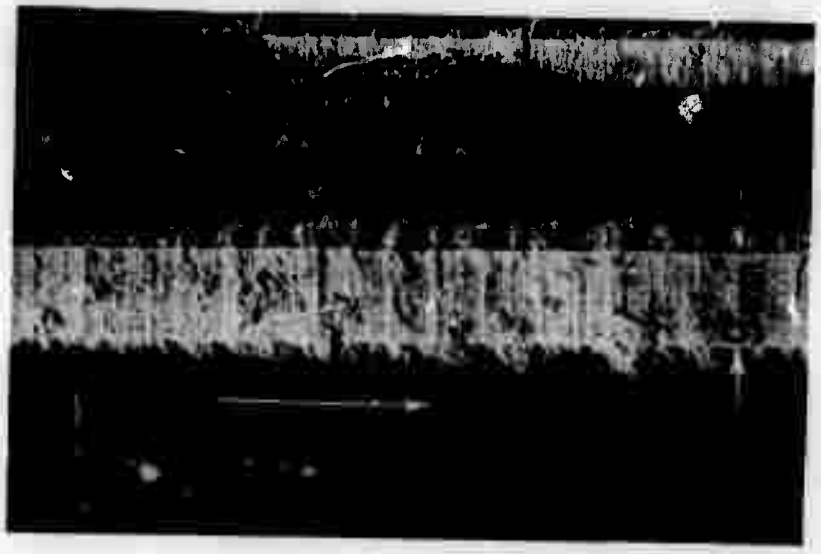

Figure 5. The Cut Surface of an Andesite Sample.

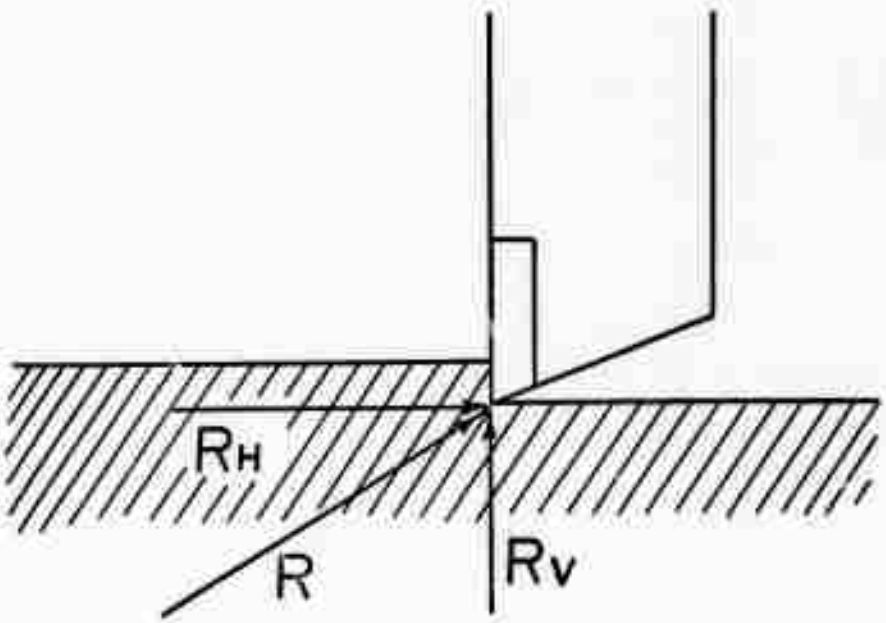

Figure 6. Diagrammatic representation of the forces acting on the cutter tip.

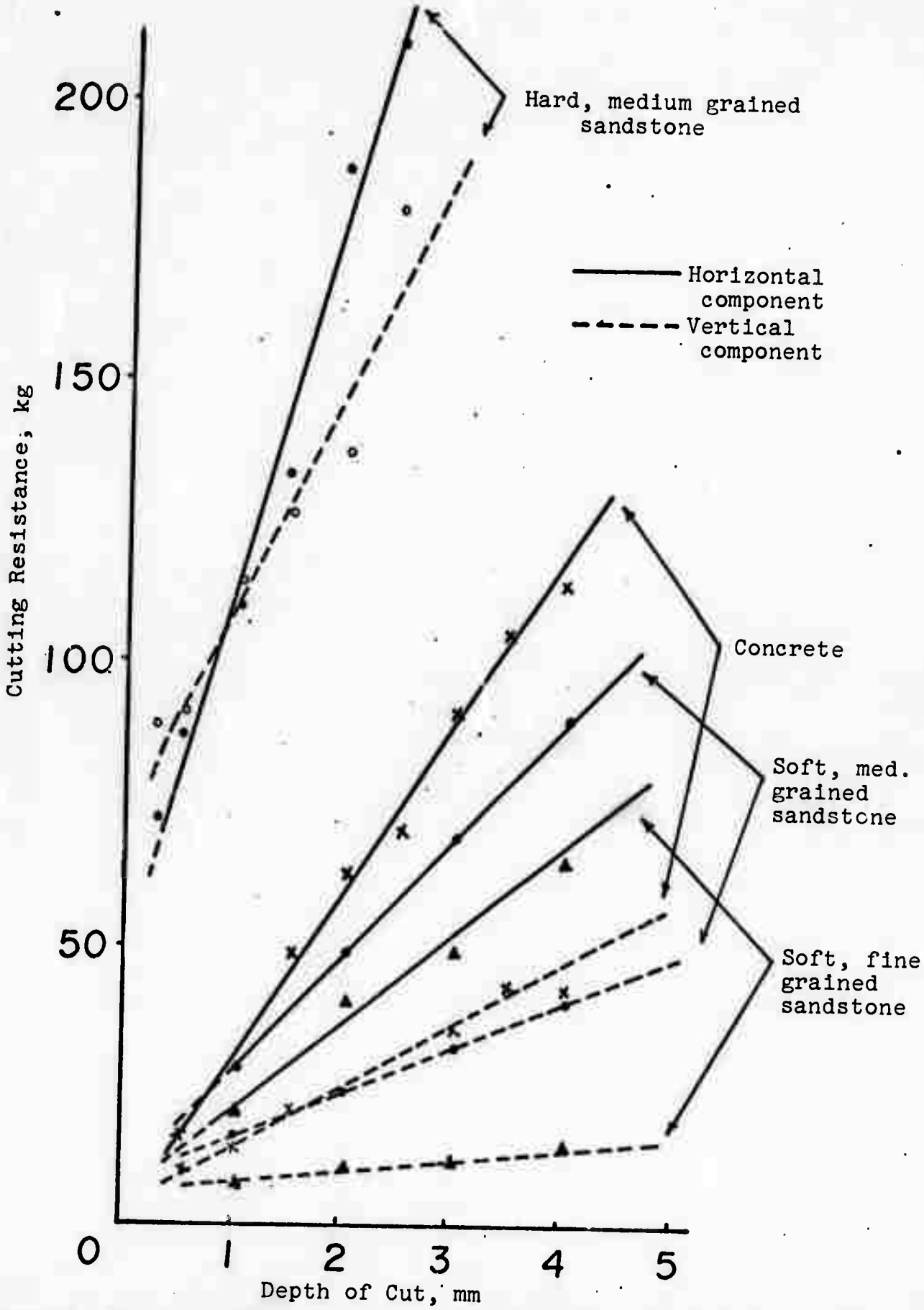

Fig. 7. The relationship between the cutting resistance and the depth of cut for various materials.

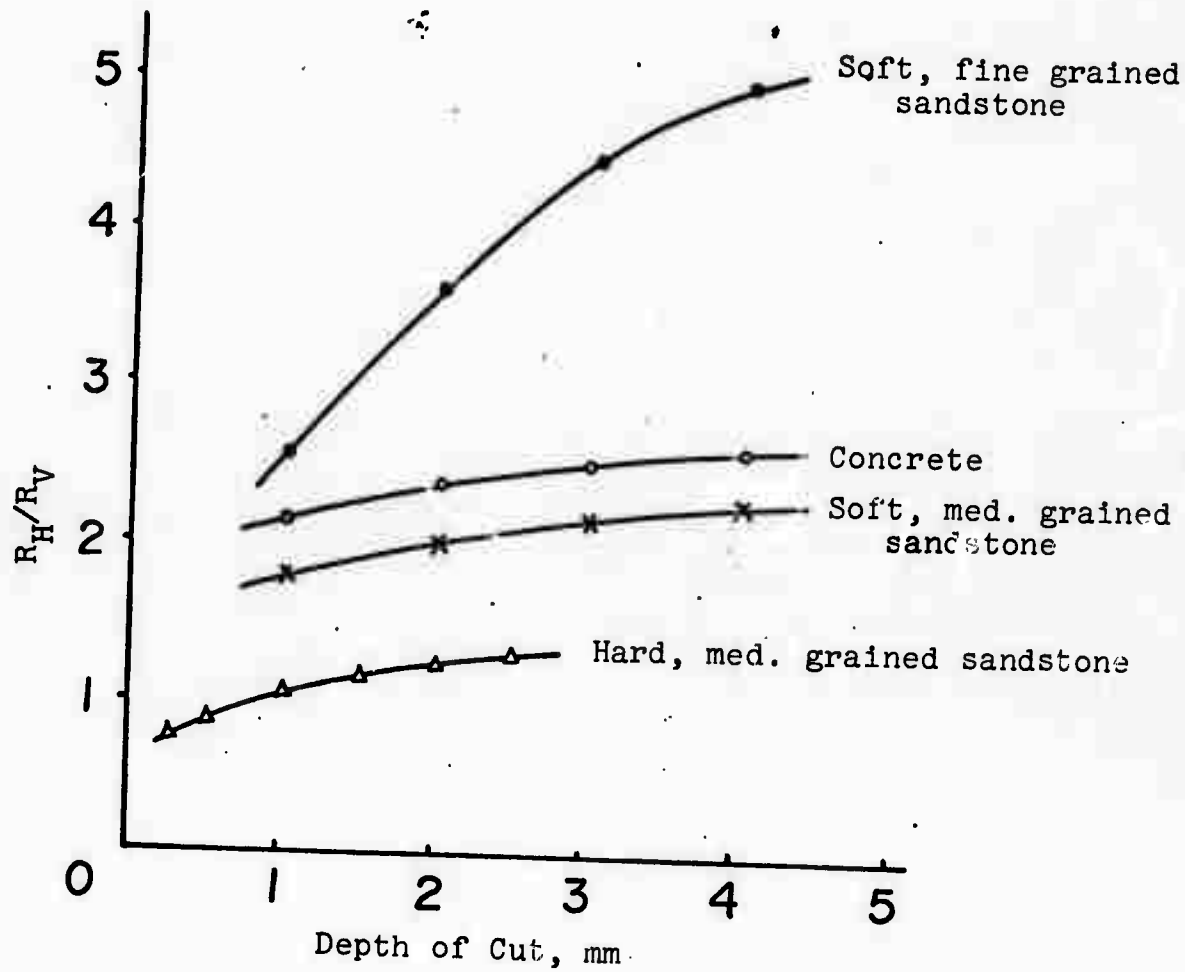

Fig. 8. The relationship between R_H/R_V and the depth of cut for various materials.

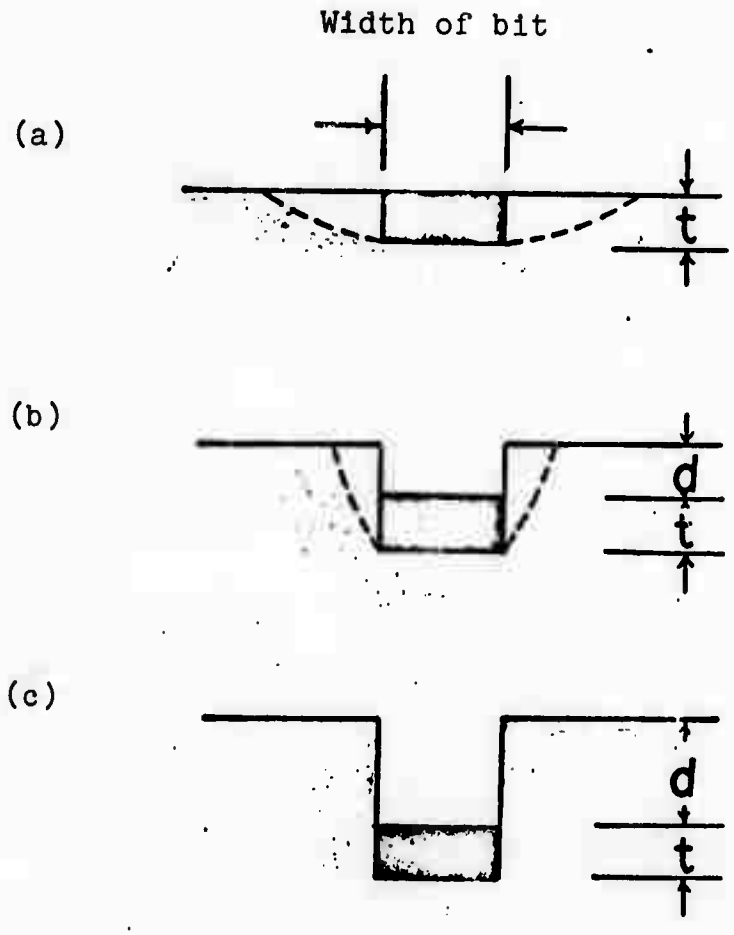

Figure 9. Diagrammatic representation of how the breakage pattern depends upon the cutting position.

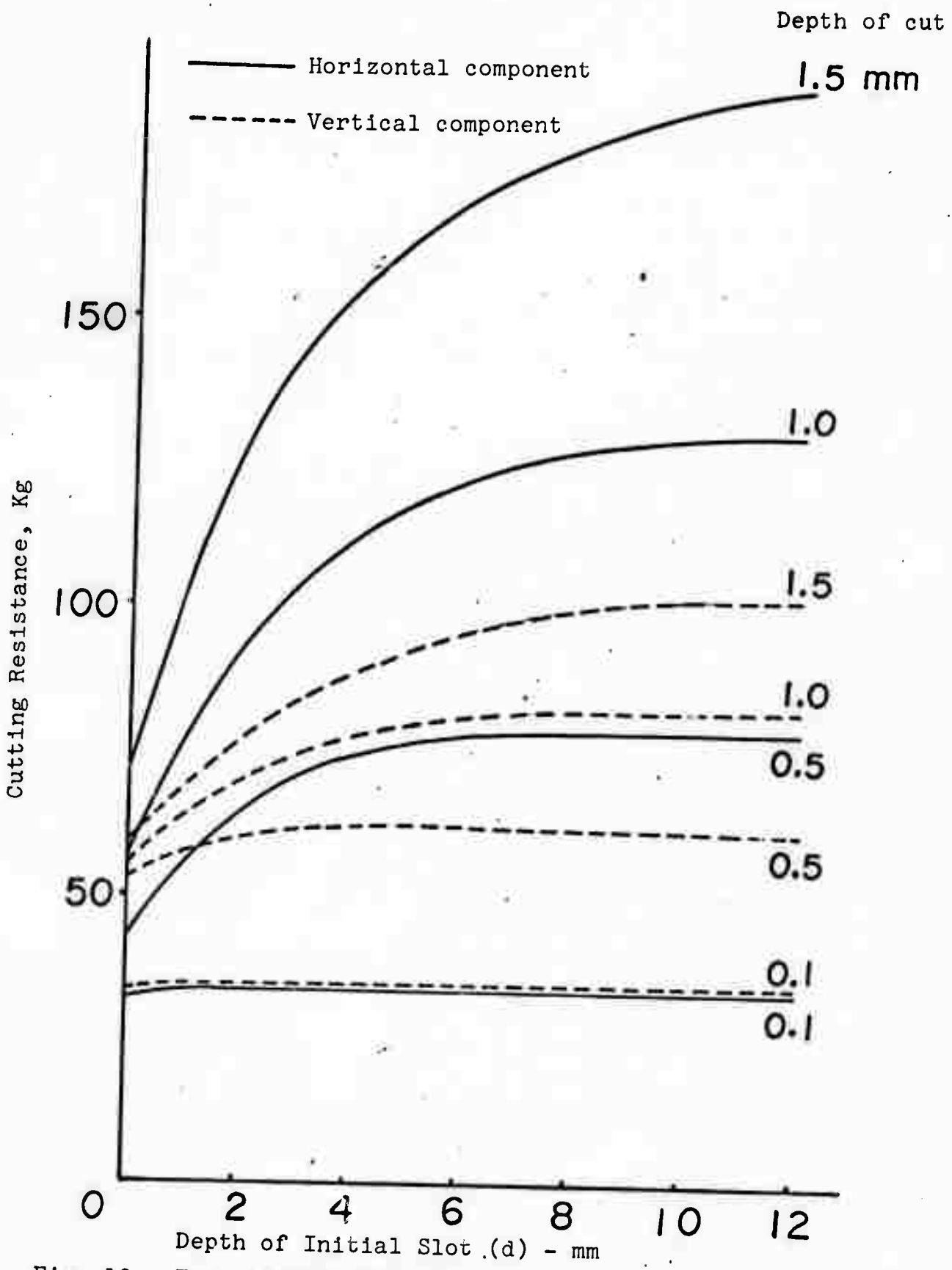

Fig. 1C. The relationship between the cutting resistance and the depth of the initial slot for various depths of cut.

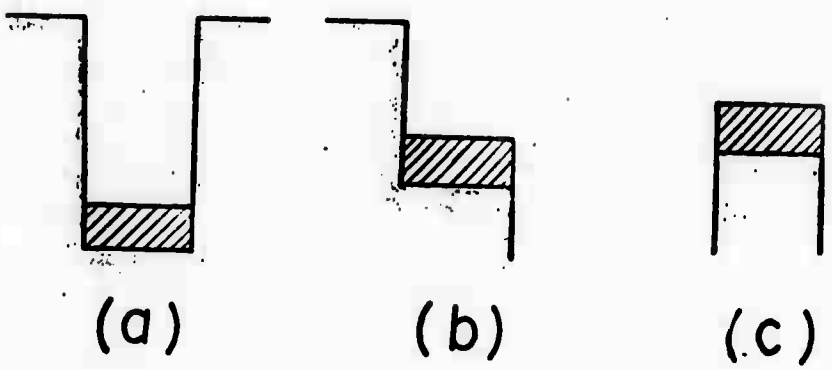

Figure 11. Cutting geometry showing one, two, and three free surfaces.

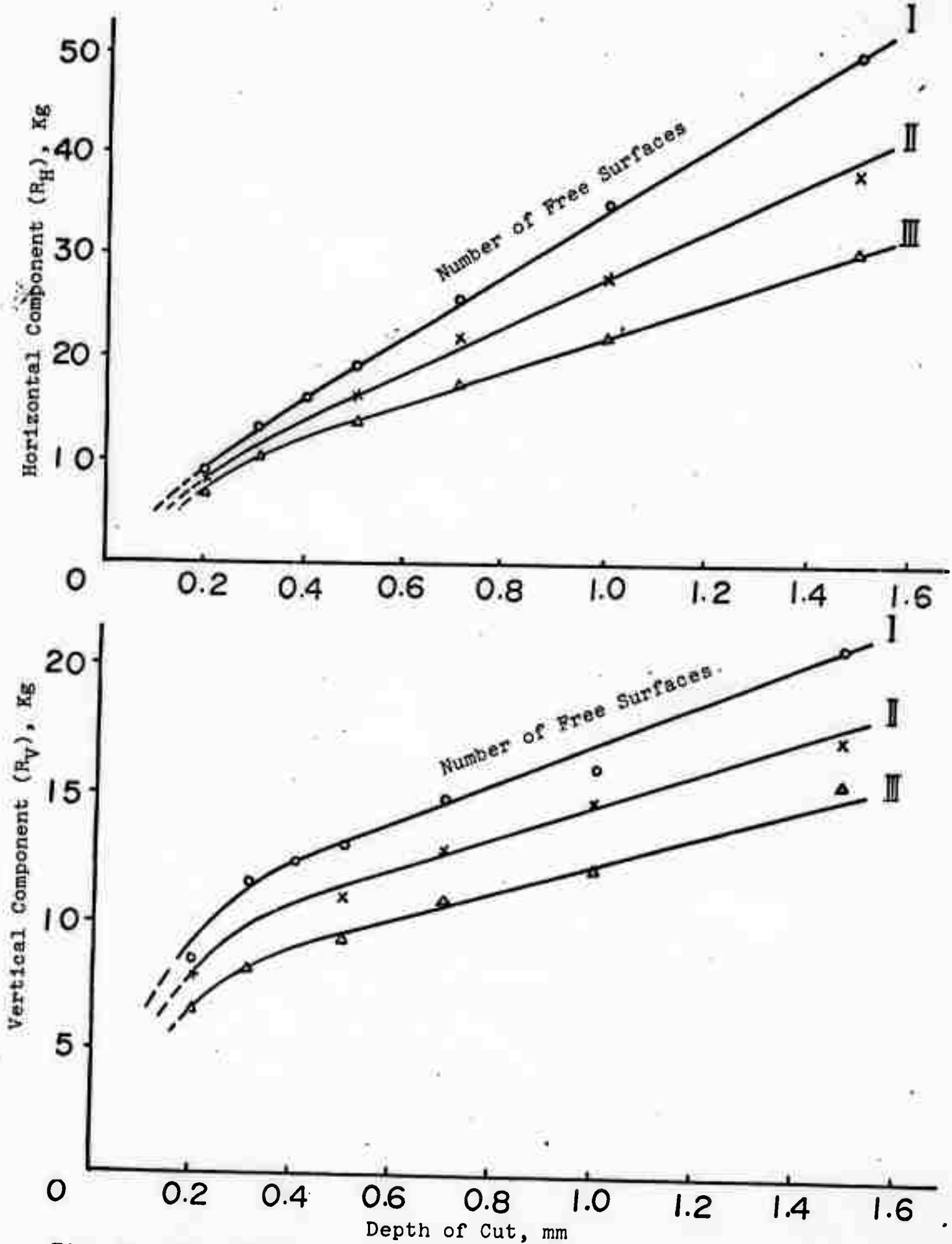

Fig. 12. The relationship between the cutting resistance and the depth of cut for various numbers of free surfaces.

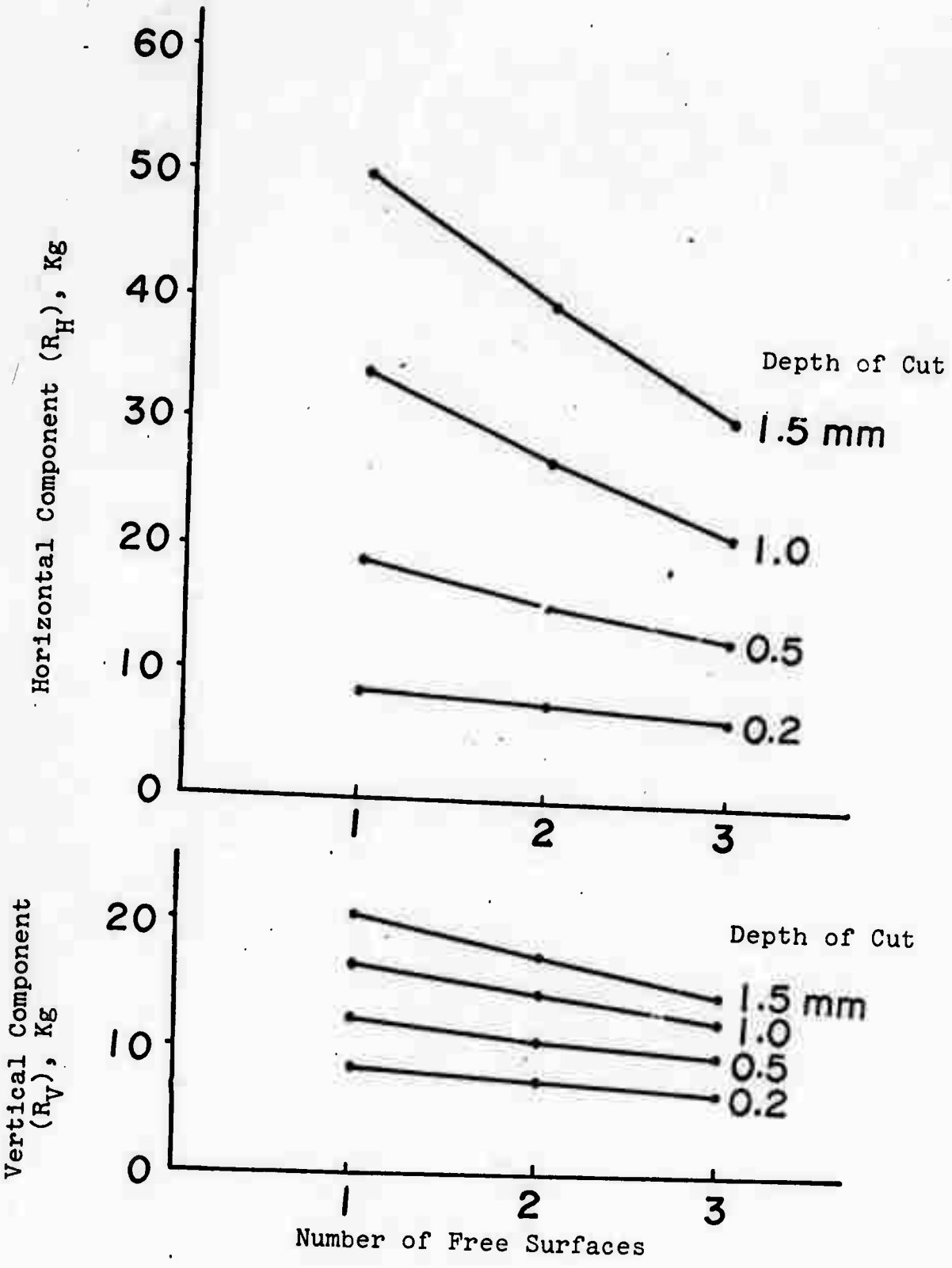

Fig. 13. The relationship between the cutting resistance and the number of free surfaces as a function of the depth of cut.

The Roman numerals I, II, and III represent the number of free surfaces. The numbers to their right give the depth of cut in mm.

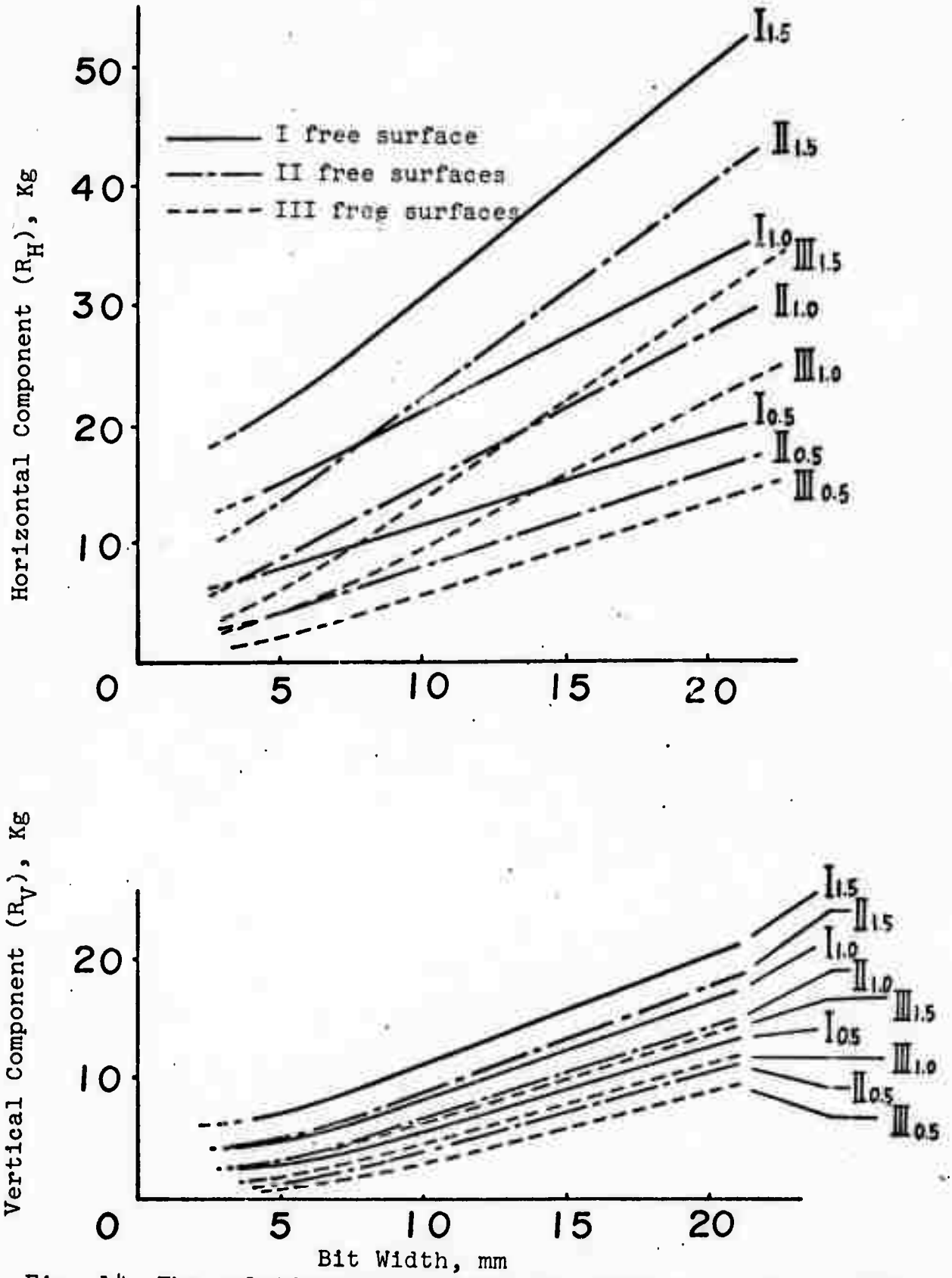

Fig. 14. The relationship between the cutting resistance and the bit tip width.

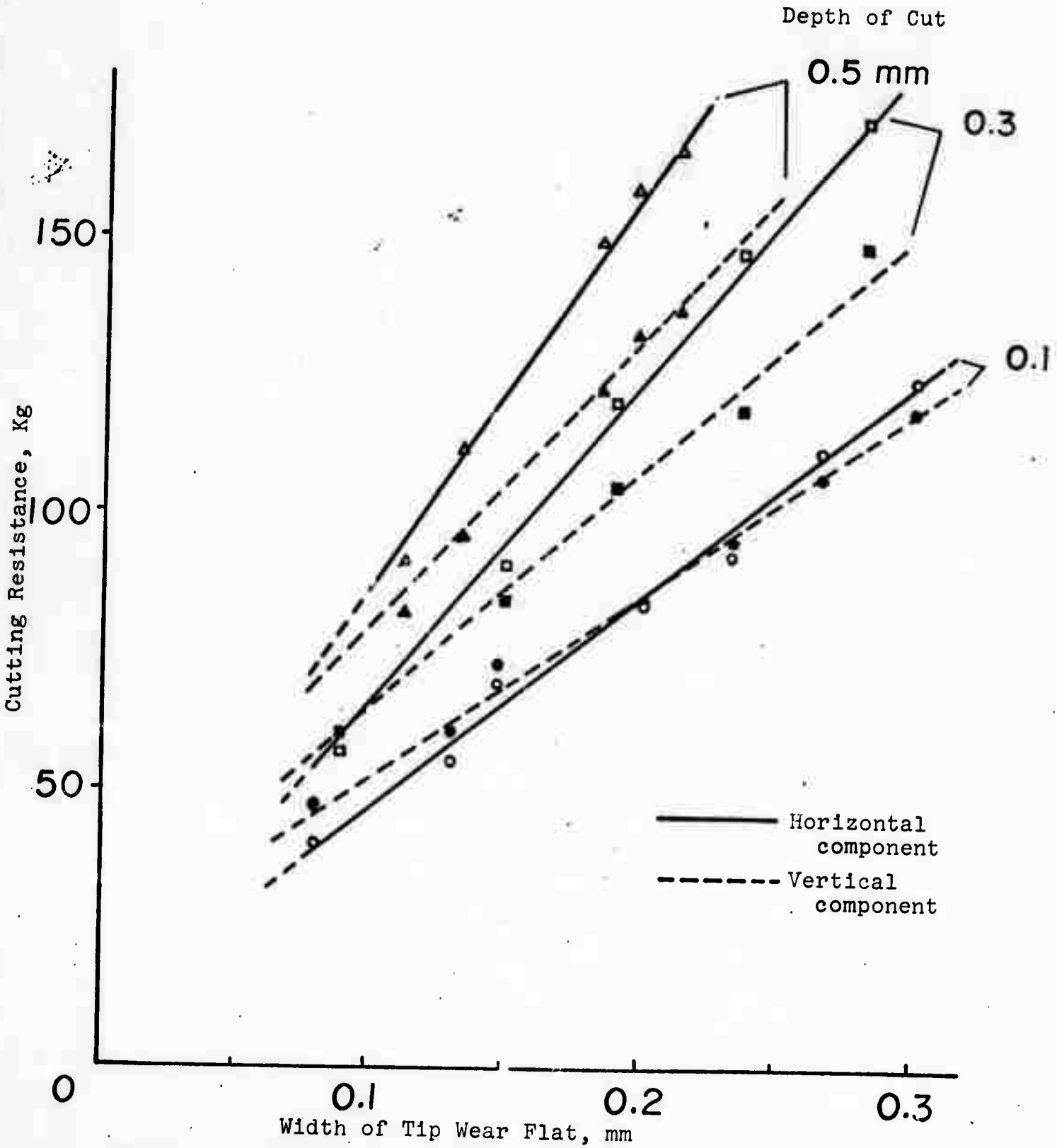

Figure 15. The relationship between the cutting resistance and the width of the tip wear flat.

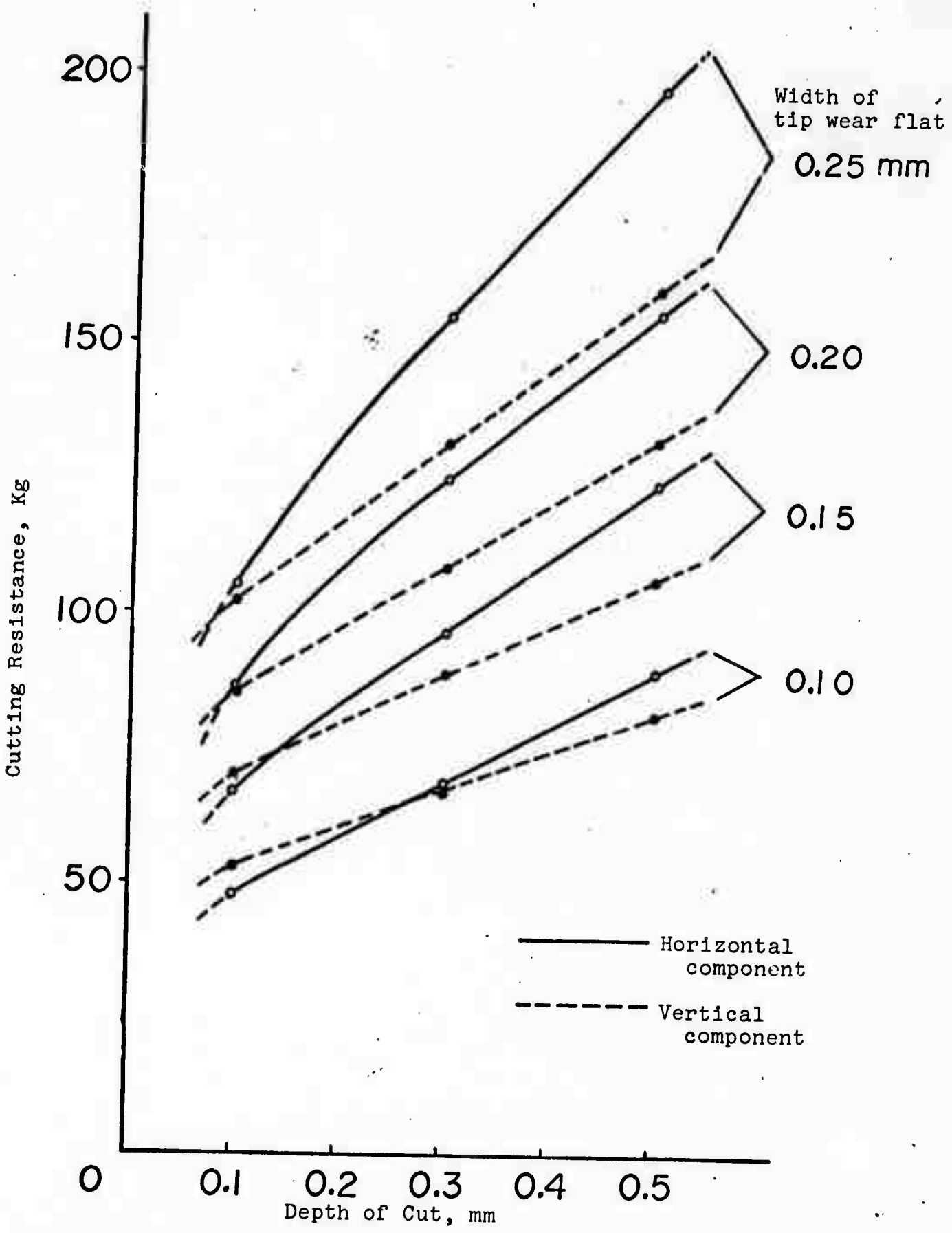

Fig. 16. The relationship between the cutting resistance and the depth of cut as a function of tip wear.

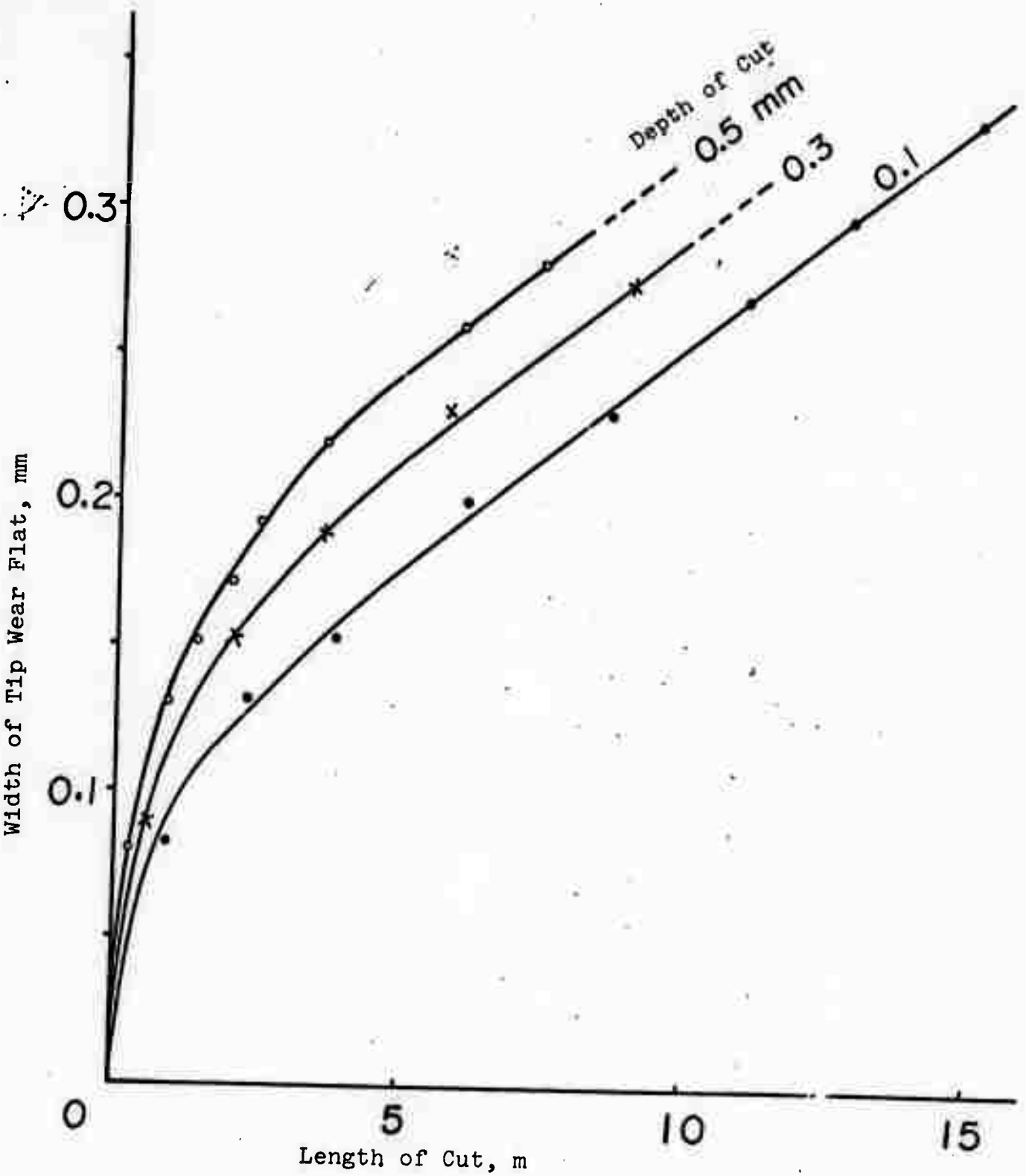

Fig. 17. The relationship between the width of the tip wear flat and the length of cut as a function of the depth of cut.

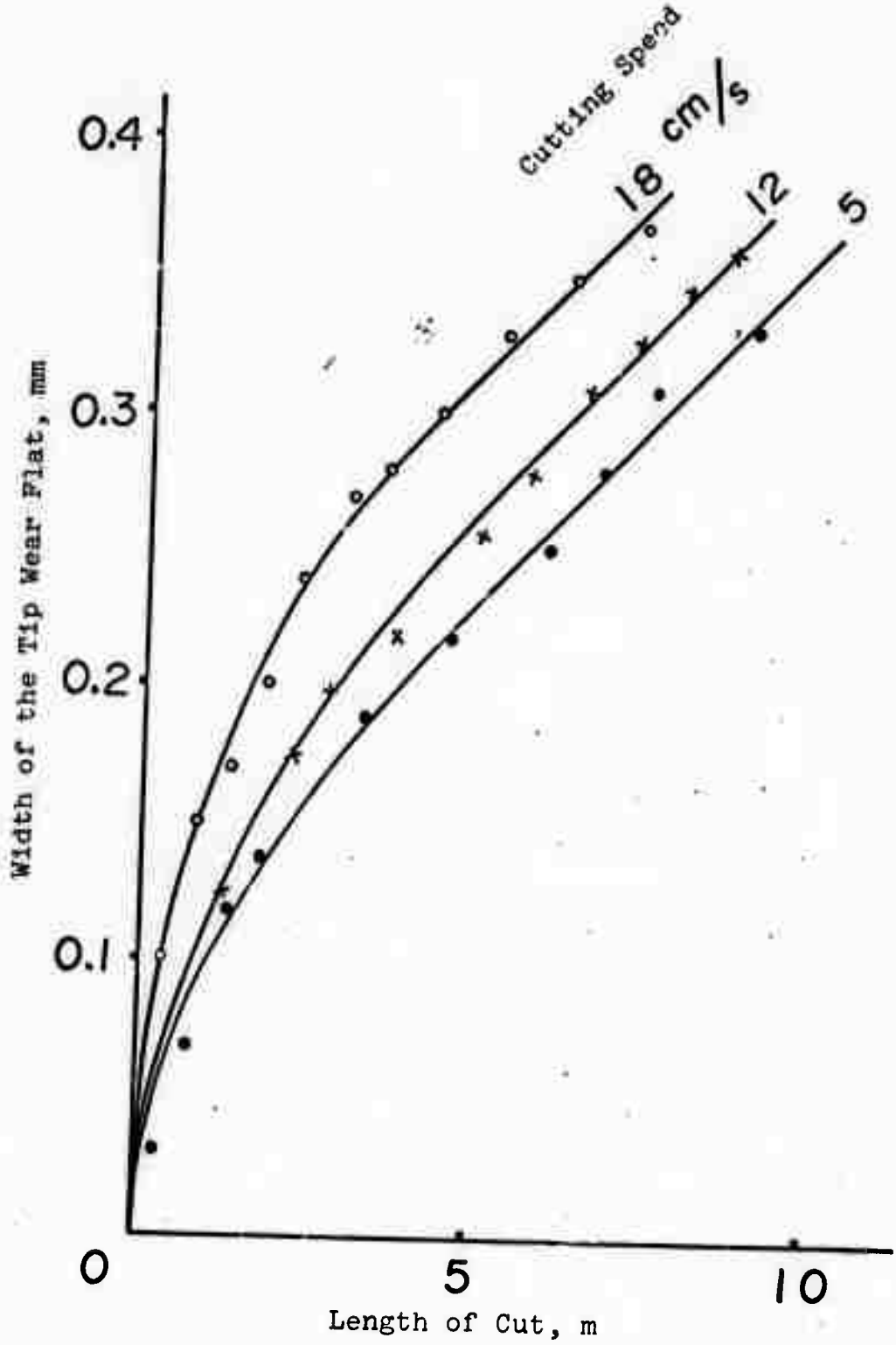

Fig. 18. The relationship between the width of the tip wear flat and the length of cut as a function of cutting speed.